

Central Asian Institute for Applied Geosciences (CAIAG)

**REMOTE- AND GROUND- BASED EARTH EXPLORATIONS
IN CENTRAL ASIA**

BISHKEK 2016

UDC 551. 8+551. 244

LBC

B.D. Moldobekov., Sh.E.Usupaev., A.V.Zubovich., A.N.Mandychev., R.A. Usubaliev., L. Joldybaeva., Z.A. Kalmetieva., A.Shabunin., Y. Podrezova., O. Kalashnikova., and etc.

“REMOTE AND GROUND EARTH EXPLORATION IN CENTRAL ASIA”.

Bishkek.: Publishing house "City Print", 2016. 206 p.

The monograph shows the remote and land-based applications in the Earth exploration derived from established by CAIAG and GFZ and the latest network monitoring changes in the environment of Kyrgyzstan and cross-border areas with the countries of Central Asia (CA).

The results presented the priority directions: network monitoring, climate, water and ecology, geodynamics and disasters, IT geodatabase and infrastructure, scientific and educational potential in Central Asia.

The book is designed for wide range of scholars and experts studying the Earth science in the region of Central Asia.

Bibliography. 152 references. Fig. 180. Tables 10.

Published by the decision of the Academic Council of CAIAG

Reviewers:

K.A Kozhobaev PhD (technical sciences) ., Professor of Kyrgyz-Turkish University "Manas"

I. Sadybakasov. PhD (geology, mineralogy), a consultant of the Resource Centre "TEMPUS"

Institute of Mining and Mining technologies named after Academician U. Asanaliev.

Editors in chief: B.D. Moldobekov, Doctor, PhD (geology, mineralogy)
J. Lauterjung Prof, Dr. physics and minerology.

ISBN

CONTENT

History of Foundation

Introduction

CHAPTER 1. GEODYNAMICS AND GEORISKS

1.1. Preliminary geological and geophysical research of Sary-Djaz River basin

1.1.1. Selection of the study area and geological development of the area (Mikolaichuk A.V., Moldobekov B.D.)

1.1.2. Description of geomorphology, regime of recent movements and dangerous natural processes related to them (Usupaev Sh.E., Ormukov Ch.)

1.1.3. Seismicity of the area and surface movements (Zubovich A.V., Kalmetyeva Z.A., Mosienko O.I.)

1.2. Landslide dynamics survey

1.2.1. Landslides Tatyr, Gulcha, Mailisu and Minkush (Mandychev A.N., Dudashvili A.S., Detushev A., Shabunin A.G., Azisov E.A., Mosienko O.I., Abdybachiev U.)

1.2.2. Landslides in Alay district (Abdybachiev U., Usupaev Sh.E.)

1.3. Landslides, seismicity and geodynamics of Tien Shan

1.3.1. Landslides in Chui and Fergana hollows and their mountain framings (Kalmetyeva Z.A., Moldobekov B.D.)

1.3.2. Analysis the time of landslides activation (Kalmetyeva Z.A., Moldobekov B.D.)

1.4 The Nura earthquake of 2008 ($M=6.6$; $I_0 = 8$ MSK64)

1.4.1. Field study (Meleshko A.V., Usupaev Sh.E., Michailiev V.N.)

1.4.2. Structural position based on geological, seismological and GPS observations (Zubovich A.V., Kalmetyeva Z.A., Mikolaichuk A.V.)

1.4.3. Results of remote study (Teshebaeva K., Sudhaus H., Echtler H., Motagh M., Roessner S., Schurr B., Wetzel U.)

1.5. Specifics of spatial and time distribution of strong earthquakes in Central Asia (Kalmetyeva Z.A., Moldobekov B.D.)

1.6. Seismic microzonation of the territory of large cities

1.6.1. Bishkek city (Bindi D., Parolai S., Pilz M., Moldobekov B.D., Orunbaev S. Zh., Tokmulin Zh.A., Usupaev Sh.E.)

1.6.2. Karakol town (Bindi D., Parolai S., Pilz M., Orunbaev S.Zh., Usupaev Sh.E.)

CHAPTER 2. CLIMATE AND WATER RESOURCES

CONTENT

2.1. A study of climate change

- 2.1.1 Comparative analysis of the results of measurements by automatic weather stations and traditional types of weather equipment (J.Podrezova, A.Podrezov, A.Shabunin, A.Mandychev)
- 2.1.2. High-elevation snow cover area assessment using GIS and remote sensing technologies (J.Podrezova)
- 2.1.3. Analysis of climate changes in Issyk-Kul lake basin (A.Shabunin)
- 2.1.4. Assessment of the present-day regime of the surface temperature of the Issyk-Kul lake using MODIS/TERRA data (A.Shabunin)
- 2.1.5 Atmospheric dust monitoring station (A.Shabunin, E. Azisov, Schettler G.)

2.2. A comprehensive study of the mountain glaciers dynamics

- 2.2.1. Enilchek glacier research (R.A.Usabaliev, E.A.Azisov, A.Osmonov, A.Shabunin, A.Dudashvili, A.Mandychev, M.Dayirov)
- 2.2.2. Geophysical studies of glacial-dammed Merzbacher lake dam (I.Torgoev, B.Omorov, A.Torgoev, S.Burette)
- 2.2.3. Seismic noise measurements on the Southern Engelchek Glacier in the area
- 2.2.4. Lake Merzbacher (Sh.Usupaev, S.Orunbaev, T.Konokov)
- 2.2.4. Magnetometric studies in the area of the confluence of the North and South Enilchek glaciers near the Merzbacher Lake (A.Shakirov, Sh.Usupaev, R. Usabaliev)
- 2.2.5. Study of the Abramov, Golubin, Adygene, Petrov and Karabatkak glaciers (R.Usabaliev, E.Azisov, A.Mandychev)

2.3. Study of regime change of rivers, lakes, water reservoirs and groundwater

- 2.3.1. Forecast of water flow into the Toktogul water reservoir in the vegetation period (Kalashnikova O.Yu., Karamoldoev J.J.)
- 2.3.2. Longterm change of climatic features and water flow at Naryn river head during the vegetation period (Kalashnikova O.Yu.)
- 2.3.3. Change of annual flow of the Issyk-Kul basin in the long-term period (Kalashnikova O.Yu.)
- 2.3.4. Study of consistent patterns of southern Kyrgyzstan surface discharge related to climate change, and assessment of the intensity of erosion processes and transportation of sediments in the pool of the Toktogul reservoir (Shabunin A.G., Mandychev A.N., Dudashvili A.S., Azisov E.A., Mosienko O.I., Detushev A.)
- 2.3.5. Monitoring and assessment of mountain outburst lakes in the northern slope Terskey Ala-Too and the Kyrgyz ridge (Dayirov M.A.)
- 2.3.6. Groundwater studies (Mandychev A.N.)
- 2.3.7. Analysis of Landsat 8 satellite imagery with respect to mapping of aquatic and terrestrial objects of Issyk-Kul lake basin (Shabunin A.G.)
- 2.3.8. Study of the possibilities of application and adaptation of various climatic, hydrological and erosion models (Shabunin A.G.)

CONTENT

2.4. Study of the impact of Makmal gold mine on the environment (U.A. Abdybachiev, B.D. Moldobekov, A.S.Dudashvili, E.Mamabetaliev, K.E.Uzakbaev, E.Kylychbaev)

CHAPTER 3. NATURAL PROSESSES MONITORING AND GEOINFORMATION SYSTEM

3.1. Monitoring System

3.1.1. Research Monitoring Network (A.V. Zubovich, A.E.Shakirov, A.K. Sharshebaev, S.S. Barkalov)

3.1.2. Seismic monitoring (A.K. Sharshebaev, Z.A. Kalmetyeva, A.V. Zubovich)

3.1.3. Hydro-meteo monitoring (A.V. Zubovich, A.E. Shakirov, A.K. Sharshebaev, S.S. Barkalov, M.N. Borisov).

3.1.4. GNSS monitoring (A.V. Zubovich, O.I. Mosienko, A.E. Shakirov)

3.2. Information systems and geodatabase

3.2.1. The storage system of sensory data (A.V. Zubovich, D.A. Mandychev)

3.2.2. Geodatabase (A.V. Zubovich, D.A. Mandychev, M.M. Jantaev, V.V. Savin)

3.2.3. Geoinformation systems in engineer communication services (A.V. Zubovich, D.A. Mandychev, M.M. Jantaev, V.V. Savin, W.A. Abdybachiev, O.I. Mosienko, S.S. Barkalov, K .E. Uzakbaev)

3.2.4. Information system on security of schools and preschool educational organizations (A.V. Zubovich, D.A. Mandychev)

3.2.5. Data Platform for Disaster Risks in Kyrgyzstan (M.M. Jantaev, A.V. Zubovich, D.A. Mandychev, S.S. Barkalov).

CHAPTER 4. CAPACITY BUILDING AND SCIENTIFIC COOPERATION

4.1. Scientific cooperation (L.Y. Joldubaeva, A.Sh. Ainabekova, Ch.Sh. Zhaparkulova, A.A. Meleshko)

4.2. Capacity building (L.Y. Joldubaeva, A.Sh. Ainabekova, Ch.Sh. Zhaparkulova, A.A. Meleshko)

PREFACE

History of CAIAG foundation

According to the history research an international organization like the Central-Asian Institute for Applied Geosciences (CAIAG) was not founded suddenly as indicated Doctor W.Michajljow and Professor Ch. Reigber , but emerged from close cooperation of researchers from Germany and scientists from the Central-Asian countries, with the goal of implementing joint research projects.

In the early 90s of the last century the director of Department 1 “Kinematics and Dynamics of the Earth” of the German Research Centre for Geosciences Potsdam (GFZ), Prof.Ch.Reigber, suggested his colleagues from Kazakhstan, Kyrgyzstan, Uzbekistan and Russia to establish a network of GPS control points for monitoring recent deformations and movements of the Earth's crust in this region and to coordinate the joint activities in project named “Central Asian Tectonic Sciences (CATS)” (Figure 1a).

In 1992 the first 40 control points were installed and surveyed on the territory of Kazakhstan, Kyrgyzstan and Uzbekistan after having signed initial agreements with three institutes of the Russian Academy of Sciences –Research Station IVTRAN (U.A.Trapeznikov), the Institute of Geoecology (V.I.Makarov), the Institute of Astronomy (S.K.Tatevyan) - and with the Institute of Geological Sciences and Seismology of Ministry of Education and Science of Kazakhstan (A.K. Kurskeev), the Geodesic Service of Kyrgyzstan (V.G.Tzurkov) and, the Institute of Seismology (K.N. Abdullabekov) and Institute of Astronomy (T.S.Yuldashbaev) of the Academy of Sciences of Uzbekistan.

Results from this first GPS observation campaign in Central Asia were presented already in autumn 1992 at the IAG International Symposium “Geodesy and Physics of the Earth” in Potsdam (Reigber et al., 1993).

In 1994 a final collaboration agreement between GFZ, IVTRAN and the Geodetic and Cartographic Services of Kazakstan, Kyrgyzstan and Uzbekistan was signed with an addendum that State Cartography Service of Tajikistan (M.C. Ishanov) would join this activity. In the same year in addition to a re-survey of the existing GPS-points, additional control points were installed and measured in the Northern Pamir and the Tajik depression [1, 3].

In 1995 to 1996 the GPS network was extended to 90 markers over an area of 1200 x 1800 km in the region, including 8 points around the Tarim basin, established in collaboration with the National Bureau of Surveying and Mapping (J.Y.Chen) of PR China [6].

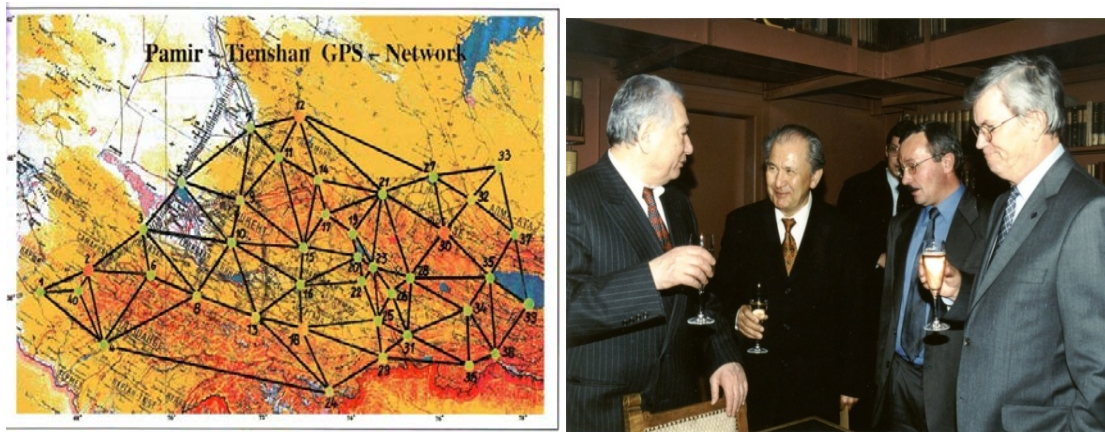
This network of GPS stations was re-surveyed in the time period between 1995 and 1998 and the related data analyses enabled to quantify the distribution of deformation within the seismically active Tien Shan and North Pamir region and the ongoing rotation

PREFACE

of virtually undeformed tectonic blocks, such as the Tarim and Fergana. (Reigber et al., 1999, Reigber et al., 2001) [2, 3, 5-9].

In 1995, within the CATS project, the GFZ Potsdam in collaboration with the Institute of Seismology NAS KR started activities on studying paleo-seismology of the Tien Shan. Expeditions to Suusamyr valley were conducted and area of Talas-Fergana fault and some areas of Inner Tien Shan were investigated.

The next year this kind of works was carried out in Alai valley, and then in the northern spurs of Kyrgyz range. Finally, in 1999 paleo-seismic-dislocations of the northern part of Issyk-Kul basin had been studied.



a.

b.

Figure 1. a. GPS observation network in Central Asia.

b. Documentary photograph: discussion of strategy of CAIAG foundation, left to right: world-famous writer and ambassador of Kyrgyzstan in the Benelux countries Ch.T. Aitmatov, the ambassador of Kyrgyzstan in Germany doctor A.D. Djumagulov, doctor W.Michajljow, Professor Ch. Reigber.

These studies became a valuable addition to GPS-network results, enabling to identify the location, intensity and frequency of major seismic events in the Tien Shan during past few thousand years (Chedia et al., 1997; Michel et al., 2000, Chedia et al., 2000; Korjenkov et al., 2006) [5, 7, 10].

In 1997 it was decided to supplement and expand the research activities in Central Asia by acquiring modern satellite remote sensing data. On the basis of an agreement between the Ministry of Emergency Situations (MES) of the Kyrgyz Republic, the German Research Centre for Geosciences Potsdam (GFZ) and the German Aerospace Center (DLR) a mobile 4m dish RS satellite receiving station was established in 1998 near Bishkek in the Vinsovhoz village, in the area of the Kyrgyztelecom relay station. This station received information from satellites with radar sensors (ERS-1, ERS-2 and RADARSAT), as well as from satellites with optical sensors (LANDSAT-5, SPOT-1 etc). Specialists of DLR and GFZ were involved in this work. From the Kyrgyz side specialists

PREFACE

of MES and Kyrgyz Geodesy had been specially trained as operators on this mobile station.

The next year according to an agreement with the Ministry of Defense of the Republic of Uzbekistan the station continued its operation in Kitab town in Uzbekistan. For the first time in Central Asia satellite RS data, received from the European radar satellites ERS-1 and ERS-2, were preprocessed using a quick-look Synthetic Aperture Radar (SAR) data processor on a powerful computer, producing accurate calibration of the data [8]...

Finally processed radar and optical data provided valuable information on the surface dynamics and endogenous geological processes on the territory of Central Asia, which, in turn, served as basis for the creation of a database in this field.

It also provided an opportunity to carry out an areal monitoring of mass movements, occurring in connection with catastrophic events, such as earthquakes, landslides, mudflows, avalanches, glaciers etc. That is, to significantly complement pointwise GPS-derived information of such events.

In 1998 GFZ decided to study within the CATS project the impact of modern tectonics and crustal deformation on the occurrence and distribution of landslides in the region. To do this, researchers of the GFZ (U.Wetzel, S.Rössner) together with colleagues from MES KR (B.Moldobekov, A.Sarnagoev, V.Ponamarev) started to study landslides in the mountain chain of the Fergana valley [3 – 6, 11].

In august of the same year the first field works in the Maily-Suu, Jalal-Abad, Osh area, and further in Gulcha and Sary-Bulak had been carried out. In the following years until 2004 specialists of MES KR (Sh.Usupaev, H.Ibatulin and A.Meleshko) from the Kyrgyz side had actively participated in these works [4 - 6].

From 1999 until the end of CAIAG's history period several expeditions on this subject to the Fergana valley were been carried out, and a good number of scientific papers was published (Roessner et al., 2000; Wetzel and, Roessner, 2000; Xia et al., 2000, Roessner et al, 2006) [4, 10-12]. In general, utilization of new research technologies as GPS, SAR-interferometry (ALOS and TeraSAR X), and broadband seismic stations led to a breakthrough in understanding the formation of landslide structures and primary characteristics of their occurrence. In addition, in the course of these activities digital databases were developed not only on landslides, but also on geological and tectonic conditions of the described region.

At a meeting on February 19, 1999 with the former Prime Minister of the Kyrgyz Republic J.Ibraimov, Prof. Ch.Reigber gave a report on these already implemented projects and the numerous contacts with geoscientific institutions in the region and expressed the need and interest for the creation of an international geoscientific institute in Central Asia.

Stimulated by further contacts with Kyrgyz governmental organizations and subsequent negotiations with a number of interested organizations in Kyrgyzstan, GFZ Potsdam in collaboration with the Center for International Development (ZEU) of the Giessen

PREFACE

University and with representatives of the Ministry of Emergency Situations of the Kyrgyz Republic developed a concept paper for the establishment of a Central-Asian Institute for Applied Geosciences (CAIAG). This document, written in German and Russian languages and available in its final version in July 2001 (GFZ, 2001), was a compilation of initial deliberations on main directions of research, organizational structure and initial financing for such an institute.

In the time frame 2001-2002, between the Government of the Kyrgyz Republic and the GFZ Potsdam the basis for concluding a cooperation agreement on the foundation of the institute was established.

On March 5, 2002, during his state visit of Germany the former President of the Kyrgyz Republic, A.Akaev, together with the world-famous writer and ambassador of Kyrgyzstan in the Benelux countries Ch.T. Aitmatov, the ambassador of Kyrgyzstan in Germany A.D.Djumagulov and further representatives of the Government of Kyrgyzstan had visited the GFZ in Potsdam (Figure 1b).

During this visit a Memorandum of Intent to found the Central-Asian Institute for Applied Geosciences (CAIAG) in Bishkek was drawn up. President A.Akaev thanked the chairman of the GFZ Executive Board Prof.R.Emmerman by saying: "Foundation of such geo-scientific institute is a valuable gift in the "Year of Mountains". For us it is a great honor that the institute will be located in our capital city Bishkek".

In October 2002, the final Cooperation Agreement on the establishment of CAIAG was signed by the Kyrgyz government and the GFZ Potsdam, coinciding with the Global Mountain Summit, conducted under the auspices of UNESCO from October 29 to November 1, 2002 in Bishkek.

In October 2002 the CAIAG Steering Committee, appointed by the Cooperation Agreement to deal with all current affairs on the initial establishment of CAIAG, met for the first time in Potsdam. The SD consisted of an equal number (5) of representatives from Kyrgyzstan and Germany: from the Kyrgyz side the director of the Institute of Geology NAS KR Prof.A.B.Bakirov, the director of the Institute of Water Problems and Hydropower NAS KR Prof.D.M.Mamatkanov, the director of the National Geodetic Survey KR Dr.V.E.Tsurkov, the director of MES Monitoring Center Dr.B.D.Moldobekov, the ambassador of KR in Germany Dr.A.D.Djumagulov; from the German side the director of the Institute of Geography of the Giessen University Prof.E.Giese, the director of the Center for International Development of the Giessen University Prof.H.-R.Hemmer, the director of the Dept. 1 of GFZ Potsdam Prof.Ch.Reigber (Chairman of the Steering Committee), researcher of the Dept.1 of GFZ Potsdam Dr.H.-U.Wetzel.

In November, 2002 the two first co- directors of CAIAG were appointed: by the Government of the Kyrgyz Republic Dr. B.D.Moldobekov, by the Board of GFZ Potsdam Prof.Ch. Reigber.

From 2003 to 2004 the Steering Committee had another three meetings in Bishkek and Potsdam to discuss, develop and recommend outlines for the charter of CAIAG, the

PREFACE

institute's structure and main directions and priorities of research, its governing bodies, the staffing and salaries requests and the provision of a modern working environment.

In accordance with the obligations of the Cooperation Agreement the Government of the Kyrgyz Republic provided in autumn 2002 a two building complex in Timur Frunse street 73/2 on long-term lease for the institute.

The official hand-over by representatives of the Kyrgyz government took place on October 31, 2002 in the administrative building №1. In the sequel, in 2003 by order of GFZ Potsdam, a technical documentation for total renovation of building №1 was prepared and delivered by "BishkekProject" bureau.

In May 13, 2004 CAIAG received from the Ministry of Justice of the Kyrgyz Republic the certificate of state registration of the legal entity with registration № 21388-3300-PF (IS).

On May 17, 2004- as amendment of the "Cooperation agreement" from 29.10.2002, and approved by Regulation №720 of the Government of the Kyrgyz Republic, dated 14.11.2003- the Foundation Treaty on founding the Central-Asian Institute for Applied Geosciences in the legal form of a non-profit organization as Fund was concluded between the Government of the Kyrgyz Republic and GFZ Potsdam. O

In June 2004 a contract on the renovation services was signed with the «Neman» company, winner of the open call for tenders. On June 17, 2005 the State Commission on Construction of KR had accepted the renovated building.

INTRODUCTION

In the preface of the book shown the history of the Institute's foundation, where the Founders of the new CAIAG research organization considered it necessary to realize the idea of the need for cooperation between scientists and politicians in solving social problems for ensuring sustainable development of Central Asian countries.

In the developed concept of the Institute, priority areas are: the development of an interdisciplinary network for the environment monitoring, climate change, water problems, geodynamics and geo-catastrophes, and increasing research capacity.

In the CAIAG Strategy one of the main principles of applied research is the creation of multi-purpose monitoring networks and assessment of changes in the natural environment, installation of modern geophysical, geodetic, glaciological, seismic, and meteorological stations in Central Asia. In this regard, the Institute's strategy is aimed at: carrying out complex studies of socially important problems in disaster risk prevention, water resources management and adaptation to climate change, providing scientifically based support to decision-making communities in Central Asia.

Priority directions of applied geosciences of CAIAG are: 1. Processes of global changes negatively affecting the Environment. 2. Monitoring and assessment of disasters (multi-hazard approach), disaster risk prevention (multi-risk) and early warning methods. 3. Applied interdisciplinary studies of water balance and cycle, glacier researches, land use assessment, the impact of active use of water resources on the Environment. 4. Developing the potential of education and socially-oriented programs.

CHAPTER 1. GEODYNAMICS AND GEORISKS

1.1. Preliminary geological and geophysical research of Sary-Djaz River basin

1.1.1. Selection of the study area and geological development of the area

The area of the Sary-Djaz River basin is 10.700 km². Its average annual discharge is known only for the upper part at the inflowing Kuylyu River and is 42 m³/s [Mamatkanov *et al.*, 2006]. Taking into account that downstream major tributaries flow in the Sary-Djaz river such as Enilchek, Uchkel, Akshiryak, Dzhangart, Kayindi, Kuyukap and Maybash, which are fed by the largest glaciers in the Tien Shan, we assume that the average annual water flow is at least 120 m³/s, whereas the flow on Naryn River at the site of Toktogul hydropower station is 475 m³/s [Mamatkanov *et al.*, 2006]. Thus, the study area represents about 20% of water resources of Kyrgyzstan.

It is quite obvious that geological zonation should not coincide with the area's hydrography; therefore the geological study area should be a bit wider and cover all tectonic units which are present in the Sary-Djaz river basin. Eastern bound of the study area is the Meridional ridge with the peak of Khan Tengri in its southern part. The Khan Tengri plexus of mountains is the eastern bound of the Central Tien Shan. Further to the east we find the Halyktau ridge of the Eastern (Chinese) Tien Shan. The northern boundary of the study area goes along the marginal fault which separates Terskei Ridge from Issyk-Kul and Tekes hollows. The western border is open and provisionally extends along the watershed between the Sary-Djaz and Naryn river basins. The southern boundary subsequently goes along Kipchak Fault between Kokshaal Ridge and Tarim Hollow. The total study area is 15 000 km² (**Figure 1.1.1**). Seismological data were taken within the coordinates 41° - 43° in latitude 77.5° - 80.5° and in longitude in order to cover the location of existing GPS-observations points.

At the territory of the Kyrgyz Republic there are few published data. Study of this region's neotectonics, is essentially limited by the work of Schultz S.S. [1948] and preliminary geological and geophysical studies carried out during seismic risk zoning of the territory in 1981-85 [Knauf, 1988]. It is quite obvious that just the general tectonic zonation was highlighted in these works. At that time there was no methodology for study of active faults and isotopic dating of Cenozoic complexes. In recent years there was just one publication dedicated to stratigraphy of Sary-Djaz Pliocene-Pleistocene deposits [Charimov, Fortuna, 2007].

There is much better situation with the unpublished data presented as reports in the archives of the State Geological Agency of the Kyrgyz Republic. First of all, it is the report on geomorphology and Cenozoic stratigraphy of that region in a scale of 1:500 000 [Turbin, 1966]. Besides, in this area medium-scale geological surveys were carried out in which the data on the recent tectonics must be reported [Grishchenko, 1985; Severinov, 1994; Chernov, 1993].

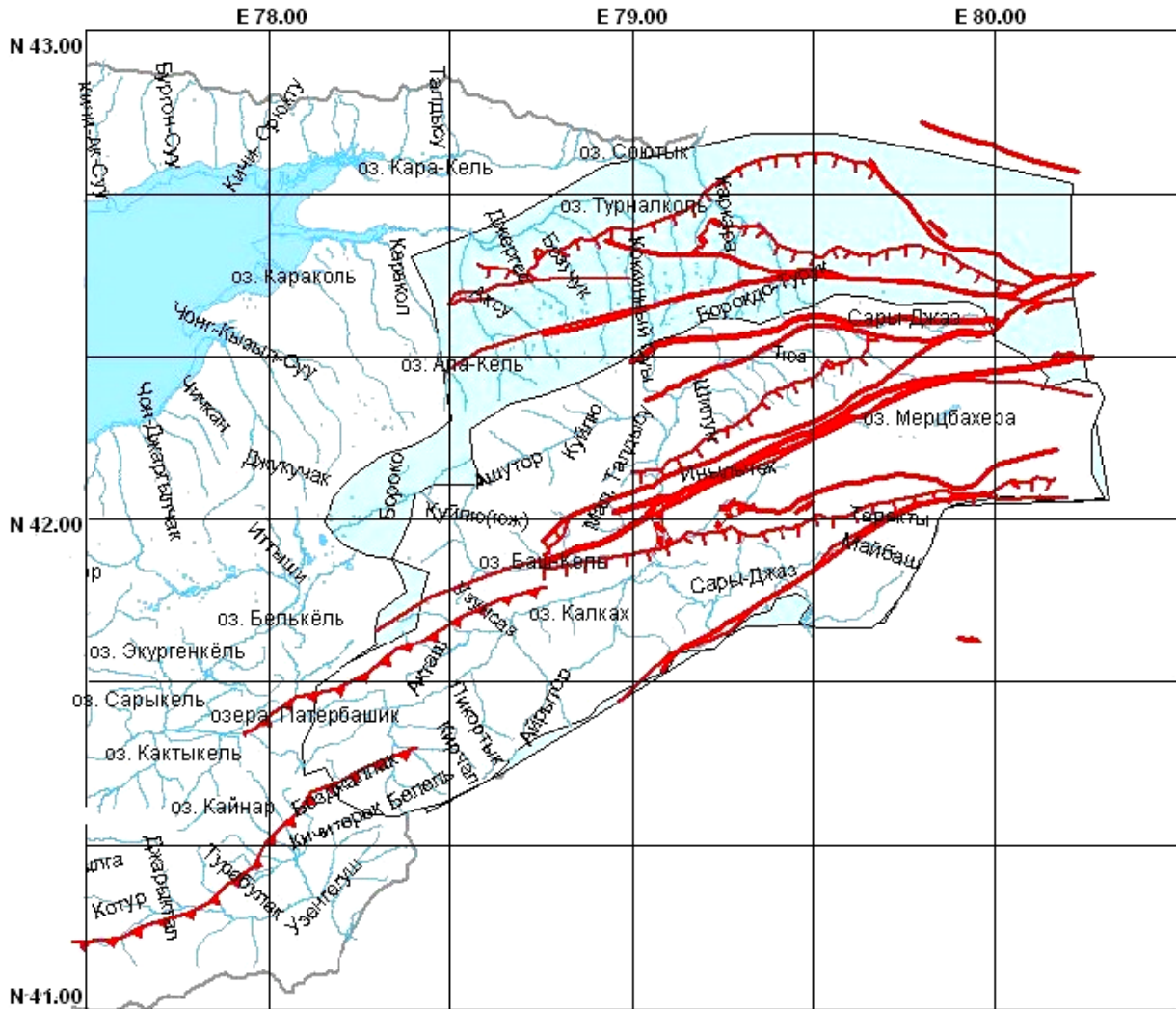


Figure 1.1.1. Study area

1.1.1. Description of geomorphology, regime of recent movements and dangerous natural processes related to them

The main elements of pre-recent structure of Sary-Djaz area are Caledonides of Northern Tien Shan, Caledonides-Hercynides of Middle Tien Shan and Hercynides of Southern Tien Shan, separated by deep faults – Nikolayev line and Atbashi-Enilchek regional faults.

This zoning is reflected in the modern structure, as well. Within the Northern Tien Shan, East Terskey mega-anticline is located. Within the Middle Tien Shan Mountains, there is Kuylyu-Sary-Djaz mega syncline and adjacent from the south meganticline of the same name. Complexly built folded structures of the Southern Tien Shan in the newest structure are divided into three parts: Enilchek-Kainda, Kuyukap and Kokshaal.

East-Terskei meganticline occupies the northern part of the area where there are two types of fold groups: north-western Terskei horst-anticline and north-eastern Ashutor

CHAPTER 1. GEODYNAMICS AND GEORISKS

horst-anticline. The indicated structures have southern asymmetry – low-lying northern and steep southern wings. The amplitude of the total uplifts reaches 3750-4500 m. The identified two fold groups on the meridian of the Upper-Sary-Djaz hollow are separated by a low (3500-3750 m).

Kuylyu-Sary-Djaz megasyncline has a northeast strike. Its most distinguished part's axis – Upper Sary-Djaz graben synclines – forms a gradual curve convex to the north. From the west to the east mega syncline extends from Kyulyu Transfer to lower reaches of Adyrtoz River. Total amplitudes of the latest movements within the discussed structure vary from 2500 m in the axial part up to 3250 m in the west wing. From the south, the mega syncline is bound by Kuylyuk fault and the eastern branch of Sary-Djaz Fault. The latter has a southern low; the amplitude of uplift of its hanging wing reaches 400-900 m.

Kyulyutau-Sary-Djaz meganticline consists of four horst-anticlines. In the western part, the meganticline is broken by a chain of breaks, with the amplitudes of displacement on them up to 100-150 m. Total amplitudes of elevations of this block ranges between 3500 and 4700 m.

From the south, the considered mega anticline is bound by Atbashi-Enilchek Fault being an active deep seam in the latest time. The amplitude of relative shifts of the fault's wings reaches 900-1300 m. In terms of regime of movement, the area under consideration is included to the domain of sustainable newest uplift. Total velocity of uplifting for the entire latest stage is estimated at tenths of mm /year; for the Quaternary period of 1-2 mm / year.

Modern high-relief area formed by the latest movements leads to the development of dangerous natural disasters such as landslides, mudflows and avalanches. Sary-Djaz River basin includes areas of different degree of mudflow hazard. Areas with potential mudflows from 100 to 1000 m³/s are located on the right bank of the upper reaches of Ak-Shiyrak and Baralbas Rivers, in the left bank of the upper reaches of the Sary-Djaz river, on the left bank of Uch-Kul River and the upper reaches of the Kuyukap river. Areas prone to possible mudflows of 10 to 100 m³/s cover the body of the Enilchek glacier and middle mountain parts of the Sary-Djaz River basin. Mudflows with volume up to 10 m³/s are possible in the low mountain and valley parts of Sary-Djaz River basin and its tributaries.

Avalanches are also among the natural hazards in the study area. Within the relatively small and isolated areas along the Sary-Djaz river valley at the place of confluence with Kuylyu River, near the village of Enilchek, as well as along the right and left banks of Ak-Shiyrak River, avalanches occur only in snowy years with volume of up to 500 m³. Areas located in low and, rarely, in the mid mountain parts of Sary-Djaz, Kuylyu, Ak-Shiyrak and Baralbas river banks, are characterized as prone to potential avalanches timed less than 1 time in 10 years, with a maximum volume of 10 thousand m³. Within the remaining areas of medium and high altitudes, excluding the area occupied by the Enilchek glacier, avalanches occur from 1 to 10 times in 10 years, from 1 to 5 avalanches running on 1 km of the valley floor, with the maximum volume of 10 to 100 thousand m³.

1.1.2. Seismicity of the area and surface movements

The main document used for description of seismicity of the area is the catalogue of earthquakes by the Institute of Seismology, National Academy of Science of the Kyrgyz Republic (IS) which was created on the basis of published data (for the period of time since 250 B.C. to 1961) and their own instrumental observations (since 1962). The extract from the catalogue for the study area was provided to us by the IS in accordance with the cooperation agreement. The full information (listed without gaps) in this catalogue are available for the strongest ($M \geq 6.5$) earthquakes since around 1800, for events with $M \geq 5.5$ - since 1865, with $M \geq 4.5$ - since 1929, with $M \geq 3.3$ - in 1955 and, finally, from the mid-1970s, after the establishment of a regional network of seismic stations, the catalogue becomes representative for events with $M \geq 2.2$ [Djanuzakov *et al.*, 1977].

For the monitoring of surface movements a network of GPS-stations was installed by CAIAG. In this report data from three permanent GNSS-stations located in the marginal parts of the study area were used. These stations are Merzbacher-1 (MRZ1), Taragai (TARA) and Kerege-Tash (KRGT) (**Figure 1.1.2**). All stations are equipped with GNSS-receivers Topcon GB-1000. Observation data are automatically transferred to CAIAG where they are processed with the help of Gamit/Globk programs (MIT, USA).

The view of the area seismicity is given by the map of earthquake epicenters (**Figure 1.1.2**). Epicenters of strong ($M \geq 5.5$) earthquakes from ancient times till 1980s are shown by black asterisks. For the period of 1981-2013 the epicenters of all recorded earthquakes are shown.

The frequency of occurrence graph (see **Figure 1.1.3**) shows that the earthquakes of $M \geq 2.5$ are representative for this sampling. Epicenters of earthquakes of different energy ranges are shown on the map in different colors to more clearly emphasize the characteristics of their location. Thus, one can see that the strongest earthquakes ($M = 5-6$), marked on the map in pink and as black asterisks, for a period of about two thousand years occurred only in the edge parts of the study area, bounding the Sary-Djaz river basin from a part after entering the territory of China. From the northwest, Sary-Djaz River basin is limited by a line of earthquake epicenters, known as the South-Issyk-Kul section of North-Tien Shan seismic active zone [Djanuzakov *et al.*, 1977; Knauf, *ed.*, 1988]. The strongest earthquake within this seismically active zone happened in 1970 - Sarykamysh earthquake, $M=6.8$, $l_0=8-9$. In the south-east of the study area there is South Tien Shan (Hissar-Kokshaal) seismic zone [Djanuzakov *et al.*, 1977; Knauf *ed.*, 1988]. The strong earthquakes took and take place here. For example, Kokshaal earthquakes - 1969 ($M=6.6$, $l_0=9$), 1971 ($M=6.1$, $l_0=8$ points), 1987 ($M=6.1$), 2005 ($M=5.5$). In the middle of the area one can clearly see a line of epicenters (red) of earthquakes of $M=3.3-4.4$ with south-west strike, known as the Central Tien Shan seismic zone. It is characterized as relatively weakly active [Knauf, *ed.*, 1988]. Referred by Djanuzakov K.D., 1915, $l_0=8$ Kokshaal earthquake within this zone belongs to a class of earthquakes, the epicenter of which is determined with an accuracy of more than 50 km. By this reason, it is difficult to talk about its affinity to this area. The interest is presented by the epicenter lines of weak ($M \leq 3.3$) earthquakes of the north-western

strike (transverse to the above seismically active zones) – Akshiyarak and Sary-Djaz lineaments [Knauf, ed., 1988]. Within Sary-Djaz lineament there is Sary-Djaz river midstream representing a big interest in terms of the planned construction of hydraulic structures. The detailed study of seismic hazard in the eastern part of the territory of Kyrgyzstan was carried out by scientists of IS [Knauf, ed., 1988]. The result of fault-plane solutions analysis was interpreted as follows [Belenovich and Bagmanova: Knauf, ed., 1988].

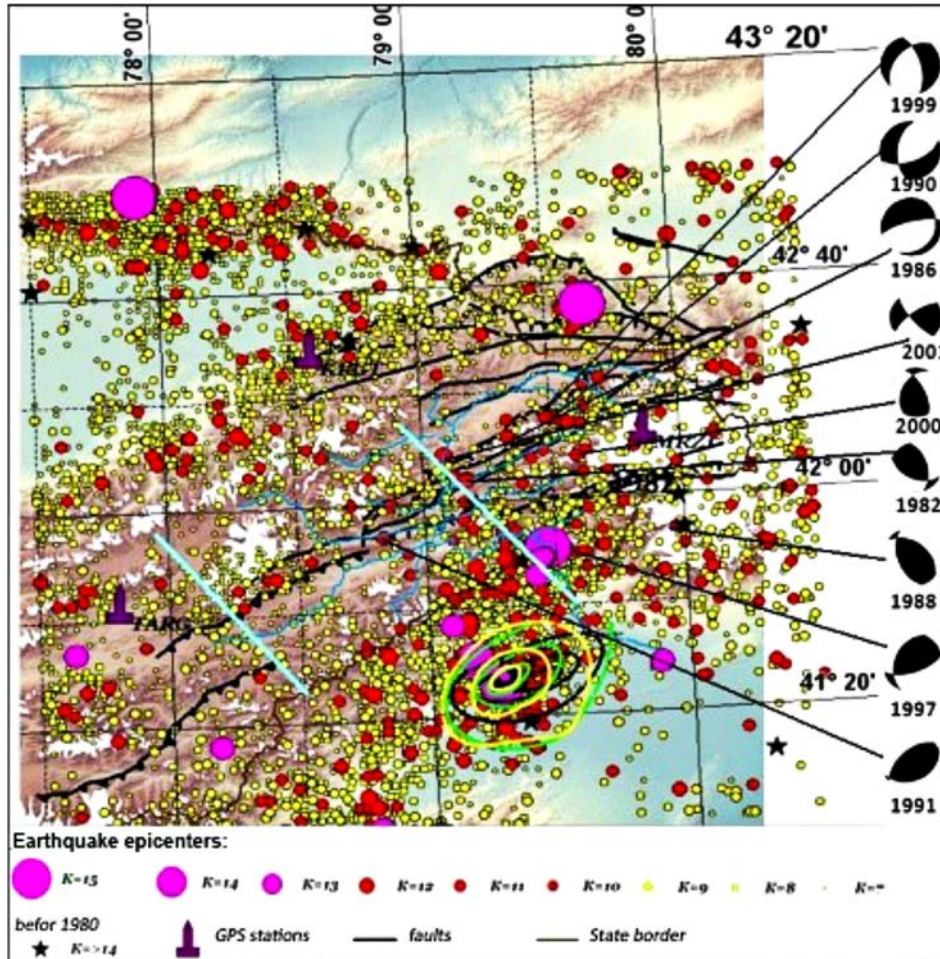


Figure 1.1.2. Map of earthquake epicenters for 1981-2013. Mechanisms of the earthquake sources are according to the Yearbook “Earthquakes in Northern Eurasia” and isoseismic lines of Kokshaal earthquakes according to [Djanuzakov et al., 2003]: 1969 ($M = 6.6$, $I_0 = 9$) – in black, 1971 ($M = 6.1$, $I_0 = 8$ points) – in green and 1987 ($M = 6.1$) – in yellow. Blue lines indicate the boundaries of the blocks according to [Knauf, ed., 1988]. $K = 1.8 M + 4$.

The area of the Sary-Djaz river basin is divided into three regional blocks, the boundaries of which go along Akshiyarak and Sary-Djaz lineaments. In earthquake sources within the western and eastern blocks uplift-slip motions occur under the influence of near-horizontal sub-meridional compression (i.e. directed across the strike of geological structures); mass movement is directed to the north. The central block is in turn subdivided by the Kuyukap fault into separate sections. To the north of the fault in earthquake sources oblique-normal motions occur with the direction of movement to the east. In the areas bounded by the Kuyukap fault, type of motions in earthquake sources becomes different and the direction of movement changes to the west. Furthermore, if

within the whole central block near-vertical position of the compression axis is observed, in the range of the Kuyukap fault it changes to the horizontal position. These facts give reason to characterize the Kuyukap fault as a shear boundary of the latitudinal strike. The authors also note that according to the data on weak earthquakes in the central block the unstable nature of the signs of the first displacements is observed.

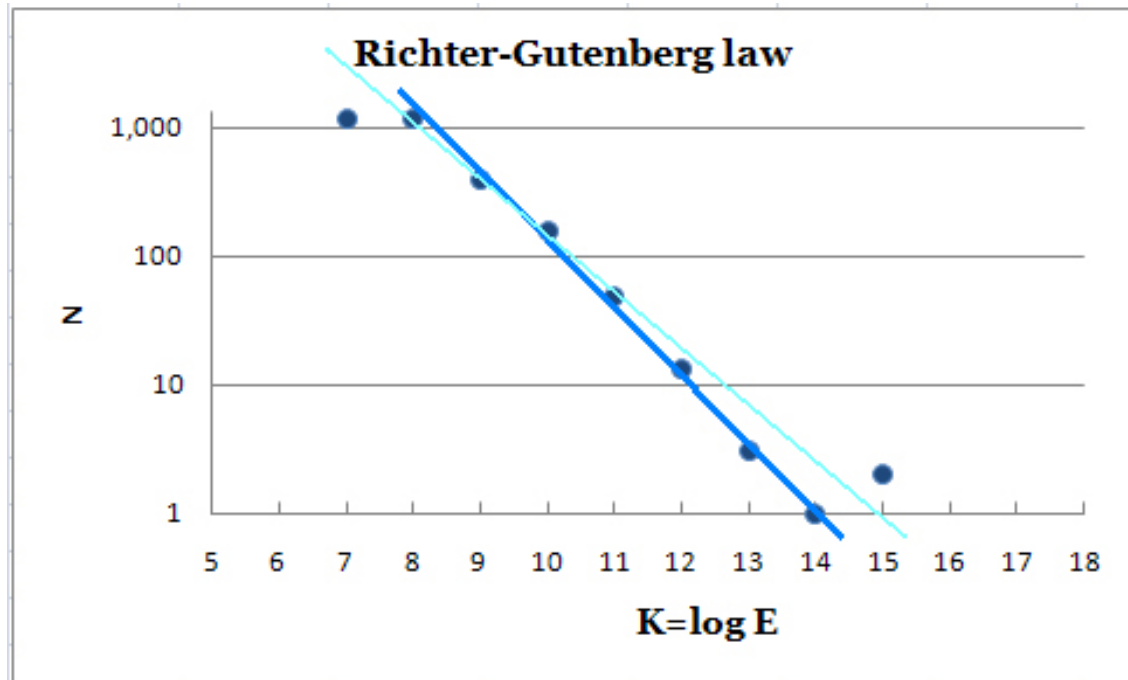


Figure 1.1.3. Recurrence graph for 1981-2013

Let's compare these findings with the observation data for latter years, 1986-2013. **Figure 1.1.2** shows the available data on mechanisms of earthquake sources with $M \geq 4$. It is possible to visually determine areas of uplift (within Sary-Djaz lineament), normal (the eastern end of the Central Tien Shan seismic active zone) and oblique-slip motions (to the south of Kuyukap Fault, even within the South Tien Shan seismic active zone). For more information about the movements in earthquake sources one can refer to findings of macroseismic surveys of big events. Isolines of the three Kokshaal earthquakes with intensity $I_0 = 8-9$ in the South Tien Shan seismic active zone in 1969, 1971 and 1987 are evidences of seismic movements along major geological structures of the South Tien Shan seismic active zone, whereas to the north uplift motions occur in a northerly direction.

All the complexity of the nature of the movements in the study area is clearly demonstrated by an earthquake on February 14, 2005, which occurred near the junction of Sary-Djaz lineament with Southern Tien Shan seismically active area (**Figure 1.1.4**). The peculiarity of this earthquake is that it was preceded by a series of foreshocks, the strongest of which occurred approximately one month before the future main shock, 17 km north-west from it [Djanuzakov *et al.*, 2011]. Aftershocks of this earthquake within the first two weeks filled the space between the main shock and the abovementioned foreshock. **Figure 1.1.4** shows that the mechanisms of sources of the foreshock, the main shock and strong aftershock that occurred in 11 hours, practically coincided

indicating that the same type of motions in the focal zone extended to the north from the main shock. But then aftershocks went in the north-eastern and south-western direction from the main shock. And after one month they occurred only along the line of the north-eastern strike.

Focal mechanism solution of the strongest aftershock in this series (**Figure 1.1.4**, top) shows that uplift movements were replaced by normal and sub-meridional direction of movements changed to near-latitudinal, in agreement with the direction of stretch of isolines (**Figure 1.1.2**) of the above three Kokshaal earthquakes.

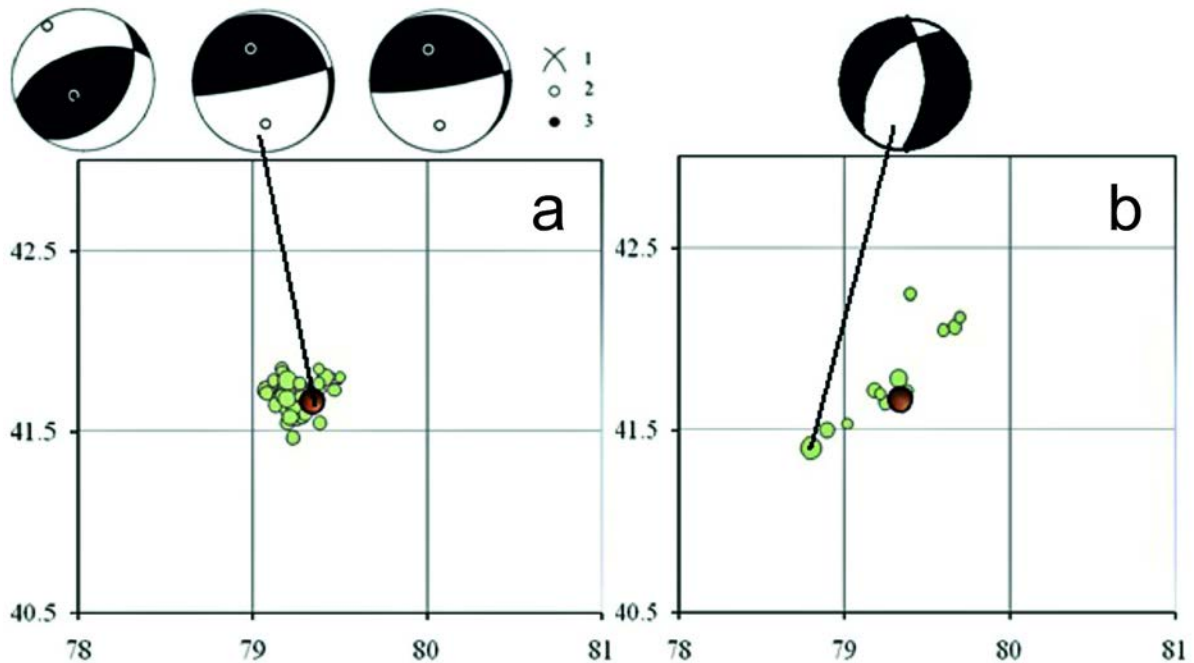


Figure 1.1.4. Mechanisms of sources of the Kokshaal earthquakes

Top: focal mechanisms of the foreshock, the main shock and the strongest aftershock of earthquake February 14, 2005 ($M=6.1$), which occurred the day after the main shock (left) and strong aftershocks that occurred two and a half months after the main shock (right). Below: The epicenters of aftershocks that occurred within the first month (a), and after two months (b) according to [Djanuzakov *et al.*, 2011]. Brown circle shows the epicenter of the main shock.

These data are generally consistent with the conclusions made by [Knauf, *ed.*, 1988] on the complex picture of the seismic deformation of the study area, and in particular, within the Sary-Djaz lineament. However, the analysis shows that within this transverse zone (Sary-Djaz lineament) in historical time there were no strong ($M>5$) earthquakes. The devastating events begin at the point of junction of this structure with the South Tien Shan seismically active area on Kuyukap fault. In the work by [Knauf, *ed.*, 1988], this section is defined as the North Kokshaal seismogenic zone with potential events of $M=6.6-7.0$.

CHAPTER 1. GEODYNAMICS AND GEORISKS

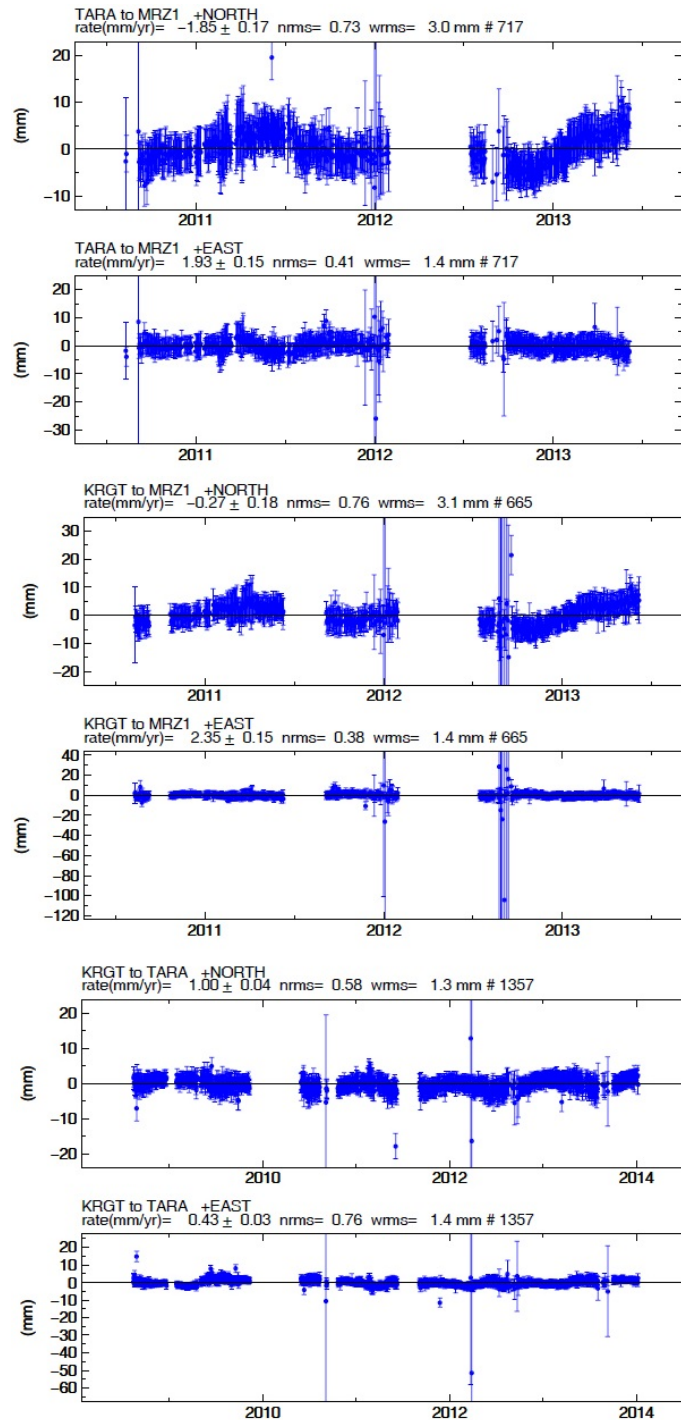


Figure 1.1.5. Northern and eastern elements of the changes of the baseline length between the stations of Taragai, Merzbacher-1 and Kerege-Tash

According to the observation data from GNSS stations, time series of changes in the lengths of the horizontal components of the baselines between stations were constructed (**Figure 1.1.5**). Analysis of changes in baseline length of the Keregetash station relative to the Taragai station (**Figure 1.1.5**) shows that the northern component of the velocity of baseline length change is about ~ 0.5 mm/year. Eastern component - even less - about 0.1 mm/year. This is a very low velocity at a level of error, although the distance between stations is more than 100 km. Such velocity suggests that the stations are arranged in a massif which now behaves as a single unit.

CHAPTER 1. GEODYNAMICS AND GEORISKS

Analysis of the location of the Kerege-Tash station relative to the location of the Merzbacher-1 station (**Figure 1.1.5**) shows a component-wise change. Here velocities are not high either, although somewhat higher than in the previous case, 1.16 and -2.54 mm/year - respectively the northern and eastern parts. The values of the velocity component and the relative locations of the stations indicate that KRGT in relation to MRZ1 is slightly shifting to the south-east.

During GPS-observations (June 2010 – December 2013) between Taragai and Keregetash stations there were no earthquakes of representative class. While between Merzbacher and Kerege-Tash stations there were two earthquakes with $K=9$ and seven earthquakes with $K=8$, i.e. rather weak events. Nothing is known about the direction of movement in the focuses of these earthquakes, because there are no data on the mechanisms of their sources. If we assume that the nature of the movements within the specified time is maintained, then we can consider the above data on focal mechanisms (see **Figure 1.1.2**) for the last 10-20 years. Then it is obvious that the GPS-data on surface movements are in good agreement with the data on earthquakes on a qualitative level. **Figure 1.1.2 shows** that between KRGT and MRZ1 stations there are series of faults within the Central Tien Shan seismically active zone. In the earthquake sources occurring within the area normal, strike-slip and oblique-slip motions take place. To evaluate the quantitative ratios it is required to accumulate data.

Conclusions:

- The study area is mostly composed of ancient Paleozoic rocks. To assess the risk of dangerous geological processes, additional geophysical surveys are needed, as well as field work in conjunction with the use of methods of remote sensing and determining the absolute age of rocks;
- The middle flow of Sary-Djaz River is located within Sary-Djaz lineament within which historically there were no strong ($M > 5$) earthquakes. Strong earthquakes occur to the south, near the junction of Sary-Djaz Lineament with the Kokshaal seismically active area along Kuyukap Fault, where Sary-Djaz River goes to China;
- According to data on earthquake source mechanisms and the results of the macroseismic surveys of severe earthquakes, it follows that in the area of Sary-Djaz river exit into China the geological environment is in a complex stress state. This is evident in the difference between types of movements in earthquake sources on opposite sides of the river bed, as well as to the north and south of Kuyukap fault. Moreover, in the epicentral areas of strong earthquakes there may be rupturing deformations extending in different (mutually perpendicular) directions;
- Despite the short period of observation, there is a qualitative agreement between the observation data obtained using the methods of GPS and seismology, which may indicate a predominance of brittle fractures in the area.

1.2. Landslide dynamics survey

1.2.1. Landslides Tatyr, Gulcha, Mailisu and Minkush

The mountain relief prevails at the territory of the Kyrgyz Republic that at foothills with widely spread abundance of loosely bound clay and loess deposits from the Quaternary to Mesozoic conditions for numerous landslides are composed. Their study is very important for developing forecast methods of landslide processes and measures to reduce the damages caused by landslides to objects of human activities ^[1].

One of CAIAG's projects under which landslide surveys have been implemented is the project called "Landslide survey with ground observation methods and remote sensing techniques (in the pilot area of upland framing of Fergana Basin, northern and inner Tien Shan)". The purpose is to study the main factors and mechanisms of the formation of typical landslides in key areas and to identify the functioning and evolution trends of the landslides in order to develop landslide behavior forecast methods and risk management measures. The basic methods of survey are the interpretation and analysis of satellite imagery using special software and GIS technologies, field topographic measurements of morphometric features of landslide bodies using GPS and tacheometers, the study of movements of ground control points (**Figure 1.2.1**), the laboratory testing of soil and groundwater, and finally the analysis of archived data on key factors of landslide formation.



Figure 1.2.1. Field studies of landslides near Gulcha, Mailisu and Minkush towns

During the project, collection and analysis of archived information was performed with regard to geological, lithological, hydrogeological, geomorphological characteristics of four landslides located in the area of Mailisu, Gulcha, Minkush towns and Bishkek city (**Figure 1.2.2**). At the same time, preliminary field studies were conducted during which morphometric and topographic parameters of landslides were measured through measurements by GPS devices "Timble 4000 SSE" and "Topcon GB-1000". Also, geological and hydrogeological conditions of main landslides were specified: "Koi-Tash" landslide near Mailisu, "Gulcha" landslide near Gulcha, "Tuyuk-Su" landslide near Minkush, and "Tatyr" landslide near Bishkek. The location of the landslides is shown on **Figure 1.2.2** (see **Google Maps**) following the link:

<http://maps.google.com/maps/ms?ie=UTF&msa=0&msid=203965682782791499971.0004bf200bad00f222237>.



Figure 1.2.2. Location of studied landslide areas



Figure 1.2.3. Pieces of satellite images with the locations of the landslides

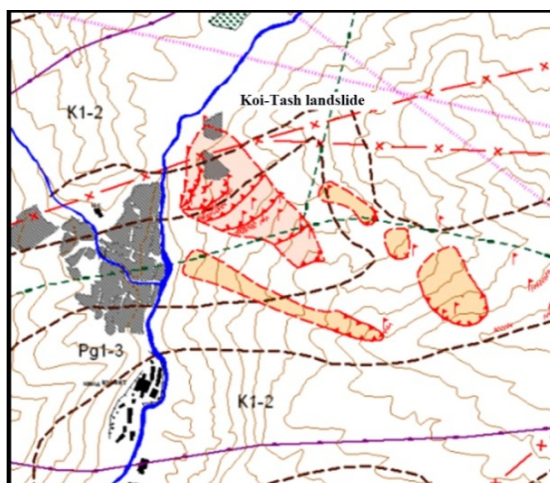


Figure 1.2.4. GIS map of Koi-Tash landslide area

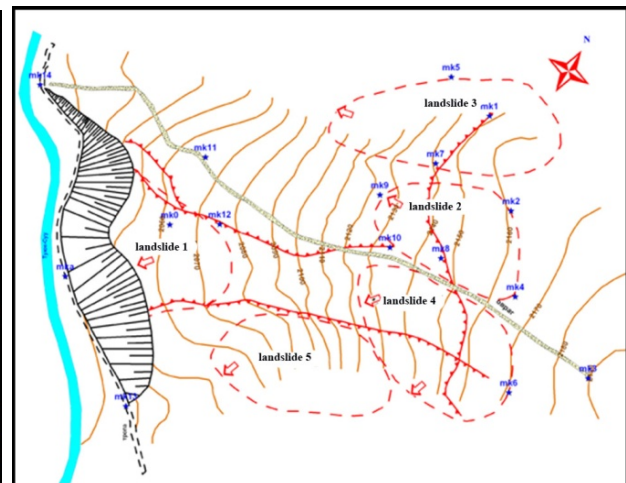


Figure 1.2.5. GIS map of Tuyuk-Suu landslide area

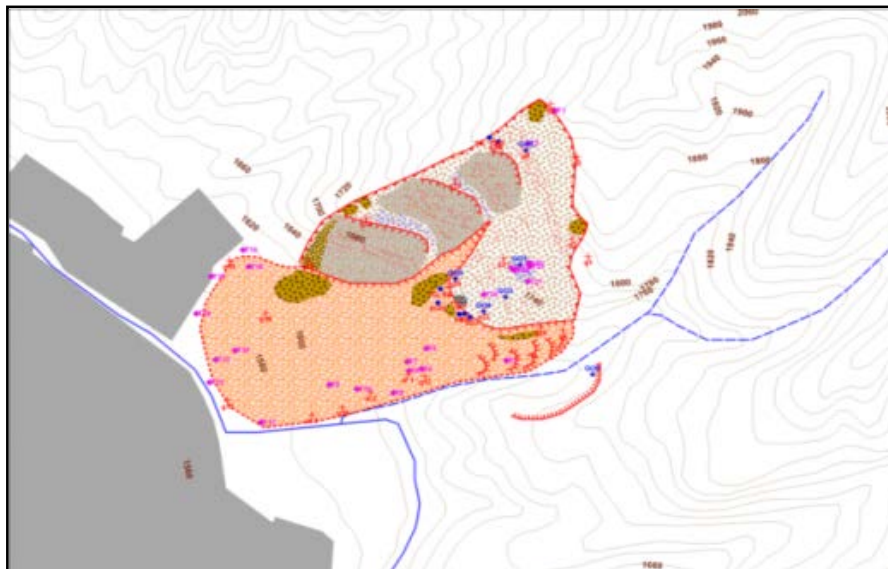


Figure 1.2.6. GIS map-scheme of Gulcha landslide



Figure 1.2.7. Quick Bird satellite image sensor: Figure 1.2.8. 3D view of the "Tatyr" landslide QB02, date: 13/07/2002, received from Google Earth server, of the Koi-Tash landslide with elements of interpretation.

According to the results of decoding high resolution satellite images (**Figure 1.2.7**), the morphometric parameters of the landslides and their contour maps in GIS MapInfo were specified (**Figures 1.2.3, 1.2.4, 1.2.5, 1.2.6**). The Landslide type as well as the mechanism of the landslide development were determined according to the morphology, lithological composition and dynamics of development, taking into account key factors climate and geology. Currently, a qualitative model of each landslide with some quantitative characteristics was established. The most likely causes of landslide activation were defined and preliminary conclusions on the most probable development of the landslides were drawn.

Within the project detailed studies are carried out on the "Tatyr" landslide (**Figure 1.2.8**). The "Tatyr" landslide (Chon-Kurchak) is located 30 kilometers to the south of the city of

Bishkek on the left bank of Alamedin River, 3 km north-east of Chon-Kurchak village. It was formed on the rocks of Suluterek and Shamsi suites in the Paleogene and Neogene period. Gypsified and saline clay rocks, conglomerates and sandstones are involved in the displacement. The volume of the landslide now stands at 6.75 million m³. Activation of the landslide process is observed since 2004. At present, the landslide is practically inactive. That is diagnosed by the position of the margins of its lower part and the individual blocks of the landslide body as well as by the development of vegetation on its borders and on the edge of front barrier.

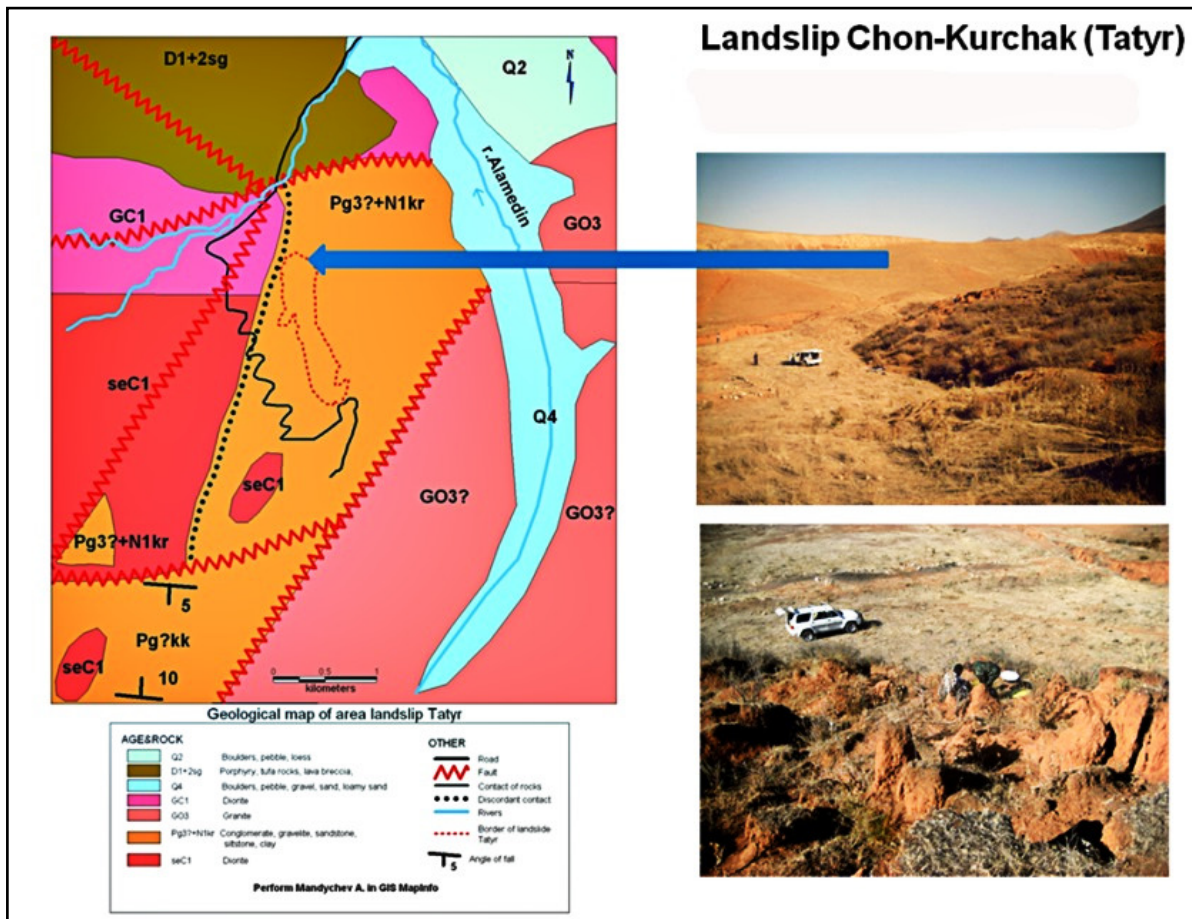


Figure 1.2.9. Map of the geological and tectonic pattern of the Taty landslide area

On this landslide a network of observation control points is shown in **Figures 1.2.10** and **1.2.11** and measurements of their coordinates and absolute height were taken by GPS Topcon GB-1000. In addition, studies were carried out on this landslide including the determination of geological conditions and GIS-mapping (**Figure 1.2.9**) and interpretation of a satellite image dated 29/09/2009, taken by the «Quick Bird» satellite and received from the «Google Earth» server with resolution of 0.6 m/pixel (**Figure 1.2.10**) and «Worldview 2» satellite image dated 27/05/2012 (**Figure 1.2.11**). The last image is presented in two options – panchromatic with resolution of 0.5 m/pixel and multispectral with a resolution of 2 m/pixel. The geographical reference error after ortho-transformation with SRTM DEM data was several meters. In the process of interpretation, the major structural elements of the landslide body, the boundaries of watersheds and the main channels of surface runoff, the tensile crack at the landslide

CHAPTER 1. GEODYNAMICS AND GEORISKS

slope and the local sites of water accumulation from precipitation on the surface of the landslide were depicted. The comparison of images obtained at different times within the period of 2.5 years allowed to identify some differences in the environment of the landslide area.

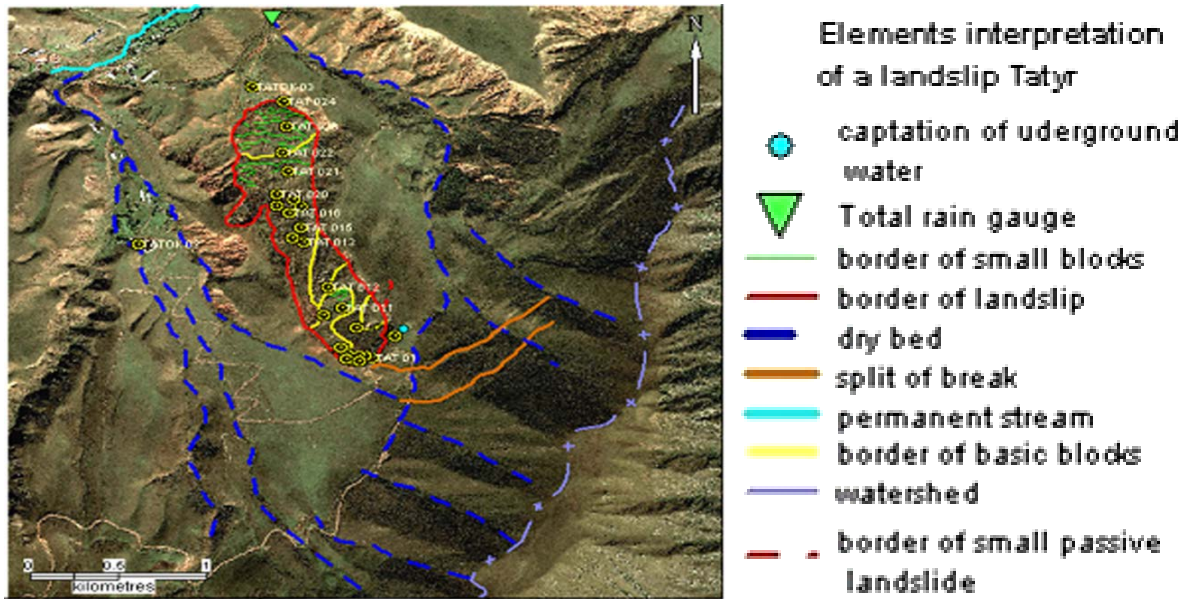


Figure 1.2.10. Quick Bird satellite image of the Tatyr landslide with elements of interpretation

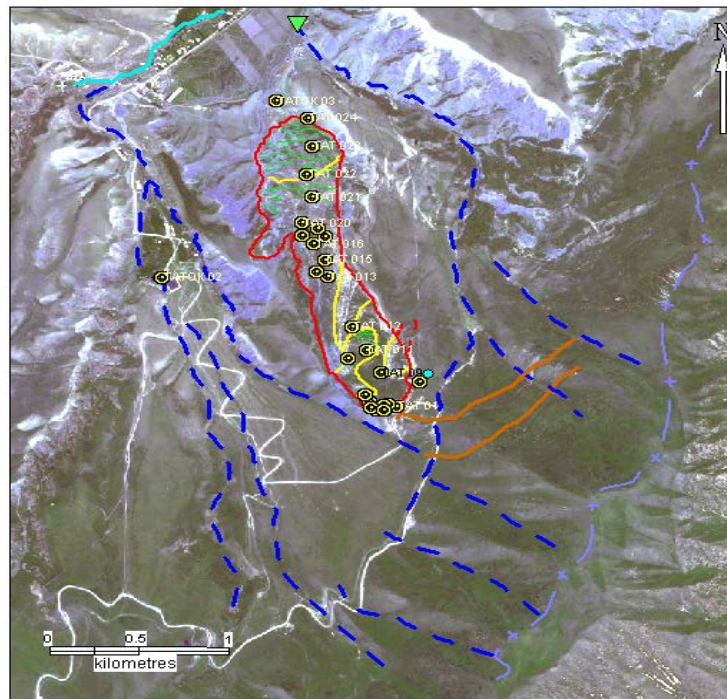


Figure 1.2.11. Worldview-2 image of the Tatyr landslide with elements of interpretation

In general, to solve the problem of improving the conditions of landslide formation and the features of its structure, it is sufficient to use the available accuracy of the satellite image geopositioning. Additional possibilities are provided by three spectral channels of the original image and the possibility of combining them to identify in more detail the different elements of the structure of the landslide. More precise studies of changes in

the geometric landslide characteristics are only possible by repeated measurements of coordinates and the height of reference points using geodetic GPS and tacheometer instruments.

To determine the general morphologic parameters of the landslide we analyzed the SRTM DEM (digital elevation model), provided on the “Google Earth”. As shown in **Figure 1.2.12**, the profile of the central part of the “Tatyr” landslide is characterized by a relatively uniform surface slope with ill-defined ledges at 400 and 820 meters from the top level of the landslide. These ledges with an altitude of 1,700 and 1,650 meters above sea level are likely to correspond with large blocks of the landslide.

The average slope of the landslide is 0.22 which corresponds to a surface inclination angle of 12.7°. This indicator is one of the most important in forecasting a possible activation of the landslide, as it is directly related to the gradient of the gravitational potential. In the present case, it is small in size, that allows to rate the landslide as rather stable according to this criterion.

To monitor the precipitation impacting the landslide, a total precipitation gauge was installed in May 2012 near the “Tatyr” landslide (**Figure 1.2.13**) for the measurement of liquid and solid precipitation. Its location is shown by **Figure 1.2.13** (see also “Google Maps”) following the link:

<http://maps.google.com/maps/ms?ie=UTF&msa=0&msid=203965682782791499971.0004db1df0a0c263d751d>).

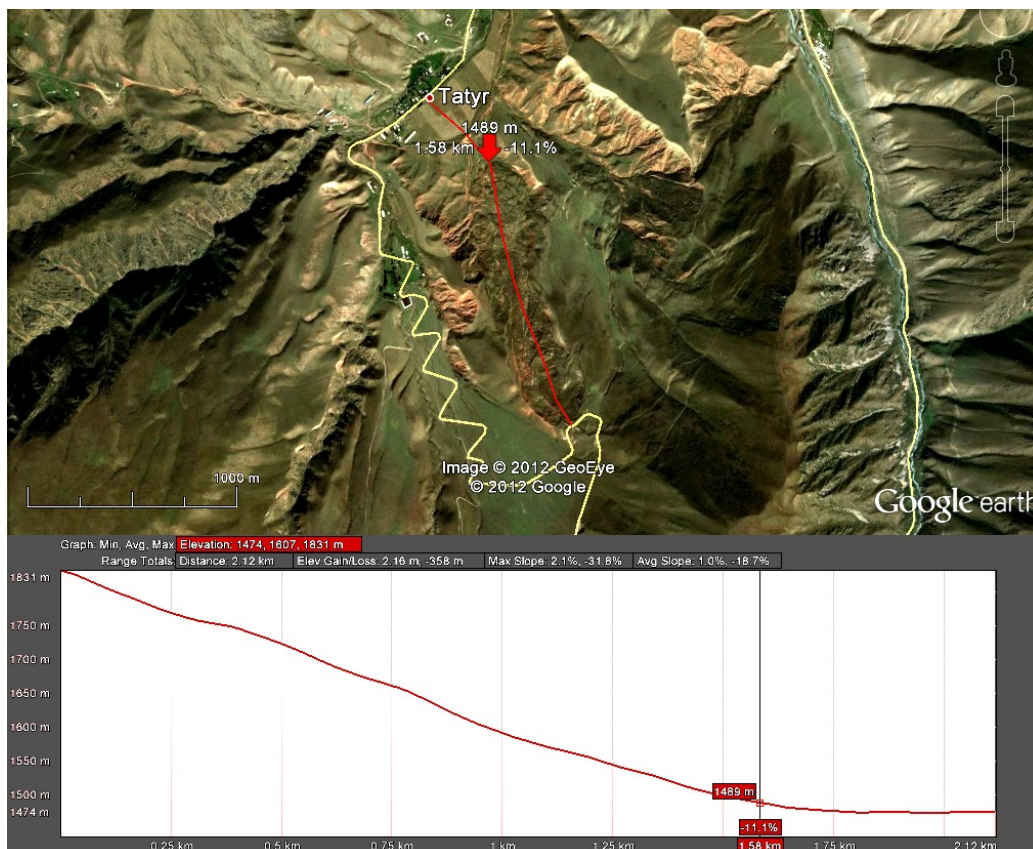


Figure 1.2.12. Profile of the central part of the Tatyr landslide

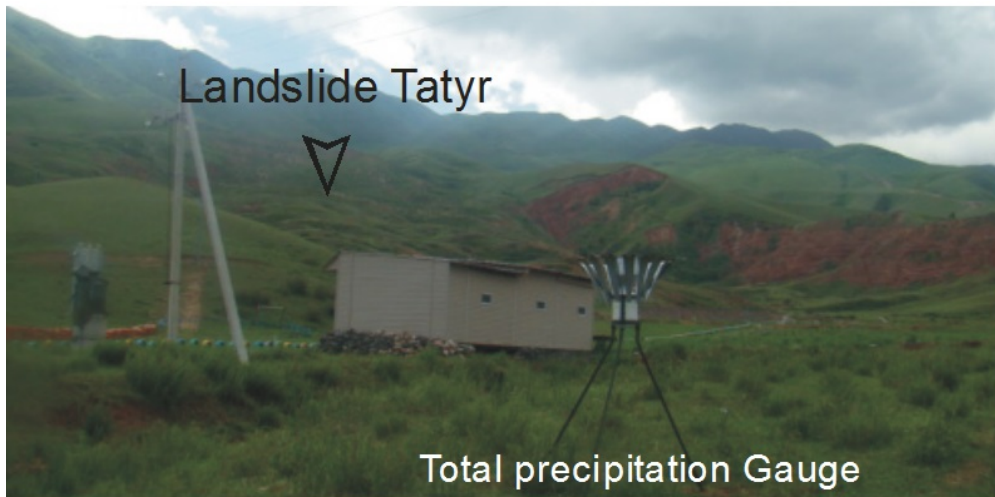


Figure 1.2.13. The total precipitation gauge located near the Taty landslide

The precipitation gauge has a wind shield, similar to a standard protection of the Tretyakov precipitation gauge, used at the moment at weather stations in Kyrgyzstan. The height of the intake from ground surface is about 2 meters and the acquisition field is 346.2 cm². Sampling frequency is once per month. **Figure 1.2.14** shows the comparison of the monthly mean precipitation for the period from 2000 to 2009 according to the Baytik weather station (alt. 1543 m) located near the precipitation gauge “Taty” (alt. 1.464 m) as well as the values measured by the precipitation gauge for 2012 and 2013. It is seen that the measured values of the precipitation gauge “Taty” in general correspond to the range and nature of changes in precipitation of the Baitik station over a period of years, which is typical for the area of Ala-Archa and the Alamedin river basins at relatively close altitudes of the area.

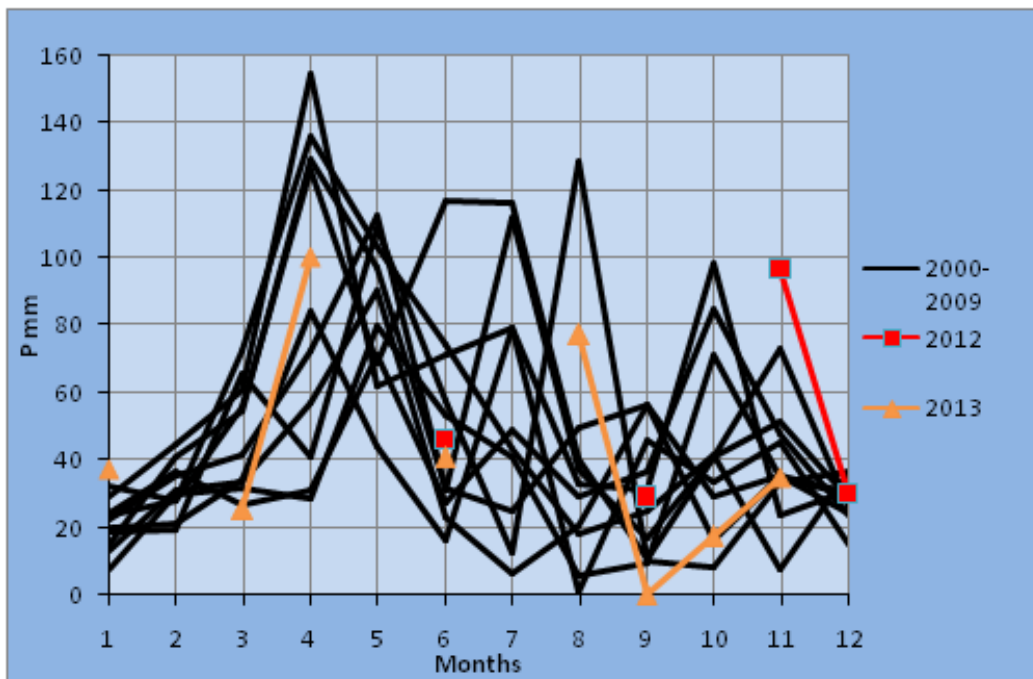


Figure 1.2.14. Precipitation recorded by the Baitik weather station for 2000-2009 and by the precipitation gauge at the Taty area for 2012-2013



Figure 1.2.15. View of site “OAU-22” near Ak-Bosogo village

Monitoring of precipitation, which is one of the key factors for the development of landslides in the “Tatyr” landslide area, allows specifying the amount of precipitation gathered in the catchment basin of the landslide. Using this information enables to develop more accurate prediction methods for possible landslide motions. In addition, it enhances the specification of meteorological parameters obtained in the network of hydro-meteorological stations in the Ala-Archa and Alamedin river basins in Kyrgyzstan, which are needed to address geotechnical, hydrological and glaciological problems.

1.2.2. Landslides in Alay district

In 2013 landslide-prone areas were examined in Uzgen and Alay districts of Osh Oblast which are included in the book “Monitoring and forecast of possible activation of hazardous processes and phenomena in the territory of the Kyrgyz Republic for 2013” and pose a threat to dwelling houses and infrastructure of settlements. The aim of these projects was to compose a single database of landslides in Kyrgyzstan and update the registry of dangerous sites. Last such work was carried out by the Geological and Hydrogeological Expedition in 1998 with the use of the topographic base of scale 1: 100 000. Preliminarily, areas of formation and propagation of landslides were identified on the previously georeferenced topographic basis of scale 1:100 000, for further research with their preparation in the form of SHP-files in the WGS-84 coordinates, KMZ. The research methodology was discussed and sources having library materials were identified. Satellite images Rapid Eye with a resolution of 5 m were acquired for decoding of hazardous locations. GPS measurements of control points were held using the methods of Rapid Static & Real Time Kinematic (RTK). Landslide-prone areas are distributed within 25 territories aiyl (village) districts. Many previously surveyed landslides were at different stages of development, and some of them required updating and continuation of monitoring surveys. During field surveys by districts 186 landslide-prone areas were described, systematized and incorporated into a single database. For all of the above areas a catalogue was created with technical documentation describing main characteristics of a landslide and slope of the landslide, as well as their typology, factors and year of formation, conditions of location, the stage

of their development, the degree of risk, photos etc. During these studies a number of thematic maps such as geological, engineering-geological, geomorphological and groundwater map were vectorized.

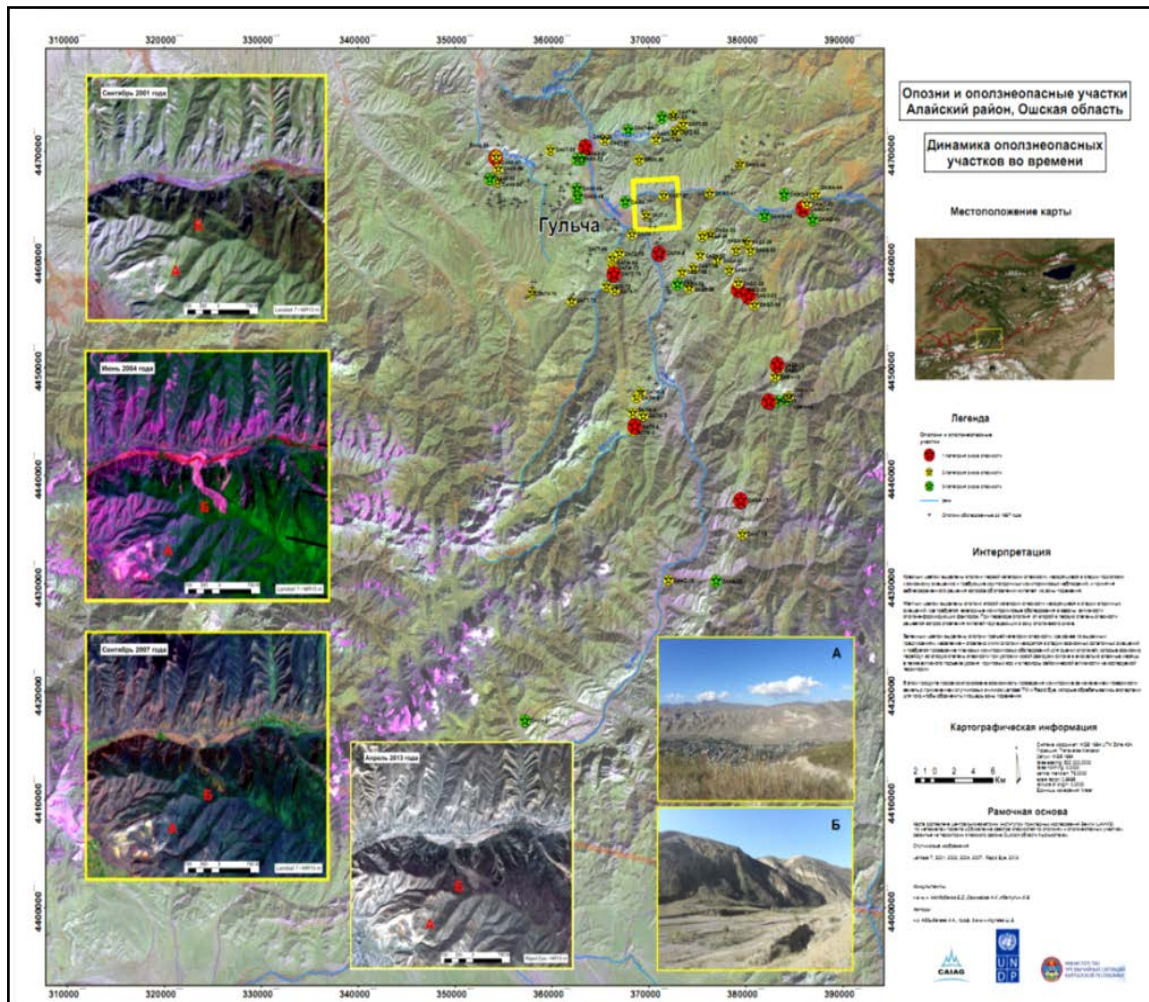


Figure 1.2.16. Final schematic map of landslide-prone areas for territory of Alay district

In 2014 works on the study of landslide-prone areas are continued for the remaining districts of the Osh province, as well as for Suzak and Bazar-Korgon districts of Jalal-Abad Oblast.

Conclusions

Based on remote sensing data, field measurements and GIS, the conditions for the formation of typical landslides as well as features of their structure and functioning were specified. At a later stage, it is planned to continue topographic measurements in the landslide areas, as well as soil sampling for the study of physical and mechanical properties, granulometric and mineralogical composition of the soils which constitute the basis of the landslide and are involved in the landslide movement process. Necessary tests will be carried out in specialized laboratories. It is also planned to conduct sampling of underground water within the areas for chemical analysis. This will allow a more complete study of the conditions of the landslide formation and the mechanism of its development.

According to the results of surveys, landslide areas were identified and mapped with geo-referencing to their localities. Based on the field research and previously studied materials, dangerous areas were analyzed and ranged, and appropriate conclusions and recommendations were handed over for further use by the Department of Emergency Situation Monitoring.

1.3. Landslides, seismicity and geodynamics of Tien Shan

Landslides are dangerous natural processes occurring on the territory of Kyrgyzstan. According to the Ministry of Emergency Situations (MES), up to 30% of the annual amount of material damage and loss of human lives accounts for landslides. Therefore, much attention is given to the study of landslides in Kyrgyzstan. For many years, in cooperation with relevant departments of MES these studies were conducted by scientific research institutes of the National Academy of Sciences of the Kyrgyz Republic: Institutes of Geology, Rock Mechanics, Seismology, and the Center for Geosciences (GFZ) in Potsdam, Germany.

Landslides are dangerous not only by themselves, but also by their possible cascade effects, such as damming rivers with the formation of ponded reservoirs, which due to natural erosion result in threat of flooding of settlements, engineering works, demolition of houses and tailings, removal of hazardous material into rivers. Therefore much of attention is paid to the individual studies of the most dangerous landslides. However, it is necessary for the successful prediction of landslide activation to understand the nature of this phenomenon as a whole, especially in its relation to other natural relief-forming processes and phenomena.

It is assumed that the main factors influencing the activation of landslides, are engineering-geological conditions and precipitations as well as the triggering impact of earthquakes. Studies of the relationship between precipitation and landslide activation in Kyrgyzstan and other parts of the world show 50-60% correlation. However, we know also examples when a landslide began to move in dry weather and independently of an strong earthquake. Triggering effects of earthquakes are usually ascertained only by the coincidence in time of these two events. A general comparative analysis of landslides and seismic activity on the territory of Kyrgyzstan has never been conducted. Research in this field was first started by the Central Asian Institute for Applied Geosciences (CAIAG) in 2009 for the territory of the Chui hollow and its surrounding mountains based on observations of the digital seismic network of KNET [*Kalmetyeva et al, 2010; Kalmetyeva & Moldobekov, 2011 (a); Kalmetyeva & Moldobekov, 2011 (b)*]. In 2011, these studies were continued for the Fergana hollow and its surrounding mountains [*Kalmetyeva et al, 2012*]. Despite the differences between these two areas in the history of development, in the underlying structure and in the nature of seismicity, we found some general regularity which gives reason to make assumptions about the nature of landslide activity.

1.3.1. Location of landslides

Northern Tien Shan (Chui Hollow and its mountainous rim)

Landslides in the Northern Tien Shan are spatially associated with the structures of recent uplifts moving onto sedimentary strata of Chui hollow and bounded in the north by a series of conjugate faults that are getting out of the Kyrgyz Range and decay in the hollow (**Figure 1.3.1**). The large landslides with more than 100 000 m³ are located along the narrow rectilinear line of sublatitudinal spread. This line is shown by the dotted line in **Figure 1.3.1**. The direction perpendicular to this line corresponds to the azimuth of 355°. This direction coincides with the direction of the compression that causes the near-latitude reduction of Tien Shan. This statement is widely accepted and confirmed by various studies, such as geomorphological studies [*Chediya, 1986 Sadybakasov, 1990, etc.*], GPS-measurements [*Zubovich et al., 2010*], and the study of the mechanisms of earthquake sources (MES) [*Ghose et al., 1998; Kalmetyeva et al., 2009, etc.*]. The work [*Kalmetyeva et al, 2009*] showed that over 50% of the earthquakes in Kyrgyzstan occur in conditions of sub-meridional compression. The maximum number of earthquakes associated with the azimuth of 355° is seen in nearly horizontal position of the axis of compression (angle with horizon varies from 0° up to 50°). Thus, we can assume that large landslides in the surrounding mountains of Chui hollow occur on the front line of a sub-meridional near-horizontal compression.

Figure 1.3.1 (**lower image**) indicates the fact that there is no distinct relation between landslide location and earthquake epicenter clusters. Another important factor is that landslides of 2002 and 2006 are spatially separated from landslides activated in 2004 as if some boundary goes along the meridian 74.9°.

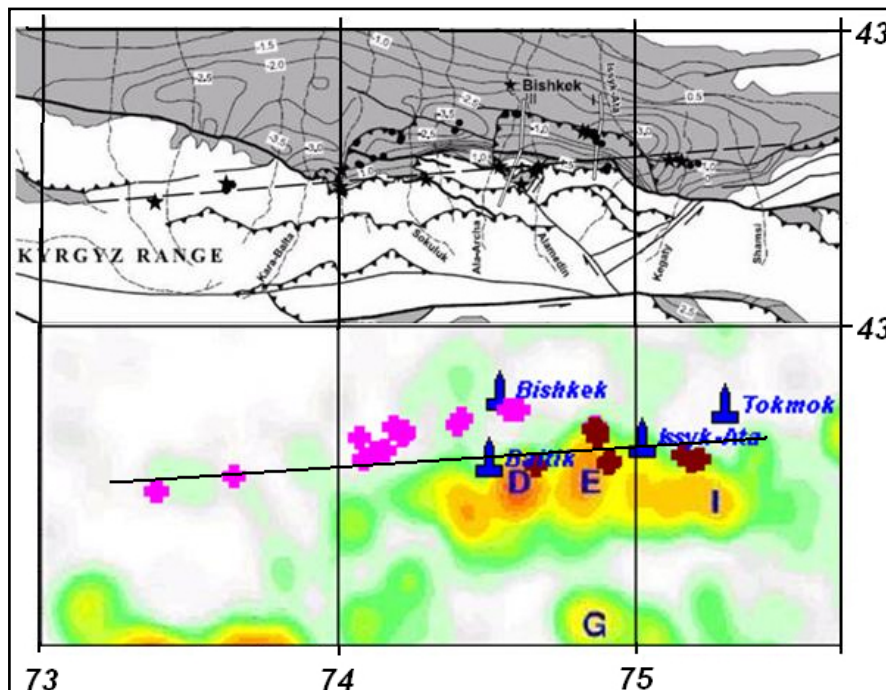


Figure 1.3.1. Neotectonic diagram (top) by [*Mikolaichuk et al, 2003*] and landslides by [*Erokhin et al, 2006*]. Ancient deposit landslides are marked with full circles, large landslides which volume exceed 100 000 m³ – with asterisks.

In fact, geological cross-sections of up to 4km depth by profiles I-I and II-II (**Figure 1.3.2**) located on different sides from meridian 74.9° are significantly different. Moreover, the location of hypocenters in clusters D, E and I, which are also located on different sides from the meridian 74.9 °, is not comparable (**Figure 1.3.4**). In cluster D and E the hypocenters occupy the range of 8-17 km depths, but in group we find two hypocenter clusters higher (5-8 km) and lower (17-25 km) of the range. Weather conditions for 2002-2006 were similar at all four meteorological posts (**Figure 1.3.1, the lower**); consequently, different precipitation couldn't be a reason for such difference in time of landslide activation.

Map of earthquake epicenters density according to [Kostyuk, 2009] (lower picture). The color shows the number of earthquakes for 1994-2006. Density values were calculated with uniform spacing of 1 km and 10 km radius of averaging. Letters refer to the densest clusters of epicenters. Pink crosses mark landslides which were intensified in 2002 and 2006, brown crosses – landslides occurred in 2004.

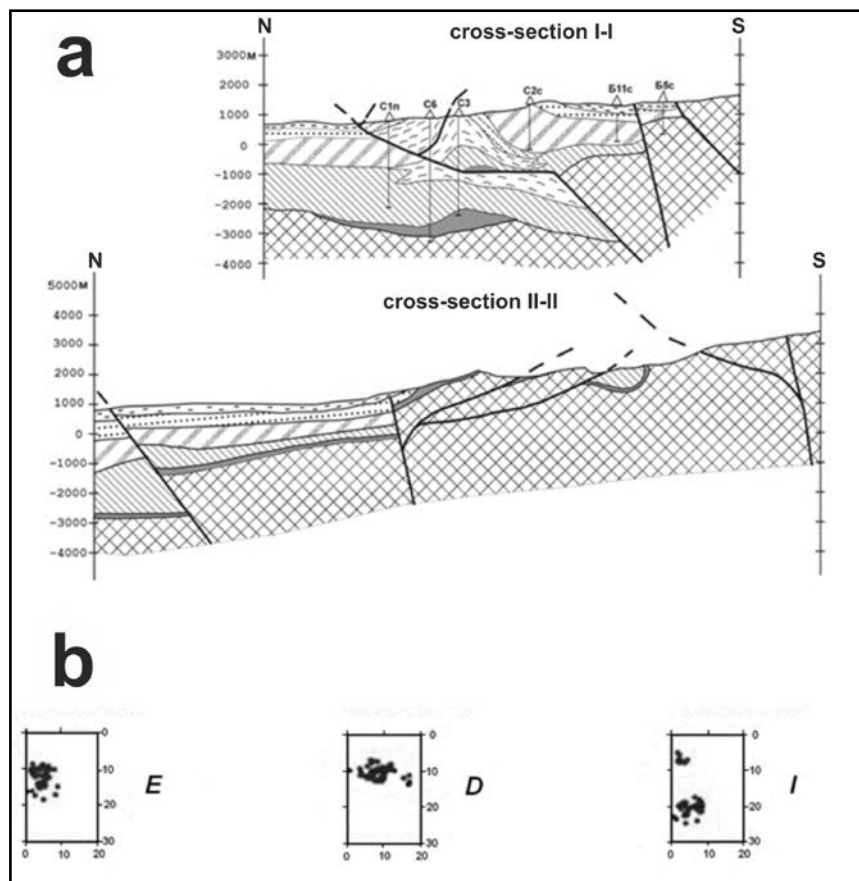


Figure 1.3.2. Geological cross-sections by profiles I-I and II-II from the work by [Mikolaichuk et al, 2003] shown on Figure 1.3.1 and latitudinal cross-sections through clusters of hypocenters E, D and I [Kostyuk, 2009].

Fergana Hollow and its mountainous frame

The territory of Fergana intermountain hollow and the surrounding mountains differs from Chui Hollow in deep structure, development history, engineering and geological conditions, and features of seismicity. As was mentioned in the work by

[Burtman, 2012]: “Kinematics of Cenozoic deformation in the eastern and northern mountain frame of the Fergana hollow is associated with the formation of Karatau-Fergana transpressive uplift, activity of Talas-Fergana fault and displacement and rotation of the Fergana hard block.”

Compared with Chui Hollow, where tectonic structures and active faults extend in parallel with Kyrgyz range, the picture here is much more complex. In the northern part of the mountain frame the tectonic zoning (border areas of permanent uplift and lowering) repeats a sketching of faults - the border of stable uplifts runs along Arslanbob Fault. In the north-eastern part these boundaries cut active faults almost at right angles (**Figure 1.3.3**). In the eastern and southern mountain frame of the Fergana hollow, boundaries of tectonic zoning again spatially coincide with the lines of active faults.

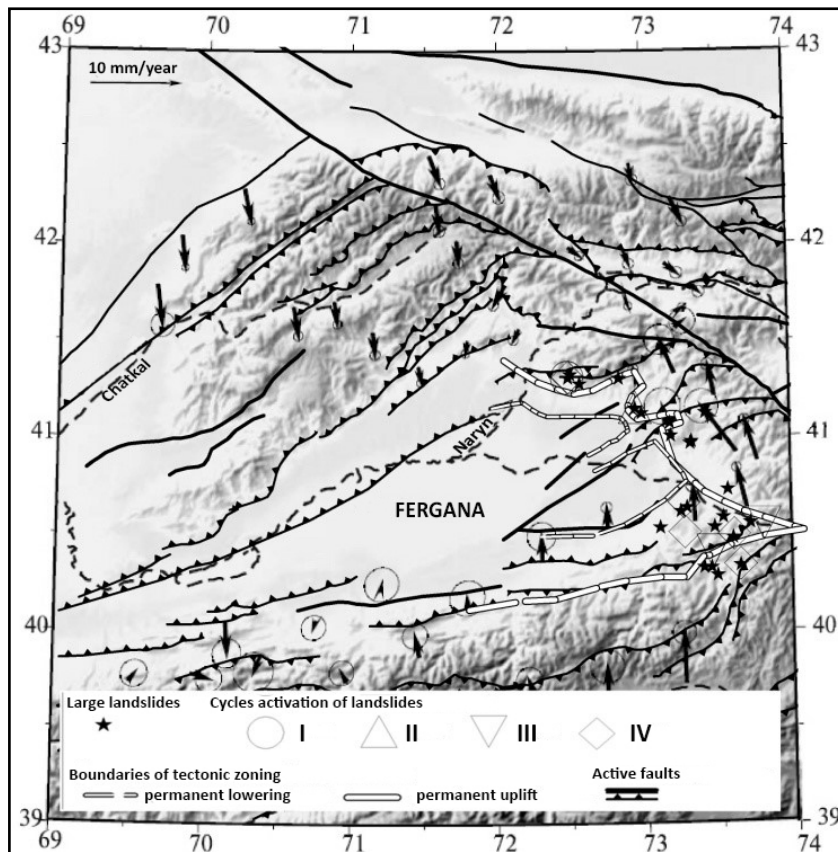


Figure 1.3.3. Vectorfield of GPS point displacements from the work by [Burtman, 2012]. The boundaries of the zones with different regime of recent movements are based on [Chediya, 1986], the active faults - according to Mikolaichuk A.V. [Kalmetyeva et al, 2009] and landslides - based on data from [Ibatulin, 2011].

Figure 1.3.3 shows that large landslides (volume of 1 million m³) like in surrounding mountains of Chu Hollow are located along a narrow line. It should be noted that in the Fergana valley landslides are considerably larger and the volume of some of them reaches 15-17 million m³. The belt of large landslides in the northern mountain frame territorially transfers on Arslanbob Fault, coinciding with the boundary of stable uplifts (Chediya, 1986). Further to the east, the belt of major landslides follows this border. In the eastern part of the hollow's border, most of large landslides are located in the area, which is characterized by Chediya (1986) as peripheral zone of intermountain hollows

presented by foothills and inner hollow lifts of 2-2.5 km height, formed in the Quaternary period in the place of the Paleogene-Neogene depression with subsidence of up to 4 km (*Chediya, 1986*). It is located between the border of stable uplift and the border of stable subsidence. There is a sharp change in the direction of the GPS point displacements from the north to north – the north-west. On the north-eastern section of the frame the direction of GPS point movement is northwest.

1.3.2. Time of landslide activation

As mentioned before, no distinct relation between the location of the landslides and the spatial distribution of earthquake epicenters was found. However, it is possible to use the data on earthquake source mechanisms to describe the stress field, namely to make an analysis of the angle between the horizon and the direction of the forces of compression. It is this parameter of earthquake source mechanisms presenting an interest, as it was previously noted that the position of major landslides are possibly controlled by the front line of near-horizontal compression. **Figure 1.3.4** shows the time-schedule of this parameter according to the data of earthquakes within the cluster D, E and I, which are the closest to the line of major landslides of mountain frame of the Chu hollow. It is clearly seen that for about 6 months before activation of landslides, which are located on the left side of the meridian of 74.9 °, in 2002 and 2006 the stabilization of horizontal compression took place. Landslide activation coincides in time with a sharp deviation of compression forces from the horizon. The same picture is observed for the landslides located to the right of the meridian of 74.9 °, which got active in 2004. Unlike areas D-E, on the area I the horizontal compression persisted longer, almost three years - since the beginning of 2001 until the end of 2003.

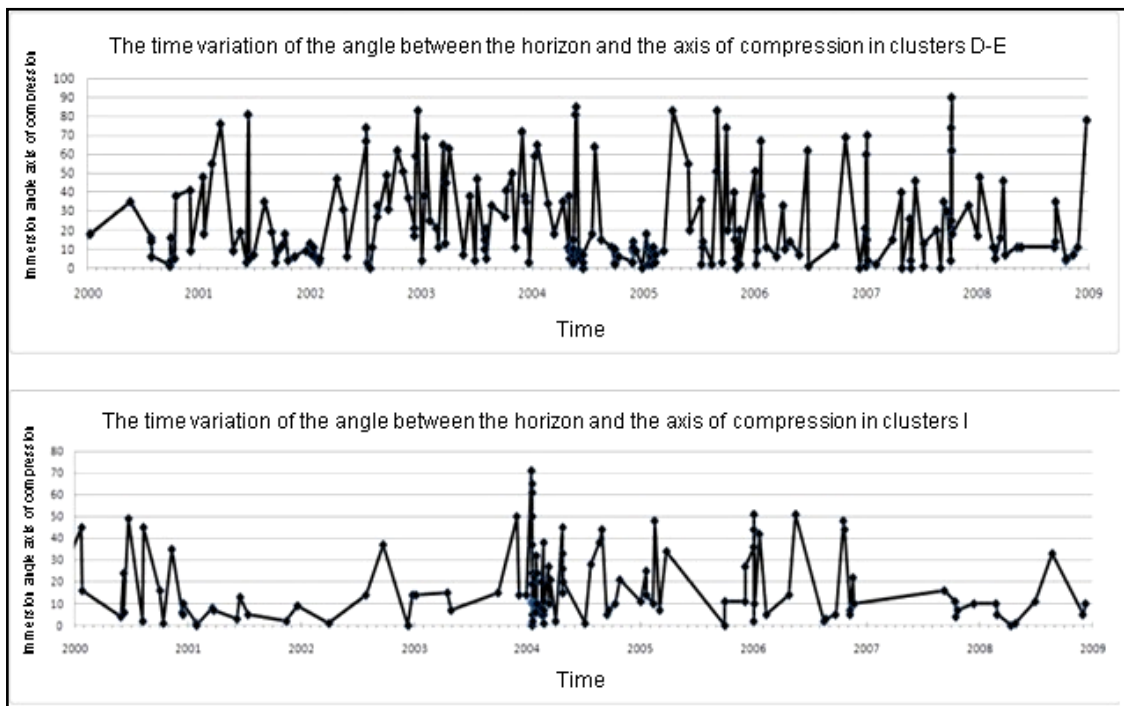


Figure 1.3.4. The time variation of the angle between the horizon and the axis of compression in clusters D-E (upper plot) and I (lower plot).

CHAPTER 1. GEODYNAMICS AND GEORISKS

On the territory of Fergana Hollow's mountain frame of the landslides also occur in cycles. *Meleshko et al.* (2002) found out four cases in the second half of the last century (**Figure 1.3.5**). The first activation of landslides began in early 1950s on the territory of Maylisay settlement on the most western end of large landslide area shown in **Figure 1.3.3**. Occurrence of multiple landslides in this area became a reason to create the landslide service in the southern part of the territory of Kyrgyzstan in 1954, and the landslide station in 1957. In the second cycle of activation landslides moved further to the eastern cycle in 1969. In the third cycle the majority of landslides occurred in the eastern part of the hollow frame. Here there was also a large number of landslides in 1993 (the fourth cycle). At the same time, in the fourth cycle, the activation of landslides took place across the whole line.

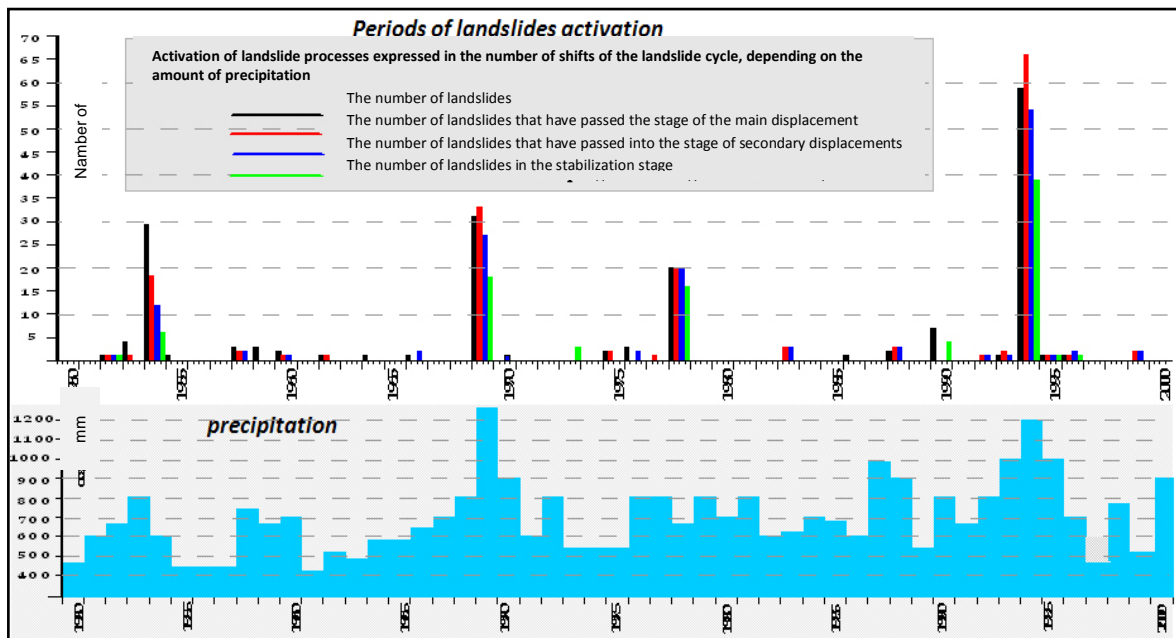


Figure 1.3.5. Time variation of the amount of activated and descended landslides (upper image) and precipitation (lower image) according to the data of works [Meleshko et al, 2002].

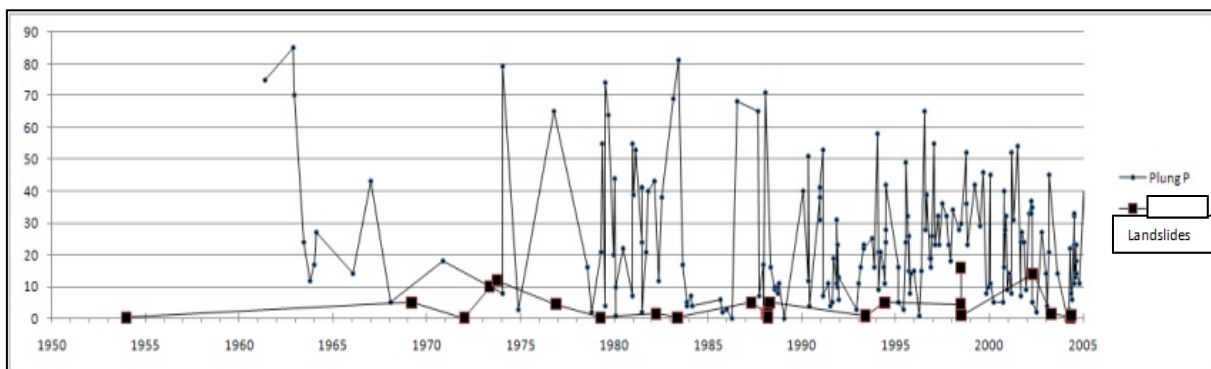


Figure 1.3.6. Time variation of the deviation angle of compression from the horizontal and the size of major landslides in million m^3 . Solutions of earthquake focal mechanisms according to [“Earthquakes in Northern Eurasia”], data on landslides by work of [Ibatulin, 2011].

Unfortunately, earthquake source mechanism solutions are systematically available only since the 70s (**Figure 1.3.6**). For earlier years such determinations were made only for

individual events. For this reason, we have no chance to track the position of the compression axis in time for the entire period. But even the data for 30 years give an idea that the direction of the compression forces does not remain constant over time (**Figure 1.3.6**). Landslides become active when the axis of compression deviates from the horizon the horizontal compression decreases and this contributes to fault displacement. **Figure 1.3.6** also gives information on major landslides. Large landslides also occur in cycles: the volume of activated landslides increases with due time, and after reaching a maximum their volume decreases again. The last of such cycles began in 1993 and after reaching a peak in 1998 finished in 2005. In 1993, two landslides of about 1 million m³ appeared: one in Maylisay, and the second – in Sary-Bulak village in the eastern part of the hollow. Both landslides occurred in the year before a significant increase in the atmospheric precipitation was measured. The mass of landslides coincide in time with a significant increase in atmospheric precipitation. At the same time, however, the compression axis angle with the horizon sharply increases. The largest landslides in this cycle (up to 17 million m³) occurred in 1998, when the amount of precipitation significantly reduced. But the graph (**Figure 1.3.6**) shows at this time an overall increase of the compression angle with the horizon. Obviously, the precipitation affected the stability of slopes covered with clay rocks. But the main effect for landslide occurrence appears to be the change of the direction of compression forces, namely, its deviation from the horizontal plane.

1.3.3. Conclusion

The results of these studies lead to the conclusion that the landslide processes are initially determined by the recent geodynamic setting. Large landslides occur within narrow linear zones which are spatially confined to the marginal parts of recent structures of uplift. Cyclic activation of landslides coincides in time with a significant abrupt deviation of the compression axis direction from the horizontal plane. Atmospheric precipitations weaken the resistance of covers on the slopes and create conditions for their slumping.

However, using data on the geodynamic setting of the region, we deal with the history of development (modes of recent movements - 20-30 million years, active faults - 10 thousand years), while landslides, that we are discussing, have intensified in the last 50 years and reflect the state of the geodynamic processes today. In order to identify locations of landslide hazards it is required to widely use such research methods as GPS, satellite images and seismic observations. **Figure 1.3.7** shows the earthquake epicenters of the top part of the seismically active stratum in the Fergana region. They form a broad belt of north-western spread. The belt of major landslides has the same spread but it forms a separate belt that does not coincide with the belt of earthquake epicenters. At the same time **Figure 1.3.8** depicts that even the smallest movements of landslide, that are recorded instrumentally, coincide in time with the occurrence of earthquake micro tremors that are recorded by seismic stations. We think that this indicates that the landslide activity and seismic activity (excluding the strong, destructive earthquakes) are independent processes caused by one and the same reason.

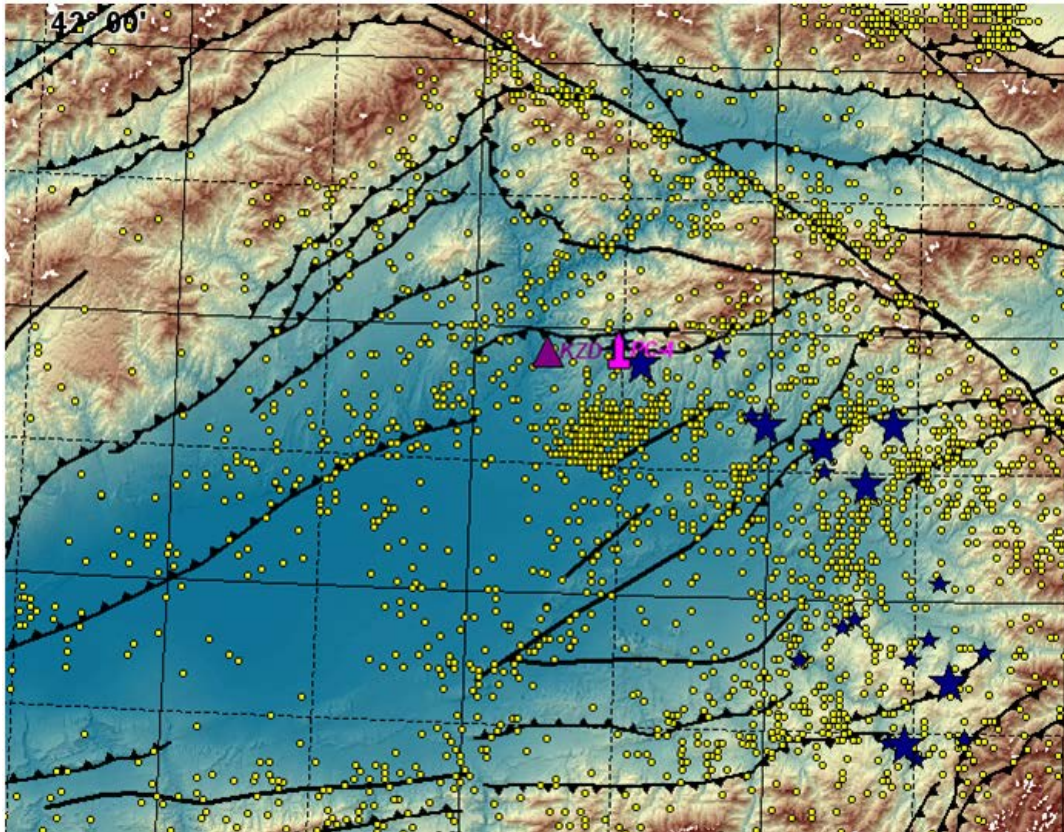


Figure 1.3.7 Map of earthquake epicenters within 1996-2010 with depth of hypocenters 0-15 km. Large mudslides are marked with asterisks according to [Ibatulin, 2011]. Active faults are set according to Mikolaichuk A.V. [Kalmetyeva et al, 2009].

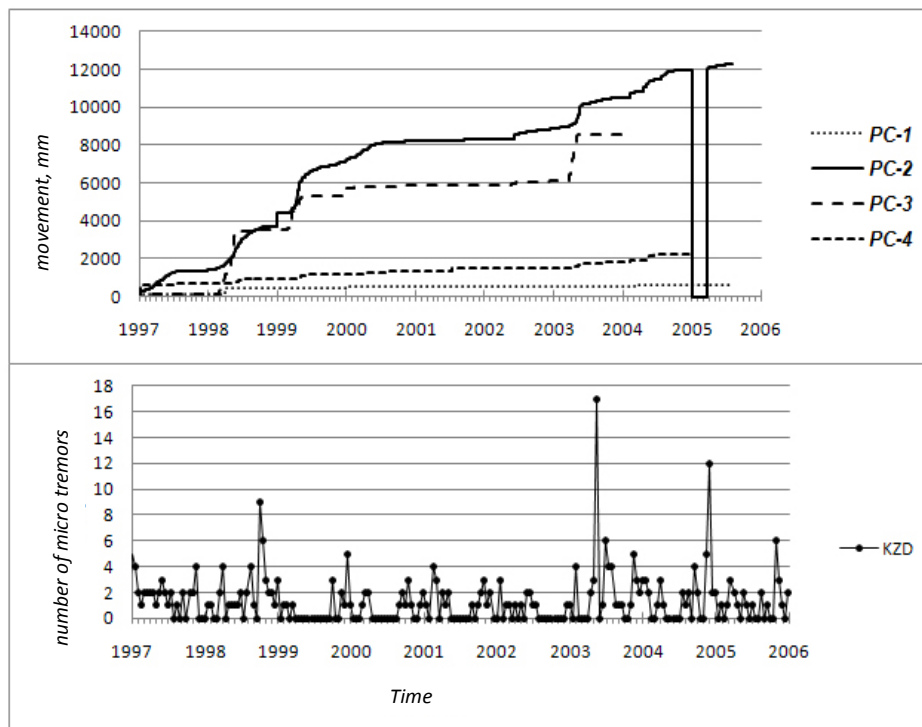


Figure 1.3.8. Comparison of a number of micro tremors (according to [Kalmetyeva et al, 2012]) recorded by the seismic station Kyzyl-Djar with the movement of Mailisay landslide recorded instrumentally at two points: PC-1 – “Tectonics” (bottom graph) and PC-4 – “Upper Koi-Tash” (top graph) according to [Torgoev, 2004].

Outside of the conducted research there are some issues such as the types of landslides, the age of initiation and relationship with rupture structures of different ranks, engineering geology conditions. We realize fully that, of course, these factors and characteristics are very important for making predictive assessment of slope stability. It is also important to have record of earthquakes in the study area in a wide energy range. All these tasks are subjects for further and more detailed studies that we plan to conduct on the basis of a local network of seismic stations operating in the Fergana region in 2009-2010.

1.4. The Nura earthquake of 2008 ($M=6.6$; $I_0 = 8$ MSK64)

1.4.1. Field studies

On October 5, 2008 at 15:52 p.m. by Greenwich time, in the eastern segment of Alai basin (Kyrgyzstan) a strong earthquake occurred. These scale events are of great scientific interest as they give material for the study of an area modern geodynamics. However, different research methods must be involved to their study since the surface manifestations of these events cover a large area, including sites difficult of access.



Figure 1.4.1. Nura village after the earthquake (A), typical structural damages (B) (photo taken by Meleshko A.V.)

CHAPTER 1. GEODYNAMICS AND GEORISKS

Field surveys revealed the following. A large territory including Osh, Batken, Jalal-Abad and Naryn Oblasts of Kyrgyzstan as well as border areas of Uzbekistan, Tajikistan and China were affected by seismic shaking. Nura settlement was completely destroyed, 74 people were died (**Figure 1.4.1-A**). Houses built from clay and straw were completely destroyed (152 constructions) (**Figure 1.4.1-B, left**), panel wooden houses were only slightly damaged (**Figure 1.4.1-B, top right**). Through cracks appeared in the building of the hospital built from burnt brick. Only one new school building which was constructed in accordance with building codes, remain intact (**Figure 1.4.1-B, lower right**). Concrete bridge over the Nura river was damaged. The ruptures of 5 cm width arose on the asphalt road to the south and north of the bridge. They were repeated there every 90 m generating folds of “consolidated” wave of deformation (Figure 1.4.2). Between these ruptures small cracks of up to 1 cm width appeared and were repeated every 30 m [Abdrakhmatov *et al.*, 2008; Annual Report of CAIAG, 2008].



Figure 1.4.2. Cracks (lower part of photo) and “waves of deformation” (upper part) were observed in the vicinity of Nura settlement at distances up to 2-3 km (photo taken by Meleshko A.V.)

1.4.2. Structural position based on geological, seismological and GPS-observations

Description of the structural position of the Nura earthquake was performed by CAIAG employees on the basis of the analysis of geology of the area, materials GPS-observation and processing of seismograms of the main shock and the strongest aftershocks recorded by the digital stations of temporary network installed under TIPAGE project [Zubovich et al., 2009]. The Nura earthquake occurred as a result of the movement of Trans-Alay Range onto Alai Basin due to NNW-SSE oriented compressional stresses, induced by the movement of the Indian plate towards the north with a velocity of ~35 mm/year with respect to the Eurasian plate [Zubovich et al., 2007]. The main morphological-structural elements of this region are Alai Basin and Alai and Trans-Alay Ranges.

Alai Range is made of Paleozoic rocks of the South Tien Shan. Cretaceous-Paleogene sedimentary rocks of Tajik sea and continental deposits are discordantly bedded on the southern slope of the Alai range [Burtman, 2000]. The southern part of this region is limited by a watershed and the southern slopes of Trans Alay range.

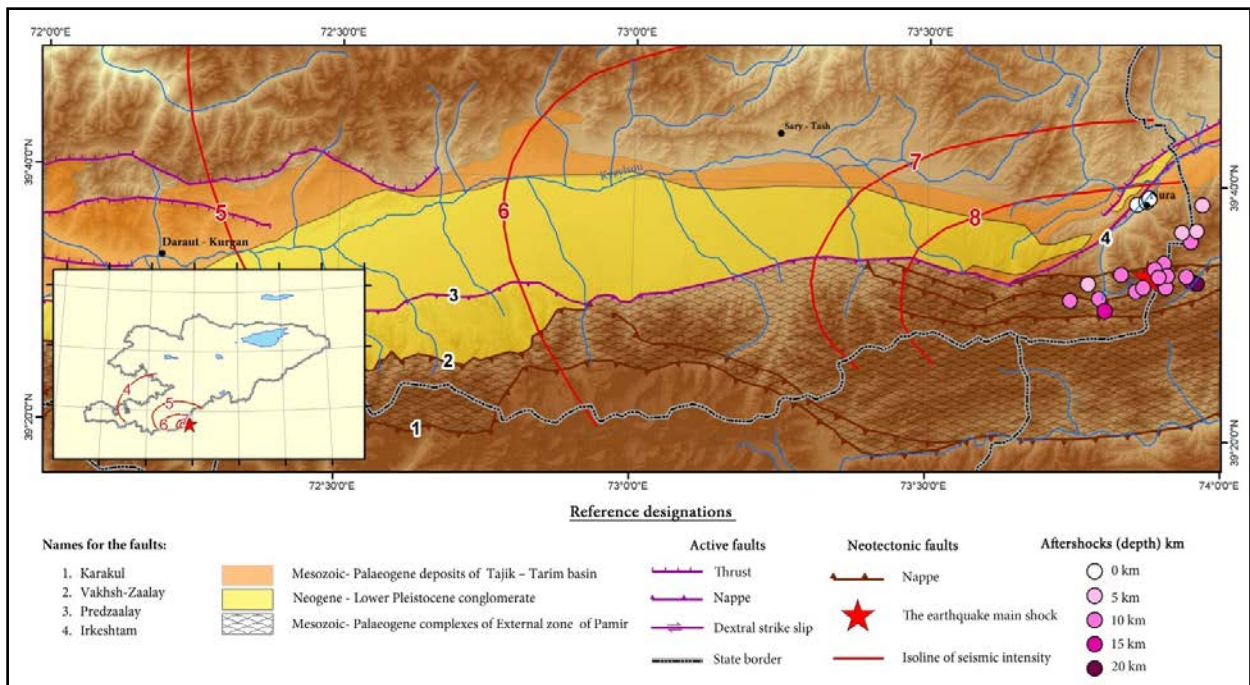


Figure 1.4.3. Neotectonic scheme of source area of Nura earthquake in 2008, $M_L=6.6$, $I_0=8$ by Mikolaichuk A.V. [The Atlas of Earthquakes of Kyrgyzstan, 2009]

Paleozoic complexes of the North Pamir moved along Karakul thrust (1 on Figure 1.4.3) to the north by more than by 300 km. They tectonically overlapped the southern zones of the Cretaceous-Paleogene Tajik basin [Burtman, 2000; Trifonov, 1999; Strecker et al., 2003]. The external zone of Pamir is represented by a cascade of overthrust masses made of Jurassic, Cretaceous and Paleocene deposits. These masses are compressed into asymmetric and overtilted folds formed as a result of the Pamir offset in the front part of Karakul nappe [Trifonov, 1999]. The Northern border of Pamir is the Vakhsh-Trans Alay nappe (2 on Figure 1.4.3); related overthrust masses overlap

relatively undeformed deposits of Cretaceous-Paleogene section of the bottom of Alai Basin [Burtman, 2000; Trifonov, 1999; Nikonov et al. 1983].

The basin is made of Neogene-Early-Pleistocene conglomerates along the northern slope of Trans Alay range; these are also involved in uplifts, making a new series of thrusts. These are the youngest nappes (**3 on Figure 1.4.3**), in essence, being the further development of cascades of nappes of the Pamir External zone. [Trifonov, 1999; Strecker et al., 2003].

Surface deformation in the pleistoseismic areas of strong earthquakes show that these thrust faults have been reactivated in modern times, thus inducing the seismicity of the region [Nikonov et al., 1983]. The seismic zone at the connection of Pamir and Tien Shan is one of the most active of the world in terms of frequency of occurrence, density of epicenters and intensity of earthquakes (**Figure 1.4.3**) [Nikonov et al., 1983]. The intensity of earthquakes can reach $I_0 \geq 9$, for maximal possible magnitude of $M \geq 7.5$ [Bune, Gorshkov (ed.), 1980; Turdukulov, 1996]. The width of the seismically active zone is 30 km. All pleistoseismic areas of the strongest events are part of it. Here, earthquakes of magnitude $M \geq 6$ occur more often than in other seismically active regions of Central Asia: 1949 $M=7.4$ Khait earthquake, 1974 $M=7.3$ Markasui, 1978 $M=6.8$ Daraut-Kurgan and 1983 $M=6.1$ Alai. For the earthquakes with $M < 6$, the majority of motions are also thrusts and strike slips [Kalmetyeva, 2005; 2006; Kuchay, Bushenkova, 2008; 2009].

The Nura earthquake in the region of Alai valley was recorded by several temporary stations of the German Research Center for Geosciences (GFZ), equipped by digital broad-band seismometers. It allowed determining rather accurately the location and depth of the hypocenters of the main shock and aftershocks [Zubovich et al., 2009]. The hypocenter of the main shock is located at the depth of 10 km and in the place of the larger accumulation of aftershocks, formed a line of EN-E strike of 15-20 km width. Along this zone some faults rejuvenated from the south to the north are marked.

Nura settlement destroyed by the earthquake is located close to the outcropping of Irkeshtam thrust fault which is the most northern and youngest of the aforementioned series. Several shallow aftershocks occurred close to it. The hypocenters of the other aftershocks are shifted to the south. Their depth is increasing towards the south. It is obvious that aftershocks activity is related to a fault zone plunging obliquely to the S-SE with hypocenters located at a depth of more than 15-20 km.

On the basis of the depth of the main shock and its distance from the line of Irkeshtam thrust one can estimate the slope angle of the fault zone equal to $\sim 45^\circ$. This slope angle is confirmed by the solution of the focal mechanism of the main shock defined in the Center of Data of the Geological Service of USA (www.neic.cr.usgs.gov).

The main source of information about modern geodynamics of this region is based on GPS data. Vectors of deformation velocities were calculated according to observational data of the Scientific Station (SS RAS) and Seismological Bureau of Xinjiang-Uighur Autonomous Region [Abdrakhmatov et al., 1996; Zubovich et al., 2004] (**Figure 1.4.4**).

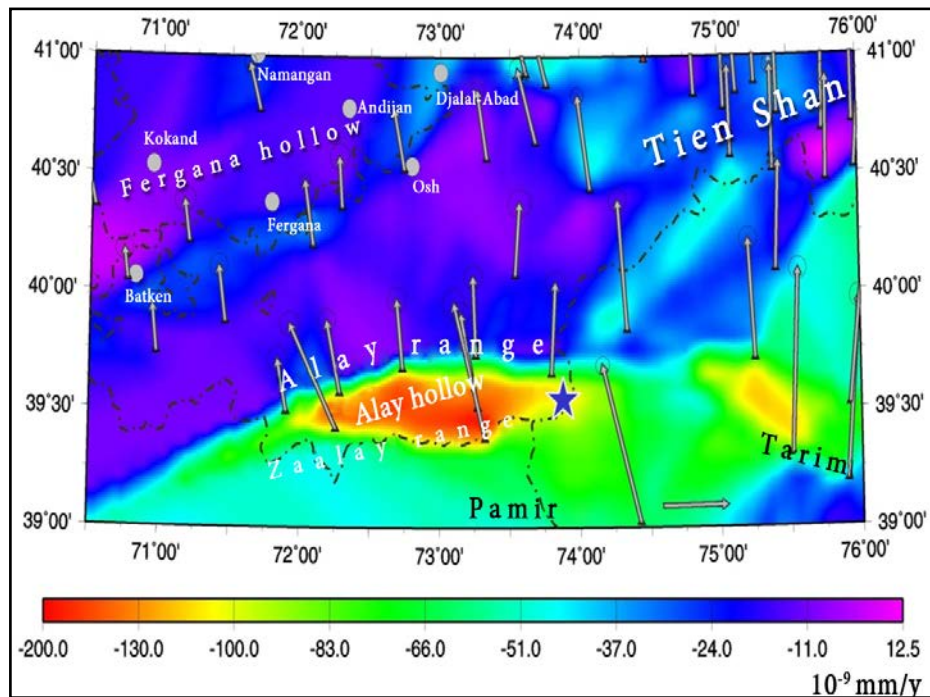


Figure 1.4.4. Map of velocity vectors (arrows) and velocities (in color) of deformation. Blue star is the epicenter of the Nura earthquake.

The results show the velocity of movement of Pamir towards the Tien Shan is at least 7 mm/year. The velocity of deformation is also shown in the figure. In contrast to vectors it does not depend on the reference system and therefore allows us to better outline some details. One of the zones of increased deformation extends along the border between Pamir and Tien Shan, but as it can be seen in Figure 20, the main shock of the Nura earthquake occurred outside deformation zone, at its eastern flank.

Most probably, it is not accidental. Data of GPS measurements allow detecting slow creep movements that are not registered by other non-geodesic methods. The detected zone of increased deformation at the front section of the Pamir indenter reflects, probably, creep movements related to the thrust of Pamir on Alai that shall lead to constant discharge of stresses in this area. There are no such movements along the lateral borders of the zone. Therefore, elastic strain energy is not continuously discharged and its accumulation creates conditions for the preparation of the earthquake. The earthquake occurred on October 5, 2008, near Nura mountain settlement when the level of stresses exceeded the limit of rock strength.

1.4.3. Results of remote study

More detailed information on surface deformations can be obtained with the use of remote sensing techniques. Radar satellite remote sensing, in particular L-band ALOS/PALSAR and C-band ENVISAT imagery we use in this study to analyze surface deformation related to the earthquake and mass movements by applying SAR interferometry (InSAR) and pixel offset techniques [Teshebaeva *et al.*, 2014]. We processed 16 ascending ALOS and 7 descending ENVISAT images spanning from May

8, 2008 to August 20, 2009, and we formed differential interferograms and pixel offset maps.

In the ascending ALOS interferograms, we observe a clear coseismic surface displacement north of the footwall of the Pamir Frontal thrust and at the hanging wall of the Irkeshtam fault. At these locations, we measure large and sudden changes of negative and positive line-of-sight displacements that amount to approximately -24 cm and 48 cm, respectively. In the corresponding descending ENVISAT interferogram, we observe widespread motion towards the satellite north of the Irkeshtam fault, with up to 6 cm of line-of-sight displacement (**Figures 1.4.5, 1.4.6**).

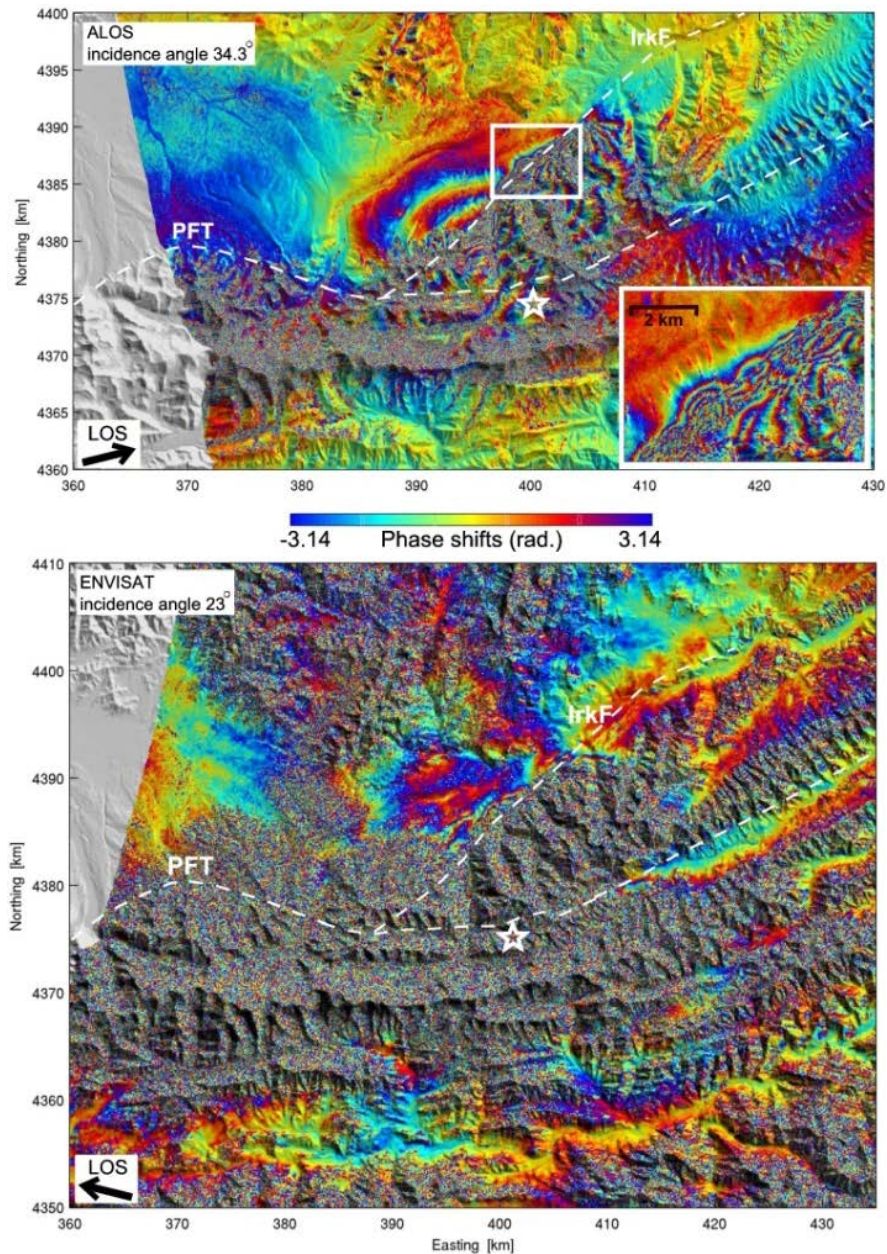


Figure 1.4.5. ALOS (top) and ENVISAT (bottom) interferograms over a shaded relief show the line-of-sight (LOS) surface displacement close to the Nura earthquake epicenter (white star). The white dashed lines outline the Pamir Frontal thrust (PFT) and the Irkeshtam fault (IrKF). The inset in the top panel shows an enlarged image of the in white outlined area, where steps in the interferometric phase values point to surface rupture (Figure 1.5.6) [Teshebaeva et al., 2014]

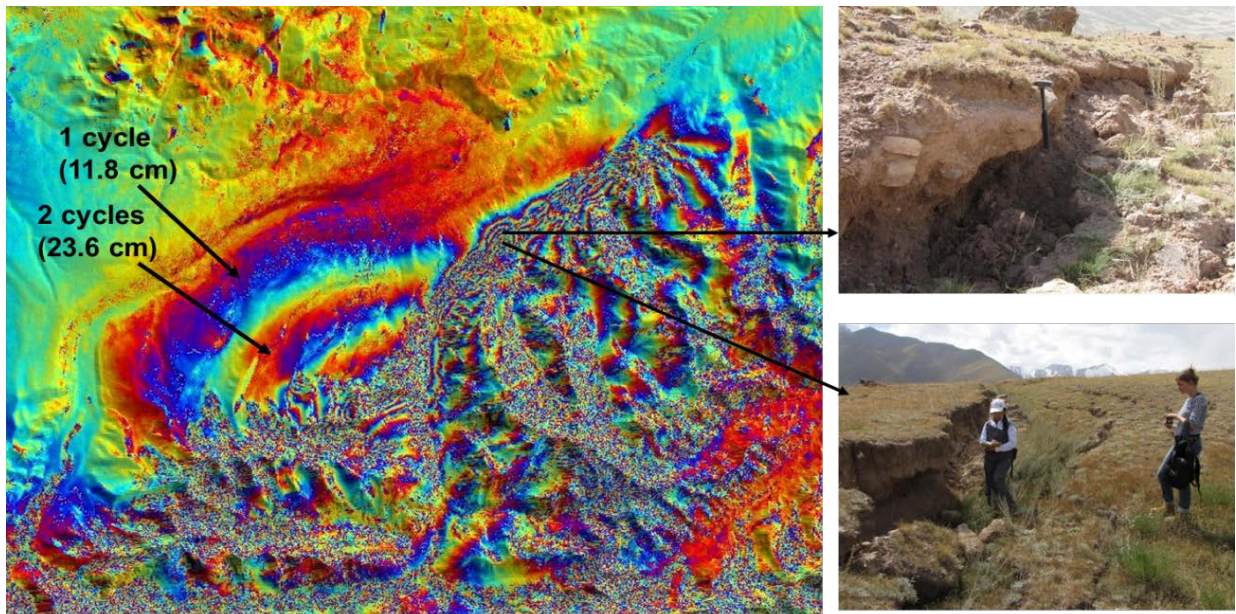


Figure 1.4.6. ALOS interferogram close look for the deformed area verified from the field observations. Black arrows show location of the surface ruptures obtained during field investigations in 2012 [Teshebaeva et al., 2014]

The pixel offsets add new information at and south of the Irkeshtam fault, where no InSAR data are available (**Figure 1.4.7**). Our offset measurements using the ALOS data show a sharp displacement discontinuity across which the surface movement is in the opposite direction. The boundary length of this feature extends continuously for approximately 25 km in a northeast-southwest direction, and this is identical with the strike of Irkeshtam Fault [Teshebaeva 2012; 2014]. The purely horizontal azimuth pixel offsets show, similar to the range pixel offsets, a clear discontinuity parallel to Irkeshtam Fault (**Figure 1.4.7**).

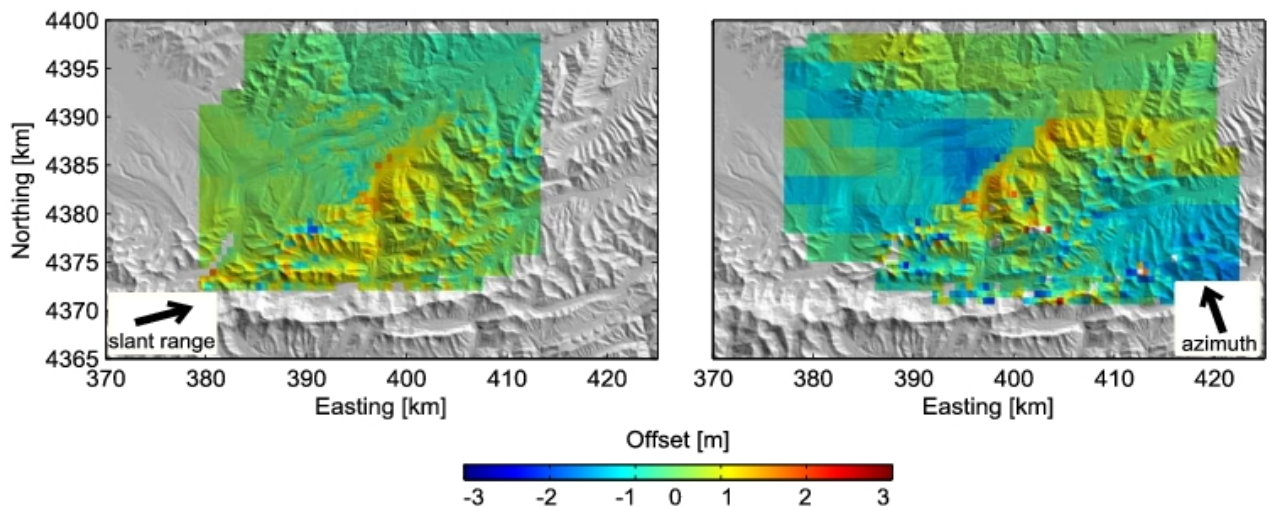


Figure 1.4.7. ALOS range (left panel) and azimuth (right panel) pixel offset measurements. Azimuth offsets give purely horizontal surface displacements in the direction parallel to the satellite flight direction (right panel, black arrow) [Teshebaeva, 2014]

This analysis leads to the following results:

- the Nura earthquake nucleated at the Pamir Frontal thrust, where a major part of co-seismic deformation took place in the footwall;
- we can observe surface ruptures along the Irkeshtam fault to the north of the Pamir Frontal thrust, where no aftershock activity is observed [Teshebaeva, 2014].
- we can find generally larger surface displacements in the hanging wall of the Irkeshtam fault than in its footwall (**Figures 1.4.5, 1.4.6, 1.4.7**) [Teshebaeva, 2014].

1.5. Specifics of spatial and time distribution of strong earthquakes in Central Asia

On November 2010 CAIAG proceeded to creation of its own catalogue of earthquakes. Through the SeisComP system data the wave-formed continuous flow from CAIAG seismic stations, CAREMON, KRNET, and KNET network stations and from nearly 30 seismic stations of the international network were transferred to CAIAG. Initial processing was made automatically by the SeisComP complex. Then the operator selected events within the coordinates: 26° - 57.5° , N and 46.5° – 87° , E from the automatic occurrence events. In cases of time error in the center (RMS) was more than 2 seconds, the operator performed a manual picking of phases and repeated defining of the epicenter. If such events had happened at the territory of Kyrgyzstan, then their records were processed also by Seisan and Elwin programs. It turned out that events with large RMS occur in selvages of the territories when all observation points were located on one side from the seismic event (i.e. $\text{gap} > 180^{\circ}$). At that the results of processing by the Seisan and Elwin programs have shown lower RMS values. The reason of differences was that the direct-wave traveltime graph laid in the SeisComP program conforms to the platform-type earth crust averaged traveltime graph, as in the Seisan and Elwin we have laid the traveltime graph for the territory of the Kyrgyz Republic (*Green, Kalmetyeva, 1978; Green, 1993*).

Besides, in cases when direct wave raypath from the earthquake epicenter to CAIAG's seismic stations transferred through Kokshaal Ridge the traveltime was increased significantly (till few seconds), that added errors in defining of the epicenter coordinates. If the earthquake epicenter had been located to the north of Kokshaal Ridge, there were no such errors. The facts stated are well coordinated with data available on the earth crust velocity structure in Kokshaal area. According to Sabitova T.M. [*Bakirov et al., 2006*] here the Mohorovicic boundary is lowered at the depth of nearly 100 km. We have decided not to make changes in the SeisComP program's initial data as it is provided for defining the epicenter coordinates within the whole Central Asia and not only on the territory of Kyrgyzstan.

In July 2011 the KNET network data were ceased to transfer to the FDSN and, consequently, to CAIAG. Obviously the further composing of catalogue for the territory of Kyrgyzstan became meaningless, all the more so that catalogue had been creating in the Institute of Seismology of the National Academy of Sciences of the Kyrgyz Republic.

CHAPTER 1. GEODYNAMICS AND GEORISKS

Switching off the KNET network from the FDSN did not affect condition of the monitoring network of the Institute of Seismology, as it receives these data directly. Ceasing of data transfer from the KNET to the CAIAG did not bother registering strong earthquakes ($M \geq 5$) on the whole territory of Central Asia (**Figures 1.5.1-1.5.2**). Automatic catalogue of these events is available on the CAIAG site: www.caiag.kg. Essentially, the catalogue composed by us is a catalogue of destructive earthquakes in Central Asia. Analysis of spatial and time behavior of earthquakes based on that catalogue enables to study laws of destructive earthquake effects in Central Asia. This is what we will discuss further.

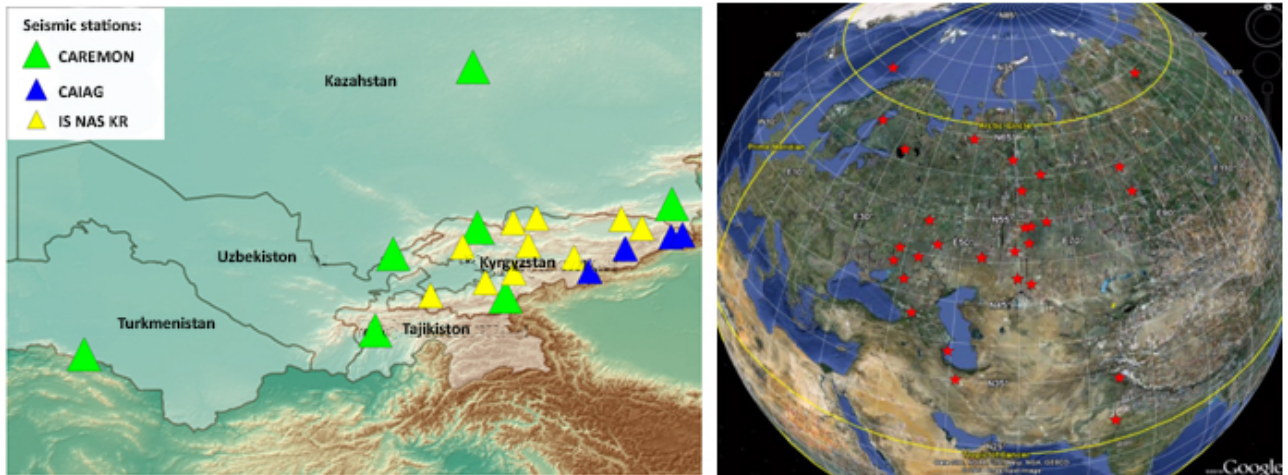


Figure 1.5.1. Seismic stations whose data are transferred to CAIAG

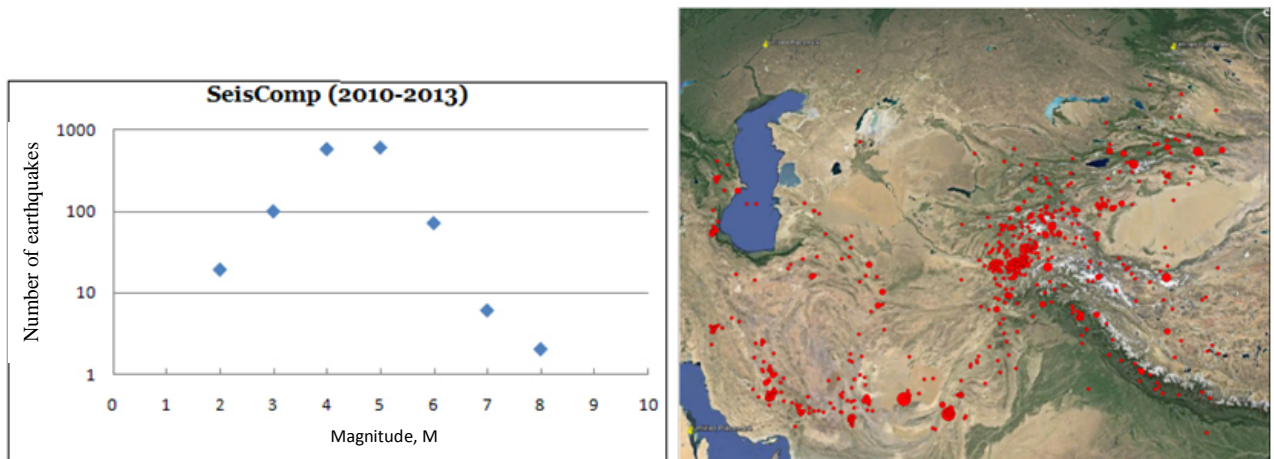


Figure 1.5.2. Recurrence graph (on the left) and the map of earthquake epicenters (on the right) according to the catalogue of CAIAG for 2010-2013.

Figure 1.5.2 (right) shows the epicenters according to the CAIAG catalogue for 2010-2013. It is visible that epicenters are distributed regularly along some lines. For comparison with the region's seismicity in the previous years we have used the map of epicenters for 1900-2012 located on the USGS site (<http://earthquake.usgs.gov>).

Figure 1.5.3 shows this map with earthquake epicenters according to the CAIAG catalogue for 2010-2013 (red circles). It is clear that epicenters of strong earthquakes in

2010-2013 are distributed within the same narrow lines where strong earthquakes took place in last 100 years.

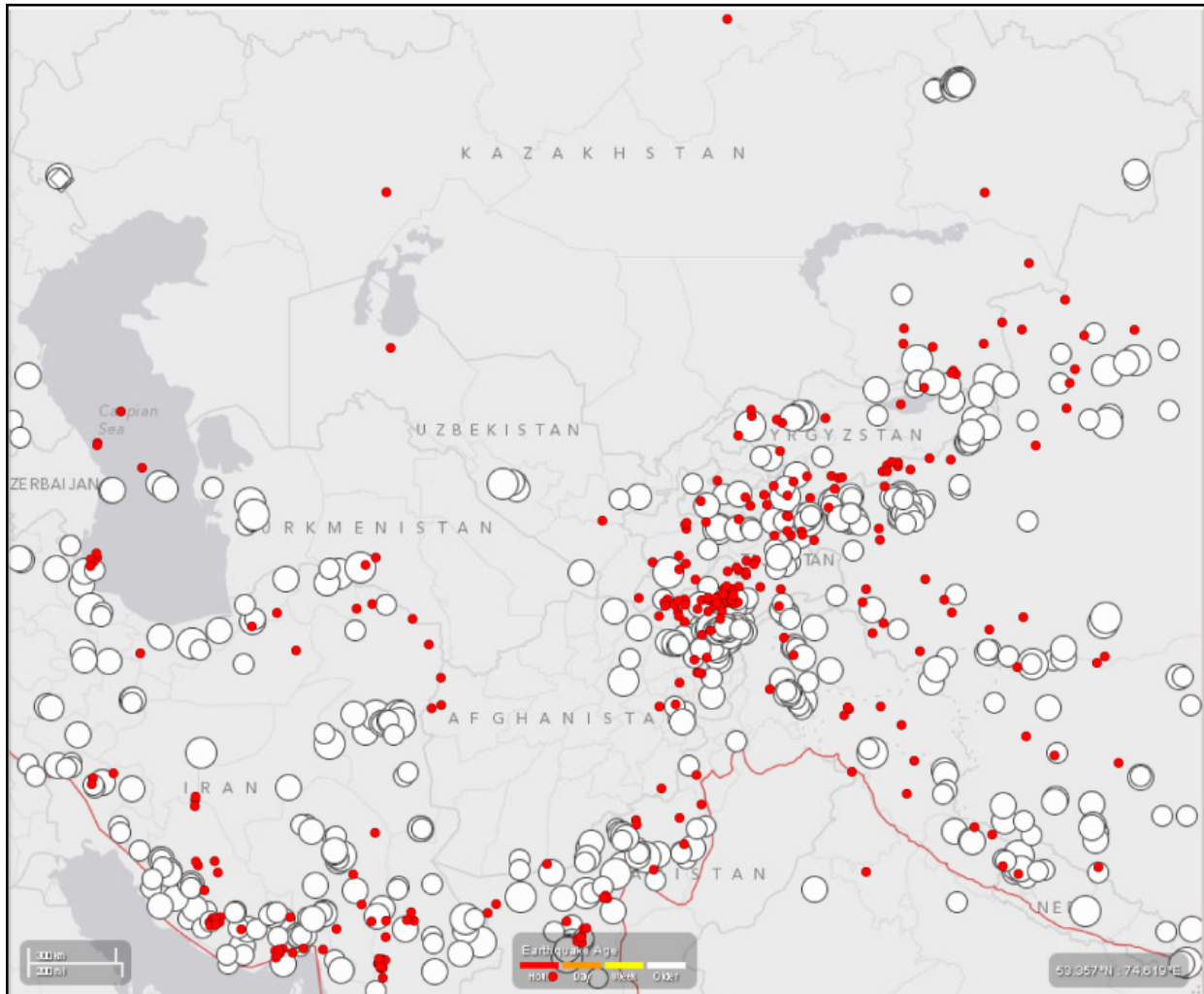


Figure 1.5.3. Map of earthquake epicenters with $M \geq 5$ according to USGS (copy of the map from the site: <http://earthquake.usgs.gov>) for 1900-2012 (empty circles) and the CAIAG catalogue for 2010-2013 (red circles)

For analysis of the spatial and time distribution of the area earthquakes we have composed a cumulative catalogue for 1850-2013 based on USGS, GFZ, the Institute of Seismology of the National Academy of Science of the Kyrgyz Republic, CAIAG and the catalogue composed within the project ISTC-KR1176. We should note that composing of the cumulative catalogue according to data from various catalogues is a difficult task.

Epicenters of strong earthquakes according to data from various catalogues are located at a distance till 100 km from each other. Energy estimations of earthquakes in different catalogues are shown by different magnitude estimations. Therefore the results of the analysis executed should be considered just in the broadest sense.

The time-magnitude charts and also charts showing change of earthquake epicenter coordinates by latitude and longitude as along the whole territory as on separate areas.

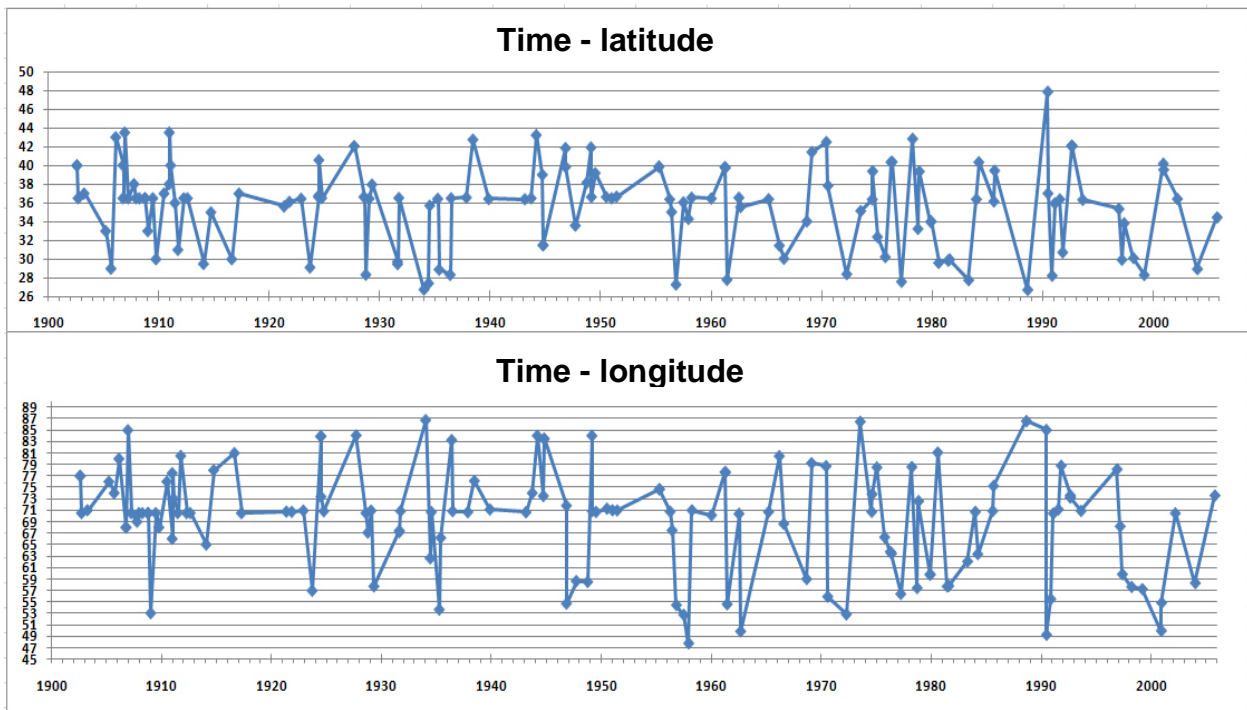


Figure 1.5.4. Time change of latitude (upper) and longitude (lower) of strong earthquakes in Central Asian region.

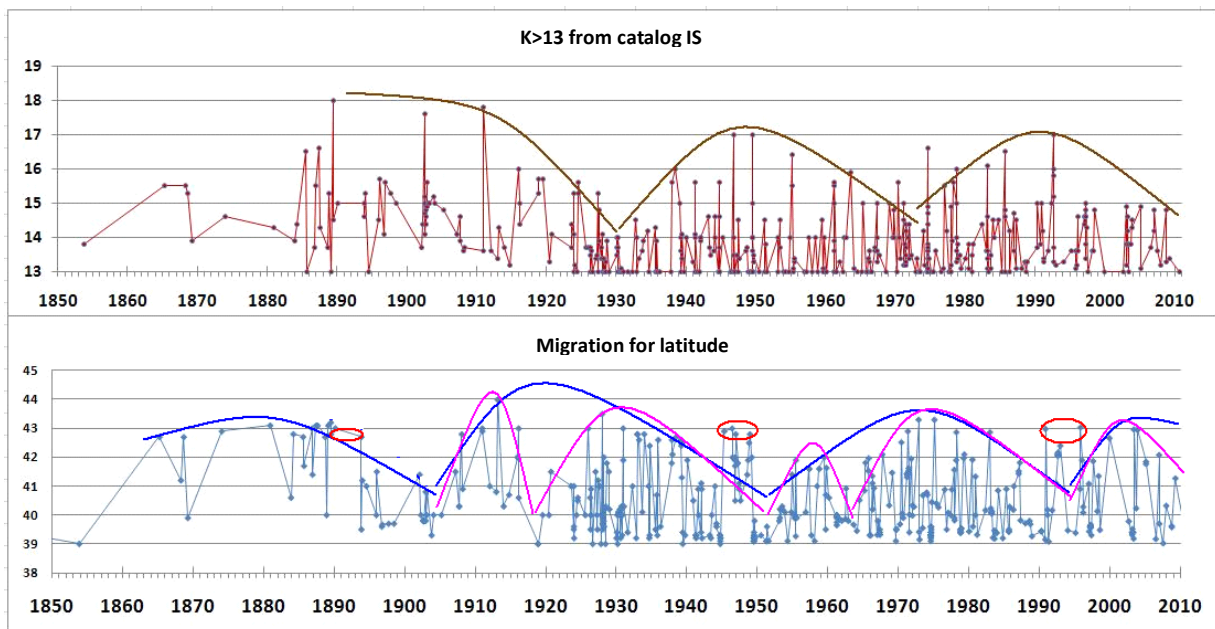


Figure 1.5.5. Time change of energy class of seismic events (upper) and latitude their epicenters (lower) for Pamir-Tien-Shan region.

Charts in **Figure 1.5.4** show that epicenters of strong earthquakes move in time, moving away and to the point with coordinates approximately 36° - 37° N by latitude and 70° - 71° E by longitude, i.e. relatively deep-focus Gindukush zone. Creation of such kind of charts on separate areas of the territory observed shows that such moving happens in cycles with length of 40-50 years. Thus, in Pamir-Tien-Shan area (**Figure 1.5.5**) there is an approximately 45-year cycle as in the earthquake energy class change (upper image) as in moving of epicenters at the north-south direction (lower image). It is clear

that, in general, the energy level of events increases by moving of earthquake epicenters to the south (i.e. the upper chart's maximums correspond to the lower chart's minimums). At that the epicenter movement cycles consist of a kind of two subcycles. Moreover, at the end of every epicenter movement cycle (lower chart) some events that break the common pattern appear. They are strong events occurring in Northern Tien Shan. They happen when earthquake epicenters move southwards and the north seems to become quiet. In other words, strong earthquakes in Northern Tien Shan happen when it is quiet. In 1946 it was the Chatkal earthquake ($M=7.4$), in 1992 – the Suusamyr ($M=7.3$). If these charts are prolonged mentally, supposing that the pattern will be fulfilled in the future, then the next epicenter migration cycle will be completed to 2030. Then, approximately in 2020-2030 a strong earthquake with M no less than $M=7$ on Northern Tien Shan in the latitude range of 42° - 43° is expected.

Epicenters of strong earthquakes migrate in circles to the west of Hindukush. On Figure 1.5.6 yellow asterisks on the left show epicenters of strong earthquakes occurred from 1930 to 1985. Nearby numbers 1-10 show the order of occurring of these earthquakes in time. As a result, from 1930-1985 epicenters of these earthquakes were moving away at first, and then approached Hindukush moving in circular motions counterclockwise.

The same movement pattern is observed also for weaker events ($M=5-6$) according to the CAIAG catalogue for 2010-2013 (Figure 1.5.6 on the right). Numbers near the epicenters show that at the upper side of the area the epicenters move westwards, and at the lower side – eastwards, i.e. in circular motions counterclockwise.

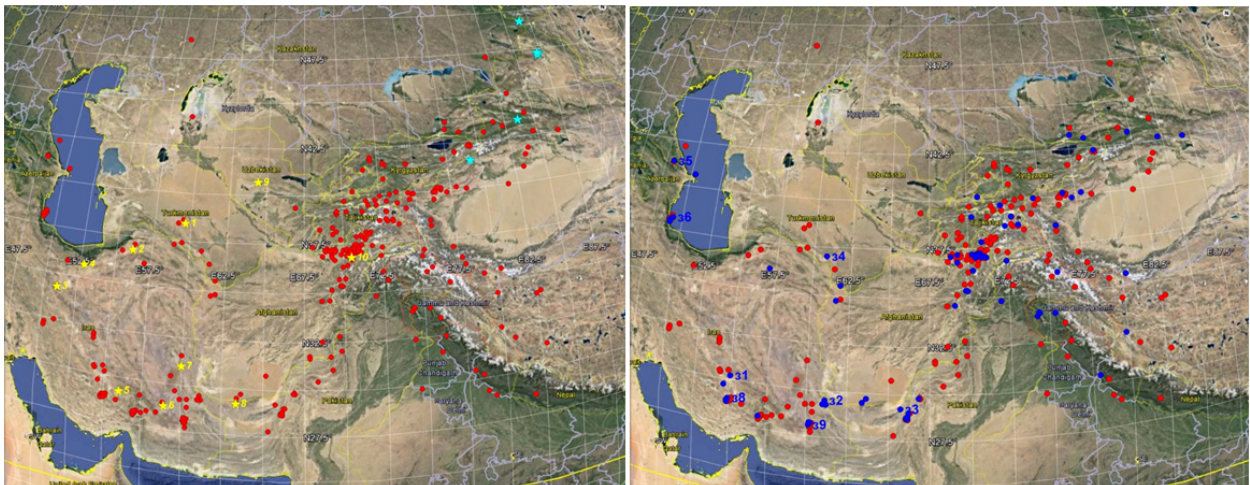


Figure 1.5.6. Epicenters of strong ($M \geq 6.5$) earthquakes in Central Asia from 1900 to 2005 (on the left) according to the CAIAG cumulative catalogue data and epicenters of earthquakes with $M \geq 5$ for 2010-2013 according to the CAIAG catalogue data.

Here just few episodes of the region's seismic activity were given. But even these episodes best speak with sufficient proof that the whole Central Asian region undergoes a unified geodynamic mechanism that defines the seismic activity. In this relation we need to highlight a necessity of cross-boundary cooperation, joining efforts for clear understanding of seismicity patterns and, consequently, correct estimation of seismic risk of the region.

1.6. Seismic microzonation of territories of large cities

Seismic microzonation is aimed at quantitative assessment of ground shaking affecting the territories of industrial and civil constructions. This allows conducting calculations of seismic resistance of certain constructions and, as a result, selecting appropriate places for allocation of constructions and facilities. This is considered to be one of the most important measures, contributing to the safety of housing and civil, industrial, and rural constructions in seismic – prone regions.

Existing maps of seismic microzonation in Kyrgyzstan were developed in the Soviet period. Since then the configuration of settlements has changed, new types of constructions have been constructed. In the meantime new technologies for seismic effect assessments have been created. Under this project the studies on ground resonance frequency characteristics in Bishkek and Karakol (Kyrgyzstan), Dushanbe and Khorog (Tajikistan) cities have been conducted. Similar studies were started for Naryn (Kyrgyzstan) and Almaty (Kazakhstan) cities.

Three types of instrumental measurements were carried out:

areal seismic noise measurements

Sites with different seismic intensity rates were selected, as illustrated on the last map of seismic microzonation in the considered settlement. The measurements were conducted during 4 hours. The task was to estimate the velocity profile of the upper Earth's crust layers in each site according to transversal and surface Love and Rayleigh waves.

point seismic noise measurements

30-minutes noise measurements in selected points were carried out. The points were distributed along the area of the settlement, taking into account existing area and territory of planned building activities for the next 10-15 years. Selected noise recordings were processed using a standard Nakamura's method to estimate the resonance frequency and thickness of the upper layer.

earthquake measurements

Seismic stations were installed in the areas covering all basic ground types to record earthquakes. Measurements took few months. Two approaches were used, depending on the location of the stations, distance between them and from earthquake epicenter.

In cases when the distance between two stations was at least 5 times less than the distance from the hypocenter, and one of the stations is located on rocky grounds, while another one is on sedimentary structure, the method of standard spectral ratio (SSR) was used. This process is illustrated schematically on the left figure. The spectral ratio of measurement on sedimentary structure to the ratio of measurement on rocky grounds shows the action effect of sedimentary rocks.

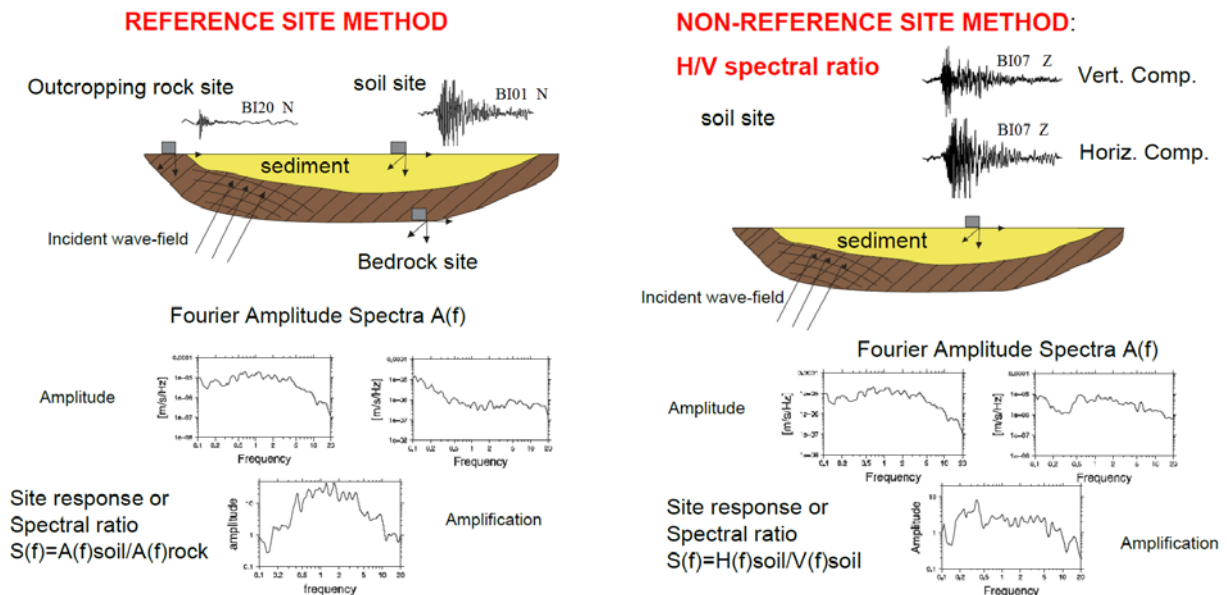


Figure 1.6.1. Methods of processing of earthquake recordings: SSR (left) and Non-Reference H/V (right).

If this condition is not fulfilled (left figure), the method with no reference point is used. To assess the effect of impact area, the spectral ratio of horizontal component of seismograph to vertical component spectra is calculated.

Conducted studies resulted in the composing of resonance frequency ground characteristics of the studied area.

1.6.1. Bishkek city

Field and office research work was conducted together with researchers from GFZ, Potsdam, Germany and INGV International Institute of Geophysics and Volcanology, Italy.

To conduct earthquake measurements the following equipment was used:

- 16 stations Mark 1Hz + EDL and 4 stations Lennartz LE3D + Reftek stations were installed in order to record earthquakes;
- sensors Mark L4C-3D, Lennartz LE3D-5s and digitizers EarthData Recorder PR6-24 were used for recording noises;
- GPS antennas.

Surveys of the area were conducted in 4 sites:

- Close to CAIAG
- On the northern side of the active Issyk-Ata fault, eastwards of Orto-Sai settlement,
- Central stadium named after D. Omurzakov and
- Experimental facility of the Institute of Biology NAN KR (**Figure 1.6.2**).

CHAPTER 1. GEODYNAMICS AND GEORISKS

Half-hour point measurements of seismic noises were conducted in 208 points, distributed in accordance with a city building plan until 2025.



Figure 1.6.2. Location of area's survey points

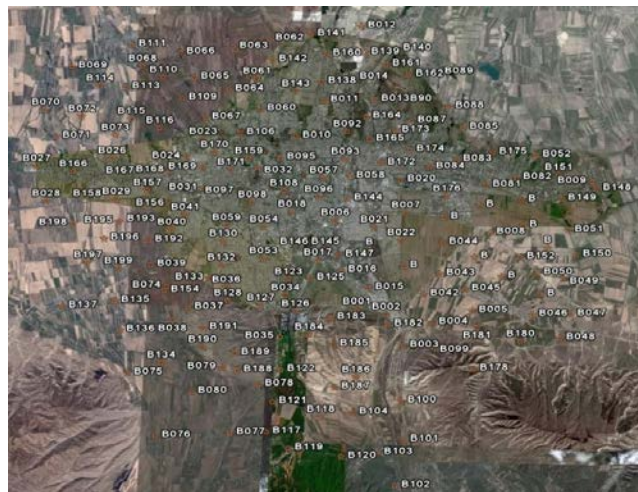


Figure 1.6.3. Point seismic noise measurement



Figure 1.6.4. Location of seismic stations

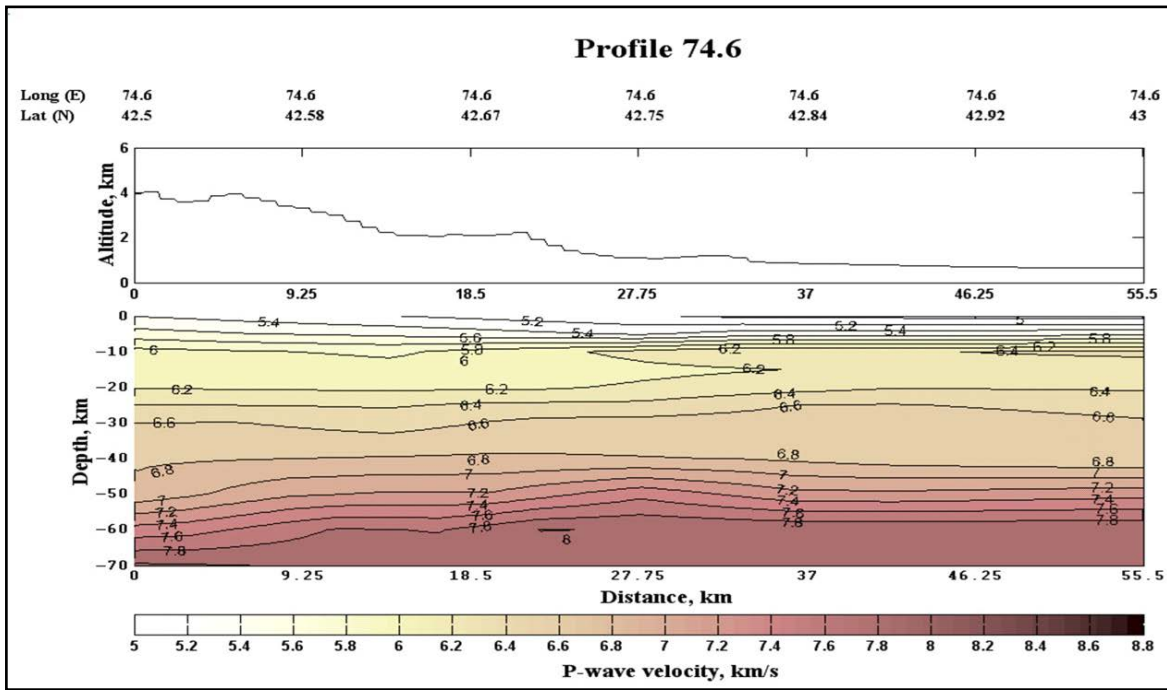


Figure 1.6.5. Velocity profile along the meridian 74.6° E (Sabitova et al., 2006).

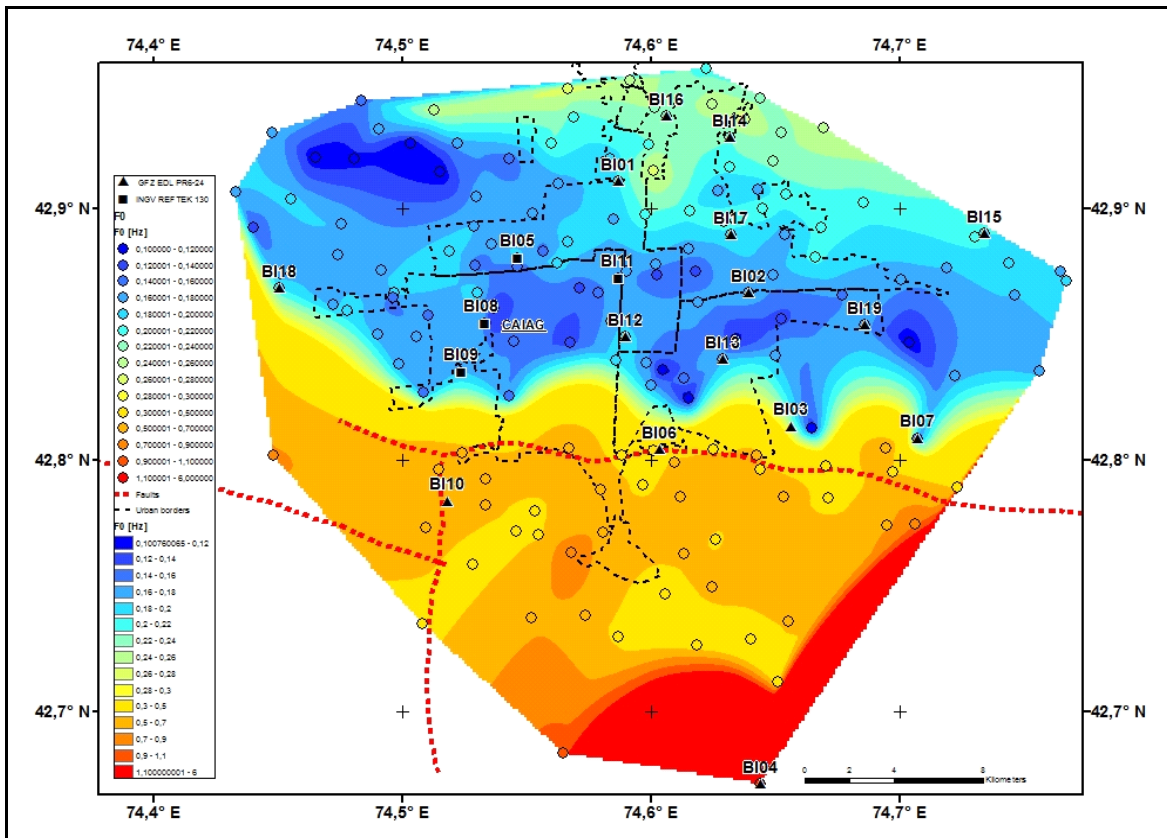


Figure 1.6.6. Map of frequency resonance ground characteristics on the territory of Bishkek city

Sites for stations were selected considering the requirements for zones with different intensities, as well as considering the deep structure. Position of the stations along meridional profiles is specified by peculiarities of velocity structure of the Earth's crust of the Chui depression according to 3D model data (Sabitova et al., 2006) represented on

Figure 1.6.5 as a velocity profile. For the period from 15.08.2008 to 1.12.2008 more than 200 seismic events have been recorded. Of those events, 48 strong earthquake recordings were selected for spectral processing.

As a result, the map of frequency resonance ground characteristics for the territory of Bishkek was created (**Figure 1.6.6**). For Kyrgyzstan this work is of importance for the reason that up-to-date methods of seismic zonation were used for the first time and meet international standards. In 2014-15 it is planned to introduce in Building Codes of the State Agency of Construction of the Kyrgyz Republic the parameters of frequency resonance ground characteristics.

1.6.2. Karakol town

For Karakol town three types of seismometric observations: area's survey (**Figure 1.6.7a**), point noise measurement (fig.7b), and earthquake recordings (**Figure 1.6.7c**) were conducted using the seismic stations Mark C34L+ EDL (20 sets were provided by GFZ and 4 sets belong to CAIAG), Geophone 4.5 Hz + SOSEWIN (20 sets provided by GFZ), as well as one seismic station from CAIAG - Guralp CMG3D + EDL.

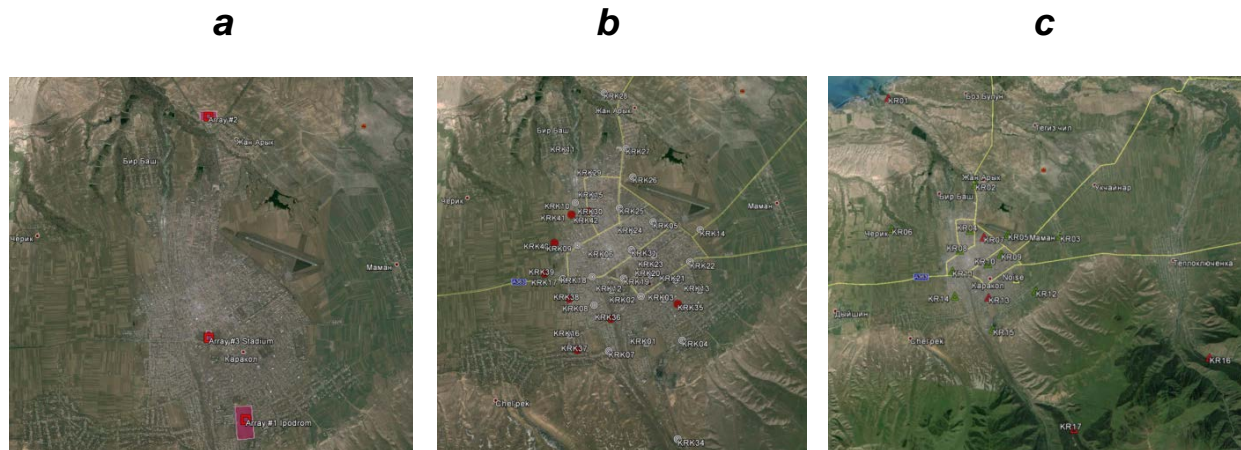


Figure 1.6.7. Location of stations taking into account types of observations: a) area's survey, b) point noise measurement, c) earthquake recordings

In order to conduct areal measurements, three sites were selected: road junction in the northern part of the city, Central Stadium, Hippodrome. The sites were selected in such a way as to locate stations in areas with different seismic intensity, as shown on the map of seismic microzonation of Karakol town (1995). Materials obtained on every site were processed. The task was to define the velocity section of surface layers of earth crust under every site according to recordings of transversal waves and surface waves of Love and Rayleigh.

30-minute recordings of noises were carried out by three stations during two days. 42 recordings were chosen for analysis. The standard methodology of noise processing was used for defining the resonant frequency of the upper layer and its power.

CHAPTER 1. GEODYNAMICS AND GEORISKS

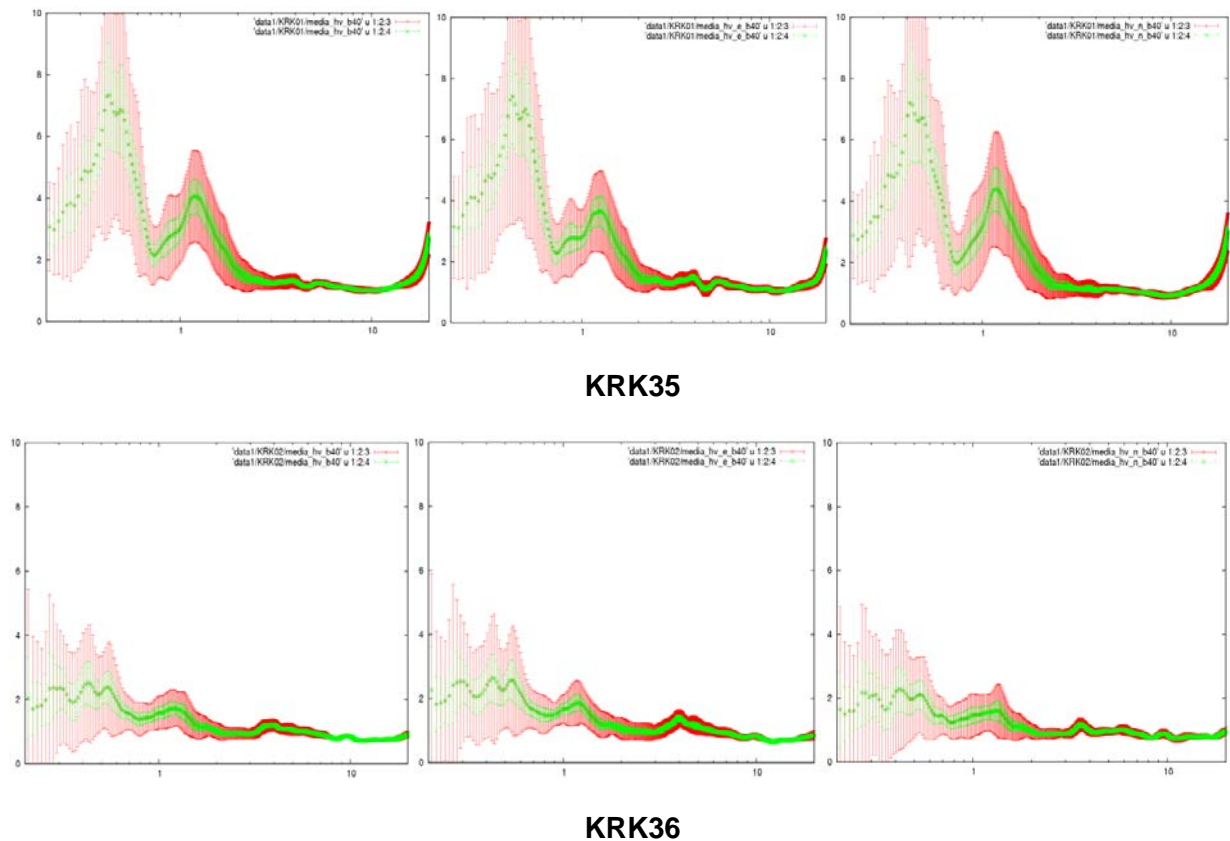


Figure 1.6.8. Site at the northern part of Karakol

Velocity profiles of the upper ground layers of the city were drawn up using the recordings of transversal and surface waves.

Earthquake recording was carried out by 22 seismic stations, 17 of them were installed within Karakol town and 5 stations – around the town. This network of stations worked for 4 months – from July to October 2011. **Figure 1.6.8** shows examples of processing of earthquake recordings for two points: KPK35 and KPK36. Graphs of correlation of spectral curves of full horizontal vector to vertical component (on the left) are shown by red, latitudinal component to vertical (in the middle) and meridional component to vertical (on the right). Average values and standard decline are shown by green. These data are in the final stage of processing.

According to the processed area's survey data (together with Matteo Picozzi) the following results were obtained:

According to the area's seismic survey results in the northern part of Karakol town, two layers of ground thickness were detected: the upper one is 4 m with S-wave velocity of 220 m/sec, and the second layer of 40 m with S-wave velocity of 440 m/sec.

At the territory of the Central Stadium there were three ground layers observed: the upper one is 8 m with S-wave velocity propagation of 450 m/sec, the middle one of 40 m with S-wave velocity propagation of 800 m/s, and the lower layer which is 150 m and its S-wave velocity propagation is 1500 m/sec.

CHAPTER 1. GEODYNAMICS AND GEORISKS

At the territory of the Hippodrome of Karakol town there were two ground layers observed. One layer is 7 m with S-wave velocity propagation of 300 m/sec and another layer which is 40 m and its S-wave velocity propagation is 900 m/sec.

According to the data obtained, it is possible to draw a preliminary result that the ground conditions within Karakol town are not homogeneous and vary with depth of the cover thickness. In order to make the town's microseismic zonation map, we need to carry out more detailed studies.

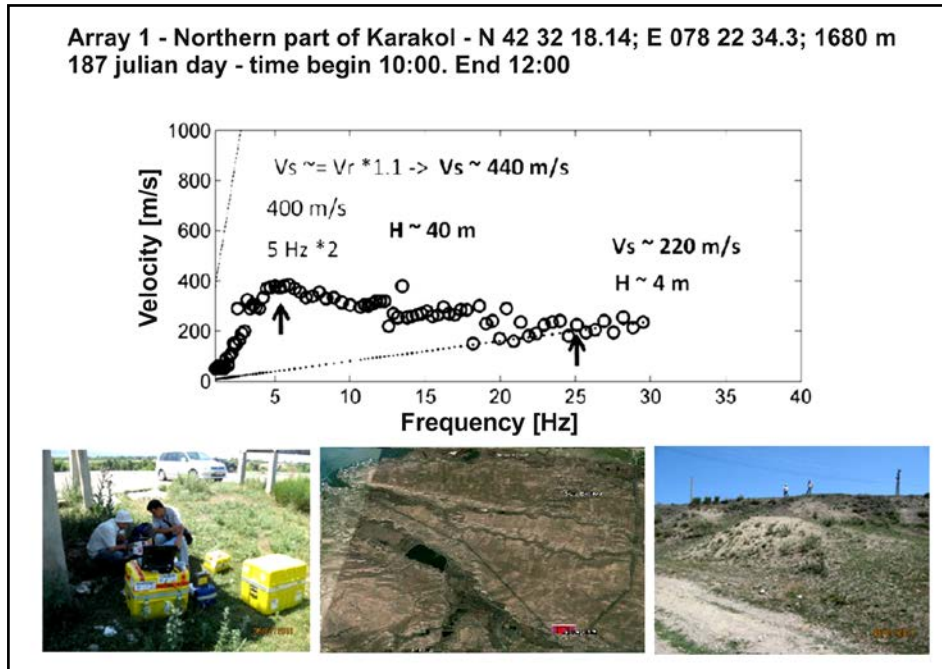


Figure 1.6.9. Site in the northern part of Karakol town

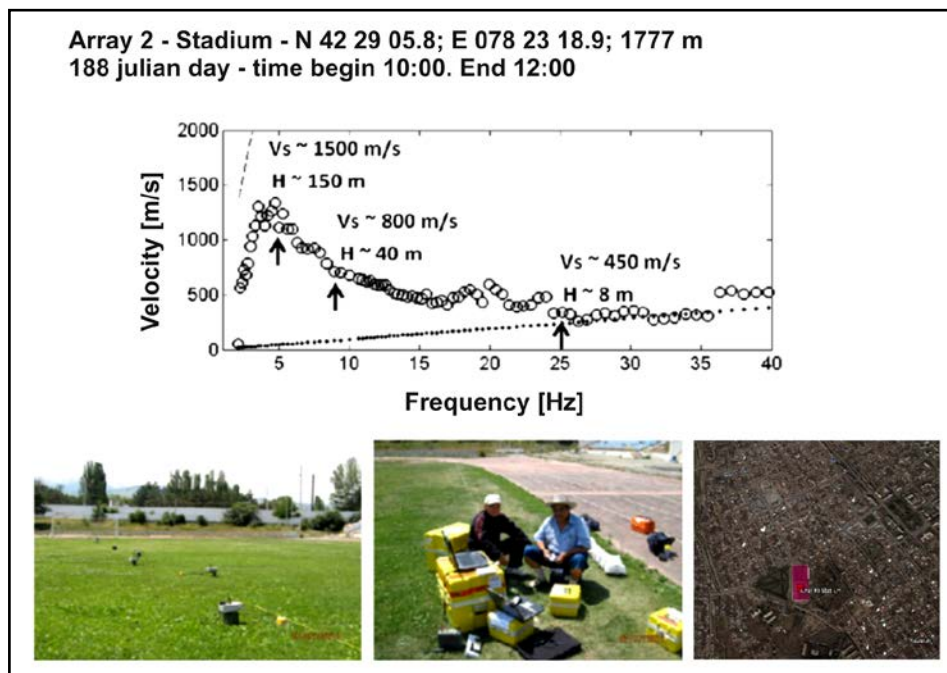


Figure 1.6.10. Central Stadium site in Karakol

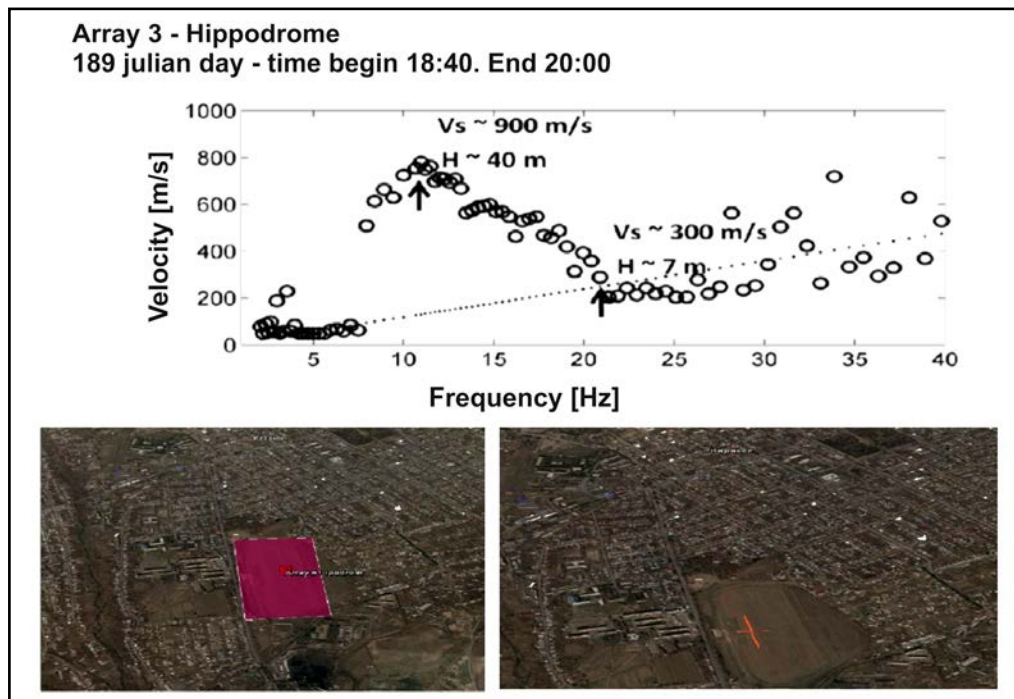


Figure 1.6.11. The Hippodrome site in Karakol town

CHAPTER 2. CLIMATE AND WATER RESOURCES

2.1. A study of climate change

Climate studies are of great practical importance and CAIAG pays considerable attention to instrumental measurements and analysis of the major climatic parameters in Central Asian region.

At the same time, the focus is on modern methods of remote atmospheric research using automatic weather stations and meteorological data from different satellites.

To present time in CAIAG were conducted a number of studies in the field of climate monitoring, these are comparative analysis of observations obtained with a traditional hydro-meteorological equipment and data from automatic weather stations, study of atmospheric dust on the basis of special station set to the south of Bishkek city, definition of areas of high altitude snow covered areas in different regions of the country, comprehensive analysis of climate change in the Issyk-Kul Lake basin.

2.1.1. Comparative analysis of the results of measurements by automatic weather stations and traditional types of weather equipment

In order to assess the comparability of the results of meteorological parameters measurement obtained by traditional instrumentation used at meteorological stations of Kyrgyz Hydrometeorological Service and at automatic weather stations, the measurements by automatic weather station and traditional instruments were made on the meteorological site of the Department of MEEP KRSU in Bishkek city.

Based on an agreement between the Central Asian Institute of Applied Geosciences and the Kyrgyz Russian Slavonic University an AMS Vaisala WXT510 instrument [2] was installed at the meteorological observation site owned by the Hydrometeorological Observatory (HMO) of the Department of Meteorology, Ecology and Environmental Protection (MEEP) of the Faculty of Natural and Technical Sciences (NTSF) of the Kyrgyz Russian Slavonic University (KRSU) in Bishkek. The installation aimed to:

- Obtain twenty-four-hour meteorological data from the AMS WXT510 in the territory of Bishkek by CAIAG and KRSU
- Compare the meteorological data of WXT510 and data from HMO KRSU (measured by standard hydrometeorological equipment);
- Assess the reliability of the WXT510 operation in autonomous mode for continuous measurements and the required level of preventive maintenance.

The AMS Vaisala WXT510 instrument was installed on a metal tower at a height of 3 m above ground level on 18.09.08. Debugging took until 4.10.08, and starting from

October 4th, 2008 the station operated in a continuous mode with a 10 minute sampling interval.

Meteorological site HMO is located on the territory of NTS KRSU in Bishkek, its height is 759.3 m above sea level; the barometer height is 760.3 m above sea level, the coordinates are 42°51 north and 74°38 east. The meteo-site HMO conducted triple measurements every working day starting from 01.09.2002 at 09, 12 and 15 o'clock local time (except Saturday and Sunday). [1]

AMS WXT510 measures wind speed and direction, precipitation, barometric pressure, temperature and relative humidity. A comparison of measurement data of the WXT510 and the HMO equipment was made for atmospheric pressure, temperature and relative humidity taken at 09, 12 and 15 o'clock local time. For the period from September 18th to December 29th in total 171 pressures, temperature and relative humidity measurements have been taken.

Comparing wind speed and direction was not conducted, because the sensors WXT510 were located at a height of 3 m and the sensors M-63M-1 on the roof of a 4-storey building at a height of around 15 m.

Air temperature

Figure 2.1.1.1. shows air temperature of the sensor WXT510 (blue line) and of a thermometer (red line) placed in a psychrometric booth. Both lines are in good agreement, and show that the air temperature measured by the meteorological thermometer is slightly higher than the air temperature recorded by the weather sensor.

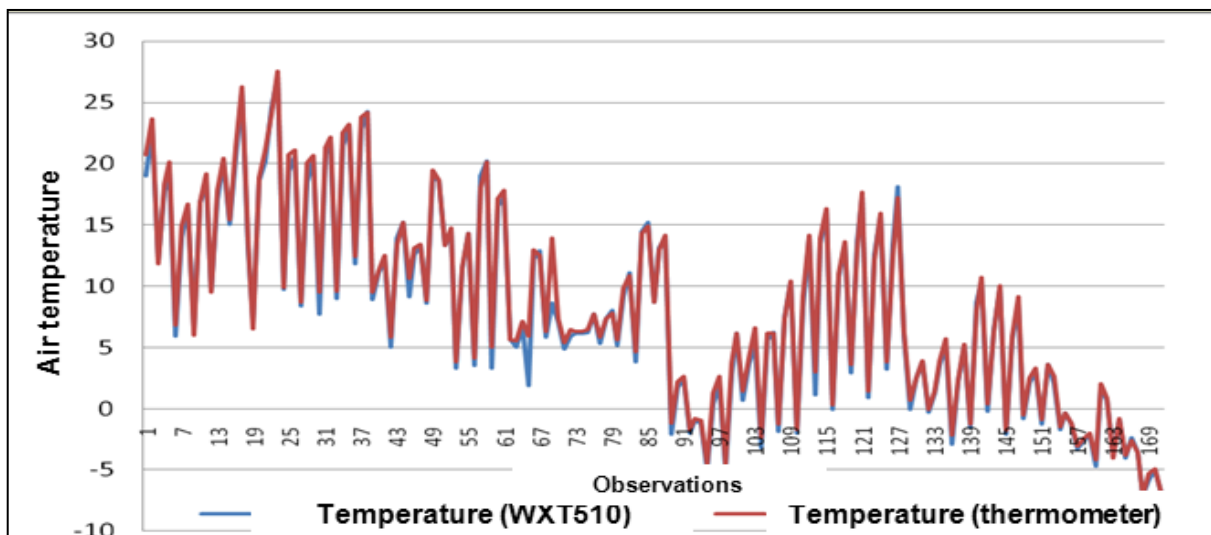


Figure 2.1.1.1. Air temperature graphs according to the data of the sensor WXT510 (blue line) and thermometer (red line) of the meteorological station HMO KRSU

The temperature deviation between the two devices, except for two cases, is in the range of -1°C to $+2^{\circ}\text{C}$. A mean value of the deviation and its mean-square deviation (MSD), as well as the asymmetry coefficient were calculated using the complete data set. Besides, the temperature series were divided into gradations 5°C , and for each gradation the statistical characteristics were calculated.

The average temperature deviation between both instruments is 0,4 ° C for the whole temperature range. Since the accuracy of the temperature sensor WXT510 and psychrometric thermometer is the same and about $\pm 0,3$ ° C, the deviation may be considered to be quite small at the average.

Relative humidity

Fig. 2.1.1.2. shows the relative humidity data from the sensor WXT510 (blue line) and psychrometer (red line) of the meteorological station HMO KRSU. Evidently the relative humidity measured with two different devices, are in bad agreement.

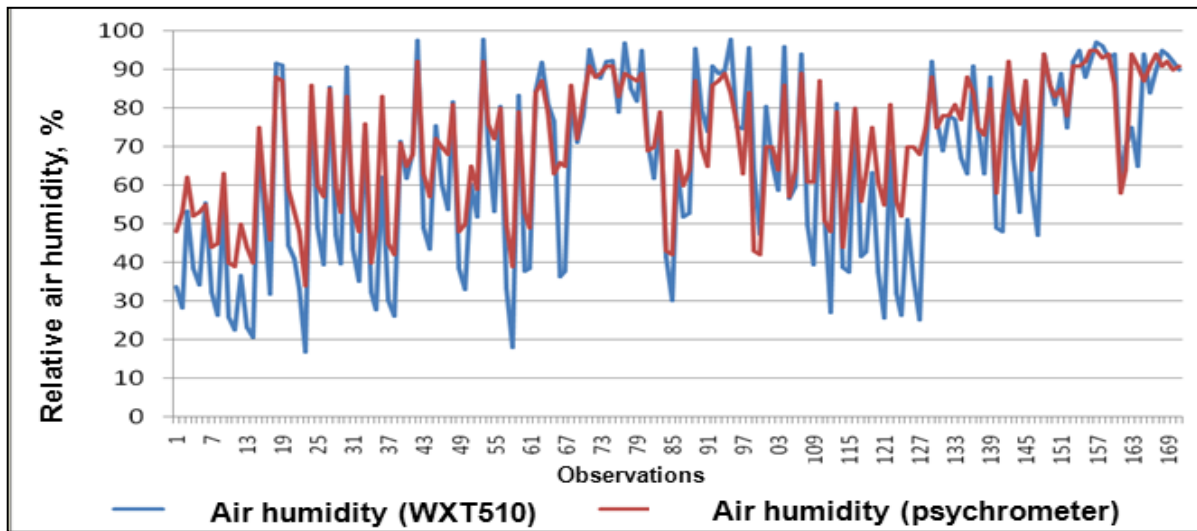


Figure 2.1.1.2. Graphs of the air relative humidity change according to the data from the sensor WXT510 (blue lines) and psychrometer (red lines) of the meteorological station HMO KRSU

Relative humidity measurement deviations are in a wide range from -21% to +42%. The comparative analysis of deviations shows that the deviations are largely dependent upon air temperature. Therefore, the average values, mean-square deviation values, and asymmetry coefficients were calculated for the whole observation series and on different air temperature gradations.

Atmospheric pressure

Atmospheric pressure graphs according to the data from the sensor WXT510 and station cistern barometer are in quite good agreement. Atmospheric pressure deviations are in the range from -2 hPa to +2 hPa.

The average air pressure deviation according to the barometer from the sensor WXT510 across the whole range constitutes -0.1 hPa, for different temperature gradations these deviations are in the range -0.5 ...+0.2 hPa. These values are within the accuracy range of the atmospheric pressure WXT510. Mean-square deviations for different series are large enough 0.4 ... 1.4 hPa. Empirical series of distributions have basically very strong, both the left and right asymmetry.

The results showed that temperature measurements of the two compared devices differ slightly, but these deviations do not exceed the measurement errors of these devices.

The relative humidity values according to the sensor WXT510 differ from the relative humidity value obtained by psychrometric observation within the range of measurement error of the instrument (6%). Relative air humidity measured by the WXT510 is highly dependent on air temperature. In the range of air temperature values -7°C to $+10^{\circ}\text{C}$ the humidity deviations according to both devices are observed to be minimal and constitute 1-4%. At higher air temperature (above $+10^{\circ}\text{C}$) the humidity values differ significantly and the average deviation reaches 14-18%.

The values of atmospheric pressure according to two compared devices are virtually identical, and the differences of the values are within the measurement accuracy of the pressure sensor WXT510.

Reference

1. <http://www.planet.elcat.kg/>
2. Vaisala Weather Transmitter WXT510. // User's Guide. - Helsinki, Vaisala Oyj, 2006. - 152 p.

2.1.2. High-elevation snow cover area assessment using GIS and remote sensing technologies

The purpose of this study is to consider a new approach in the assessment of snow cover area using GIS tools and digital information from the device AVHRR of the satellite NOAA [1].

Water resources are considered to be a special and strategic type of "raw material", particularly in those rapidly developing countries, where water consumption increases considerably. Water resources accounting, proper planning and rational management is required. Of particular importance is the solution of these problems for the region of Central Asia, including Kyrgyzstan.

This paper demonstrates the possibilities of the use of GIS tools and remote sensing data in the assessment of the area of snow cover, presenting the river basin Kara-Darya in the Kyrgyz Republic as a case study. The Kara-Darya river is a left tributary of the Syr-Darya river that flows across the Fergana Valley. The area of the basin above the Andijan reservoir is about 12,300 km², its height is from 0.8 to 5.0 km. The main river feeding is coming from seasonal snow and ice melting. Rainfall contributes significantly only to the formation of flashfloods [2].

Initial data for the analysis were the data of the five-band radiometer satellite imagery AVHRR from the hydrometeorological satellite NOAA.

To decode the satellite information about snow cover the AVHRR bands 1, 2 and 4 were used. As a software tool the programs ERDAS Imagine and ArcGIS were used.

Image processing was carried out in the program ERDAS Imagine:

CHAPTER 2. CLIMATE AND WATER RESOURCES

-the data reference was carried out by means of a digital elevation model, as well as images of the study area were obtained;

-three type - classification of images was conducted: cloudiness, snow and earth;

-the total snow cover area was determined.

Processed satellite images from the program ERDAS were loaded as an img-file into the program ArcGIS, which enables converting these files into the GRID-format. Calculations of snow line elevation head and snow-cover areas at high altitude zones were carried out in ArcGIS (Fig. 2.1.2.1).

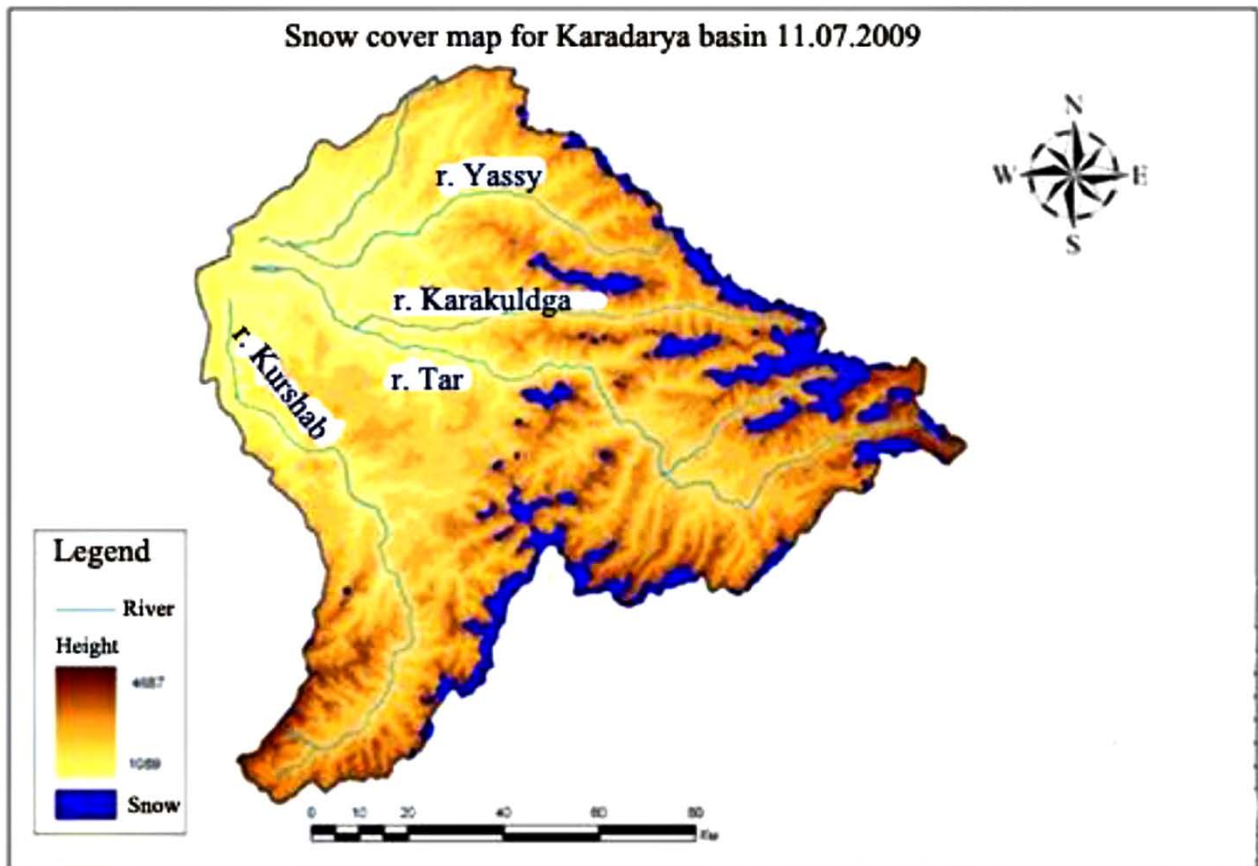


Figure 2.1.2.1. Map of snow-cover area in the Kara-Darya River for July 11, 2009

Thus, remote sensing data obtained from satellites can be rather successfully processed using GIS technology, and the results of the calculations applied practically. For example, for the purpose of conducting a mountain river runoff forecast, prevention of avalanche hazard, calculation of snow load, agriculture estimations and other cases.

Reference

1. <http://noaasis.noaa.gov/NOAASIS/ml/avhrr.html>
2. The Great Soviet Encyclopedia: Volume 30- M.: "Soviet Encyclopedia", 1969-1978.

2.1.3. Analysis of climate changes in Issyk-Kul lake basin

The importance of studying climate changes in the Issyk-Kul Lake depression is first of all due to the uniqueness of the region [12, 15] and its recreational significance. The first systematic studies of climate of the Issyk-Kul region have been started in the late XIX century (with an opening of the weather station Karakol in 1881 and in Balykchy in 1894). By the year 1949 already 10 operating and maintained meteorological stations were in the Issyk-Kul basin. From 1962 to 1979 the meteorological network was improved to a considerable degree. Some stations were closed or relocated, some new stations were opened. The total number of them remained practically unchanged (9 - 11 stations). Such a reorganization is not always, from our point of view, rational, this influenced the length and homogeneity of the observation series, what significantly effected data selection for our research.

From 1992 to 1999 six weather stations have been closed in the Issyk-Kul basin; today there are only four stations left. One of them - Chon-Ashu – is located at a height of 2800 m. This is station of Kyrgyzhydromet, which belongs to the department of the Ministry of Emergencies of the Kyrgyz Republic, and was responsible for hydrometeorological monitoring in the Issyk-Kul basin in the recent years. A wide meteorological monitoring coverage of the territory in the past allowed for many authors to conduct quite complete studies of climate in the Issyk-Kul region. The results were published in scientific papers; a detailed list of publications is given in [15]. This study aimed to continue previously performed research work and to analyze recent and possible future developments and changes of some climate indicators of the basin and their connection with water level of the Issyk-Kul lake.

For this purpose, the data on the average monthly air temperature and monthly precipitation totals have been collected. The choice fell on these indicators, since they are integral indicators of climatic conditions in the basin. When selecting the weather stations, the preference was given to the stations in Cholpon-Ata operating since 1928, and in Balykchy town, where continuous observations are available since 1927. These stations are located in the central and western areas of the Issyk-Kul region. Using such an approach there is an information gap for the eastern part of the basin, which is the area of heaviest precipitation and specific temperature regime. Unfortunately, the station Karakol (Prjevalsk) located in that area of the Issyk-Kul region that had conducted observations since 1881, was closed in 1997. Considering the importance of the contribution of the eastern zone to the lake water balance, we decided to take other precipitation and temperature data available for this region. The station Karakol was relocated in 1943, thereby interrupting the observation continuity. From 1932 to 1953 the station Karakol AMSG was operating in parallel with the station Karakol. The analysis of temperature and precipitation data for the period of the parallel operation of these stations shows that these data are weakly correlated and that it is not correct to integrate the data series obtained for the period before 1943 with the data series obtained after this period (1943 - 1997). For this reason we decided to use the data of the station Karakol only for the period of homogeneous observations, i.e. since 1943 (Fig. 2.1.3.1).

CHAPTER 2. CLIMATE AND WATER RESOURCES

Studying two climate indicators - precipitation and air temperature, we have observed the changes in the last decades according to three selected stations. For each of the stations the following values were calculated: the average annual, average winter (November-March) and average summer (April-October) air temperature and annual precipitation values. Linear trends of the data series were calculated using least squares method, considering the elements of the series to be independent. Fig. 4.1.11 shows the average annual, average summer and average winter temperature values for the station Cholpon-Ata for every moving five-year period for the years 1929-2007. A five-year window allows leveling the sharp drops on diagrams, identifying general variability trends and keeping the series sufficiently long. [4]

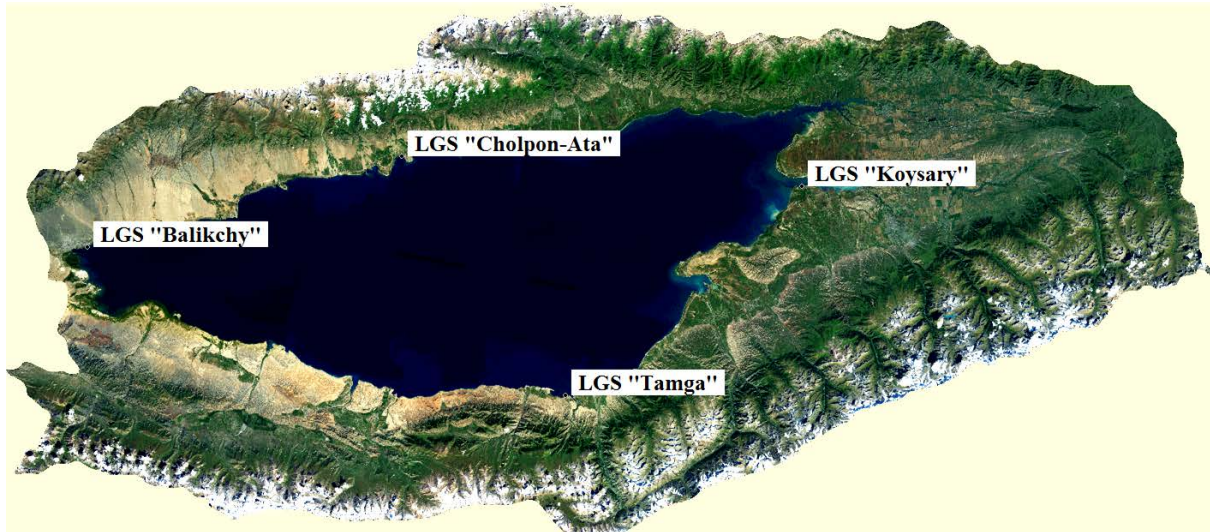


Figure 2.1.3.1. Issyk-Kul Lake basin and location of meteostations “Balykchy”, “Cholpon-Ata”, “Karakol”

The figure 2.1.3.1. shows that, on average, there is a continuous rise of the average annual air temperature values and also the summer and winter values. For the period of 79 years (1929 -2007), the average annual temperature was rising at an average of 0.027°C per year. Moreover, the rise of winter temperature ($0,034^{\circ}\text{C}$ per year), has contributed more to this temperature rise, than the rise of summer temperature ($0,021^{\circ}\text{C}$ per year). Similar calculations were carried out for the meteostations Karakol and Balykchy (Figure 2.1.3.1.). It turned out that for 53 years (1944 - 1996) in the town Karakol the average temperature was rising in the mean by 0.023°C per year, and the same is true (0.023°C per year) for Balykchy for the period of 79 years (1928 - 2006).

The second important climate element is precipitation. Figure 2.1.3.2 shows a long-term course of annual precipitation totals at the station Cholpon-Ata. It is clear that if the entire observation period is considered – the trend is positive. Similar situation is observed at the two other stations. Because the long-term average annual precipitation totals at the stations Balykchy and Karakol are different, we provide the values expressed in percent of average long-term totals (mm per year) for the entire observation period. The linear precipitation variability values at the station Karakol for the period 1944-1996 results to $1,7\text{ mm/year}$ (0.42% per year), while the result for the station Cholpon-Ata for the years 1929-2007 is 0.9 mm/year (0.34% in year) and the

CHAPTER 2. CLIMATE AND WATER RESOURCES

station Balykchy for 1928-2006 years is 0.5 mm / year (0.42% per year). Evidently the percentual increase of precipitation is comparable at all three stations.

A very important question is if it is possible to characterize a long-term climate change in the Issyk-Kul basin through observations only on one station? To some extent this can be judged by analyzing the observed data. For this purpose, pairwise correlation coefficients were calculated for average annual air temperature and annual precipitation between the three stations (Table 4.1.1). Apparently there is a rather good relationship between mean annual temperature values according to all three stations. At the same time, the interconnection between annual precipitation values is much worse, moreover, virtually there is no interconnection between precipitation values from the Karakol and Balykchy stations.

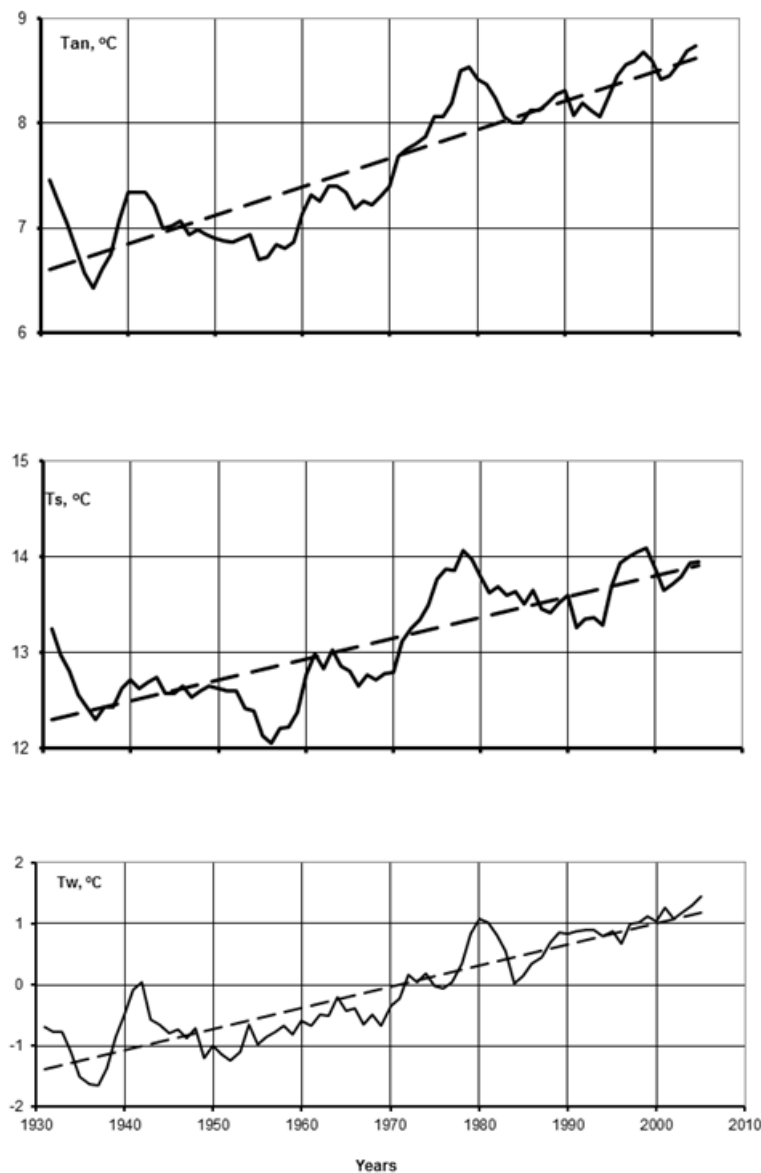


Figure 2.1.3.2. Long-term yearly average (T_{an}), average summer (IV-X) (T_s) and average winter (XI-III) (T_w) air temperature at station Cholpon-Ata. Initial series are smoothed by moving five-year periods. The dotted line shows linear trends.

CHAPTER 2. CLIMATE AND WATER RESOURCES

Thus, it can be concluded that each of the three stations reliably characterizes air temperature, but not air moisture.

It should be noted that similar calculations for these stations were carried out by us earlier [3], but at that time the observations series were considerably shorter and limited to the year 1976. Therefore, the results were significantly different from those listed in the Table 2.1.3.1.

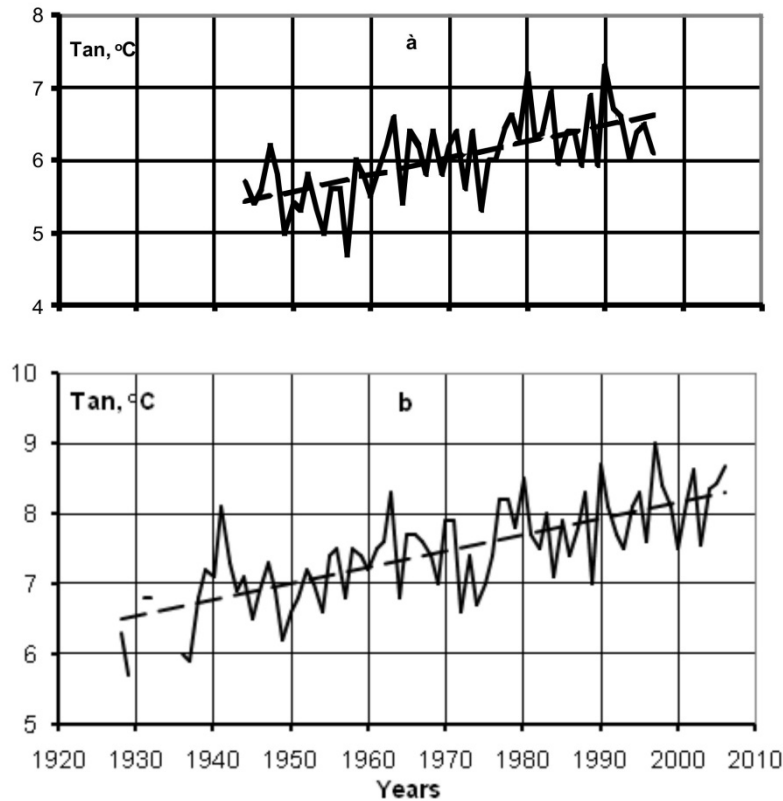


Figure 2.1.3.3. Long-term annual air temperature at stations Karakol (a) and Balykchy (b). Initial series are smoothed by moving five-year periods. The dotted line show linear trends.

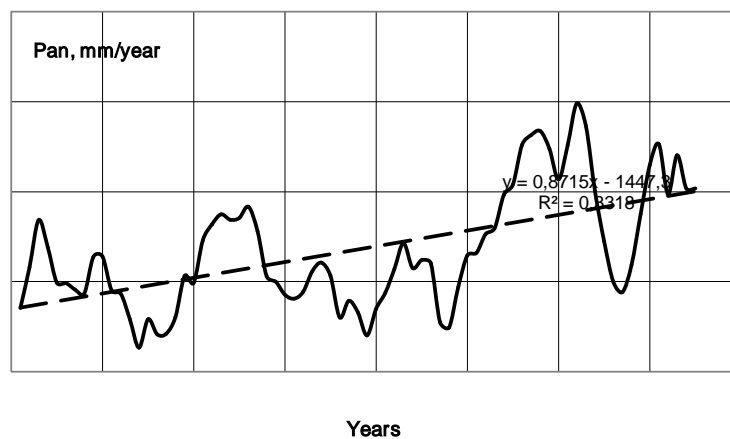


Figure 2.1.3.4. Long-term annual precipitation at station Cholpon-Ata. Initial series are smoothed by moving five-year periods. The dotted line shows linear trends.

CHAPTER 2. CLIMATE AND WATER RESOURCES

Table 2.1.3.1. Coefficients of mean annual air temperature and annual precipitation (in brackets) correlation between three station in the Issyk-Kul basin.

Station	Karakol	Cholpon-Ata	Balykchy
Karakol	1	0,877 (0,521)	0,880 (0,190)
Cholpon-Ata		1	0,838 (0,414)
Balykchy			1

The most important issue, both practical and theoretical, is the water level fluctuation in Issyk-Kul Lake, the connection of these fluctuations with climate and anthropogenic factors, and the forecast of lake level change in the future as well.

Instrumental observations of the water level of Issyk-Kul have been started in 1927 by the only existing station Balykchy. In 1947 already three gauging stations were operating in the lake basin, which, to a considerable degree, have contributed to the accuracy of the estimation of both average lake water level for a certain period, and water level for a certain date. For these calculations we used the data on water level for the period 1947-2007 at the end of each calendar year, as required by all water-balance calculations performed by Kyrgyzhydromet for Lake Issyk-Kul. To avoid random errors in the lake level values for the date - December 31, arisen from downsurge, upsurge, and seiche, we took a ten-day mean value for the water level at the end of year (from December 27 to January 5, [2,11]). Based on this values of water level changes for the whole year were calculated.

The next step was an attempt to find a correlation between water level changes of the lake and selected climate parameters (temperature and precipitation). It should be noted that such attempts were made repeatedly in the past [6, 9, 16, etc.]. The parameters varied during these investigations were climatic parameters, duration of the observation series, the number of involved stations, rates of economic activity, etc. The results obtained were rather different: starting from the findings about a total dependence of the lake level on climate factors [1, 18] to their secondary role under a suppressive influence of anthropogenic factors [6, 9].

We decided to focus only on the total annual precipitation and the mean annual air temperature for the following reasons. Annual precipitation characterizes the water inflow into Issyk-Kul Lake, which is composed of precipitation on the lake surface area, surface and groundwater flow into the water body. The effect of temperature is considered to be more complicated: on one hand with increasing temperature, the evaporation from the water surface increases and the water level in the lake decreases; on the other hand intensive ablation results in the increase of the glacier runoff, what leads to a lake level increase. Another important reason that influenced our choice is that for all scenarios of long-term climate change forecasts, annual precipitation and mean annual air temperature were used [5].

CHAPTER 2. CLIMATE AND WATER RESOURCES

Now we can return to the question of interconnection between annual changes of the lake level and average temperature and annual precipitation. It would be reasonable to calculate the interconnection of these values with the lake level change, but since the change rate of the Issyk-Kul lake does not exceed 1,4 % [10], we can confine our calculations to the level change values. When looking for such a connection, we could use only the data of the meteorostation Cholpon-Ata, because the Karakol station was closed 11 years ago, and the Balykchy station poorly characterizes the humidity of the basin. An attempt to use the data of the stations Balykchy and Cholpon-Ata for the calculations did not bring any improvement. Search of linear connections of annual water level changes with temperature and precipitation was carried out by the least square method using the data for the period 1947 - 2007. The dependence is described by the following equation (1):

$$dH_i = -20,3 + 0,112 \cdot Pan_i - 1,571 \cdot Tan_i, \quad (1)$$

dH_i – is the lake water level change for an i –year (from the 31 December of a previous year to 31 December of a current year)

Pan_i – is the annual precipitation totals according to the station Cholpon-Ata

Tan_i – is the annual average air temperature according to the same station. Correlation coefficient of original and calculated level change values turned out to be equal to 0,63.

We pay attention to the point that the precipitation coefficient sign is positive, and the temperature one is negative, what is quite logical. This shows the general trend of climatic parameters: the higher the annual precipitation, the higher the water levels, and the higher the temperature, the lower the water levels.

The obtained relation can be considered to be sufficiently close for this rough calculations not taking into account many other influences (wind speed, solar radiation, humidity, etc.), as well as the impact of economic activity.

Similar calculations can be performed using as variables not the air temperature and precipitation values themselves, but their normalized values:

$$\frac{Pan_i - Pm}{\sigma Pan} \quad \text{и} \quad \frac{Tan - Tm}{\sigma Tan} .$$

Here Pm – is the average long-term precipitation amount,

Tm – the average long-term air temperature

σPan и σTan – are the average quadratic deviations of the respective values. The quality of the dependence does not change, but it is possible to estimate a relative contribution of fluctuations of each argument to the relation equation. A relative contribution of precipitations appeared to be 6 times larger than of the air temperature. This can be explained by the different effect of temperature on the water balance of the lake, as stated above.

CHAPTER 2. CLIMATE AND WATER RESOURCES

One of the most pressing issues regarding Issyk-Kul is the question about possible future lake water level changes. Attempts to forecast the water level were made starting from the 70-ies to 2000 [6, 13, 14]. Unfortunately, all the attempts were not successful.

The forecast of water level for a quite long period after the year 2000 is available only in two known publications: - that is [15] with a forecast available till 2033, where the lake level is told to be 1605.6 m, and [7], which shows the calculations for the year 2028 (1606.1 m) and 2078 (1605.3 m). The latter work provides the equation enabling calculation of the level for any year till the year 2078.

Our equation (1) allows calculating the future changes of the level of Lake Issyk-Kul, if future climate changes are known (mean annual air temperature and annual precipitation).

Currently, there are many long term climate change forecasts. These expected climate changes vary over a wide range. In particular, the temperature rise in Kyrgyzstan by 2100, with respect to the norm of 1961-1990, is expected to constitute 1,8-4,4 ° C, while the forecasted precipitation change is in the ranges from -6% to +54% [5].

We decided to limit our calculations till the year 2050. Since the range of forecasted climate change variability by 2050 is wide, we made calculations on three change values - 0,5; 1,5 and 2,5 °. Two trends of precipitation change were observed a) a monotonous at a rate equal to the trend over the last decade (0.915 mm / year), since most of scenarios show an increase in precipitation in the future [15, 17, etc.]; b) a constant and equal to the average value over the last 20 years (1978-2007 gg.) - 294 mm / year, because during this period the amount has not increased in Cholpon-Ata and Balykchy.

Both annual precipitation and temperature fluctuate from year to year. The existing climate change scenarios provide only some values for the end of a forecast period. In other words, we had to use only monotonous temperature and precipitation change values from year to year, which are quite unreliable. Thus, the only thing that can be forecasted for possible climate change scenarios is a general trend of changes of the level of Lake Issyk-Kul.

On fig. 2.1.3.5, provides calculated using the equation (1), level changes from 2007 to 2050, under monotonously increasing and unchanged precipitations for three scenarios of temperature changes for the end of the estimated year. As is seen from the figure, in case of monotonous increasing precipitation: if the temperature increases by 0.5 ° C, the level of Lake Issyk-Kul in 2050 will rise by 98 cm, if the temperature increases by 1.5 ° C, the level will rise by 63 cm, and if the temperature growth constitutes 2.5 ° C, the lake level will only rise by 29 cm.. If the annual precipitation amount remains unchanged, while the temperature rise is the same (0.5, 1.5 and 2.5 ° C), the level of Lake Issyk-Kul in 2050 will decrease respectively by 38, 73 and 107 cm.

We express our deep gratitude to Prof. G.E. Glazyrin for recommendations and useful discussion of obtained results.

CHAPTER 2. CLIMATE AND WATER RESOURCES

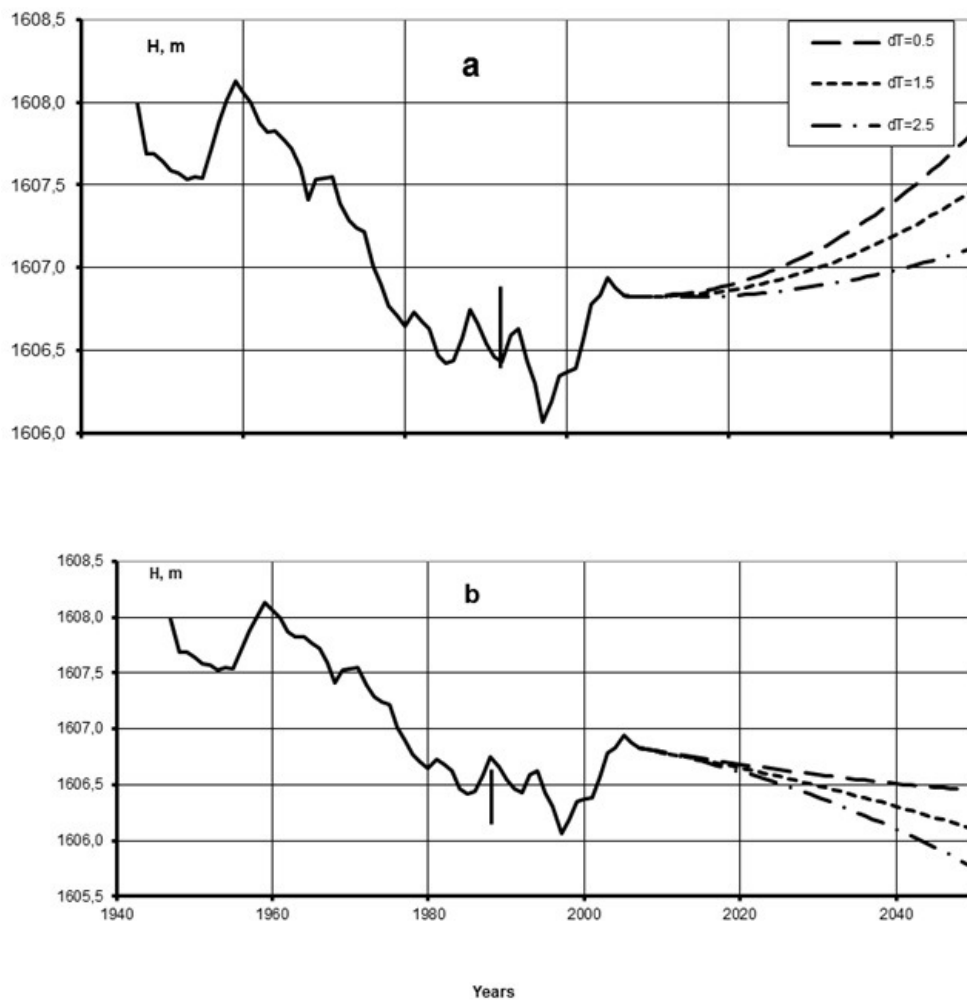


Figure 2.1.3.5. Real (up to 2007) and forecasted change of the level of Issyk-Kul Lake under different long-term climate change scenarios by the year 2050: a) as a result of monotonous increase in annual precipitation amount; b) as a result of unchanged precipitation rate. Examples of temperature changes are shown in legends.

Thus, all three meteorological stations located in the Issyk-Kul basin show a monotonous increase of mean annual, summer and winter temperatures. In general, the annual precipitation rate year over the past half century has been growing by about 0.4% per year. However, in the last 20 years, according to data of the stations Cholpon-Ata and Balykchy it remains constant.

None of the stations separately can provide sufficiently reliable characteristics of the climate of the basin, particularly with respect to precipitations. Annual changes in water level in lake Issyk-Kul are well described by a linear function which has the annual precipitation and mean annual air temperature as arguments. Correlation quality can be considered quite good, taking into account the fact that the calculations were made using only the data of one meteorological station. The relative contribution of changes of annual precipitation to the changes in the level of Issyk-Kul is 6 times higher than the contribution of changes in mean annual air temperature.

Clarification of long-term forecasts of climate change will enable to estimate the water level change in the lake more precisely.

Reference

1. Bolshakov M.N. Against the hypothesis of anthropogenic lowering the level of Lake Issyk-Kul in the twentieth century // Proceedings of the Academy of Sciences of Kirghiz. SSR. – 1982. - № 4, - p. 20-25.
2. Glazirin G.E., Stavisskiy Y.S., Shabunin G.D. A new approach to the study of the water balance of the Issyk-Kul lake. – SARNIGMI Proceedings, 1980, vol. 77 (158) p. 57-63.
3. Glazirin G.E., Glazirina E.L., Shabunin G.D. Statistical characteristics of some indicators of climate Issyk-Kul basin. - Proceedings SARNIGMI, 1982, Issue 87 (168), p. 30-40.
4. Glazirin G.E., Grupper S.R. Tashkent climate and its changes in the XX - beginning of XXI century. Tashkent, Ed. NIGMI, 2008. – 52 p.
5. Global environmental conventions: Opportunities Kyrgyzstan, Issue Brief, Bishkek, 2004. -155 p.
6. Gronskey T.P. Water balance and the expected water levels of Lake Issyk-Kul: Author. Diss. Candidate. of Geogr. Sciences. – Leningrad, 1983. – 16 p.
7. Denisov V.M. About a long-term decrease in the water level of Lake Issyk-Kul. - Proceedings SARNIGMI, 1981, issue. 81 (162), - p. 43-52.
8. Dikih A.N. Glaciation of the Issyk-Kul basin and its flow formed role. Nature and people of Kyrgyzstan, a special edition of "Biosphere Territory Issyk-Kul", Bishkek, 2000, p.32-33.
9. Krivoshey M.I., Gronskey T.P. Water balance of Lake Issyk-Kul // research problems in large lakes of the USSR. L.: Science, 1986. – p. 276-280.
10. Kuzmichenok V.A. Estimation of some detailed morphometric characteristics of Lake Issyk-Kul // Study hydrodynamics of Lake Issyk-Kul using isotopic methods. Part 1 -Bishkek Ilim, 2005. p. 64-80.
11. Lake Issyk-Kul / ed. I.V. Molchanov. - L.: Gidrometeoizdat 1946. -148 p.
12. Nature and people of Kyrgyzstan, a special edition of "Biosphere Territory Issyk-Kul", Bishkek, 2000. -59 p.
13. Ratkovich D.Y. Water balance and level regime of the Issyk-Kul Lake // Water Resources. -1977. – Volume 5. –p. 20-33.
14. Romanovskiy V.V. The course of the Lake Issyk-Kul level to the year 2000 and the impact on his business activities // Coastal zone of Lake Issyk-Kul. - Frunze: Ilim, 1979. – p. 34-50.
15. Romanovskiy V.V., Kuzmichenok V.A., Mamatkanov D.M., Podrezov A.O. All about the Issyk-Kul Lake in the questions and answers. Bishkek, Ed. Kyrgyz-Russian Slavic University, 2005. – 406 p.
16. Heyphed M.N. The reasons for reduction the lake level over the past decade. - Proc. Lake Issyk-Kul. -Frunze, Ilim, 1978. – p. 117-121.
17. Chub V.E. Climate change and its impact on the natural resource potential of the Republic of Uzbekistan. -Tashkent, SANIGMI, 2000. -252 p.

18. Shnitnikov A.V. Water resources of Lake Issyk-Kul // Water Resources. – 1977. – Volume 5. – p. 5-19.

2.1.4 Assessment of the present-day regime of the surface temperature of the Issyk-Kul lake using MODIS/TERRA data

Temperatures of water reservoirs are extremely important characteristics determining many details of functioning. It determine almost all physical and biological processes in a reservoir: hydrodynamics, species and quality composition of hydrobionts, trophic state of the water. The main objective of this work is to obtain average long-term, average monthly and average annual temperatures of the Issyk-Kul lake surface on the basis of data provided by the MODIS tool of the TERRA satellite. The work includes the results of MODIS data verification by field studies, estimations of average monthly and average annual surface temperatures of the lake for a long-term period, comparison of obtained data with data of previous years.

Issyk-Kul lake is a mountain lake located approximately at 770 east longitude and 420 north latitude, in the northern part of the Tien Shan mountain belt in the Kyrgyz Republic (Central Asia). It is situated at 1607 m above sea level and surrounded by high mountain chains: Kungei Alatau chain in the north reaching 4770 m and Terskei Alatau in the south with peaks of 5200 m.

According to the First National Communication of the Kyrgyz Republic, in average for the entire territory of Kyrgyzstan the average annual temperature in the twentieth century in terms of 100 years rose by 1.6 0C, that is much higher than the global warming of the Earth, equal to 0.75 0C for this period of time. And for the Issyk-Kul hollow the increase of the average annual air temperature for this period was 2.4 0C [6].

The climate warming in the Issyk-Kul region, outlined since the 60s of XX century, influenced the lake temperature. An increase of the surface temperature in the inshore zone is recorded by lake hydrological posts since 1975. Thus, according to Romanovski V.V. and Shabunin G.D. [4] the increase of February temperature of water at the Tamga lake post from 1975 to 2001 was 0,8 0C. And according to Romanovski V.V. and Shabunin A.G. [5] the temperature of deep water increased by 0,5 0C from 1981 to 2005.

Observations of the thermal regime of the Issyk-Kul Lake in the 60s - 80s of the last century were made by the Department of the Hydrometeorological Service of the Kyrgyz SSR (DHMS) on the basis of monthly thermal surveys on eleven vertical profiles confined to the central part of the reservoir, and later, on six vertical profiles located in eastern and western parts of the lake [8].

In addition, the observation of the surface water temperature of the lake was conducted on the lake DHMS posts located around the perimeter of the pond. Currently, thermal survey of the lake surface is not conducted (due to lack of funds) and out of previously functioning lake posts, only four are still active. Episodic studies on the water area are

CHAPTER 2. CLIMATE AND WATER RESOURCES

conducted under some international projects such as the KR 330.3 "Study of hydrodynamics of Issyk-Kul Lake using isotopic methods", in the framework of which, in 2003-2005, an international group of scientists (with the participation of the authors of this paper) made lake water temperature measurements at different depths, on some standard DHMS verticals.

All of these suggests the need to develop new approaches and methods for studying the temperature regime of the lake. This work shall evaluate the potential of satellite technologies, in particular MODIS tool located on the TERRA satellite, for this kind of studies.

The spectroradiometer MODIS (Moderate Resolution Imaging Spectroradiometer) is a key tool of the American satellites EOS (Terra (EOS AM-1) and Aqua (EOS PM-1)). MODIS has 36 spectral channels with 12-bit radiometric resolution in the visible, near-, mid-and thermal infrared ranges [1].

One of numerous products produced on the basis of MODIS is Sea Surface Temperature (SST) [3]. This product is distributed by the NASA through Ocean Color site [2] and has the following key features: spatial resolution of 1 km (with Issyk-Kul area of over 6000 km² it enables about 6000 simultaneous measurements of water area); measuring range from -2 0C to +32 0C (which is acceptable for the lake); measurement error (stated by the producer) + / - 0.4 0C (which is also more than acceptable for this kind of research.)

The primary data during this work was the MODIS/TERRA data on Sea surface temperature (SST), provided by the NASA and Ocean Color Group upon request for the study area, for the 13-year operation of the radiometer (February 2000 to March 2013). Sampling of the data and their geolocation was made by the Ocean Color Group, after which the processed data were delivered.

To verify the SST data, we used DHMS data of thermal surveys on the lake surface, the measurements on water temperature at lake posts provided by the Agency for Hydrometeorology under the Ministry of Emergency Situations as well as measurements of the surface water temperature obtained in the framework of the project KR 330.3.

DHMS data of thermal surveys on the lake surface were also used to compare the average long-term and average annual temperatures of in-situ measurements with MODIS data reflecting the actual characteristics of surface water temperatures in the lake.

Methodology

The first phase of the work included verification of the MODIS data according to in-situ measurements of the surface temperature of the lake water. At this stage, the referencing of location of lake posts and DHMS standard verticals on the lake surface in the geographic coordinate system of WGS-84 (used for MODIS data) was made (Fig. 13). At the same time 9 DHMS verticals on the lake surface were chosen, which were

CHAPTER 2. CLIMATE AND WATER RESOURCES

also investigated under the project KR 330.3 in 2003-2005 (the other remaining verticals were measured in the 60s - 80s of the last century and, therefore, could not be used for comparison).

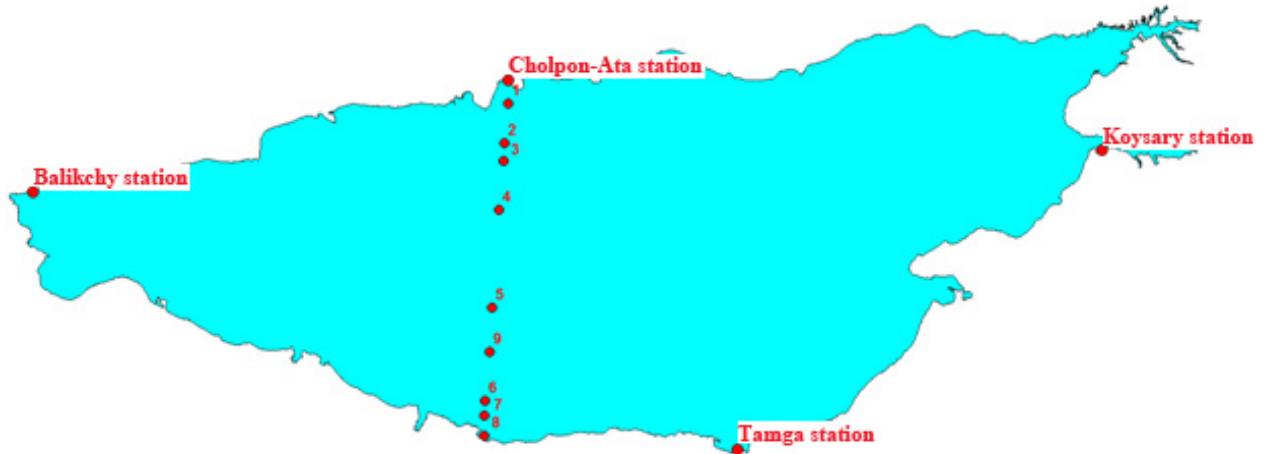


Figure 2.1.4.1. Location of lake posts and DHMS standard verticals on the lake surface used for verification of MODIS data

Next, the sampling of measurements of water temperature at these points was carried out and these data were compared with the data obtained for the same dates through MODIS observations. And in the final phase the average and maximum deviations were analyzed.

In the second stage of work the average monthly and average annual surface water temperatures based on MODIS data for the period of 2000-2013 on certain verticals were calculated. In addition, 5 verticals corresponding to the northern, western, eastern, southern and central part of the lake were chosen, on which measurements were carried out by DHMS during thermal survey.

In order to obtain the average characteristics of the surface temperatures of the lake at selected verticals, all available MODIS measurements relating to the points closest to the verticals were processed.

The third stage of the work concentrated on the average surface temperatures for the entire water body. For this, MODIS data were selected for the middle of each month (15th or closest to it) under conditions of the lowest cloudiness. To select the correct measurement points, extreme ranges of variation of lake surface temperatures for each month were determined (Table 1).

Introduction of limits for the temperature range allowed us to exclude such values from further processing that didn't relate to the lake surface, as well as the values observed in clouded areas (these values are negative or clearly distorted in MODIS data). Further, by summing up the values and dividing them into the number of measurements, the average temperature of the date of the survey was derived. This value, with some degree of acceptability, was taken as the average monthly

CHAPTER 2. CLIMATE AND WATER RESOURCES

temperature of the lake surface in a given month. Then, based on these data, the average annual surface temperatures of the lake water were calculated.

Table 2.1.4.1. Extreme values of temperatures for each month, °C

month	I	II	III	IV	V	VI
t, 0C	0,0-10,0	0,0-9,0	0,0-12,0	3,0-17,0	4,0-20,0	10,0-23,0
month	VII	VIII	IX	X	XI	XII
t, 0C	14,0-25,0	15,0-26,0	13,0-24,0	6,0-21,0	6,0-18,0	0,0-13,0

At the final stage of the work, we compared the data for previous years 1963-1978 and 1968-1978 received as a result of DHMS thermal survey with modern MODIS/TERRA data (2000-2013). For the comparison we used the average long-term and average annual data obtained previously [8] through the DHMS thermal survey and the same values obtained as a result of this work.

On the basis of MODIS/TERRA data, changes in temperature of the surface water of the lake were also analyzed for the 12-year measurement period (2001-2012).

Results of MODIS data verification according to data from the lake posts of Kyrgyzhydromet, at sufficiently high correlation coefficients, showed significant differences in the absolute values of temperatures, and therefore, this verification was not confirmed. In our opinion, this is due to the proximity of the land and, consequently, the introduction of errors to the signal by reflecting from dry surfaces.

The results of MODIS data verification with data received under the project KR 330.3 showed good accordance both on the correlation coefficient and the absolute values: the correlation coefficient was 0,98; average difference -0,35 0C, the maximum difference 3 0C. A good indicator for MODIS data verification according to these data is that in-situ measurements were carried out in all seasons.

MODIS data verification results show that these data are fully applicable to continue the series of measurements of surface temperatures (Figure 2.1.4.2), to derive the average characteristics of the lake surface temperature and to use them for other practical tasks.

It should be noted that the accuracy of the MODIS data verification by instrumental observations adversely is affected by several factors. The main ones are: the absolute difference of the measurement procedure, a small number of compared values (80 values of the surface temperature), the measurement time (at diurnal temperature up to 2 °C, wherein the time shift might be up to 2 days), the place of measurement (in this case, the MODIS value closest to the vertical was used, while the horizontal displacement could reach 0.5 km).

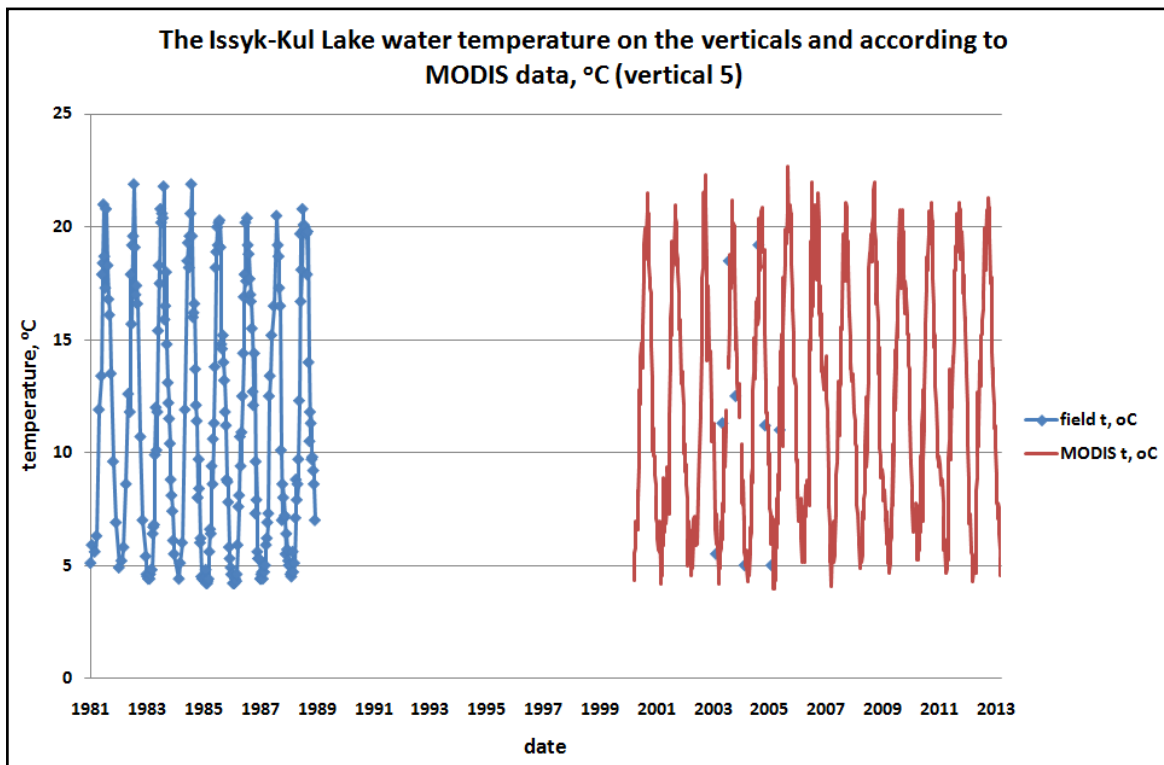


Figure 2.1.4.2. Example of continuation of series of in-situ temperature measurements on the basis of MODIS data

Thus, the verification results showed very good accordance that suggests to use this method for such studies. With the help of MODIS data, average monthly and average annual values of surface temperatures of the lake for 5 selected verification verticals were obtained. Analysis of the data showed that the average annual temperatures in all parts of the lake were 12-13 °C and are within the in the range (11,5-13,6 °C). The northern part of the lake is the warmest, with an average long-term annual temperature of 13.0 °C, followed by the eastern and southern parts where this value is 12.7 °C and 12.6 °C, respectively, then the western part with the average long-term annual value of 12.3 °C, and the coldest part is the central part of the lake with 12.1 °C. The highest average annual temperature variation is in the northern, western and eastern parts of the lake, while in the southern and central parts it is minimal, which is obviously related to the great depth of the lake in these areas. Maximum average monthly temperatures for all parts of the lake are observed in August (19,1-22,1 °C) and the minimum in February (3,8-7,0 °C).

Figure 2.1.4.3 shows an example of constructing the field of surface temperatures over the Issyk-Kul lake. Average annual temperatures for the entire lake are 12-13 °C and are in the range (12,2-13,2 °C). Average long-term and annual value, in this case, is 12.6 °C, which agrees well with the earlier data for the individual parts of the lake. The maximum average monthly temperatures for the individual parts of the lake, are observed to be 20.8 °C in August, 5.6 °C in February. Average long-term, annual and monthly values of water temperature for the entire lake are close to those values for the southern part.

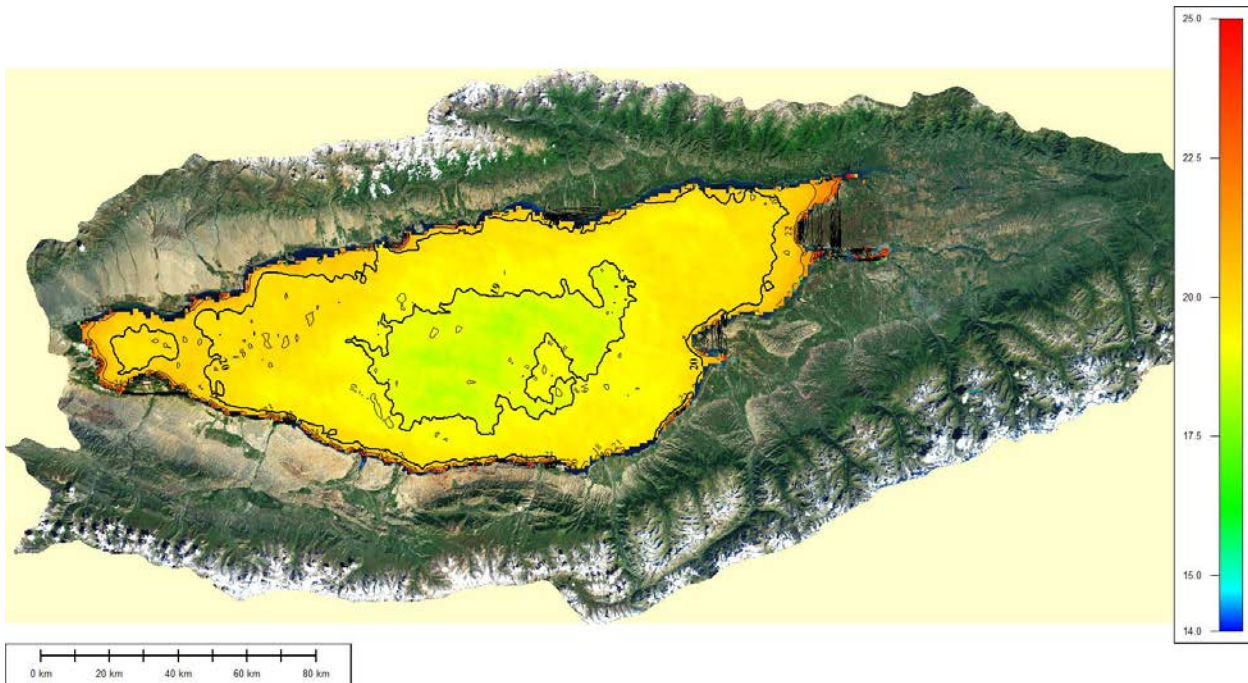


Figure 2.1.4.3. Example of constructing the field of surface temperatures for Issyk-Kul lake

At the final stage of work, a comparison was made between average long-term, average monthly and average annual surface temperatures for the periods of 1963-1978, 1968-1978 and 2000-2013. The data are presented in Table 4.3.5.

Table 2.1.4.2. Comparison of average long-term and average annual surface temperatures for the periods of 1963-1978, 1968-1978 against 2000-2013

Vertical number	Period			Difference
	1963-1978	1968-1978	2000-2013	
Vertical 1 (north)	11,7		13,0	+ 1,3
Vertical 6 (south)	11,5		12,6	+ 1,1
Vertical 31 (west)		11,0	12,3	+ 1,3
Vertical 28 (east)		11,5	12,7	+ 1,2
Vertical 26 (5) (center)	10,8		12,1	+ 1,3
Average		11,3	12,5	+ 1,2

The table above shows that the MODIS/TERRA data demonstrate a rise in the surface water temperature of the of Issyk-Kul lake in the 30-35-year period since 1978 by 1.2 °C. Moreover, this increase occurred almost equally in all parts of the lake.

It should be mentioned once again that in obtaining these data completely different techniques were used that undoubtedly introduced some minor mistakes in the results of comparison. However, good MODIS data verification indicators and their relative homogeneity and consistency with the measured data (maximum values on vertical 1 and minimum values on vertical 26 for both observation periods, a steady increase in

CHAPTER 2. CLIMATE AND WATER RESOURCES

temperature for all parts of the lake, etc.) allow us to speak about the high reliability of these data.

To estimate the change in temperature of the surface waters of Issyk-Kul lake and in order to avoid uncertainties caused by methodological approaches in the measurements, average annual MODIS data for the 12-year period of measurements (2001-2012) were analyzed. The results of this evaluation are shown in Figure 2.1.4.4.



Figure 2.1.4.4. Trends of average annual surface water temperatures of Issyk-Kul lake as per MODIS/TERRA data for the period of 2001-2012

As can be seen from the figures, most of verticals show positive trends of average annual surface temperatures of the lake. The highest (about 0.5 °C) are presented on verticals 1 and 26 - the northern and central part of the lake, respectively. For the eastern part of the lake (vertical 28) as well as for the entire lake as a whole, the trend is also positive, although it is not so pronounced (about 0.1 °C). On vertical 6 which

CHAPTER 2. CLIMATE AND WATER RESOURCES

corresponds to the southern part of the lake there is almost no trend, and for vertical 31 it is even negative (about -0.05°C).

Due to the lack of funding for field monitoring in state institutions and the accompanying reduction of the ground observation network, remote sensing (RS) techniques are of growing importance. These methods, despite all its disadvantages, have several advantages such as large area coverage, data availability, etc. These advantages can effectively be used in the work with relatively flat surfaces i.e. large lakes.

This work assessed the applicability of RS data, in particular MODIS/TERRA data, to study the thermal characteristics of the surface of Lake Issyk-Kul. Options for practical use of the data for further research were shown.

Results of MODIS data verification with the measured field data showed a good accordance, both on the correlation coefficient (0.98) and on the average and the maximum differences (-0.35°C and 3°C respectively).

Analysis of the data showed that the average annual temperatures in all parts of the lake are $12-13^{\circ}\text{C}$ and are within the limits ($11,5-13,6^{\circ}\text{C}$), the maximum average monthly temperatures for all parts of the lake are observed in August ($19,1-22,1^{\circ}\text{C}$) and the minimum in February ($3,8-7,0^{\circ}\text{C}$). Average annual temperatures for the entire lake are, on average, $12-13^{\circ}\text{C}$ and are within the limits ($12,2-13,2^{\circ}\text{C}$).

In addition, the MODIS data show an increase in surface water temperature of Issyk-Kul Lake for the 30-35-year period since 1978 by 1.2°C .

Also, MODIS data have positive trends of surface water temperature during the period 2001-2012, both for the greater part of the lake and for the lake as a whole. The size of the trend for change in the surface water temperature for the entire lake during this period has a value of about $0.1^{\circ}\text{C} / \text{a}$.

All these suggest the need to develop methods of remote sensing the Earth's surface parameters (including verification of RS data by ground-based data) and to assess wider applications for practical use.

Reference

1. <http://modis.gsfc.nasa.gov>
2. <http://oceancolor.gsfc.nasa.gov/cgi/browse.pl>
3. http://oceancolor.gsfc.nasa.gov/DOCS/modis_sst/, K.A. Kilpatrick et al., J. Geophys. Res. 106, 9179-9197 (2001)
4. Lake Issyk-Kul: Its Natural Environment. IV. Earth and Environmental Sciences -Vol. 13, 2002. – 302 c.
5. Romanovsky V.V., Shabunin A.G. «Study of the processes of water circulation in the Issyk-Kul Lake with the use of hydrological and isotopic data» // Coll. «Study of the Issyk-Kul Lake hydrodynamics with the use of isotopic methods» - Part II – Bishkek: Ilim, 2006. – C. 13-20.

CHAPTER 2. CLIMATE AND WATER RESOURCES

6. First National Communication of the Kyrgyz Republic on the UN Framework Convention on Climate Change. - Bishkek, 2002. – p.97.
7. Romanovsky V.V., Kuzmichenok V.A., Mamatkanov D.M., Podrezov A.O. All about Issyk-Kul lake in questions and answers. Bishkek, Kyrgyz-Slavonic University, 2005. – p.406
8. Shabunin G.D. Long-term characteristics of temperature regime of Issyk-Kul lake. – News of Academy of Science of Kyrgyz SSR, 1982, edition 3, p.39-46

2.1.5. Atmospheric dust monitoring station

An atmospheric dust monitoring station was installed at the northern slopes of Tien Shan, 40 km southwards of Bishkek, at a height of 1750 m above-sea level.

The station was installed by German researches from GFZ Potsdam together with researchers from the Central Asian Institute for Applied Geosciences (CAIAG) of the section “Climate, Water and Geoecology” and from the Russian Station of the Academy of Sciences [2] (Figure. 2.1.5.1).



Figure 2.1.5.1. Atmospheric dust monitoring station

Under the joint project between these organizations, the programme of dust control and related meteorological measurements was launched in June 2010.

Meteorological parameters and concentration of dust particles in the atmosphere are continuously measured for 32 particle size values, with a time interval of 1 minute. The mineral aerosols with a particle size of more than 2 micrometer, are automatically collected on filters for subsequent mineralogical, chemical and isotopic investigations [1, 3].

CHAPTER 2. CLIMATE AND WATER RESOURCES

Research results obtained from the analysis of dust samples and associated meteorological parameters and dust concentration values in the atmosphere are necessary as a solution of questions related to paleoclimate variability in Central Asian region, the influence of modern dust transport in the atmosphere on climate conditions, glacial and hydrological systems.

Results of primarily processed data and data analysis are shown on Figures 2.1.5.2 - 2.1.5.6.

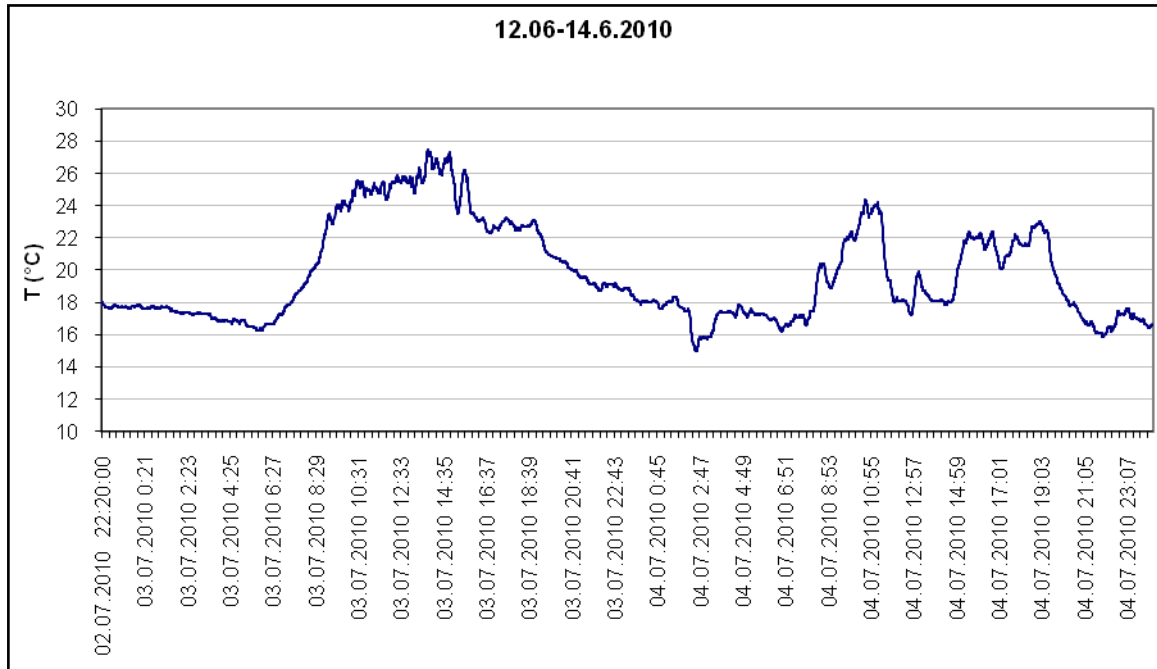


Figure 2.1.5.2. Air temperature

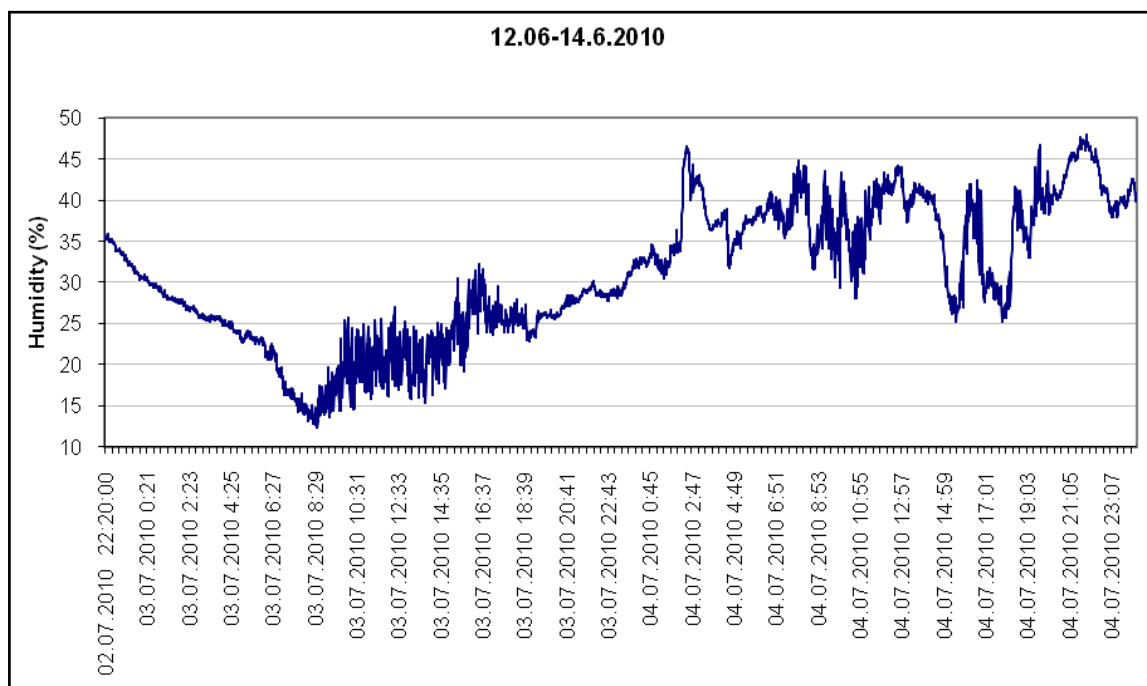


Figure 2.1.5.3. Air humidity

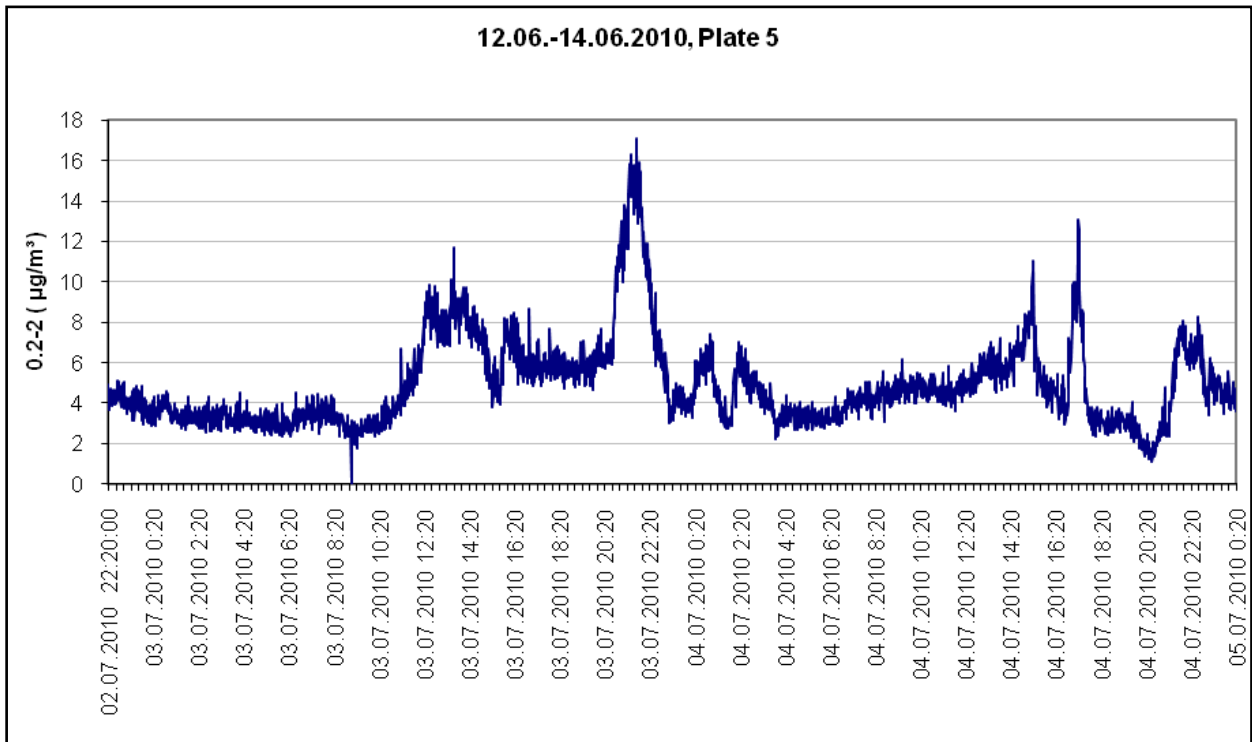


Figure 2.1.5.4. Content of particles with a size 0,2-2,0 µm in the atmosphere

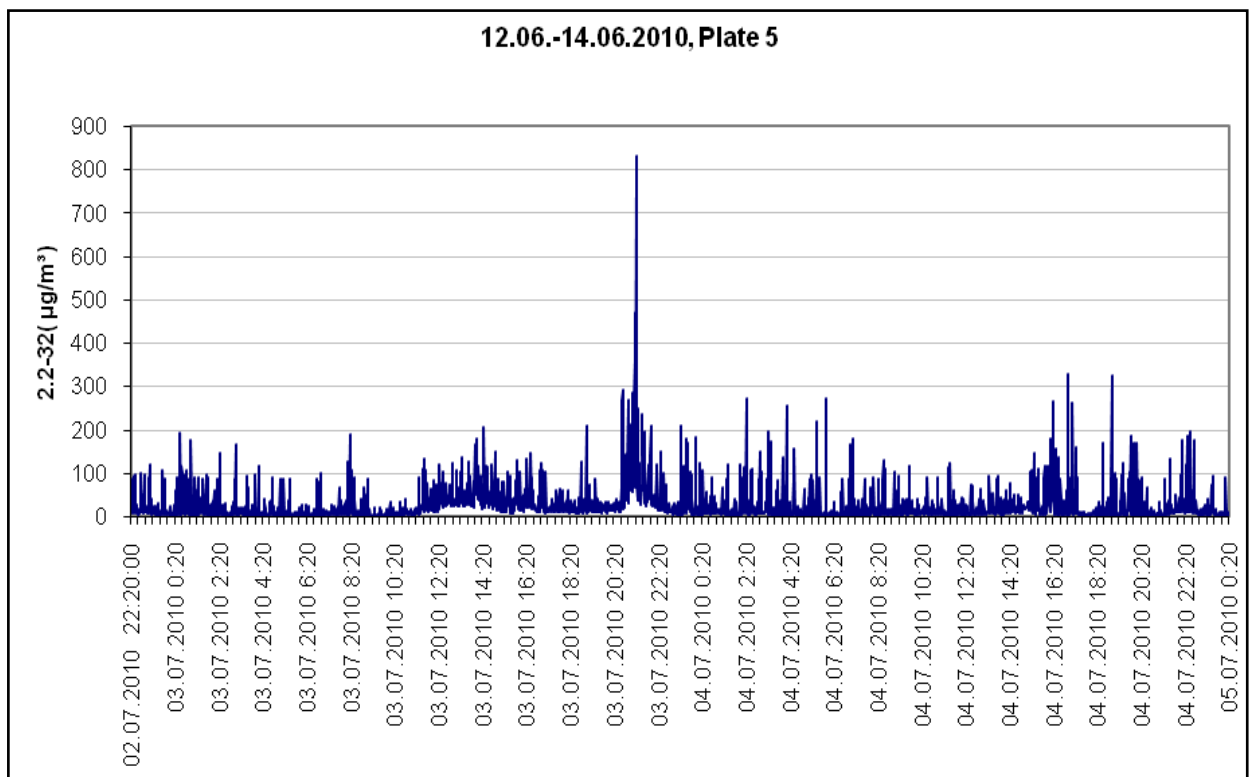


Figure 2.1.5.5. Content of particles with a size 2,2-32,0 µm in the atmosphere

Currently preliminary research findings are available, but related activities undoubtedly have a great potential and are of a profound interest both in terms of a direct analysis of dust in the atmosphere, and in terms of its influence on glacier melting, underlying surface pollution, and population health as well.

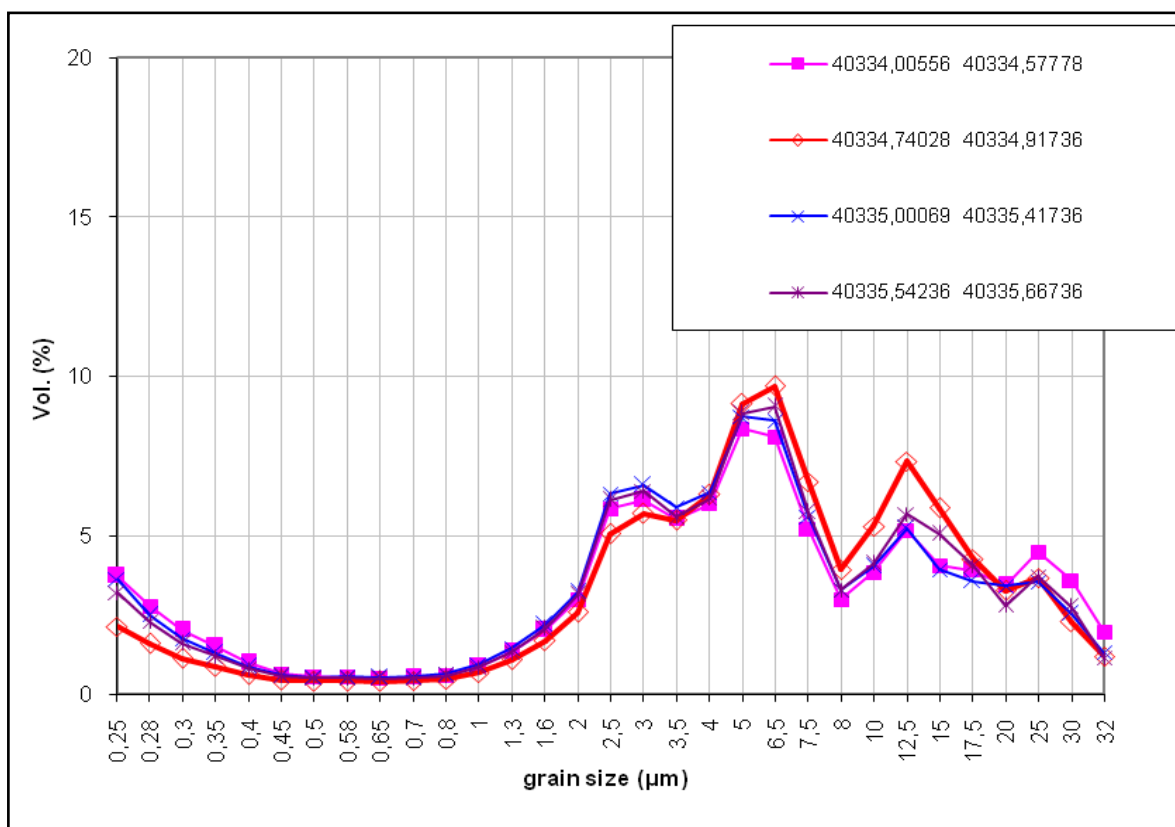


Figure 2.1.5.6. Particle size classification

Reference

1. Aerosol Dust Monitors & Counters. - GRIMM Aerosol Technik GmbH & Co. KG, 2005. - 44 p.
2. <http://www.gdirc.ru/>
3. Kleinfiltergerät LVS 3.1/MVS 6.1 // Ingenieurbüro Norbert Derenda - Germany, 2009. - 53 p.

2.2. A comprehensive study of the mountain glaciers dynamics

Glaciers are one of the components of water resources in Kyrgyzstan, their volume is 495 km³, and total number is around 5237. Glaciers provide a long-term accumulation of atmospheric ice precipitations and also following input to the river runoff. In the last century there is a tendency of glacier volume reduction, which leads to a decrease in the total amount of water resources in the region, therefore, a study of the patterns of glacier development and forecast of their changes are of big importance for economic development planning.

Specialists from CAIAG conduct research mainly together with the German partners from GFZ (Potsdam) on thematic project: "Study of the Enilchek glacier in order to determine its balance, morphological, dynamic characteristics, as well as climatic and hydrological conditions", "Monitoring of climatic, hydrological, limnological, glaciological

CHAPTER 2. CLIMATE AND WATER RESOURCES

natural and anthropogenic processes using remote sensing data and geographic information systems to solve environment-related problems in the Issyk-Kul lake basin" or "Water in Central Asia". In addition, glaciological research within CATCOS project - «CATCOS (Capacity Building and Twinning for Climate Observing Systems) are carried out together with the Swiss researchers.

Within these projects the Enilchek, Karabatkak, Petrova, Zapadnyi Suek, glacier №354 (Ak-Shyirak mass), Golubin, Abramov glaciers are investigated. Since 2004 regular field measurements of topographic-geodetic characteristics of the glaciers have been carried out on these glaciers using geodetic instruments of the Global Positioning System (GPS), as well as ablation measurement, glacier sounding using georadar, electro-sounding, decoding of satellite optical and radar images.

2.2.1. Enilchek glacier research

The Enilchek glacier system is represented by two glaciers: the North Enilchek, intricately-valley, extending to 32.8 km and the South Enilchek, dendritic, with a length of 60.5 km, which is one of the largest in Kyrgyzstan. In this system we find temporally-formed suction Merzbacher Lake [5], which periodically outbursts through the body of the Enilchek glacier and leads to flooding with the water discharge up to 1000 m³/sec in the Enilchek River. Then, for some time, the lake can vanish and then again reform due to closure of drainage channels in the glacier body and filling of the lake with meltwater, coming from the North and South Enilchek glaciers. In general, the Enilchek glacier has a complex structure, and its large moraine cover, large size and inaccessibility of both glaciers complicate their study [1, 2].

The main purpose of the Enilchek glacier project is to obtain key climatic, hydrological and glaciological parameters of the South and North Enilchek glaciers, Enilchek River and Merzbacher Lake.

In the long-term perspective we plan to identify the patterns of the Enilchek glacier development due to the global climate change and its impact on the water balance in Central Asia.

At the present time, the most important task is to measure a number of meteorological, hydrological, glaciological parameters for understanding, modeling and forecast of glacial, water, atmospheric subsystems with regard to potential hazard risks and change of the water resources.

The ultimate goal is to assess the water-ice balance of the Enilchek glacier on the basis of analysis of acquired data and formulation of multifactor models to interrelate the main natural factors, which determine the functioning and evolution of the Enilchek glacier system.

Within the above mentioned goals the following research activities were completed on Enilchek glacier project.

Study of an interrelation between geosurface temperature and outbursts of the Merzbacher Lake

For this purpose the following inputs were used:

- The surface temperature according to MODIS data, acquired from AQUA satellite, 8 days compositions - MOD11A2.005 product for the period 2000 - 2011;
- Observation data, acquired from meteorological stations of Kyrgyzhydromet for MODIS data validation;
- Daily average data on air temperature and accumulation of precipitations, acquired from automatic weather station «Merzbacher 1" for the period 2009 - 2010;
- Dates of Merzbacher Lake outbursts for the period 1902 - 2011. [6]
- The surface temperature on 8 MODIS days compositions were obtained for the investigated region from NASA service, from FTP: ftp://e4ftl01u.ecs.nasa.gov/MOLT/[10]. Then, using MODIS Re-projection Tool (MRT) software, these data were converted to GeoTiff format in UTM output projection, Zone 43, WGS84. Then, using «ERDAS Imagine 8.4» program the surface temperature parameters on 8 days compositions were obtained for two areas: lower - lower and upper Merzbacher Lake and upper - Lake Superior. According to these data, a graph of the surface temperature changes and dates of the Merzbacher Lake outbursts was formed in Microsoft Excel (Figure 2.2.1.1). This graph shows that outbursts occur during peaks of the temperature, and always occur under the surface temperature over +10 °C, mainly, when the temperature is about +15 °C.

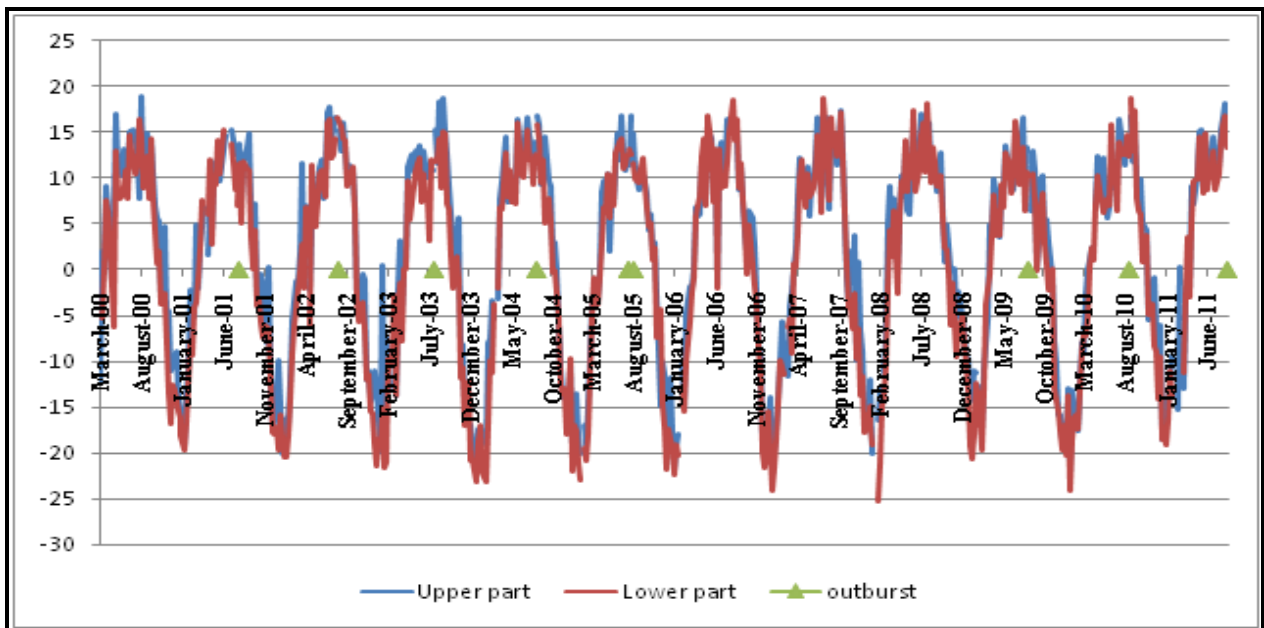


Figure 2.2.1.1. Geosurface temperature on 8 MODIS days compositions for the upper and lower areas of the Merzbacher lake basin and dates of its outbursts

Study of the Merzbacher Lake development process

Topographic maps, aerial and satellite images, acquired from Landsat, Terra-Aster, ALOS satellites within different periods, starting from 1943 and later to 2007 were used to study the changes of the Merzbacher Lake. These data were processed in GIS. The lake areas were calculated within different periods. In addition, the lake volumes were calculated for different periods as well. A DEM was generated using the module LPS 2011 of «ERDAS IMAGINE 2011" software. For this purpose, we used the data, acquired from ALOS / PRISM for 2006 after the lake outburst. The work was carried out according to the instructions of DEM generation on ALOS PRISM [4]. As a result of this work, a set of DEM was obtained for visualization and calculations. A bathygraphic curve (Figure 2.2.1.2), as well as the volume curve and a dependence of the lake volume on its surface for the upper and lower parts of the Merzbacher Lake were created [3].

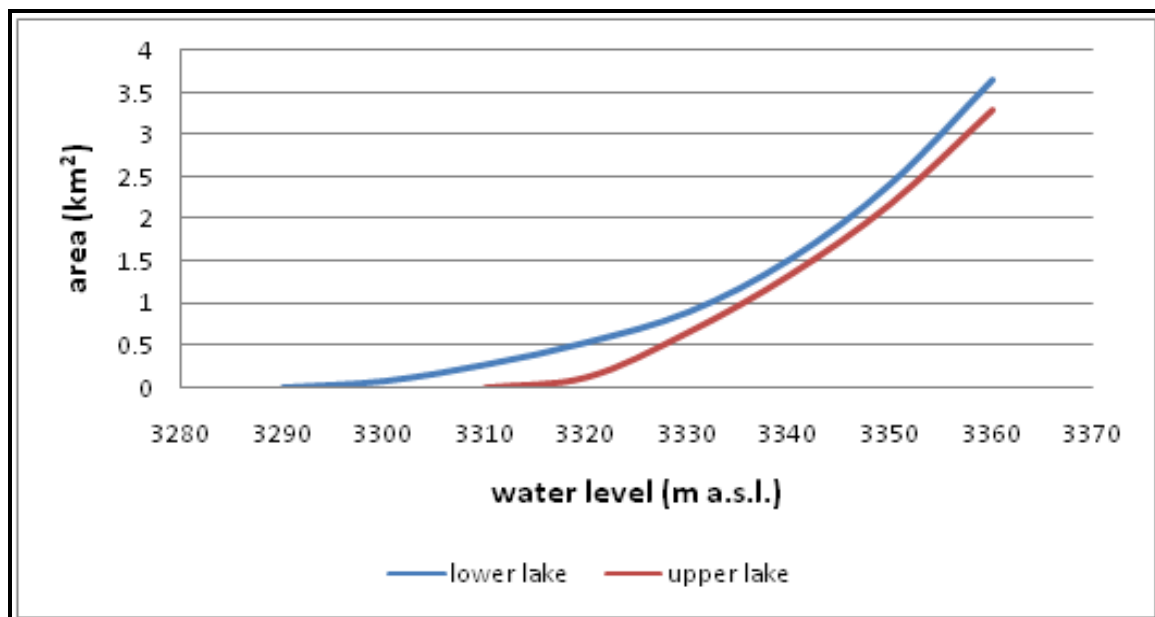


Figure 2.2.1.2. Bathygraphic curve of the upper and lower parts of the Merzbacher Lake

Monitoring and evaluation of the Merzbacher Lake outbursts for possible forecasting

Aerial and satellite images close to the lake outburst time were analyzed. The closest in time to an outburst date is an aerial image, obtained in 29/07/1990 (7 days before an outburst). On this image the area of the upper and lower lakes is roughly 3 km² each (3,016 km² and 0,054 km³ - the upper and 3,079 km² and 0,061 km³ - the lower). But, on Landsat TM image from 10.09.1990 (36 days before the outburst) the area and volume of the upper lake increased (3,777 km² and 0,071 km³, respectively), and the lower lake is completely dried. This means that only the lower lake was outburst. Therefore, a critical area for the lower lake outburst, in our opinion, is an area of about 3 km² and a volume of 0.06 km³, respectively.

Determination of ice velocity of the North and South Enilchek glaciers

The ice surface movement of the Enilchek glacier was studied using optical satellite imagery. High-quality images of 1975, 1990, 2003 and 2010 were chosen to assess the movement of glaciers' tongues of 2006, 2008 and 2010 for tracing objects on the glaciers.

The first step was a co-registration of images [8, 11]. Co-registration errors for each point did not exceed 2 pixels. Thus, for ALOS/AVNIR2 images with 10 m resolution, the error is 20 m. To determine a direction and velocity of the North and South Enilchek glaciers' surface by tracing objects ALOS/AVNIR2 images of August 23, 2006, August 28, 2008 and August 17, 2010 were used.

The same objects, well-defined on the glacier surface were selected on these images, and a value of the displacement and velocity of the glacier surface were calculated for them (Figure 2.2.1.3).



Figure 2.2.1.3. Velocities of the North and South Enilchek glaciers' surface movement

As a result, within available satellite imagery scenes a slight velocity of the ice surface movement close to zero values for about 9 km eastward from the Lake Superior is observed. Thus, by its dynamics this point is close to the passive part of the Enilchek glacier. Apparently, here a discharge of the ice, coming from the recharge area, occurs mainly due to the ablation and vaporization. Profile analysis, conducted on the central part of the North Enilchek glacier (Figure 2.2.1.4.), shows that the tongue of this glacier is located in the eastern border of the Lake Superior.

In the west we find a fragment similar to complex ultimate moraines, extending to southwest direction to the main part of the Merzbacher Lake. Due to the geomorphologic nature and according to the data of previous radar and electrical survey measurements this fragment of the glacier covers a highly thick connate ice of up to 70 m, which is melting during the formation of thermokarst funnels and small lakes, covering the surface of the complex moraines. According to the analysis of satellite images the main

tongue of the North Enilchek glacier, limited by the eastern shore of the Lake Superior, is relatively stable and over the past years not exposed to significant displacements.

The Enilchek glacier tongue is rather stable. The retreat of the glacier tongue is uneven and is max.1 km for the period 1975 - 2010. The greatest surface velocities for the period 2006 - 2010 are observed in the upper part of the Enilchek glacier and are about 0.30m/day. Where turning of the north part of the glacier reaches the discharge area in the Lake Merzbacher, the velocities reduce to 0.21m/day. Within the western passive part of the southern part of the glacier the velocities are very low from 0.09 to 0.0m/day. The data, acquired from the work performed, well-harmonized with previous studies [7, 10].

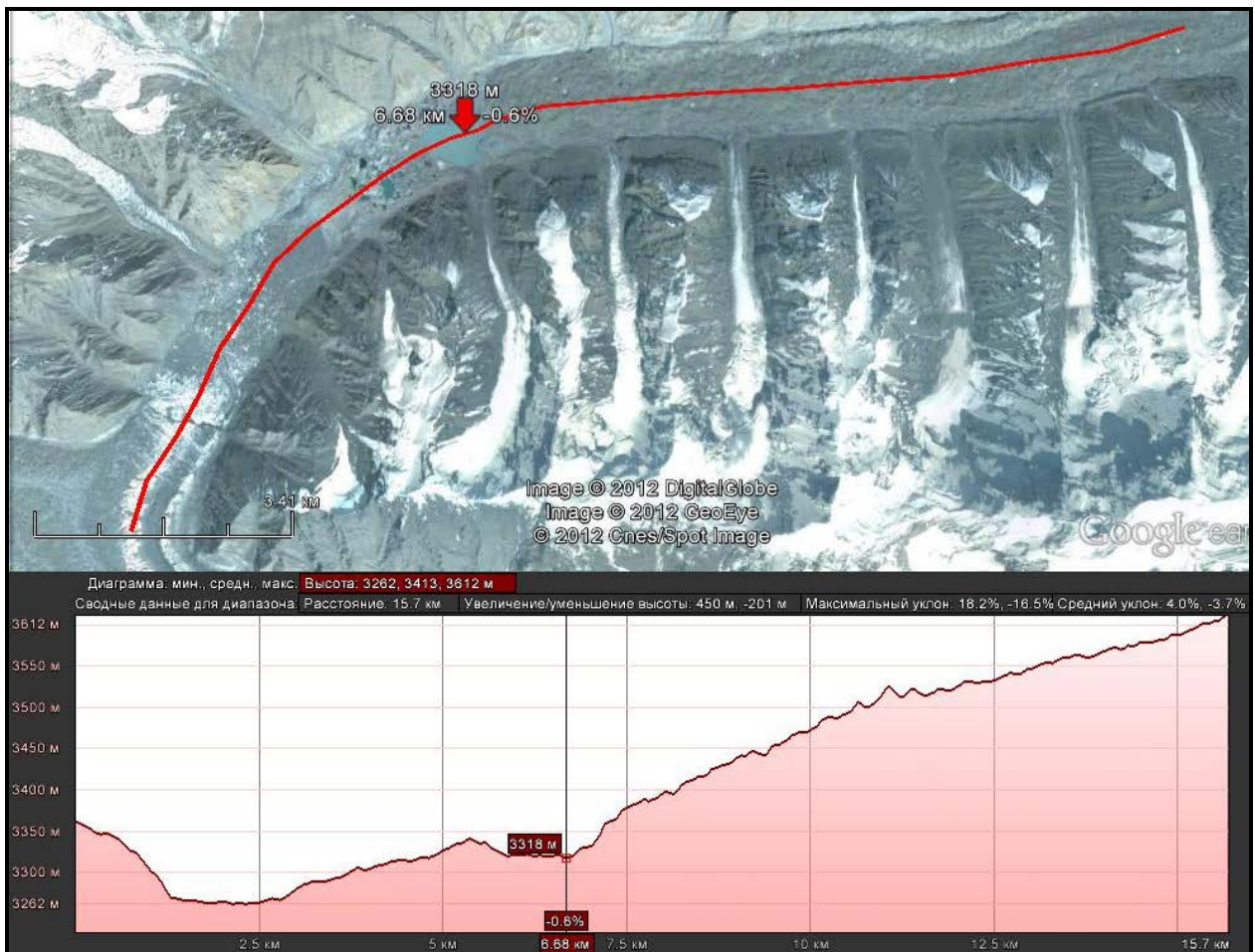


Figure 2.2.1.4. Profile along the central part of the North Enilchek glacier, left to right, from the emptying Merzbacher Lake, to the Lake Superior and further to east

In 2013 observations of changes of the water temperature in the glacier thermokarst funnels were performed using «OTT Orpheus MiniGround Water Level Sensors» sensor and automatic temperature meter with logger (Figure 2.2.1.5).

Figure 2.2.1.6. shows changes of the temperature and water pressure by «OTT Orpheus» sensor, located at a depth of about 0.5 m in the glacier water funnel. In this case, one division of the vertical scale corresponds to 10 cm of the water layer. Observations, carried out during July, showed that the water temperature varied over 88

CHAPTER 2. CLIMATE AND WATER RESOURCES

the range from 2 to 9 °C, predominantly over the range of 3 - 6°C. Changes in the level mainly varied between few cm and only at the end of the month it reduced to about 0.25 m, with following up to about 0.08 m.



Figure 2.2.1.5. Sensor that measures the water temperature on the ice surface

In this case, the main focus is on relatively high temperature of the water, filling the glacier that promotes an intensive ablation and increased volume of the glacier in the summer.

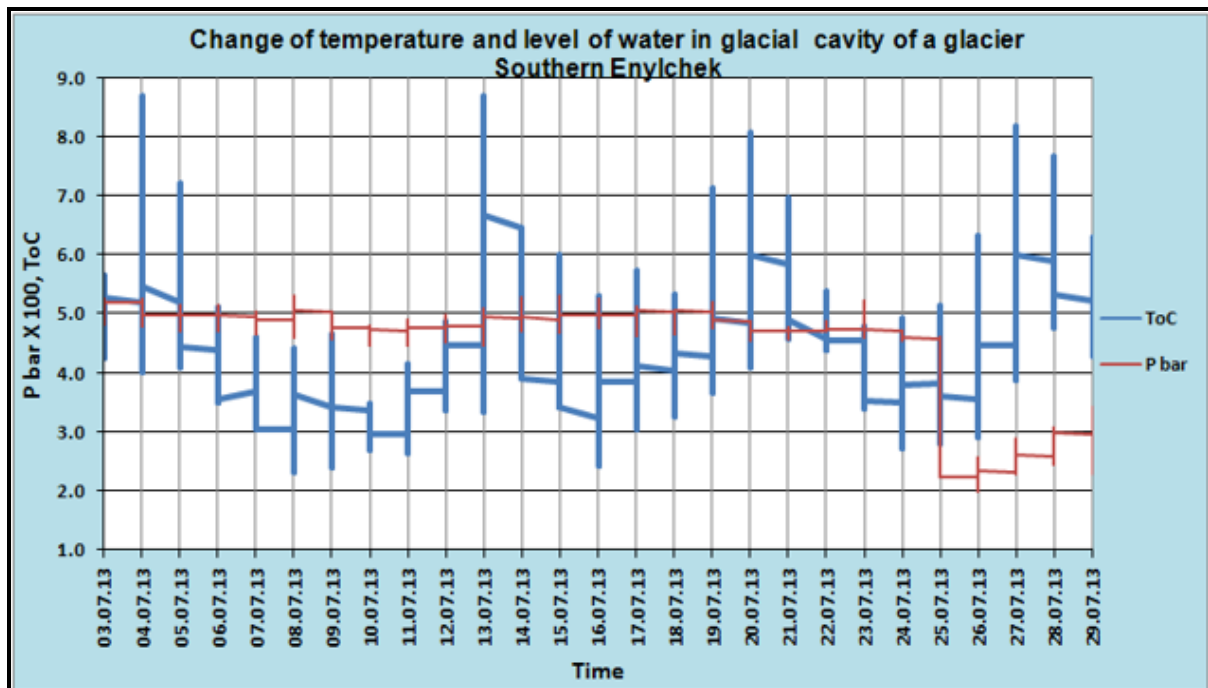


Figure 2.2.1.6. Changes in temperature and water pressure by «OTT Orpheus» sensor

Conducted comparison of 8 days compositions of the surface temperature according to MODIS data with the Merzbacher Lake outbursts showed that outbursts of the lake always occur at the temperatures above +10°C, and more frequently at its increase up to +15 °C.

CHAPTER 2. CLIMATE AND WATER RESOURCES

An assessment of the quality of MODIS data showed a good correlation by comparing with the data, acquired from the Karakol weather station.

To determine an interrelation of the lake outbursts with the surface temperature it is necessary to obtain data on the water temperature directly in the Merzbacher Lake.

ALOS / PRISM data were a good source for generating DEM in this work.

Acquired bathymorphic and volume curves, as well as curve of "area-volume dependency" of the lake can be of practical use in the further studies.

Critical pre-outburst parameters for the lower Merzbacher Lake are: an area of about 3 km² and a volume of about 0.06 km³, respectively. Critical parameters for the upper lake are: an area of about 3.8 km² and a volume of about 0.07 km³, respectively.

A very rapid regeneration of lakes is observed under the certain conditions.

A dependence of the water accumulation in the lakes on the weather conditions and conditions of the state of drainage channels is observed.

The velocity of the North Enilchek glacier surface movement in its measured western part from the end of the tongue is a slight within the measurement error.

The velocity of the North Enilchek glacier surface movement is the highest in the eastern part to the division of the northern and southern parts on the Merzbacher Lake meridian. In the western passive part of the Enilchek glacier the surface movement velocities are similar to those of the North Enilchek glacier, in the investigated area; they reduce to almost zero in the west direction towards the end of the tongue.

Reference

1. Aizen V.B., Aizen E.M., Kuzmichonok V.A. "Geoinformational simulation of possible changes in Central Asian water resources" *Global and Planetary Change* 2006.
2. Aizen V.B., Aizen E.M., Kuzmichonok V.A. "Glaciers and Hydrological Changes in Tien Shan: Simulation and Prediction" *Environmental Research Letters*, accepted for publication, May 2007.
3. Bykov V.D., Vasiliev A.V. *Hydrometry* – Leningrad: Hydrometeoizdat, 1977. – 448 p.
4. "DEM generation from ALOS PRISM_ERDAS_LPSI". Lecture material in the first phase of the JAXA Mini-Project.
5. Dikih A.N., Kuzmichonok V.A. "The Merzbacher Lake" *Herald of the KRSU*, Volume 2, 2003.
6. Glazyrin G.E. "A century of investigations on outbursts of the Merzbacher ice-dammed lake (central Tien Shan)" *Austrian Journal of Earth Sciences*, Volume 103/2, Vienna, 2010.
7. Hausler H. et al. "Results from the 2009 geoscientific expedition to the Enilchek Glacier, Central Tien Shan (Kyrgyzstan)", *Austrian Journal of Earth Sciences*, Volume 104/2, Vienna, 2011, p. 47-57.

8. "Encyclopedia of snow, ice and glaciers", Springer, The Netherlands, 2011.
9. <ftp://e4ftl01u.ecs.nasa.gov/MOLT/>
10. Mayer C., Lambrecht A., Hagg W., Helm A., Scharrer K. 2008: Post-drainage ice dam response at the Merzbacher Lake, Enilchek glacier, Kyrgyzstan. *Geogr. Ann.*, 90 A (1): 87–96.
11. Pellikka P., Rees W.G. "Remote sensing of glaciers", Taylor and Francis Group, 2010.

2.2.2. Geophysical studies of glacial-dammed Merzbacher lake dam

In 2012 a geophysical group of the Research and Engineering Center "GEORPIBOR" of the Institute of Geomechanics and Exploitation of Mineral Resources of the National Academy of Sciences on the instructions of the Central Asian Institute for Applied Geosciences (CAIAG) carried out geoelectric studies of the bottom of the glacial-dammed Merzbacher lake in the area of the dam between the major (lower) and upper lakes of the North Enilchek glacier.

Merzbacher Lake – is one of the classic examples of glacial-dammed lakes and at the same time is a unique water-ice complex. The lake is located at an altitude of 3200m, at the North and South Enilchek valley glaciers area (Figure 2.2.2.1). The North Enilchek glacier is located at 4 km away from the edge of the South Enilchek. This space between the end of the North Enilchek and the edge of the South Enilchek serves as a reservoir to collect meltwater, which form the Merzbacher Lake with an area of about 4.5 km².

The main aim of geoelectric studies was to investigate the cryogenic structure of the bottom of the Merzbacher lake using the Vertical Electrical Sounding (VES) method, in particular, to determine the occurrence and thickness of melt, frozen, fluvial-glacial and moraine sediments, which, according to available scientific publications, cover the remains of dead ice of the North Enilchek glacier [1].

The measurements were carried out using equipment as GeoTom-MK1E100 RES/IP/SP (Figure 2.2.2.2), produced by GEOLOG2000 company (Augsburg, Germany) with an installation of 100 electrodes, connected to 400 m multi-core cable and using 50% overlapping when moving electrodes and cables along the long profile.

A general view of the area and the area of geoelectric studies is shown in Fig.10. In the area of the dam two crossing VES profiles II and II-II, which mutual orientation is shown in Figures 2.2.2.3-2.2.2.4 were measured.

Figure 2.2.2.5. shows geoelectric sections (gotomograms) along mutually-crossed profiles II and II-II, went through in the area of the dam of the Merzbacher Lake. Apparently in these tomograms, the cryolithosphere resistance varies over a wide range from a few tens of ohm·m for subsurface sediments to several hundred thousand ohm·m for glacial ice at depths of 25-40 m from the ground surface.

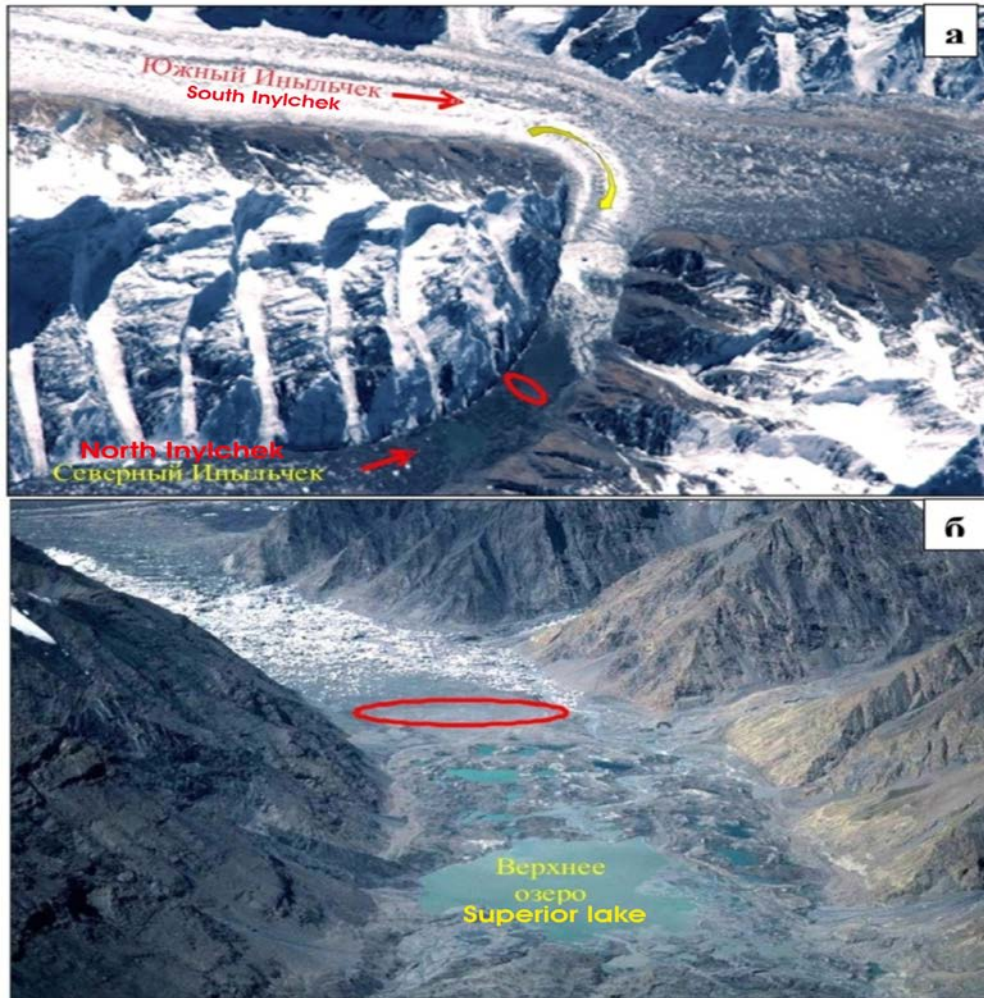


Figure 2.2.2.1. General view of the Merzbacher lake: a) satellite image of the study area - yellow arrow indicates the northward flow of the Enilchek glacier; b) view from the North Inylchek glacier; investigated area of the dam between Superior and major lakes is indicated by oval



Figure 2.2.2.2. Vertical electrical sounding GeoTom-MK1E100 and differential DGPS ProMark-3 (rover station). Electrode and multi-core cables are shown on the right picture

CHAPTER 2. CLIMATE AND WATER RESOURCES

In total, there are four different resistance layers, shown on the two tomograms (Figure 2.2.2.5), especially clearly observed in the section II-II:

Layer №1 - is an upper layer with a thickness from 5 to 10 m with a low resistance from 20 to 900 ohms·m, which is marked in blue on the tomograms.

Layer №2 – is a lower layer under №1, characterized by a resistance from 1,000 to 13,000 ohm·m and extends to depths of 15-17 m from the ground surface. The wavy layer in the longitudinal section is marked in green on the tomograms.

Layer №3 – is a layer with a resistance from 14 000 to 40 000 ohm·m, which is marked in yellow-brown, at depths of more than 20-23 m.

Layer №4 – is a layer with a resistance over 100 000 ohm·m, and marked in red-brown on the tomograms.

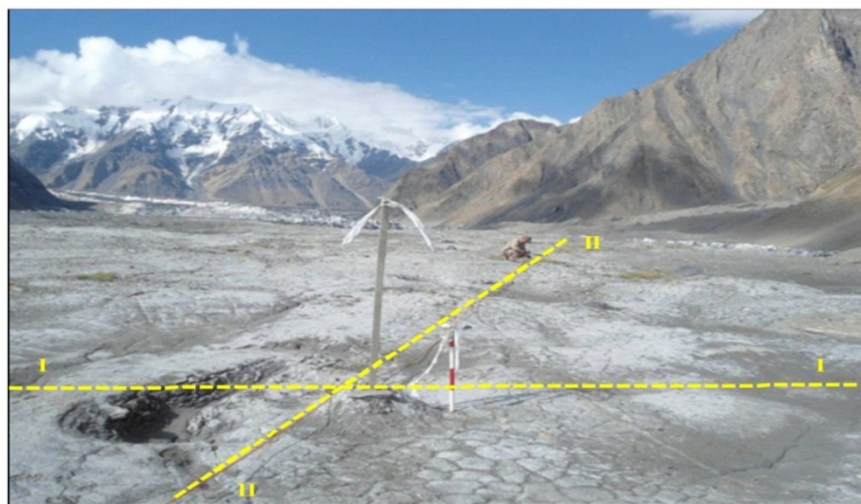
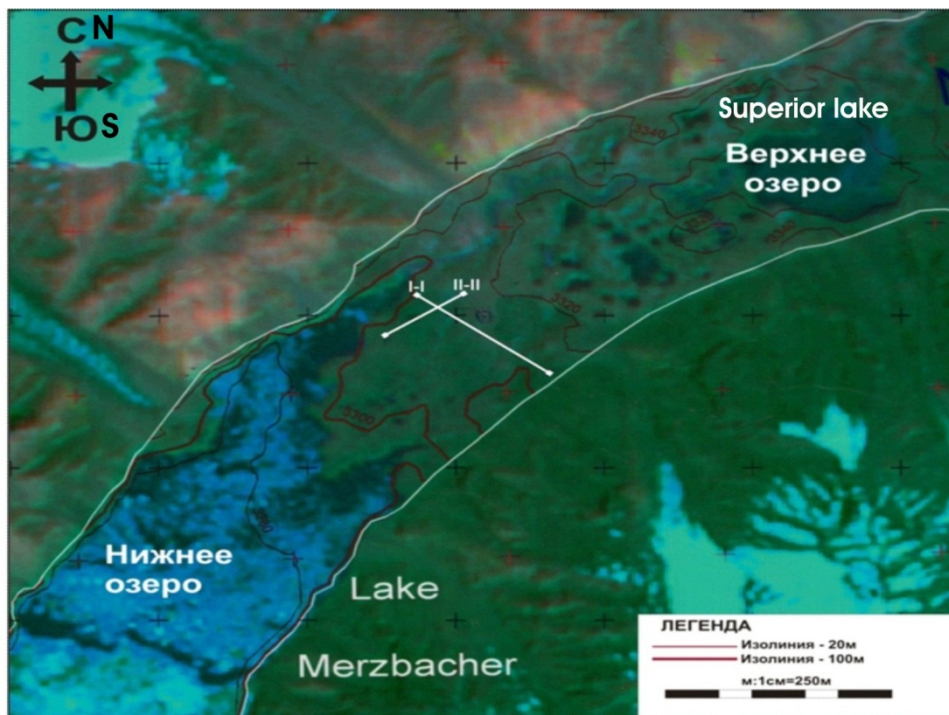


Figure 2.2.2.3. Scheme and picture of the location of VES profiles in the area of the dam

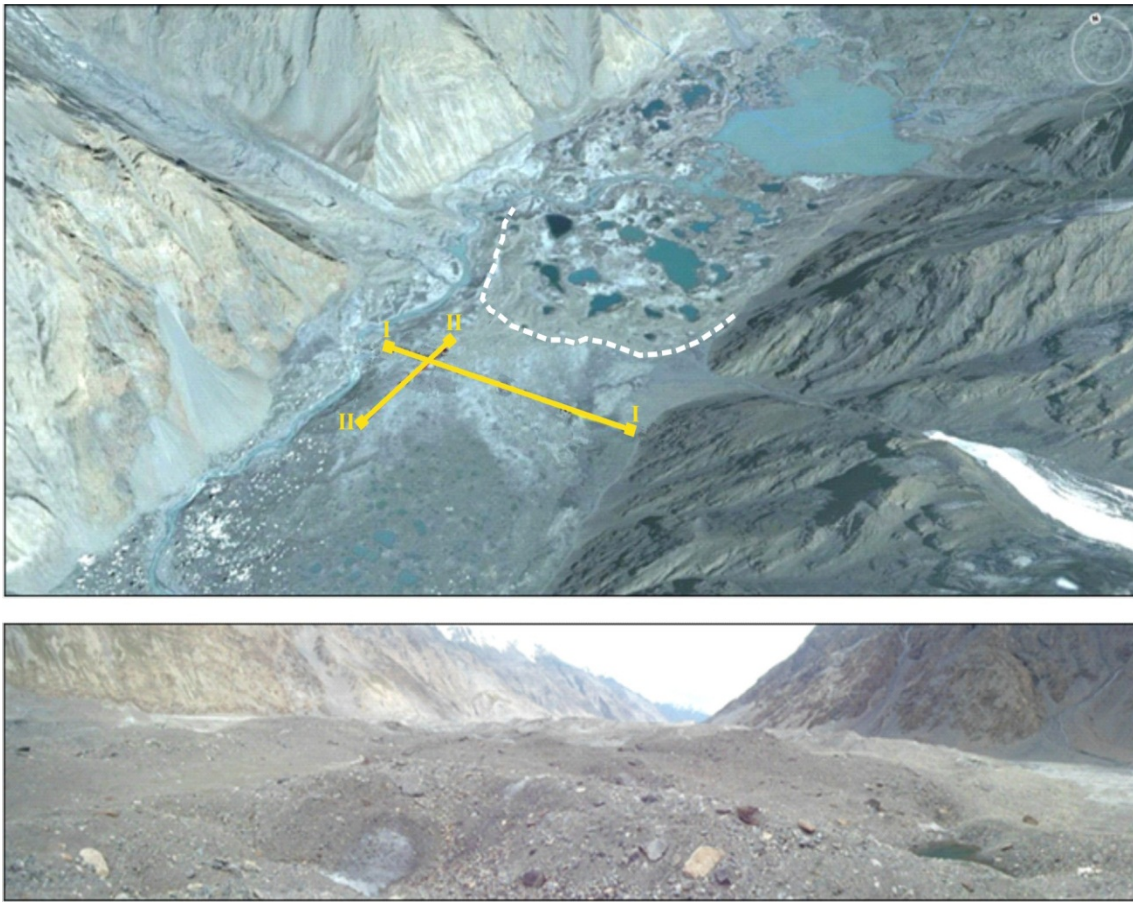


Figure 2.2.2.4. The upper picture shows the spatial location of electrical profiles II and II-II on the dam of the Merzbacher lake, below the moraine of the Lake Superior, which is shown in dotted line. The lower picture-view of the finite-moraine complex of the Superior Lake.

Also for the specified investigated area, in analogy with the Kumtor area and on the basis of cryogenic-geolectric classification, according to the temperature regime, three groups of fluvial-glacial sediments occurred in the dammed-glacial bed of the Merzbacher lake dam:

small-grained lacustrine sediments of seasonally thawed layer ($\rho = 20\text{-}200$ ohm m) with a thickness of up to 5 m in some areas, characterized by positive temperatures ($t_{cp} > 0,5$ °C). Below the depth of 1.0-1.5 m these lacustrine sediments contain pebble interlayers with impregnated rubbles;

transient or critically melt soil layers ($\rho = 200\text{-}500$ ohm m), occurring to a depth of 25 m and characterized by average temperature values t_{cp} from 0 to 0,9°C. The top of this interlayer is similar to a wavy configuration of the base of the upper seasonally thawed layer;

permafrost sediments ($\rho > 500$ ohm m), underlain by dead glacial ice and characterized by negative temperatures t_{cp} from -1 to -2,6 °C.

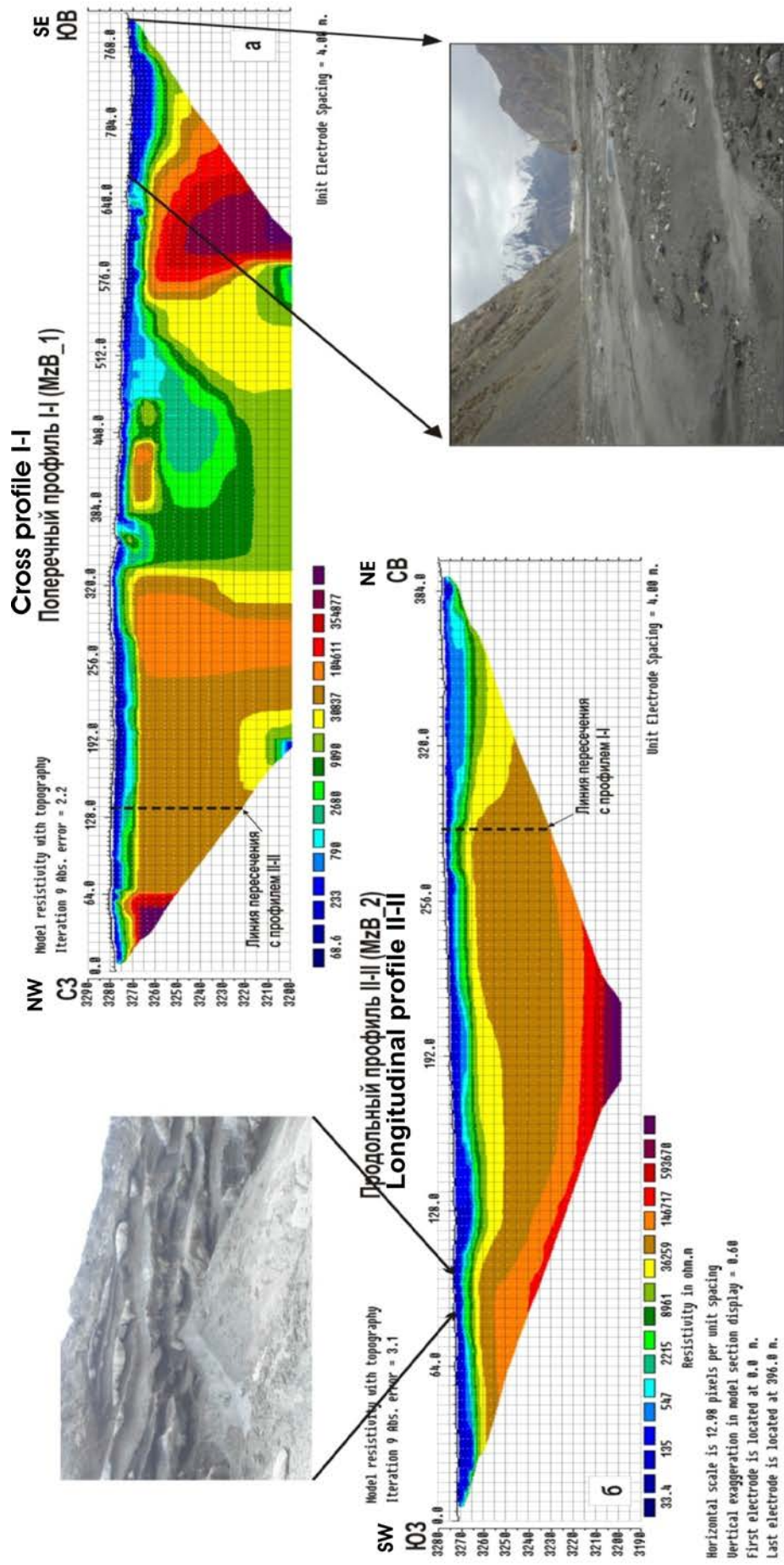


Figure 2.2.2.5. Geoelectric sections (tomograms) of profiles I-I and II-II:

- a) tomogram I-I shows a heterogeneous pattern of changes in electrical resistance in the cross-section of the valley;
- b) tomogram II-II shows a layered pattern of changes in electrical resistance along the valley of the North Enlichek

CHAPTER 2. CLIMATE AND WATER RESOURCES

As a result of study using VES investigation of the dam site around Merzbacher Lake it was found that the cross geoelectric section of fluvial-glacial sediments varies with considerable mosaic of spatial distribution of resistances in comparison with longitudinal section (along the valley), which is of clearly distinguished layered nature.

A layered nature of the distribution of longitudinal section resistances is explained by the fact that an interstratification of bottom moraine sediments with connate ice interlayers is visually observed in this study area. At the beginning and at the end of the longitudinal profile there are deep erosional incisions (Figure 2.2.2.5).

The geoelectric section of cross profile is a mosaic image that is explained by the assumption of complex physical-mechanical processes, occurred here during the dam formation.

Taking into account the global warming, it can be assumed that after some time the ice in the central part of the dam can completely melt by forming a through talik over the whole dam between the lakes. Meanwhile, there can be an alternative in subsequent emergence of another – A central channel that will connect two lakes. In this regard, it is essential to conduct a regular geophysical sounding of the Merzbacher lake dam in various cross-sections for early detection of a critical stage of the channels' formation, fraught with unpredictable hydrological consequences and/or change of the mode of emptying the main Lower Lake.

Reference

1. Airapetyans S.E., Bakov E.K. Morphology of glacial Merzbacher lake and a mechanism of its catastrophic outbursts / / Some patterns of glaciation of the Tien-Shan. Frunze: Ilim, 1971. - P.75-84.

2.2.3. Seismic noise measurements on the Southern Enilchek Glacier in the area Lake Merzbacher

The Southern Enilchek Glacier has the morphology referred to as a dendrite type, which has a length of 60.5 km, and the area of 632.3 km² according to the "Map Atlas of Kyrgyzstan" based on an assessment before 1985, while according to an assessment after 1990 the length is 60 km and the area 533 km². This decrease can be connected both with the degradation of the ice body and the reliability of the respective measurements.

Degradation of the glacier due to global climate change occurs depending on permafrost conditions of the glacier. The ice velocity rates depending on the ice body travel from the lateral glacier sides to its central part, vary in the range from 4-8 to 12-15 cm per day. To estimate the rate of deglaciation, it is necessary to calculate accurately the glacier mass balance, what requires data of the ice thickness, both in cross-section, and length profile (Leveque et. al., 2010; Chen Tsai, 2009; Macheret et al, 1992).

CHAPTER 2. CLIMATE AND WATER RESOURCES

In 1967 and in the 1990s, researchers from the University of Leningrad, Institute of Geography of the Academy of Sciences of the USSR and the Tomsk Polytechnic Institute conducted a radar sensing of the Southern Enilchek glacier in the area of Mertzbacher Lake using portable TGU-700 and MPI-8 locators.

As a result of measuring 400 sites of the ice body, it was found that the ice thickness in the vicinity of the Merzbacher lake ice dam is 375 meters. In the middle and upper part of the glacier the thickness varies from 250 to 350 meters. The ice thickness of the Southern Enilchek close to the glacier branch Shokalsky is 160 meters (Macheret et al, 1992).

In order to redetermine the thickness of the glacier in the vicinity of Lake Merzbacher researchers of CAIAG (Usupaev Sh., Orunbaev S. and Konokov T.) recorded in July 2011 seismic noise using mobile seismic stations (Figure 2.2.3.1).



Figure 2.2.3.1. Seismic noise measurements on the Southern Enilchek glacier in the area of Lake Merzbacher: left: moraine of the glacier, middle: general image of the glacier, right: left-side branch of the glacier close to the cliff glacier south-eastwards from the CAIAG observatory.

The width of the glacier is 3,5 km. The middle figure shows the lake water with floating icebergs.

The measurements were made along a profile of 22 sites (Figure 2.2.3.2). Moraine ground and glacier vibrations were recorded by the seismic station Mark (Marcl3D4 sensor and digitizer EDL). The minimal duration of each recording was 30 minutes. To determine the resonance frequencies of deposits, the method of spectral ratio of horizontal to vertical components (H / V ratio) was used. The results showed that the main peak of the ice resonance oscillations is within the frequencies 6,7 Hz and 8 Hz. The glacier thickness was calculated by the formula:

$$f = V_s / 4h,$$

where:

f - resonance frequency, Hz;

V_s - lateral transversal wave rate, km/sec;

h - layer thickness, m.

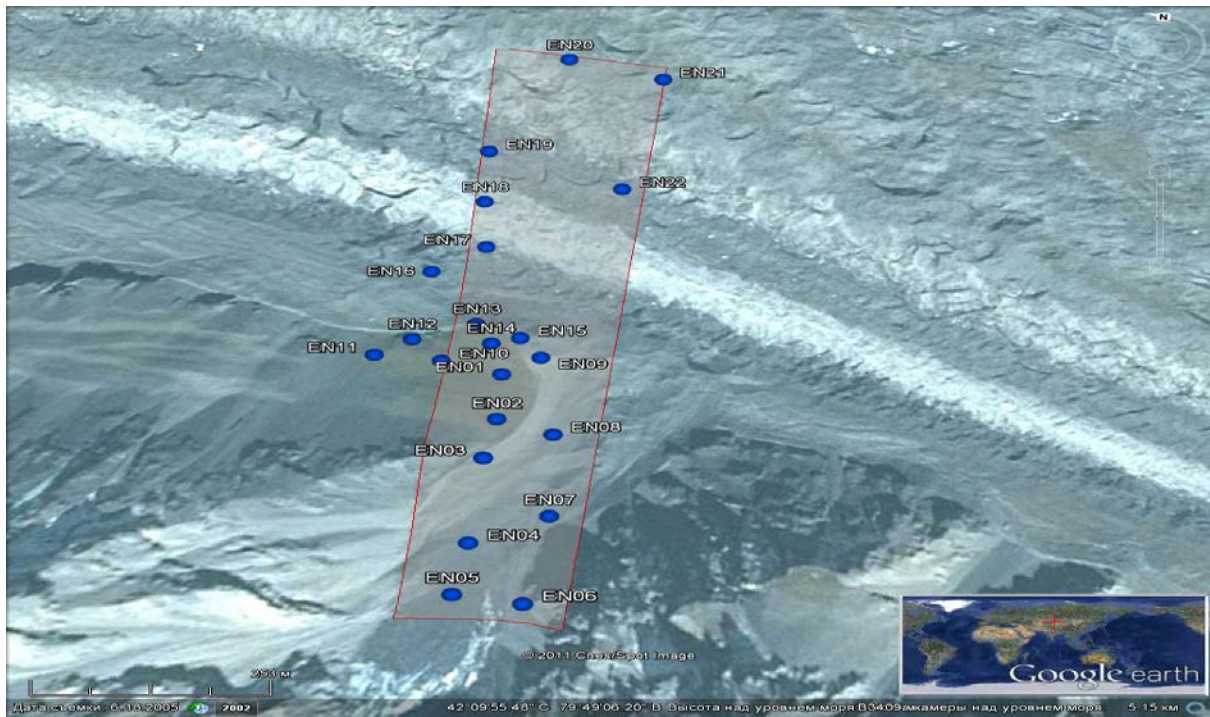


Figure 2.2.3.2. Location of seismic noise measurement sites across the profile (22 sites, profile length - 1,5 km).

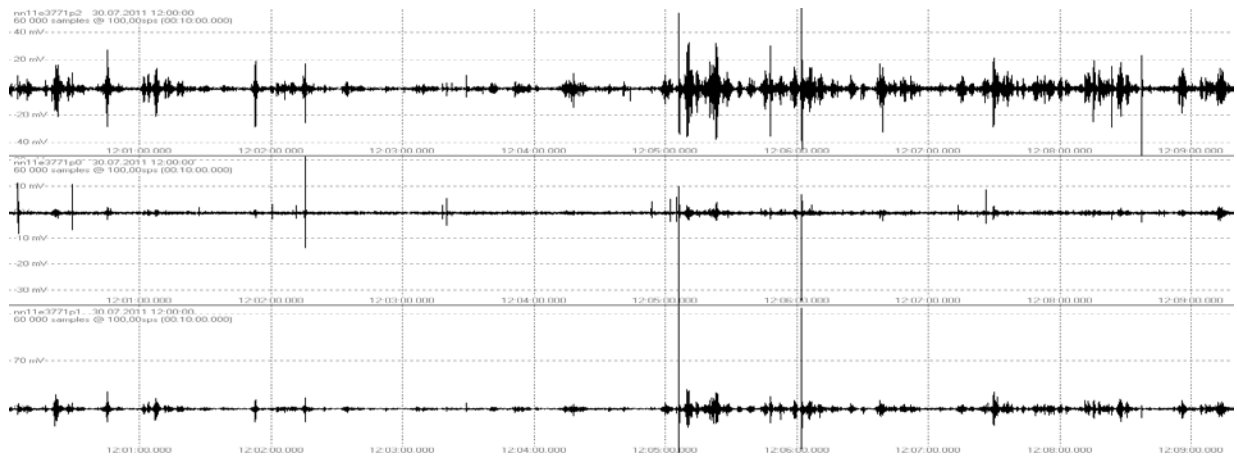


Figure 2.2.3.3. An example of the recording of three seismic noise components at the site EN22, located on the moraine 150 meters from the left side of the Southern Enilchek

The value of the transverse wave velocity was based on the results of Leveque et. al., 2010 and Chen Tsai, 2009, which state that the wave speed V_s is in the range from 2.0 km / s at a lower boundary of the glacier down to 0.9 km / s on the surface. Thereupon, in our calculations we used the value $V_s = (V_1 + V_2) / 2 = 1.45$ km / s.

Figure 4.5.23 shows an example of processing of noise recordings for the point EN05. A 30-minute recording was divided into 60-second intervals for which spectra were made. Afterwards the spectra ratio was calculated (see Figure 4.5.23.). The figure shows that the peak resonant frequency is $f = 6,3$ Hz, and therefore, the thickness h of the ice layer at this point is 42.3 m. The results of the noise processing at 22 measurement sites along the profile showed that the maximum thickness of the Southern Enilchek Glacier

is 137 meters (the left side in figure 2.2.3.5), and of the left-side tributary glacier is 42.3 m (to the right).

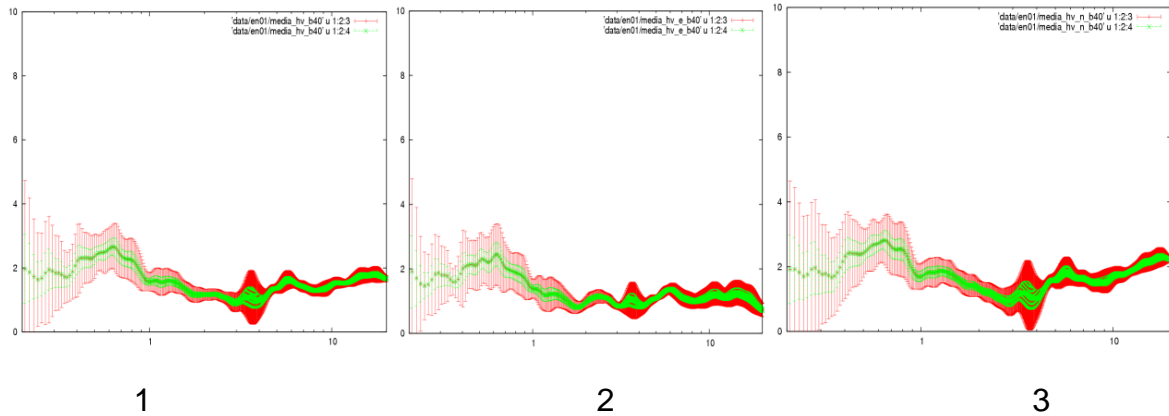


Figure 2.2.3.4. The spectra of 60-sec noise recordings according to the station EN05. 1. - The spectral ratio of vector sum of two horizontal to vertical components 2. - Ratio of E-W to Z components; 3. - Ratio of N-S to Z.

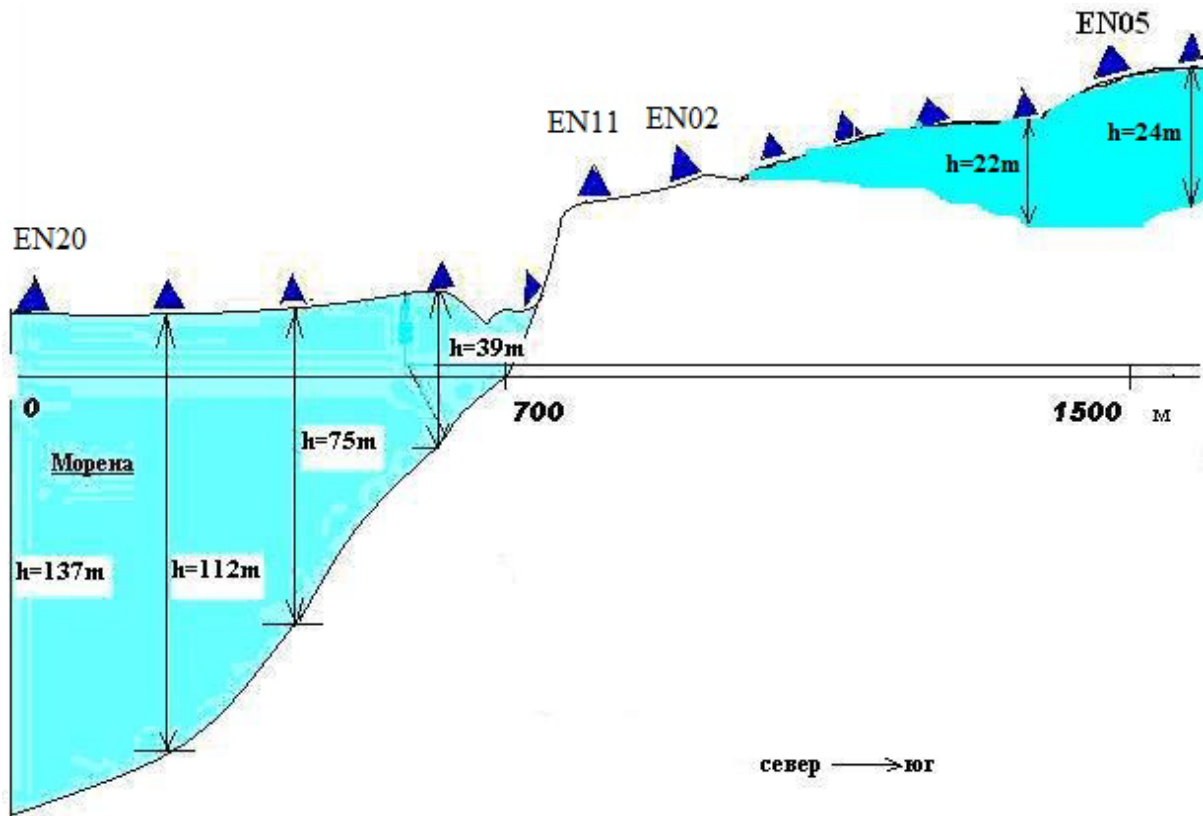


Figure 2.2.3.5. Section of the Southern Enilchek glacier (left part of the figure) and small cliff glacier (right part of the figure) along the profile

In 2012 similar measurements were conducted for four profiles on the Enilchek glacier and for the ground (moraine) dam bridge between the upper and lower Merzbacher lakes (Fig. 2.2.3.6). Obtained recordings include a complex resonance frequency, with several spectral ratio peaks. This is considered to be an indicator of the presence of complex structures, low impedance discrepancy and complex surface topography.



Figure 2.2.3.6. Location of the sites of seismic noise measurements: to the left – 4 profiles on the Elgylchek glacier (48 points) and to the right – 3 profiles on the dam (16 points).

The result of pre-processing the seismic noise revealed the following: the moraine dam thickness (according to preliminary analysis) is about 68 meters and the thickness of the glacier at the point 23 is 47 meters. The depth of the glacier valley bottom layer covered with ice is estimated to be 112 meters. Actually the upper and lower Merzbacher Lakes are located on defrosted surface of the Northern Enilchek glacier. Thus, in the annual period of existence of Lake Merzbacher its depth could possibly have a depth up to 68 meters.

The structure of the ice layer along the profile "dam bridge", extending from the north-western to south-eastern coast (Fig. 2.2.3.7), shows depths up to 300 meters. It is to be mentioned that the obtained spectra show also peaks at lower frequencies. Calculations show that at the depth of 40-50 meters there is a layer with different density properties. Possibly this layer can be identified with the dam that breaks every year, what results in the flow of water from the upper to the lower lake basins. At a depth of 170-250 m below the moraine is one more zone that is assumed to have a sedimentary cover located on the rock materials.

The Profile of "Dam Bridge" site is located 1500 meters northwest from the ice dam of Merzbacher Lake. In the area of the "Dam Bridge" site the glacier thickness is 50-100 meters less than in the area of the ice dam. Perhaps this difference is due to the cyclic nature of the glacier degradation. To understand the reasons of these changes, it requires long term (decades) measurements using a certain device (a certain method).

Reference:

1. Leveque J-J., Maggi A. and Souriau A. Seismological constraints on ice properties at Dome C, Antarctica, from H/V spectral ratios.// Antarctic Science. Volume 22 , Issue 05, Октябрь 2010. Cambridge University Press, pp 572-579
2. Victor Chen Tsai. The Use of Simple Physical Models in Seismology and Glaciology. Theses of PhD dissertation, 2009, Harvard University.
3. Macheret Ju.A., Nikitin S.A., Babenko A.N., Vesnin A.V., Bobrova L.I., Sankin L.V. Tolshhina i stroenie lednika Juzhnyj Inyl'chek po dannym radiozondirovaniya. Trudy IGAN SSSR, 1992, s.86-97.

CHAPTER 2. CLIMATE AND WATER RESOURCES

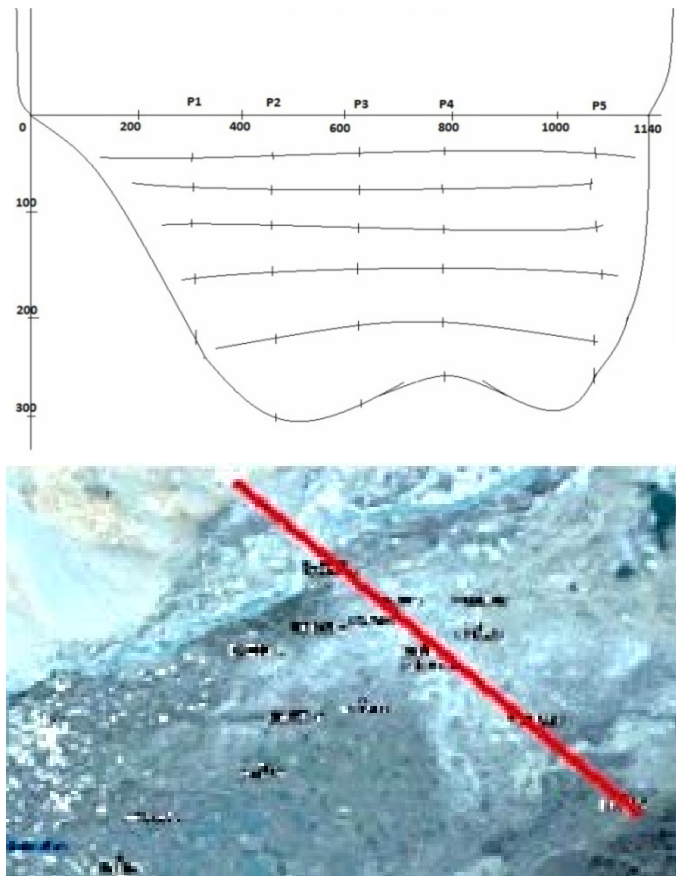


Figure 2.2.3.7. Section of the Enilchek glacier across the profile “Dam Bridge” (red line), the profile length - 1-1,2 км.

2.2.4. Magnetometric studies in the area of the confluence of the North and South Enilchek glaciers near the Merzbacher Lake

In 2011-2013 the areal and profile magnetometric survey were carried out in the area of confluence of the North and South Enilchek glaciers near the Merzbacher Lake. One of the tasks of this survey was to confirm the existence of fractured structures and crossbars under the glacier, as well as to map moraine sediments in a magnetic field. Proton magnetometers MMP-203 were used as measuring instruments.

In July-September 2011 magnetometric measurements have been carried out at 140 points for five profiles with a total length of 12 km and on the territory of the "Polyana" base camp. Before the profile observations and according to results of the micromagnetic survey an area for installing a reference point to measure the Earth's magnetic field variations was chosen in a quiet magnetic field environment. The reference point was in an area of the G.Merzbacher observatory – a concrete base of nonmagnetic materials with a height of 1.5 m was installed there.

Figure 2.2.4.1 shows the location of the PR-1 - PR-5 profiles. The faults are shown in crimson, and regional and local lineaments are shown in red (map, 1980). A known regional lineament is in black line, which was identified by satellite images. The

interpretation of obtained data of the magnetometric survey confirmed the existence of this structure. The width of this lineament with 160 m was the first time identified. Moreover, a rupture zone with a width of 50 m, hidden beneath the glacier (dark red line), was identified. According to preliminary estimates its length is limited by profiles PR-1 and PR-5.

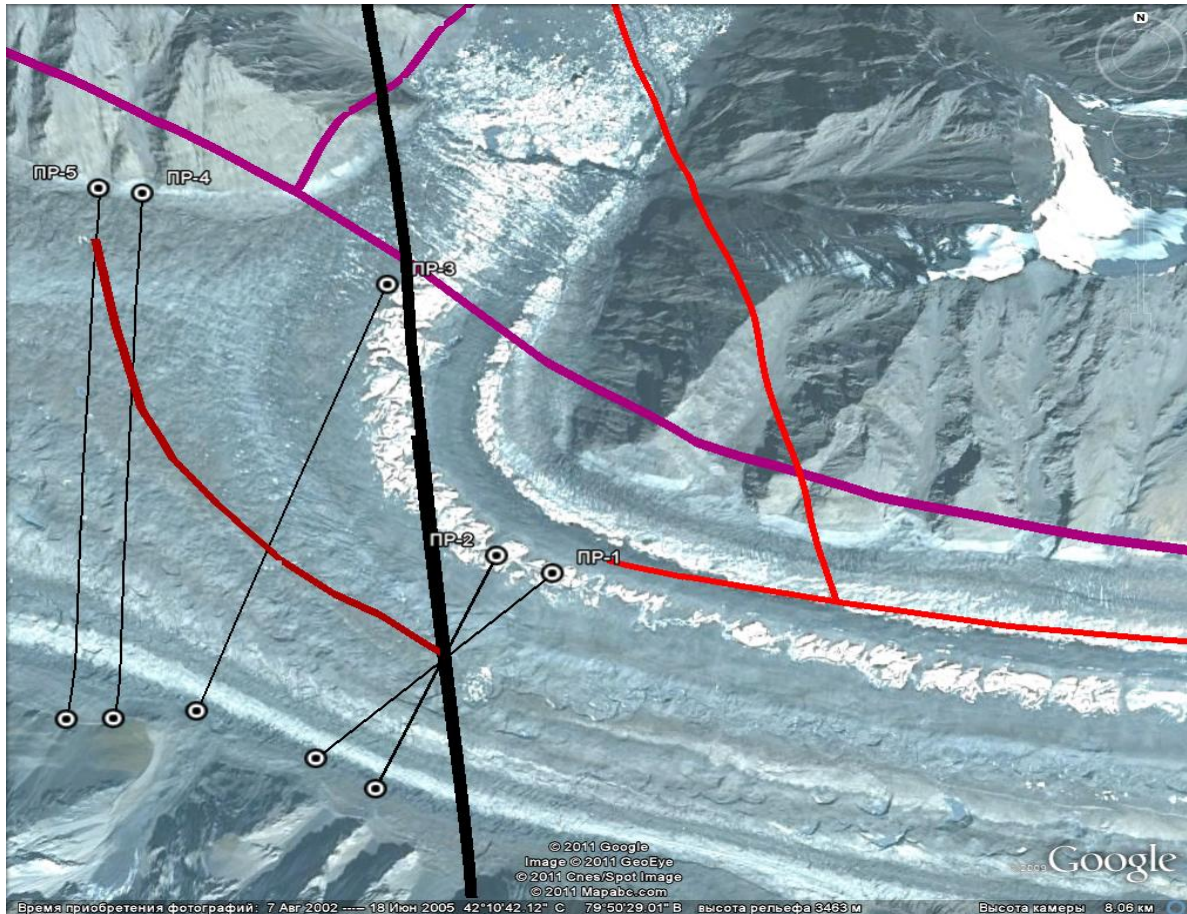


Figure 2.2.4.1. Magnetometric profiles on the satellite image

In August 2012 the magnetometric investigation of the ground dam, dividing the Merzbacher Lake into two parts, has been carried out. Its western boundary, formed by lacustrine sediments, borders with the basic basin of the lower lake, which ends by a dammed ice dam, which is part of the active Southern Enilchek glacier.

Medium and highly magnetic rocks of various intensities are shown on the map (Fig. 2.2.4.2) in red color. Weak magnetic rocks are shown in blue and violet (zero and negative values of the magnetic field).

The map of contour lines of anomalous Earth's magnetic field (Fig. 2.2.4.2) was also represented in the form of volume diagram (Fig. 2.2.4.3). Comparing diagrams of the dam relief (Fig. 2.2.4.4) with the volume diagram of magnetic anomalies (Fig. 2.2.4.3) a correlation can be seen between them.

According to magnetic features the basin of the dam has a horseshoe crossbar ledge, facing with its arc to the west, in the direction of the ice lake dam.

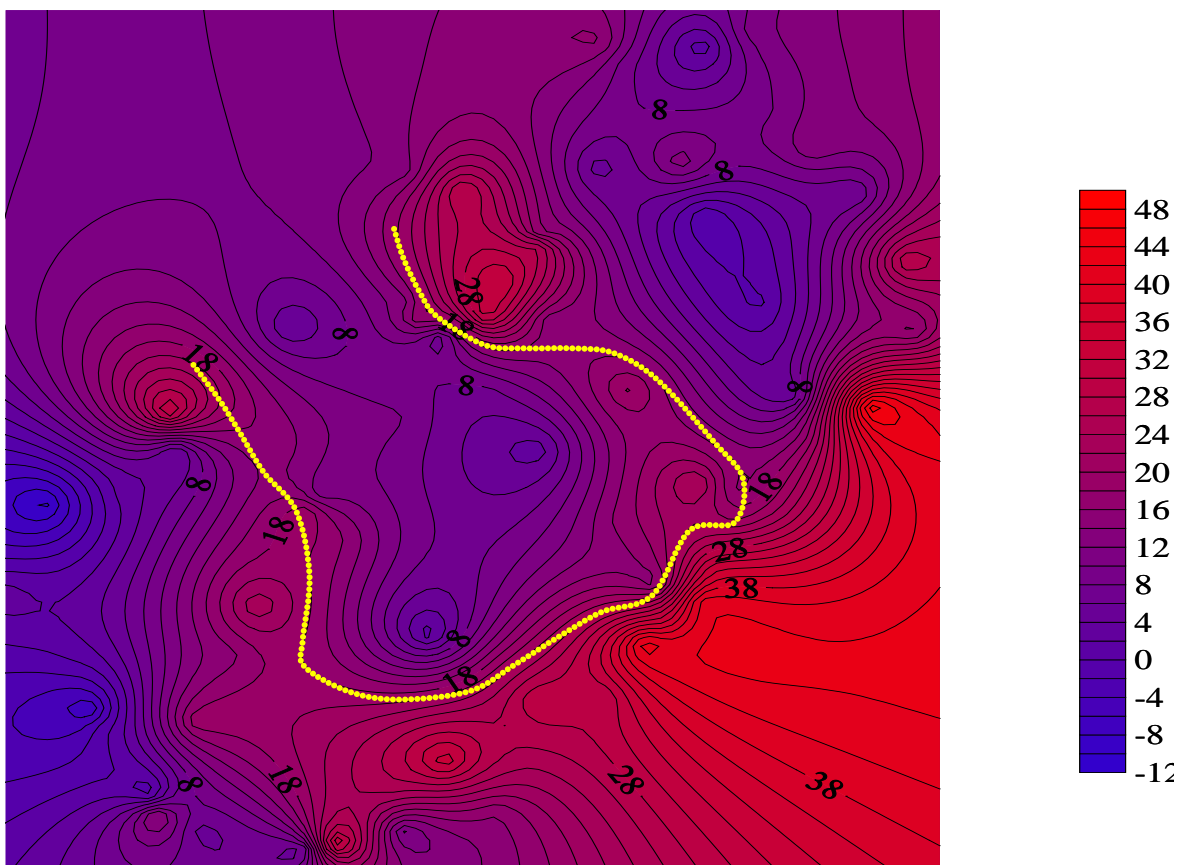


Figure 2.2.4.2. Map of contour lines of anomalous Earth's magnetic field in the dam area

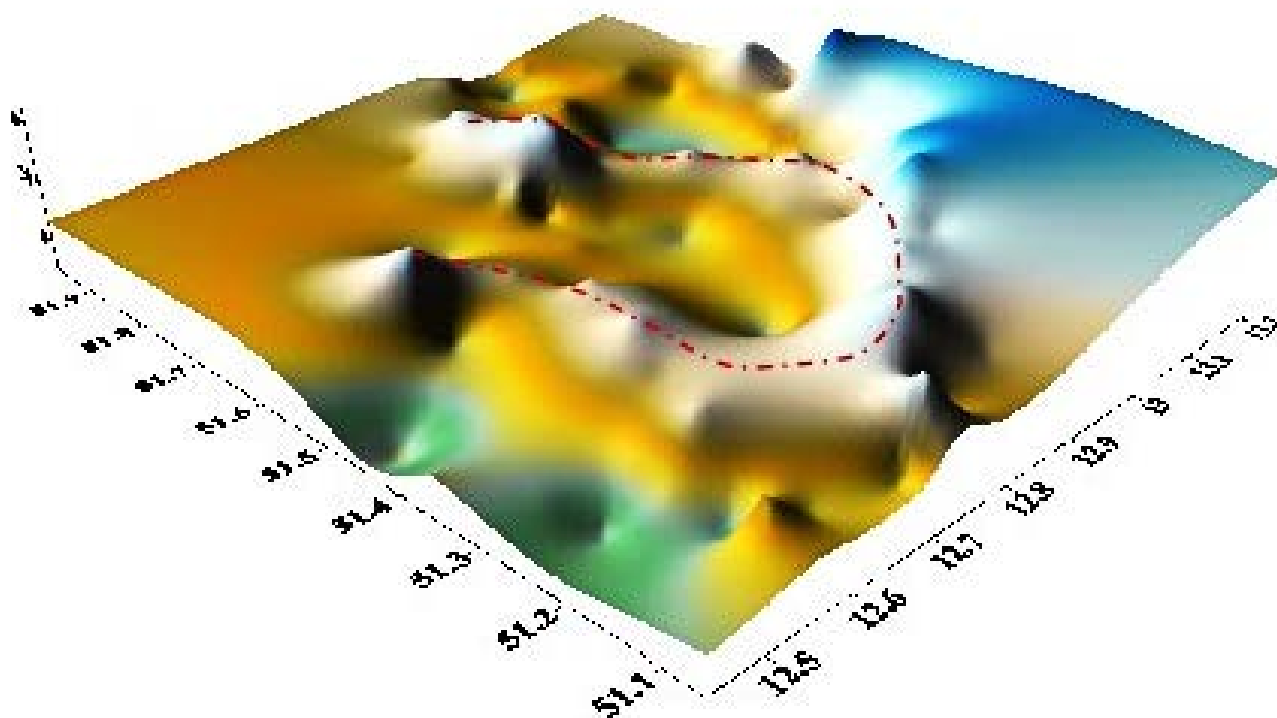


Figure 2.2.4.3. Volume diagram of magnetic anomalies in the ground dam bed between the upper and lower Merzbacher lakes

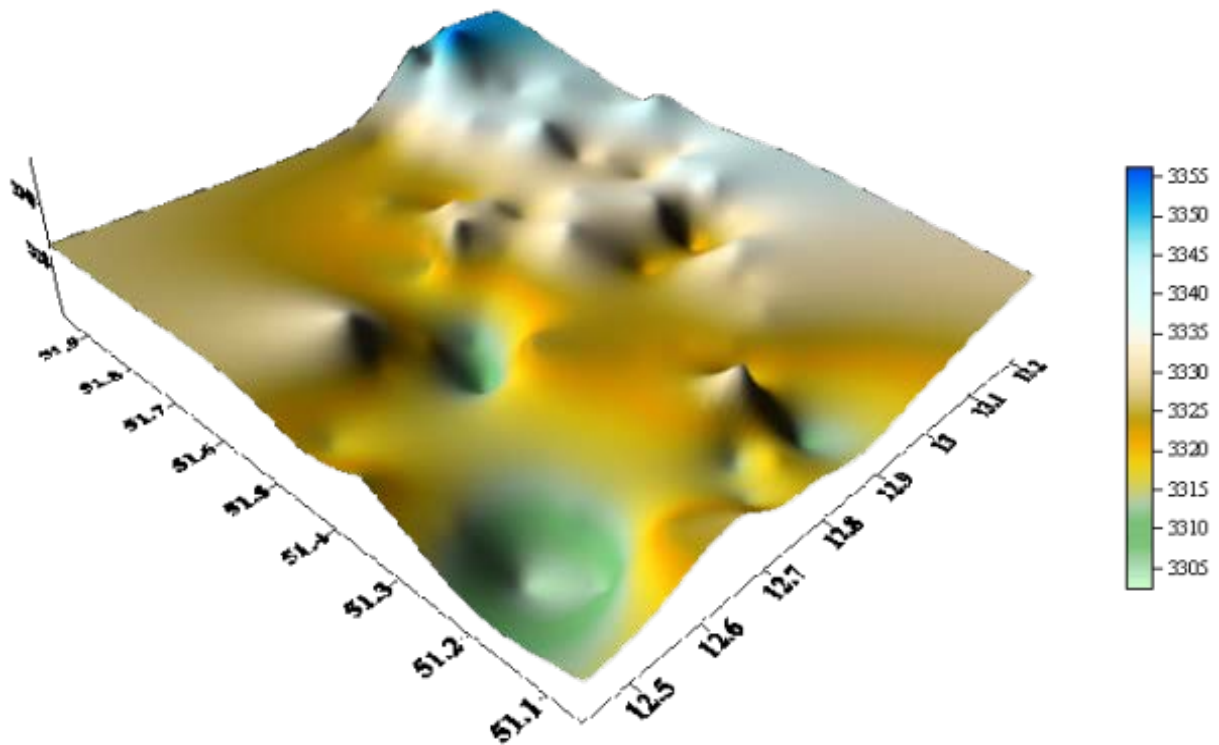


Figure 2.2.4.4. Volume diagram of the ground dam relief between the upper and lower Merzbacher lakes

Thus, we can conclude that since its formation the dam created a barrier for the accumulation of bottom sediments and formed a peculiar hydraulic fill dam, enabled to form a sufficiently broad boundary between the upper and lower parts of the Merzbacher Lake. The dam, formed by lacustrine sediments and fluvial-glacial formations, has two closure channels. In the northern part of the dam there are areas with small values of the magnetic field. Apparently, here over a long time period there was a flow channel, which developed an actual North Enilchek riverbed that contributed to discharge dammed water during filling of the reservoir from the upper basin to the lower lake. The main part of the water that fills the lower lake is supplied mainly by this river, which has a large flow, allowing over relatively short time to fill the basin of the water body. Currently the southern closure channel is represented by a temporary shallow water channel, which connects the upper lake basin with the lower. Probably, it provides an active water exchange between the two parts of the examined water body under maximum filling conditions of the lake basin.

In July-August 2013 magnetometric measurements have been carried out at 120 points for 10 profiles with a total length of 10 km. The study area was about 4 km². This measurement phase should confirm a proposed crossbar under the glacier, identified through profile measurements in previous years.

The results of the areal magnetometric survey are presented as the form of a map of the anomalous magnetic field (ΔT) (Fig. 2.2.4.5) and 3D-images (Fig. 2.2.4.6). Trough valley of the South Enilchek glacier is represented by mainly andesitic porphyries ($\alpha=1000-5000 \times 10^{-6}$ GHS) of the Silurian system (S2ld2). The South Enilchek glacier

CHAPTER 2. CLIMATE AND WATER RESOURCES

reached in former times a regional lineament, which existence was instrumentally confirmed in 2011. The glacier began plucking the weakened fractured rocks, forming a "plucking basin" and an arched crossbar, respectively, which finally developed a thrust. This caused a directional change of the South Enilchek.

On a 3D-image of the magnetic field (Fig. 2.2.4.6) non-fractured bedrocks are represented as a crossbar by intensive positive values (blue). Negative values are related to the sides of the crossbar (brown) and are interpreted as "plucking basins".

The body of the South Enilchek glacier is a confluence of several flows, coming from smaller glaciers. More powerful right flows of the South Enilchek glacier deepened its bed more than the low-power flows from the left side valleys.

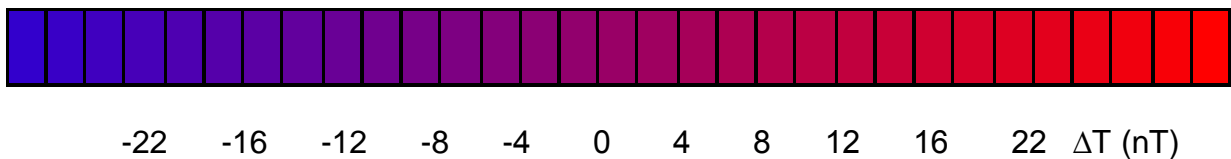
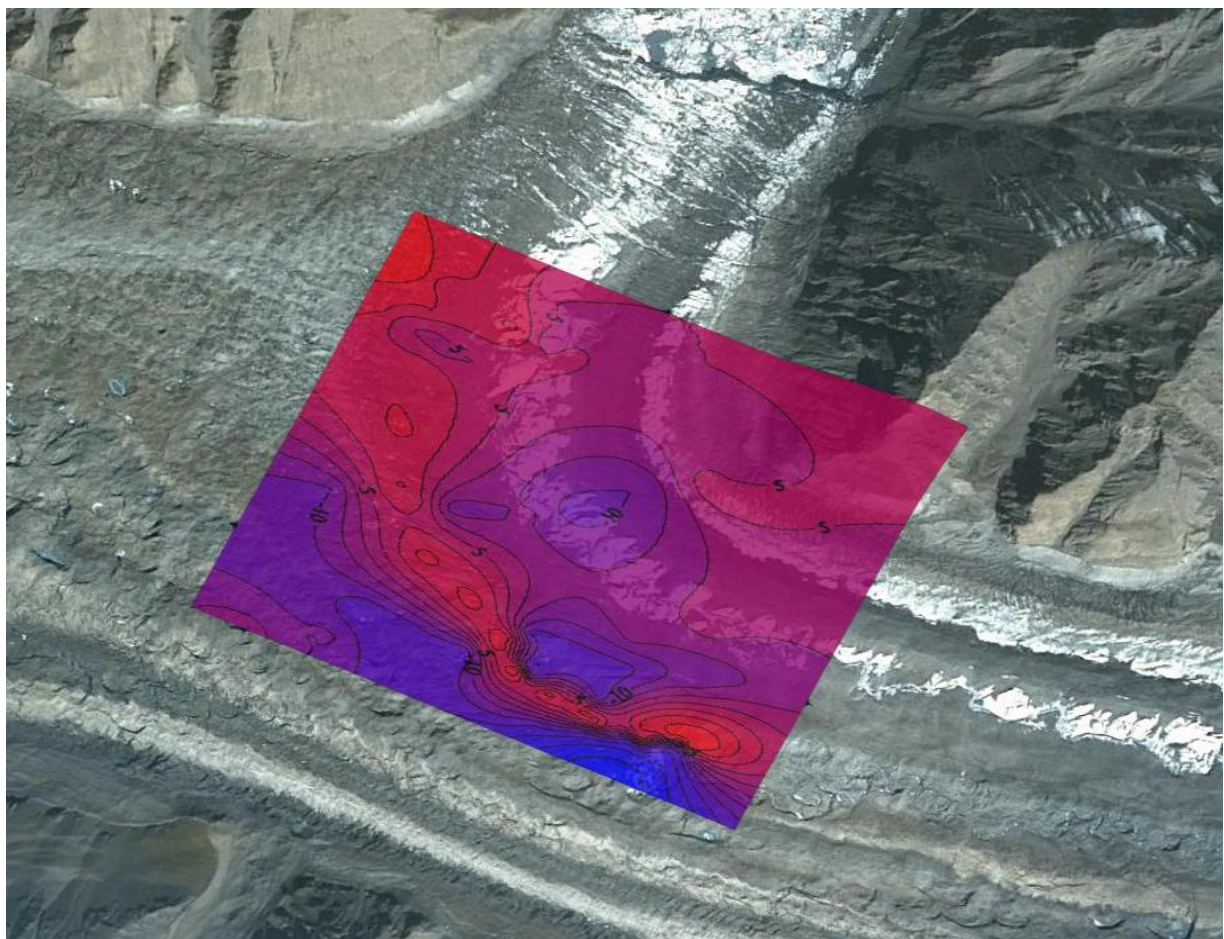


Figure 2.2.4.5. Satellite image of the North and South Enilchek glaciers with overlaid map of contour lines of anomalous Earth's magnetic field ΔT (nT)

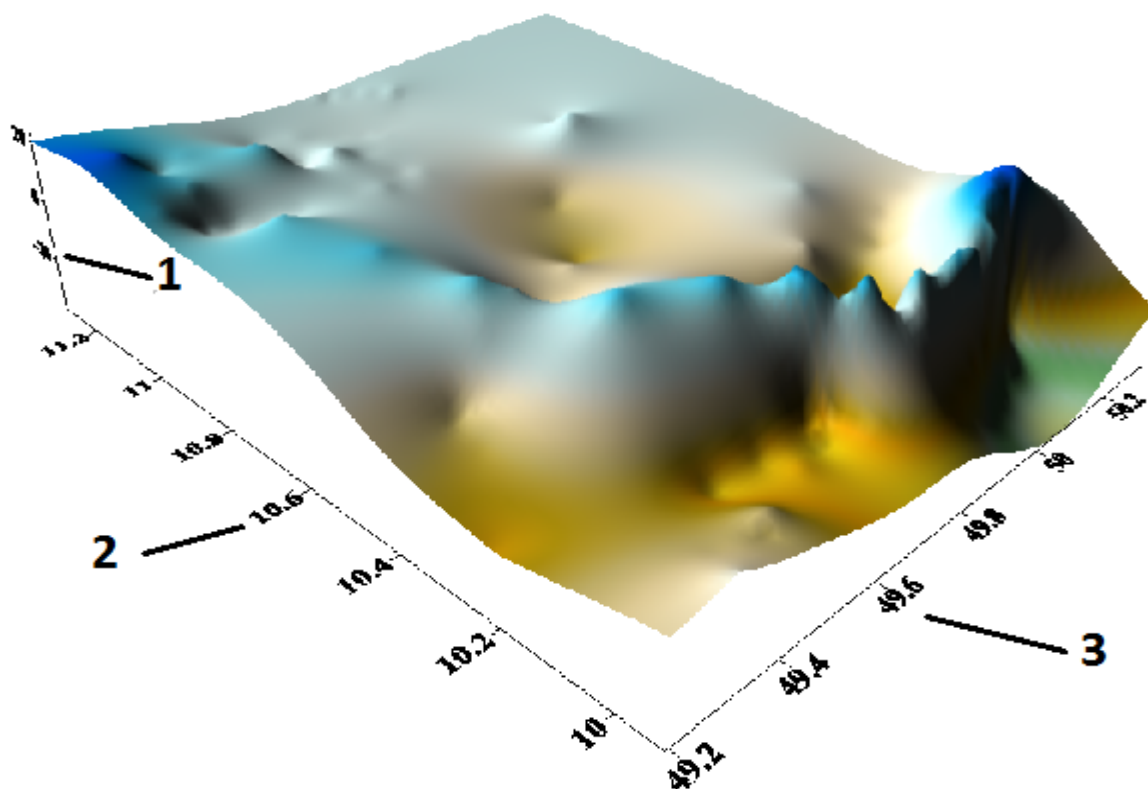


Figure 2.2.4.6. 3D-map of anomalous magnetic field (ΔT) of the North and South Enilchek glaciers confluence area, 1 - values of anomalous magnetic field ΔT (nT) (from -22 to 22); 2 - latitude 42.10.0 - 42.11.2; 3 - longitude 79.49.2 - 79.50.2

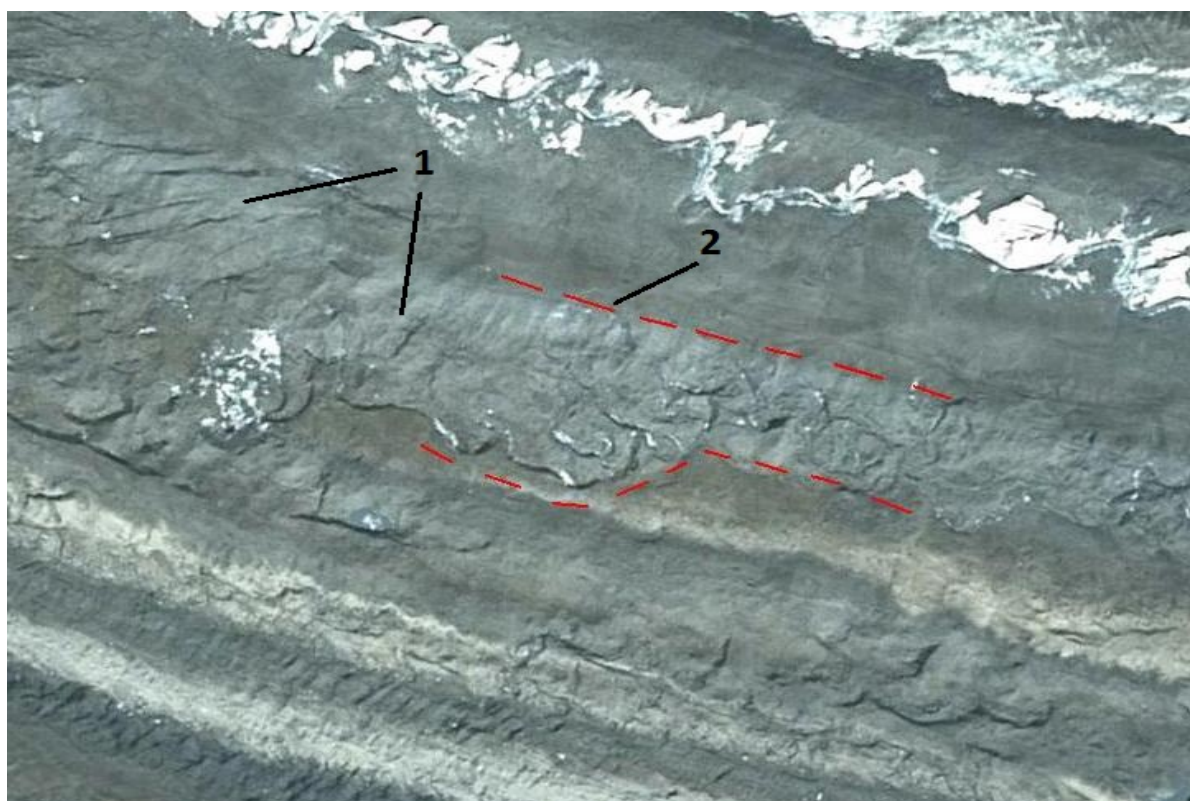


Figure 2.2.4.7. Satellite image of the upper part of examined area, 1 – cross ruptures; 2 – moraine boundaries

Visual evidence of the crossbar is also found on a satellite image of the upper part of the study area (Fig. 2.2.4.7). The satellite imagery clearly shows one of the glacier flows with gray moraine sliding over the nearby flow with brown moraine and increasing in width from 180 m to 300 m. Cross ruptures appear after 500 meters down the movement of the glacier. Probably the beginning of the crossbar is a place, where the gray moraine increases in width.

A comparison of satellite images of different years showed that the beginning of the crossbar did not change the coordinates, even when the glacier is moving. A velocity of the South Enilchek glacier movement according to GPS measurements using TOPCON TPS GB-1000 receiver of the integrated ICEDAM station reached 94 meters per year.

An analysis of graphs, created from the results of radar studies, conducted in 1990 by the Institute of Geography RAS (Macheret et al, 1992), confirmed the assumption of existence of the crossbars in the area of the confluence of the North and South Enilchek glaciers.

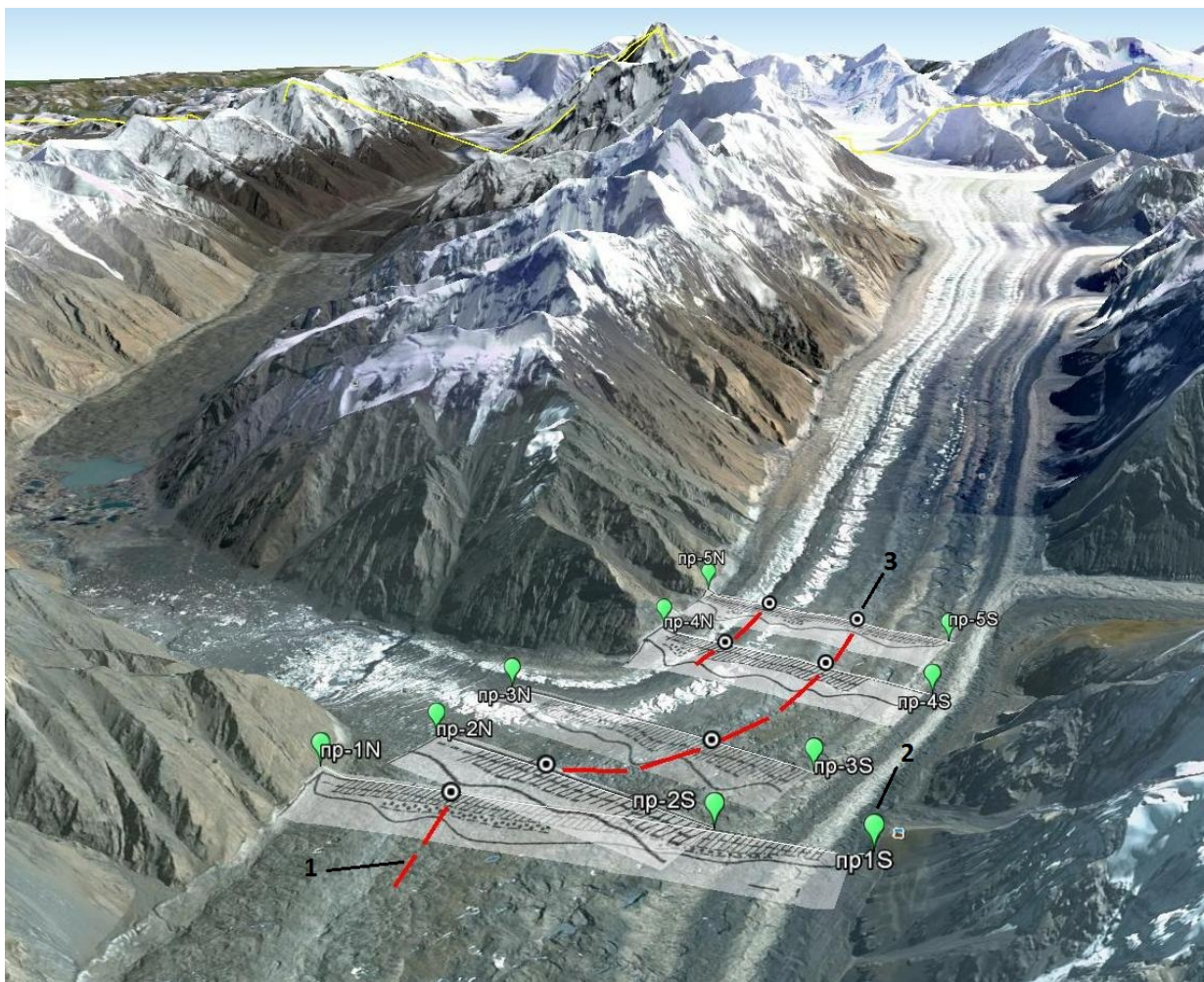


Figure 2.2.4.8. Satellite image with graphs of the bottom topography (Macheret et al, 1992) and supposed crossbars from radar sounding profiles. 1 - supposed crossbars; 2 - starting and ending points of profiles; 3 – maximum points on the graphs, identified with tops of supposed crossbars.

CHAPTER 2. CLIMATE AND WATER RESOURCES

A comparison of the results of radar sensing of the South Enilchek glacier (Macheret et al, 1992) within the PR-1-5 profiles and of magnetometric studies enabled to outline three large crossbars, formed as a result of the glacier exaration activity. The crossbars in the area of the confluence of the North and South Enilchek glaciers are longitudinal and arcuate (Fig. 2.2.4.8).

The first crossbar is arcuate, its length is 2.5 km and base width is 250-300 m, located within PR-2-5 profiles. A height of the crossbar is 100 m. This crossbar causes turning the right flows of the South Enilchek glacier towards the Merzbacher Lake.

The second crossbar is located at the northern edge of the South Enilchek glacier within PR 4-5 profiles, a base width of the crossbar of 200 m, and a height of 100 m in the north side and 50 m in the south.

The crossbars also appear at the confluence of glaciers, where they pluck strongly the bed and overdeepen the valley.

The third supposed crossbar, which is clearly shown in the PR-1 profile (Fig. 2.2.4.9) in the lower part of the study area, is located between the South Enilchek glacier and so-called "dead" non-moving part of the North Enilchek glacier.

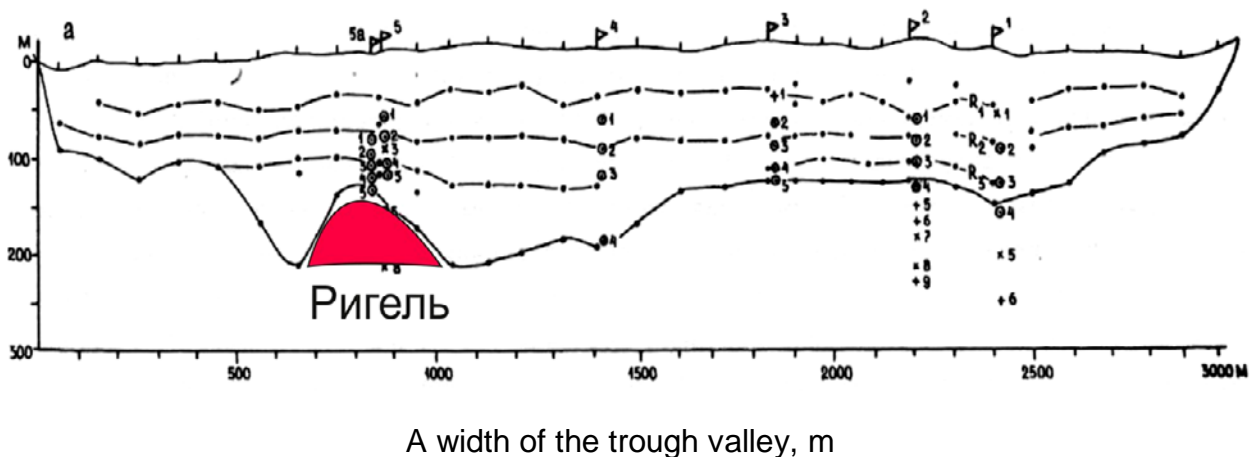


Figure 2.2.4.9. Incision of the North and South Enilchek glaciers along the cross PR-1 profile (Macheret et al, 1992)

As a result of the aerial magnetometer survey at the confluence of the North and South Enilchek glaciers, two intensive positive anomalies were observed. The first anomaly is located in the dam bed and is connected to a horseshoe crossbar ledge, facing the arc to the west, in the direction of the Merzbacher Lake. The second anomaly is arc-shaped and is interpreted by the author as a crossbar, which acts as a thrust when moving of the South Enilchek glacier and causes a change in the direction of the South Enilchek.

The presence of ruptured structures and crossbars was also observed under the glacier. Mapping of moraine sediments was performed with the help of the magnetic field survey.

Reference

1. Macheret Y.Y., Nikitin S.A., Babenko A.N., Vesnin A.V., Bobrova L.I., Sankina L.V. The thickness and structure of the Enilchek glacier according to radiosounding data // Proceedings of the USSR EGAN. 1992. Pp. 86-97.
2. Map "Lineaments and ring structures" The Head Office of Geodesy and Cartography USSR Council of Ministers. Remote Sensing 1980 1:500 000

2.2.5. Study of the Abramov, Golubin, Adygene, Petrov and Karabatkak glaciers

Within the CAWa project "Regional Research Network "Water in Central Asia" (CAWa)" [1] (2008-2013) there are observations of ablation processes to determine the balance and development trends, needed to forecast changes in glaciers and related their water resources.

In order to understand the nature and development trends of the Abramov glacier located within the Alai Ridge, satellite images of different periods, which are shown on Google Earth, USGS, Sovzond servers, as well as topographic maps, published data and aerial images from the Soviet archives were used. In addition, the results of field measurements of the glacier boundary coordinates, obtained in 2012-2013 using GPS, as well as results of the measurements of snow thickness and density of the glacier were used.

A method of the glacier boundary analysis included geological reference of satellite images and topographic maps in MapInfo GIS in the WGS 84 coordinate system with the following separation of multi-contours of the glacier boundaries and their comparison. The satellite images were referenced according to the characteristics of fixed points of the relief in close proximity to the glacier boundary, which allowed us to estimate a relative referencing error due to geometrical distortion of images of the object. Figures 2.2.5.1-2.2.5.2 show a background satellite image of the Abramov glacier tongue, which was obtained from "GeoEye1" satellite from "Google Earth" server, survey date is 19.07.2007. The data on the glacier boundary of 1978 were obtained by using a topographic map of 1:100.000 scale referenced by control points. The boundary of 1986 was fixed using a topographic map of 1:25.000 scale, developed on the basis of stereo-topographic survey, carried out in 1986 and published in 1991 by the Kyrgyz Aerogeodesic Service of the State Geodesy of the USSR. The data on the glacier boundary of 2009 were obtained using satellite images of "World View 1" satellite from the "Sovzond" catalogue, survey date is 20.10.2009. In 2011 the boundary of the glacier tongue was defined relative to the relief features in the western side of the glacier valley according to camera images, installed in 2011 in the eastern side of the Abramov glacier valley by specialists of the Central Asian Institute for Applied Geosciences together with Swiss partners (Department of Geosciences, University of Fribourg, Switzerland) within the "Water in Central Asia" project.

CHAPTER 2. CLIMATE AND WATER RESOURCES

In 2012 the boundary of the glacier tongue was recorded using GPS “Garmin e Trex” with an error <math><10\text{ m}</math>. In general, a relative error of the glacier boundary referencing in different periods is estimated to 10-20 m. On the basis of certain boundaries, a rate of the Abramov glacier area over the past decade was calculated. In Table 1. these results are compared with previously obtained data by *Glazyrin G. et al.* [3].

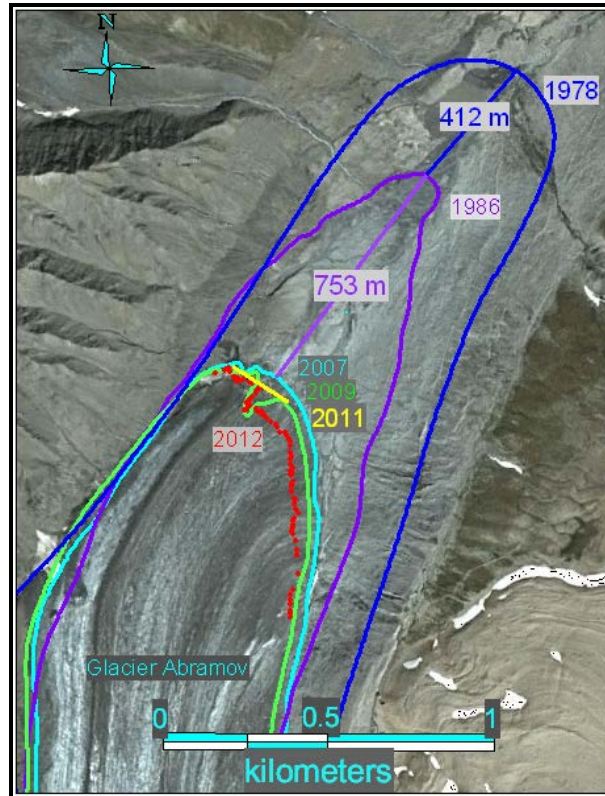


Figure 2.2.5.1. Location of the end of the Abramov glacier tongue in different periods



Figure 2.2.5.2. Position of the Abramov glacier boundary in 2013 according to an image of the “Landsat 8” satellite dated 26.07.2013

Table 2.2.5.1

Period, years	Rate of change of the glacier area (km ² /year; + increment; - reduction)	Annotations
1850-1900	-0.014	"A regime of the Abramov glacier", <i>Glazyrin G. et al. 1993.</i>
1900-1936	-0.013	
1936-1967	-0.027	
1967-1970	-0.077	
1970-1973	+0.18	
1973-1974	+0.007	
1974-1984	-0.024	
1978-1986	-0.064	CAIAG's data
1986-2007	-0.018	
2007-2012	-0.014	

Table 2.2.5.1 shows that in recent years the rate of the glacier reduction is close to that in the second half of the 19th century. This trend seems to be kept.

Besides the results of the satellite images analysis, in 2012 information on the value of ablation on the Abramov glacier using rods, installed in 2011 and measured in 2012, was acquired. These results are shown in Figure 2.2.5.3.

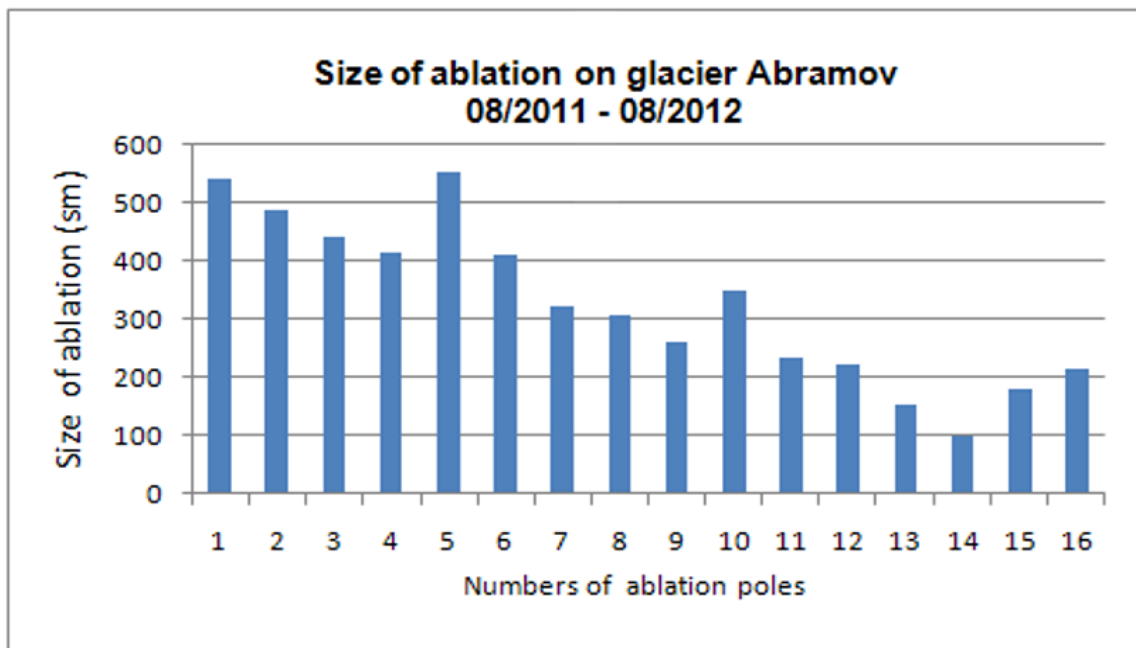


Figure 2.2.5.3. Value of ablation on the Abramov glacier

Based on the data on snow ablation, thickness and density in the accumulation area, the glacier balance was roughly estimated by CAIAG. For 2011-12 the results are made

up: specific accumulation: + 63 g/cm², ablation: - 293 g/cm², so, the ice discharge significantly exceeds its accumulation.

In general, as shown in the analysis above, with a negative mass balance, a trend of the Abramov glacier reduction at a velocity nearly 0.014 km²/year is continuing. A linear velocity of the glacier boundary retreat from 1978 to 2012, defined by the maximum distances, was 32-38 m/year, and in the period from 2007 to 2012 was about 22 m/year. A characteristic feature is the strongly different rate of the glacier retreat. Especially observed in 1973-74 as a large movement of about 300 m was observed for the Abramov glacier that resulted in increment of the glacier area. This uneven movement has to be considered when analysing trends and forecasting changes in glaciation.

In order to clarify the nature and trends of glaciers, located on the northern slope of the Kyrgyz ridge (Golubin, Adygene glaciers) satellite images of different periods, which are on the Google Earth server, aerial images and data of GPS measurements of the glacier boundary were used. In 2011-2012 the edge of the glacier tongue of the Golubin glacier was identified using GPS position; their contours are shown in Figure 2.2.5.4.

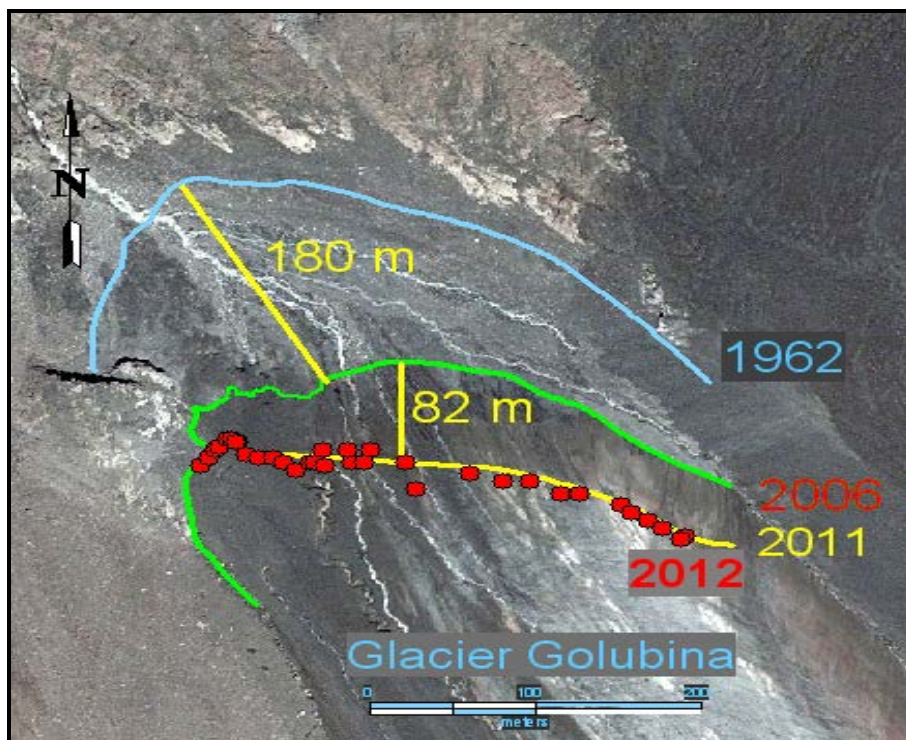


Figure 2.2.5.4. Change of the Golubin glacier tongue edge position for 1962-2006-2012

As a basis, this Figure represents a satellite image from the Google Earth server, with a resolution of up to 1 m, obtained from the Quick Bird satellite on July 24, 2006. In addition, it shows the edge of the glacier tongue of 1962, obtained by decoding the aerial image, with an error of coordinate referencing of the aerial image up to 50 m. Over 44 years, from 1962 to 2006, the maximum distances of the Golubin glacier reduced by a maximum 180 m with an average velocity of about 4.1 m/year. For 6 years from 2006 to 2012 the glacier has reduced by 82 m and a reduction rate of 13.7 m/year, i.e. over this period the rate increased about 3.3 times.

A comparison of the contour of the Adygene glacier tongue (**Figure 2.2.5.5**), which is located as well as the Golubin glacier in the Ala-Archa basin, on Quick Bird image, dated July 24. 2006. with the one obtained from an aerial image of 1962. showed that for over 44 years from 1962 to 2006 a retreat of the tongue was at a minimum of 345 m at an average velocity of about 7.8 m/year and maximum 520 m at an average velocity of about 12 m/year, with an aerial image referencing error up to 50 meters. Thus, the rate of retreat of different glaciers in one watershed during the period from 1962 to 2006 varies on average twice, maximum for the Adygene glacier and minimum for the Golubin glacier.

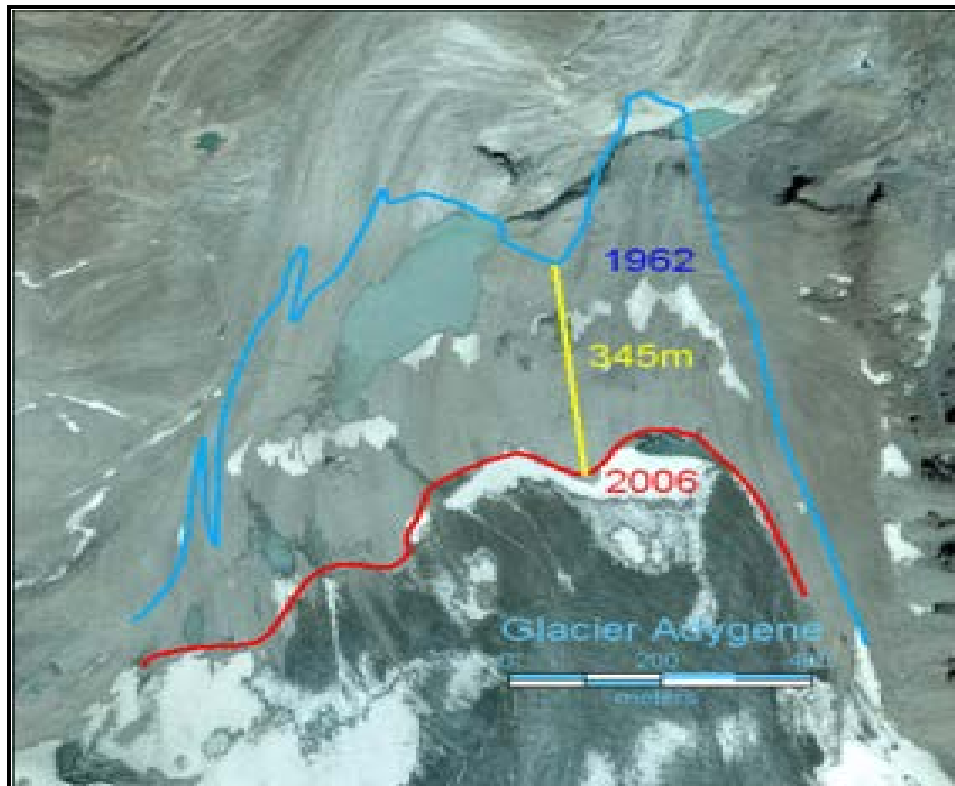


Figure 2.2.5.5. Change of the Adygene glacier edge position for 1962-2006

It needs to be said that after a long pause in 2013 the results of the study (starting from 2010) of the Golubin glacier mass balance accomplished as field work by the Cooperation between the CAIAG and the German Research Centre for Geosciences (GFZ) and the Swiss University of Fribourg (UniFR)) were published in the Bulletin of glacier mass balance No.12 (2010-2011) of the World Glacier Monitoring Service [2].

The change of the Petrov glacier edge position (**Figure 2.2.5.6**) in the Ak-Shyrak mountain range was defined by “Quick Bird” satellite images dated 4.10.2002 from Google Earth server, “Hexagon KH9” image of 1980. “Spot 5” satellite image dated 22.08.2007. obtained within the CAWa project and “Landsat 8” image dated 30.07.2013. obtained from the USGS server.

As shown in **Figure 2.2.5.6**. a linear reduction of the glacier has reached 3200 m by maximum distances for 144 years from 1869 to 2013. at an average reduction rate of about 22.2 m/year. During the last eleven years from 2002 to 2013. the uneven

reduction of the Petrov glacier made up maximum 630 m at a velocity of about 57 m/year.

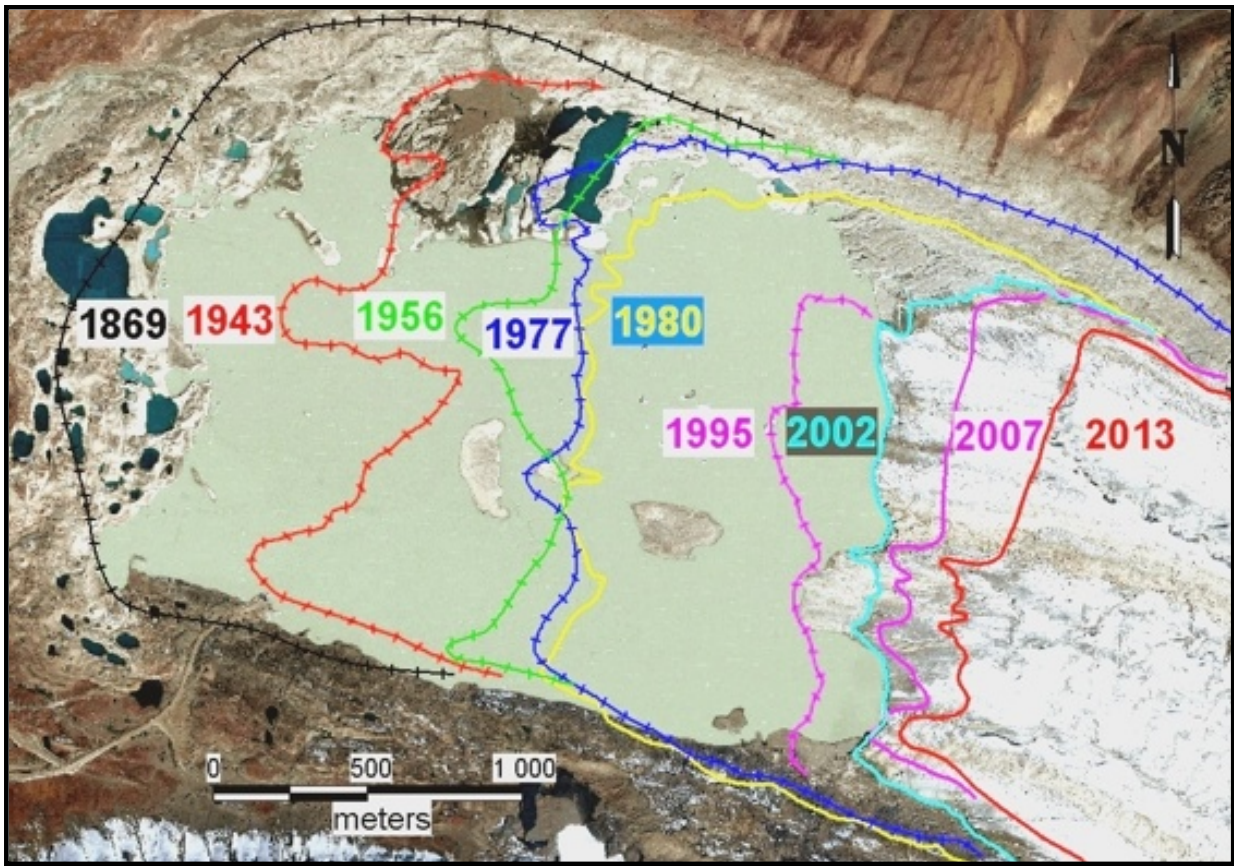


Figure 2.2.5.6. Change of the Petrov glacier edge position for 1869-2013 (lines with hachures - according to the data of Kuzmichenko V.A., smooth lines – according to the data of Mandychev A. (CAIAG))

An analysis of the reduction rate of the Petrov glacier showed a significant uneven velocity changes in different periods with change of a value from 10 to 57 m/year for several times.

A change of the Karabatkak glacier edge position (**Figure 2.2.5.7**), located on the northern slope of the Terskey-Alatoo Ridge, was defined by “Quick Bird” satellite images dated 4.10.2002 from Google Earth server, “World View1” satellite image dated 13.10.2009 obtained from the “Sovzond” server, “Pleiades” satellite image dated 25.09.2013 with a resolution of 1 m/pixel obtained within the CAWa project, and according to results of 2011 on defining the glacier contour using GPS “Garmin e Trex” with an error <10 m.

In general, a relative geological positioning error is no more than 20 m. A reduction of the Karabatkak glacier area for the period from 2002 to 2013 by maximum distances reached 120 m, at an average reduction rate of about 11 m/year. The glacier reduction occurs not only in its active eastern part, but also in the passive western moraine part. According to previous estimate, the glacier has reduced to 920 m from 1947 to 2013. at an average rate of about 14 m/year.

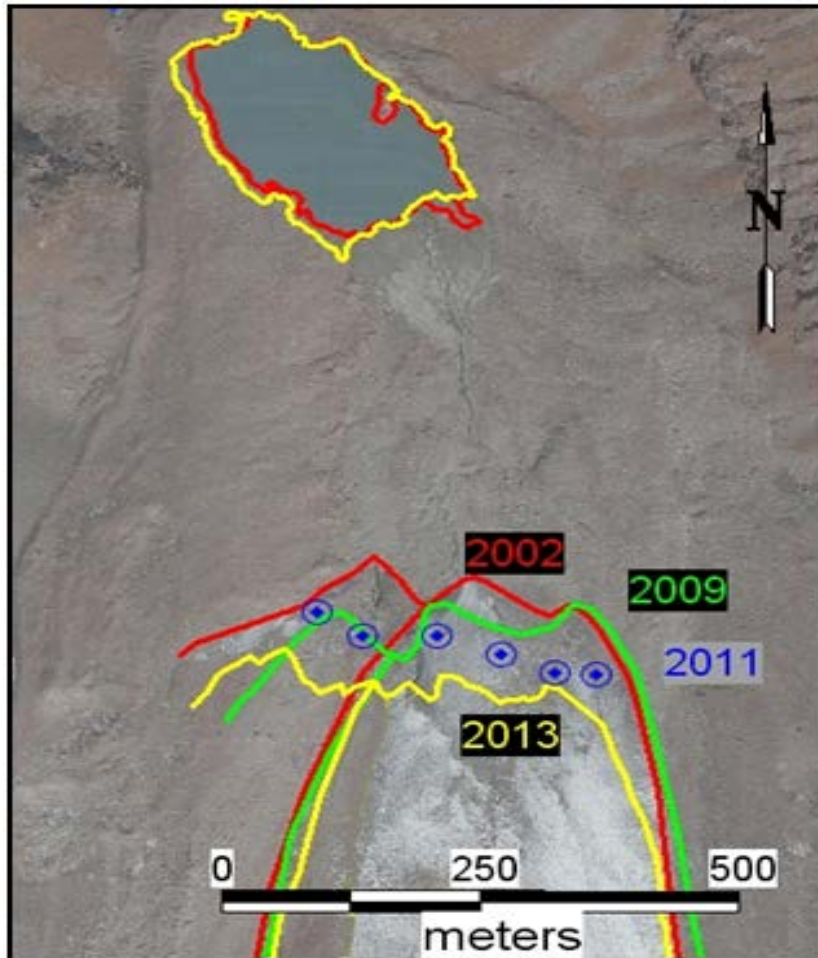


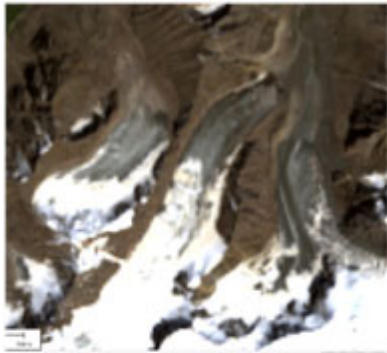
Figure 2.2.5.7. Change of the Karabatkak glacier edge position for 2002-2013

Glaciers were selected as the next objects for mapping in the high part of the Issyk-Kul basin. Glaciers in the basin as well as glaciers in the Tien Shan Mountains and around the world are of particular attention due to their actual degradation, which in turn is reflected by water resources, change of the landscape in the area, etc. Large-scale mapping and description of glaciers in the Issyk-Kul Basin were performed twice: by the Tien Shan physiographic station from 1948 to 1973 [3] and during the inventory of Randolph glaciers (RGI): World Database of glaciers' boundaries under the auspices of the Global Land Ice Measurements from Space (GLIMS) 2012 [2].

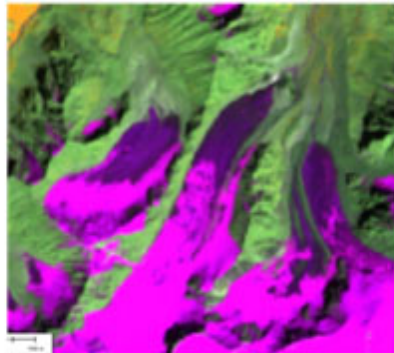
The Randolph glacier inventory, being the most modern, was performed in automatic and semi-automatic mode and has errors in determining the boundaries of glaciers. In addition, this inventory contains no narrative part. In this regard, the analysis of the current state of glaciers was based on space images of Landsat 8 and data from the Glaciers Catalogue of the USSR.

Mapping of glaciers was carried out using a combination of channels - 564. with increased resolution up to 15 m using the 8th panchromatic channel (Figure 2.2.5.8). Watershed boundaries were determined using DEM GDEM2.

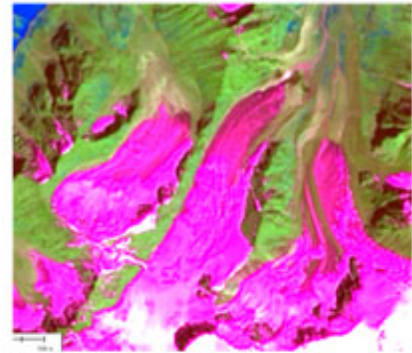
The greatest difficulties in the process of glacier mapping rose while trying to determine the boundaries in the tongue of the glacier covered with a relatively thick layer of moraine terrigenous material. A variety of image processing techniques was used as well as different combinations of channels, in particular, thermal channels. But the possibility of interpretation was limited, so that a fairly accurate determination of the boundaries could only be made for cases when the glacier tongue was covered with a relatively thin layer of moraine material, which allowed determining the ice limit.



Combining of channels 432
(resolution of 30 m)



Combining of channels 564
(resolution of 30 m)



Combining of channels 564 + panchromatic
(resolution of 30 m)

Figure 2.2.5.8. Combining of channels and improvement of the resolution of images for more accurate mapping of the glacier boundaries (glaciers are shown in white and pink).

Mapping of the Issyk-Kul basin glaciers revealed a number of inconsistencies of morphometric parameters of glaciers found from satellite images and the parameters listed in the Glacier Catalogue. If such characteristics as length or area of the glacier are typical, the inconsistencies in such parameters raise a number of questions to the accuracy of its determination during producing both the Glacier Catalogue and the DEM. In addition, a number of inconsistencies were identified in the Glacier Catalogue with regard to both exposure and morphometric characteristics.

For example, glacier #486 in the Catalogue of glaciers was shown with a clear eastern exposure, but in its description in the catalogue further exposure is referred to as the north-west. Nevertheless, this work was not dedicated to search for mistakes in the Glacier Catalogue, therefore, all the data from the catalogue were entered into the database unchanged.

In addition, the database had fields to record current (summer 2013) values of glacier morphometric parameters which can reliably be determined when interpreting Landsat satellite images and ASTER DEM data: length of the glacier, its size, the minimum and maximum heights, the geographical coordinates of the centroid of the object.

Results of the comparison of the areas of glaciers (area of over 0.1 km²) taken from the catalogue and from the decrypted satellite images are presented in Table 2.2.5.2.

CHAPTER 2. CLIMATE AND WATER RESOURCES

Table 2.2.5.2 Comparison of glacier areas (more than 0.1 km²) taken from the catalogue of the USSR glaciers (1976) and from the Landsat 8 satellite images (2013)

River basin	Number of glaciers in the catalogue	Number of glaciers by Landsat 8 imagery	Area of all glaciers in the catalogue, km ²	Area of open parts of glaciers in the catalogue, km ²	Area of glaciers by Landsat 8 imagery, km ²
Northern slope of the Terskei-Alatoo Ridge	481	599	496.7	449.6	510.7
Southern slope of the Kungei-Alatoo Ridge	150	158	139.7	135.7	114.0
Entire basin of Issyk-Kul Lake	631	757	636.4	585.3	624.7

Table 2.2.5.2 shows that the number of glaciers (with area >0.1 km²) identified as a result of interpretation of Landsat 8 satellite images exceeds the number listed in the Glacier Catalogue of about 118 for the northern slope of the Terskey-Alatoo Ridge, about 8 for the southern slope of the Kungei-Alatoo Ridge and about 126 for the whole basin of Issyk-Kul Lake. It should be noted that with the overall increase in the number of glaciers identified from satellite images compared with the number of glaciers listed in the Catalogue, there is also the disappearance of some glaciers listed in the catalogue compared to the satellite images. This is largely due to the parameter limiting the area (> 0.1 km²). I.e., the glaciers that are not defined on satellite imagery, have not disappeared completely, but their area has become less than 0.1 km² (e.g. 0.092 km²). This is certainly true for those glaciers with an area of about 0.1 km² according to the Catalogue. In turn, the glaciers with an area slightly less than 0.1 km² might not be included in the Catalogue, and a slight increase in their area has now opened their entry into the newly developed database. This does not mean that when compiling the Catalogue of these glaciers they didn't exist at all.

Glaciers' area by the results of satellite image interpretation exceeds the area for Terskey-Alatoo and is less for the Kungei Alatoo given by the Catalogue. In general, for the whole basin of Issyk-Kul Lake the area of glaciers determined from satellite images is less than the area of glaciers indicated in the Catalogue, but more than the area defined in the Catalogue as "open parts of glacier, not covered by moraine". It should be noted that in this work mapping was carried out both for open parts of glaciers and for parts covered with a thin layer of terrigenous moraine material. Identification of buried ice beneath a thick layer of moraine material is a rather difficult task, even during field research. Therefore, in this work, the most appropriate definition for the ending part of

glacier tongue, the lower bound of which was determined during interpretation, would be “an active part of the glacier,” as opposed to passive, weakly connected or not connected with the main body of ice represented by buried ice under terminal moraines.

In general, as it is seen from the above analysis, a continuous trend of reduction of the volumes of the Tien-Shan glaciers is observed, caused by an increasing average annual ground air temperature. The glacier retreat happens with an irregular reduction rate. This irregularity is observed for all glaciers, depending on the location of the slope of the ridge and all related factors of its occurrence, and for each specific glacier, depending on the characteristics of its development.

A linear estimate of the glacier retreat is only a rough approximation due to uneven boundaries of the glaciers retreat, but is justified for overall estimate of trends of the glacier change.

Reference:

1. <http://www.cawa-project.net/>
2. WGMS 2013. Glacier Mass Balance Bulletin No. 12 (2010–2011). Zemp M., Nussbaumer S. U., Naegeli K., Gärtner-Roer I., Paul F., Hoelzle M., Haeberli W. (eds.), ICSU(WDS)/IUGG(IACS)/UNEP/UNESCO/WMO, World Glacier Monitoring Service, Zurich, Switzerland, 106 pp., publication based on database version: doi:10.5904/wgms-fog-2013-11.
3. Regime of the Abramov glacier/ G.E.Glazyrin, G.M.Kamnyanski, F.I.Perziger; Central-Asian Regional н.-и. Institute of Hydrometeorology named after V.A.Bugaev, pp. 228, with illustrations 20 cm, Saint Petersburg. Hydrometeoizdat 1993.

2.3. Study of change of regime of rivers, lakes, water reservoirs and underground waters

On the territory of the Kyrgyz Republic there are more than 25 thousand rivers which belong to eight main hydrological basins: Issyk-Kul Lake, the Chu River, the Talas River, the Syrdarya River, the Amudarya River, Chatyr-Kul Lake, the Tarim River and Balkhash Lake. The main artery is the Naryn River which has a water catchment area of 58 thousand km² or about 25% of the country's area. This river is of high importance for drinking water supply and irrigation, hydropower and other needs.

The most important work done by CAIAG in the field is the forecast of water flow into the Toktogul water reservoir in the vegetation period, the change of perennial climatic conditions and the flow in the upper stream of Naryn river during the vegetation period, as well as the change of annual flow of rivers in the Issyk-Kul basin for a long-term period.

2.3.1. Forecast of water flow into the Toktogul water reservoir in the vegetation period

The study area in physical and geographical respect belongs to the Middle Asia mountain country, the Inner Tian Shan region. This is a large secluded mountainous and kettle hole region. The average absolute height is 3100 m. About 92% of the area lies in the Naryn river basin. A common feature for the area is lateral or close to it spread of mountain ranges with intermountain kettle holes and valleys.

The climate is extremely continental and arid. The cold period is longer within a year. The listed common features influence the nature of formation and geographical distribution of rivers' flow in the Naryn basin which is a resource-generating region with regard to surface and ground water. In the Naryn river basin are numerous water-users with the Toktogul hydropower station as main user, for which the forecast of water supply to the water reservoir is a principal term for developing an operating mode of reservoir cascades.

Naryn River belongs to the Aral Sea basin being the largest feeder of Syrdarya River. The water catchment area of the Naryn river is about 58 thousand km² elevation points of the water catchment basin vary within 0.7 – 5.0 km.

Table 2.3.1.1 Basic physical-geographical and hydrological features of the Naryn River and lateral inflows in the Toktogul reservoir

River site	Length of river from head to outlet (km)	Water catchment area, km ²	Average weighted altitude of catchment area, m	Period of observation on the flow, years	Average annual water discharge m ³ /sec	Type of river feeding
Naryn-Uchterek	578	52 000	2 890	1963-2011	324	Snow and glacial
Uzunakmat – Usta-Sai river outlet	73	1 790	2 360	1930-2010	28.7	Snow and glacial
Chychkan – Bala Chychkan river outlet	61	903	2 890	1938-2009	17.5	Snow and glacial
Torkent – Torkent village	45	654	2 420	1966-1997	10.3	Snow and glacial

To forecast water flow in the Toktogul reservoir during the vegetation period (April-September), meteorological data for the period from 1967 to 2011 were used hydroposts, located at different heights and slope exposures in the basins of main inflows of the Naryn River. Detailed information is given in Table 2.3.1.1. Table 2.3.1.1

CHAPTER 2. CLIMATE AND WATER RESOURCES

shows main physical-geographical and hydrological features of the Naryn River in the Uchterek gate (main intake gate) and three lateral inflows in the Toktogul reservoir.

For a forecast of the water inflow in the Toktogul reservoir for vegetation period (April-September) the meteorological information from 7 meteorological stations from 1967 to 2011 located on various heights and slope expositions in main basins of the Naryn River was used. The data on them is shown in Table 2.3.1.2.

Table 2.3.1.2 Data on meteorological stations (meteorological posts) in the Naryn River basin

No.	Name of meteorological station	River basin	Altitude, m above sea level
1.	Tian Shan	Head of Big Naryn River	3614
2.	Naryn	Head Of Naryn River	2039
3.	Atbashy	At-Bashy River	2025
4.	Baetovo	Terek River	1960
5.	Itagar	Chychkan River	2011
6.	Suusamyr	Suusamyr River	2061
7.	Chaek	Djumgal River	1642

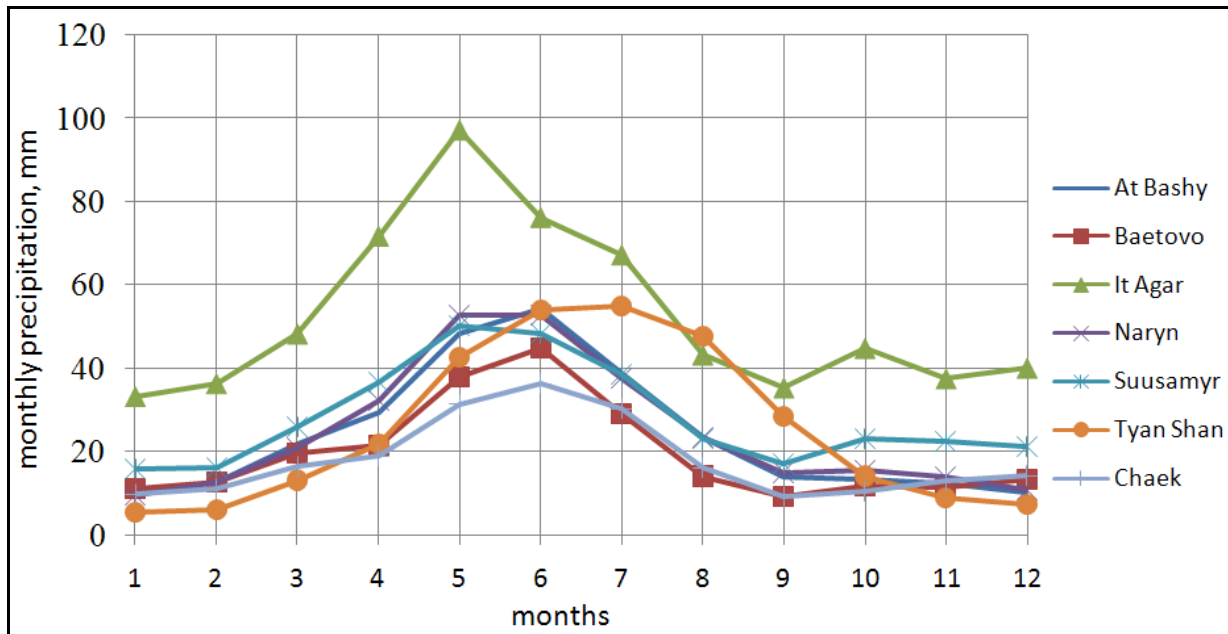


Figure 2.3.1.1. Annual precipitation trend as per historical data on meteorological stations

Figure 2.3.1.1 shows annual precipitation cycle on these meteorological stations and meteorological posts. As seen from Table 2.3.1.1, the annual trends are basically

CHAPTER 2. CLIMATE AND WATER RESOURCES

similar to each other. Maximum of precipitation is in May-June, at the upland station of Tien Shan – in June-August. Minimum precipitation is observed during the cold period – from September to February, at the Tian Shan meteorological station – from October to February.

It should be also noted that due to orography and orientation to moisture bearing streams at the Itagar meteorological station the precipitation is higher than at other meteorological stations.

The annual distribution of the flow depends, firstly, on change of precipitation within a year and air temperature and, consequently, evaporation. The annual distribution of the flow of Naryn River – at the Uchterek site, inflow to the Toktogul reservoir and lateral afflux of Chychkan, Uzunakmat and Torkent Rivers to the Toktogul reservoir – is given in Figures 2.3.1.2 and 2.3.1.3. Water inflow to the Toktogul reservoir was estimated as an amount of main incoming site to the reservoir – Uchterek site and three lateral inflows to the reservoir – Uzunakmat, Chychkan and Torkent. Starting from 1993 when the mudflow ruined the Torkent hydropost, values as $0.6 \cdot \text{Chychkan}$ were used for estimation.

As seen in Figures 2.3.1.2 and 2.3.1.2. all rivers of lateral inflow have maximum flow from May to June, in Naryn River at Uchterek site – till August. The highest flows are observed in all rivers in June. Maximum water flows in Naryn River at Uchterek site reach $2\,400\text{ m}^3/\text{sec}$ (in 1966), Chychkan river - $141\text{ m}^3/\text{sec}$ (in 2002), Uzunakmat River - $203\text{ m}^3/\text{sec}$ (in 1934), Torkent River - $177\text{ m}^3/\text{sec}$ (in 1968). The low-water season for all rivers is from October (lateral inflows to the Toktogul reservoir), or from November (Uchterek site) to March.

It should also be noted that within a year average the monthly flows in the Naryn River – Uchterek site significantly exceed flows in other rivers which is explained by the fact that the Naryn river catchment area is much larger than the areas of the rivers under study.

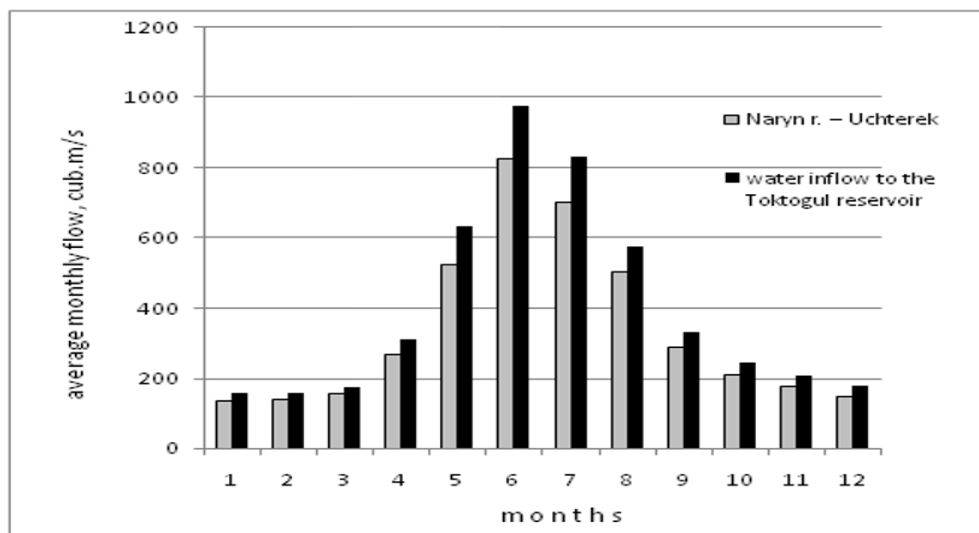


Figure 2.3.1.2. Annual distribution of flow in the Naryn River – Uchterek site and water inflow to the Toktogul reservoir

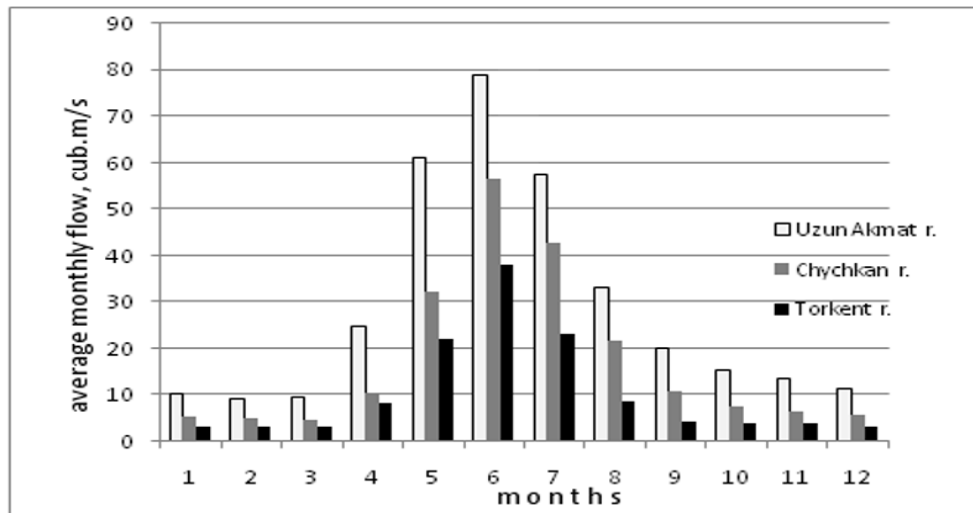


Figure 2.3.2.2. Annual distribution of river flows – lateral inflows to the Toktogul reservoir

Main sources of the rivers under investigation are melt waters and, first of all, melt water of seasonal snow (about 40% of the total feeding of the Naryn River [6]). Melt waters of permanent snow and glaciers play a big role in feeding many rivers with upland water catchments. Rain waters have no big importance in general feeding of the river flow. Feeding of the so called “basic flow” and low-water flow is mainly provided by ground waters (about 40% of the total feeding of the Naryn River [6]). The ratio of feeding sources in the total river flow alters in a wide range depending on flow formation features which are mainly determined by a vertical zonation and hypsometric properties of river basins and to a lesser degree by their geographical location. The considered rivers have the maximum runoff in June (for rivers with snow and glacial feeding). Therefore, these factors are primarily used as a guide in selecting a forecasting method.

The main source of water conservation is precipitation in the form of snow or rain. Water reserves accumulated in the form of snow, as a rule, is linked with snow retention duration i.e. duration of the cold period.

Physical and statistical methods are widely applied in the practice of hydrological forecasting. The general theoretical basis for developing long-term forecasts is a water balance equation in the river basin. In general, the water balance equation for mountain rivers in the spring-summer period can be presented as follows [6]

$$Y_0 = \sum_{i=1}^n S_i f_i + \sum_{i=1}^n X_1 i f_i + \sum_{i=1}^n X_2 i f_i + \sum_{i=1}^n h_T f_{ni} - \sum_{i=1}^n E_c i f_i - \sum_{i=1}^n E_n i f_i - \sum_{i=1}^n E_d f_i \pm \Delta_{sp} \pm \Delta_n \pm \Delta_B \quad , \quad (1)$$

where Y_0 - – river flow during vegetation period (including basic);

S_i – water reserve in snow cover of i altitude zone before melting;

i – number of altitude zone;

X_1 – amount of precipitation during snow melting;

X_2 – amount of precipitation from the start of melting to the end of estimated period;

CHAPTER 2. CLIMATE AND WATER RESOURCES

hT – layer of glaciers and permanent snows on the area disposed of seasonal snow;

E_c – evaporation from snow excluding condensation;

E_n – evaporation from soil;

$EД$ – evaporation of moisture kept by tree crown and transpiration;

f_i - areas of altitude zones;

Δp – change in reserves of ground waters located higher than layers preconditioning the basic flow;

ΔB – change in reserves of moisture in soil and ground;

Δn – change of reserves in layers preconditioning the basic flow;

f_n – areas of glaciers and snow fields.

However, it is impossible to measure or calculate many terms of equation. Therefore, in developing practical methods of forecasting a seasonal flow, the water balance equation is substituted by a similar equation which includes only principal factors.

$$Q_t = f(S_t + X_1), Q_t = f(\sum X_m), Q_t = f(S_t, Q_m, \theta_m^\circ), \quad (2)$$

Q_t – water flow within the period of time t ;

θ_m - temperature for the previous period with duration m ;

Q_m - water flow for the previous period with the same duration m ;

S_t – water reserves in snow cover by the time of making forecast t ;

X_m - precipitations within the period prior to making forecast.

As opposed to many authors who believe that only solid precipitations create spring-summer flow, Girnik found out that it is not necessary to fix starting and ending periods of solid precipitation summation for each basin and each year. She considers that as a predictor for vegetation forecast it is sufficient to take a calendar period from October 1 to March 31 [4].

Apart from the contribution of precipitation in a liquid equivalent (mm) to the flow, in multiple regressions the low water (basic) flow was taken into account that significantly improved tightness of correlation dependence with water inflow to the Toktogul reservoir during the vegetation period (April-September).

Analysis of forecasting of the rate of stream flow using physical and statistical methods was done [9] considering in mind that the rivers flow in the vegetation period is influenced not only by precipitations within the cold period but also the low water flow. For this, linear correlation dependencies could be obtained and equations of constraints of average precipitation amounts were figured out for the cold period using rates of discharge at 7 meteorological stations located in Naryn River basin with water inflow to

CHAPTER 2. CLIMATE AND WATER RESOURCES

the Toktogul reservoir during the vegetation period. The multiple regression method was also applied when as a second predictor the low runoff of water inflow into the Toktogul reservoir was used.

As a result of work, the following equations were obtained to estimate water inflow to the Toktogul reservoir during the vegetation period:

$$1. Q_{\text{aver. veg.}} = 385,7 * \Sigma \kappa \nu (\text{Tien Shan Naryn} + \text{Itagar} + \text{Suusamyr} + \text{Baetovo} + \text{At-Bashy} + \text{Chaek}) / 7 + 212.4 \quad R^2 = 0.66.$$

$$2. Q_{\text{aver. veg.}} = 1,44 * Q_{\text{low water}} + 362 * \Sigma \kappa \nu (\text{Tien Shan} + \text{Naryn} + \text{Itagar} + \text{Suusamyr} + \text{Baetovo} + \text{At-Bashy} + \text{Chaek}) / 7 - 26.1 \quad R^2 = 0.75.$$

$\Sigma \kappa \nu$ – total precipitation in rate of discharge;

$Q_{\text{low water}}$ – average water flow in low water period, m^3/sec ;

R^2 – regression coefficient.

As a result of the studies carried out it was established that:

The main sources of the rivers of the Naryn basin is melt water and, first of all, melt water of seasonal snows. Ground water plays the second big role in feeding the low water or so called “basic flow” in the Naryn basin.

The general theoretical basis for developing long-term forecasts of river flow is the water balance equation. In developing practical methods of seasonal runoff forecasting, the water balance equation is substituted by the approximate equation which includes only principal factors. For the Naryn river basin these are precipitations in water equivalent accumulated within the previous cold period and runoff during the low water period.

The rate of stream flow was analyzed using physical statistical methods of forecasting and lineal correlation dependences and regression equations were obtained which can be used for estimating water inflow to the Toktogul reservoir for the future vegetation period (April – September). Indicators of correlation dependence tightness are rather high, R^2 equals to 0.66 and 0.75.

Reference:

1. Abalian T.S. Methods of forecasting the flow during the vegetation period in the rivers of Northern Kirghizia at places with natural regime – Scientific report. Directorate of Hydrometeorological Service under Council of Ministers of the USSR. Central Institute of Forecasts. Moscow, 1956.
2. Apollov B.A., Kalinin G.P., Komarov V.D. Hydrological forecast course. Leningrad, Gidrometeoizdat, 1974.
3. Atlas of the Kyrgyz SSR, GUGK. Moscow, 1987.

CHAPTER 2. CLIMATE AND WATER RESOURCES

4. Girnik E.I. Long-term flow forecasts for the Syrdarya River basin in conditions of artificially changed regime. Directorate of Hydrometeorological Service under Council of Ministers of the USSR. SARNIGMI, Tashkent, 1971.
5. Kalashnikova O.Yu. On issue of hydrological forecasts of spring-summer runoff of mountain rivers. "Meteorology and hydrology in Kyrgyzstan". KRSU, edition 3. Bishkek, 2003.
6. Mamatkanov D.M., Bajanova L.V., Romanovskiy V.V. Water resources of Kyrgyzstan at the modern stage//Kyrgyz NAS, Institute of water problems and hydropower. – Bishkek, Ilim, 2006. - p.266.
7. Martinek J., Rango A., Roberts R. Model of melt water flow. Users' guide. Geographical faculty, Bern University, 1998.
8. Mikhailov V.I., Petriashova E.V., Smorodskaya N.S. On methods of long-term forecasts of mountain river flow in Kirghizia. // Peculiarities and methods of estimation of hydro-meteorological elements and their forecast / News of Kyrgyz Geographic Society, edition 15. – Frunze: Ilim, 1983.
9. Guide on hydro-meteorological forecasts, edition 1. Leningrad: Hidrometeoizdat, 1989.
10. Resources of surface waters in the USSR. Volume 14. Middle Asia, edition 2. Leningrad: Hidrometeoizdat, 1973.
11. Statistical methods of forecasts of mountain river flow. Works of SARNIGMI. Leningrad: Hidrometeoizdat, 1977.

2.3.2. Long-term change of climatic features and water flow at the Naryn River head during the vegetation period

The vegetation period from April to September is an important feature of river regime considered for planning the use of water resources in hydropower and irrigation sectors. The Naryn River is the main hydropower and irrigation artery in Kyrgyzstan and neighboring countries (Kazakhstan and Uzbekistan). In near future, it is planned to build hydropower station cascades on the Naryn River and its upper courses, therefore, the study of the regime of the Naryn River upstream based on the latest data becomes very important.

In this work, the study of change of hydrological and climatic features of vegetation flow (April-September) in the Naryn River upstream was carried out within the period from 1931 to 2012. In particular, it was focused on the hydrological regime of the Naryn river upstream based on observation data from the hydrological post "Naryn River – Naryn town" (HPNN); climatic features based on observation data from meteorological stations "Tien Shan" (altitude of 3614 m) in the glacial nival zone and "Naryn" (altitude of 2040 m) in the downstream of the studied catchment area. It was taken into account that in 2000 the location of the Tien Shan Station was slightly changed, therefore, data from the Naryn Station located in this basin was analyzed. In spite of the location change, data on air temperature at the upland weather station "Tien Shan" had closer correlation

CHAPTER 2. CLIMATE AND WATER RESOURCES

with the flow (HPNN data) because the altitude of the station was approximately similar to the average altitude of the study catchment area (3570 m).

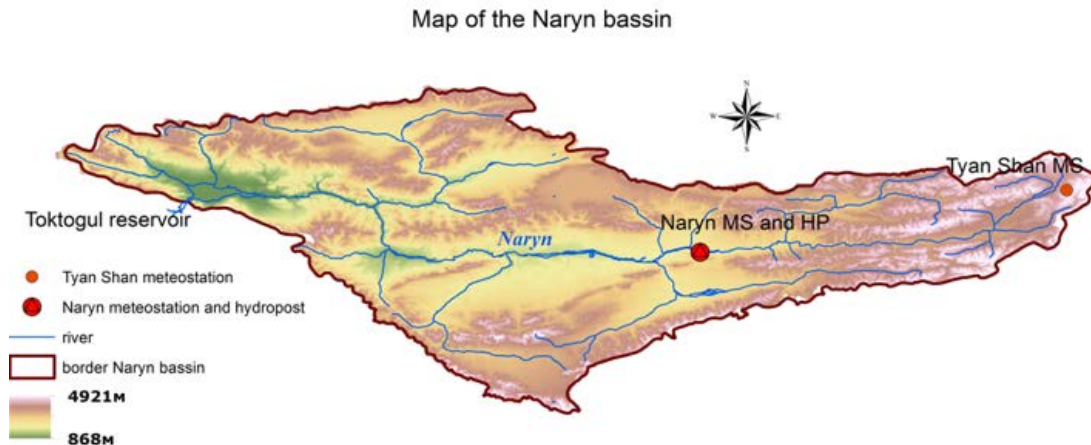


Figure 2.3.2.1. Studied basin of the Naryn River head till the hydrological post Naryn River – Naryn town

In order to identify features of the Naryn River upstream flow during the vegetation period, a five-year moving trend was built based on the HPNN data which shows an increase of average vegetation flows from 1992 (Figure 2.3.2.2). The figure demonstrates high water years (1994, 2002, 2010) with big excess – 153-162% of the average historical flows during the vegetation period. Also, on the basis of HPNN data a differential integral curve of water flow in the vegetation period was built. It also distinctly shows the period of stable increase of water volume since 1992 to present time (Figure 2.3.2.3). By estimations, the average vegetation flow for the period from 1992 to 2012 was $177\text{m}^3/\text{sec}$ or 122% as compared with the period from 1931 to 1991 when it was $145\text{m}^3/\text{sec}$.

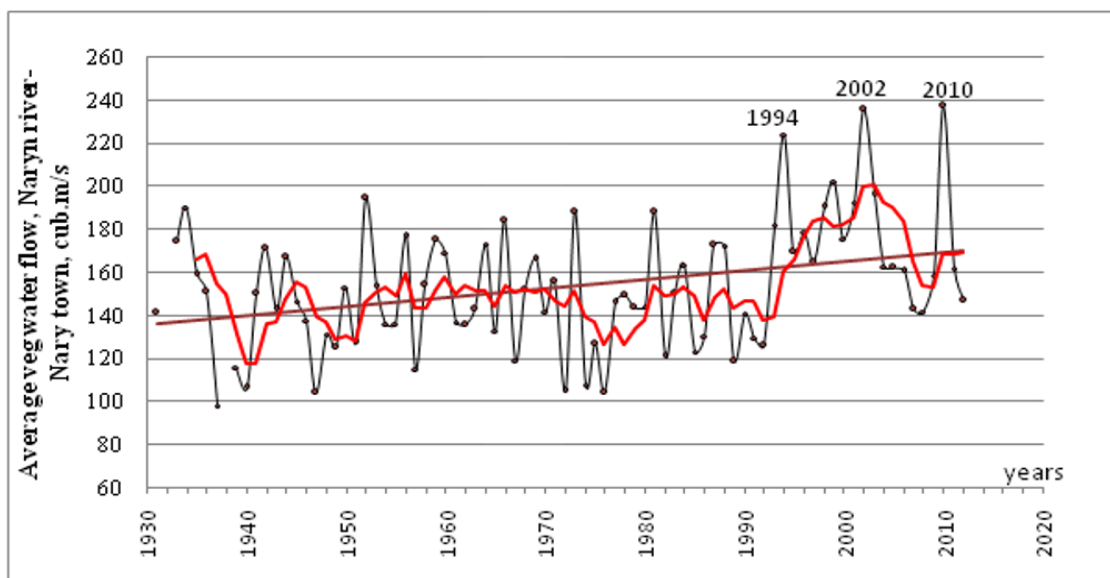


Figure 2.3.2.2. Change of water flow HPNN in the period from 1930 to 2012

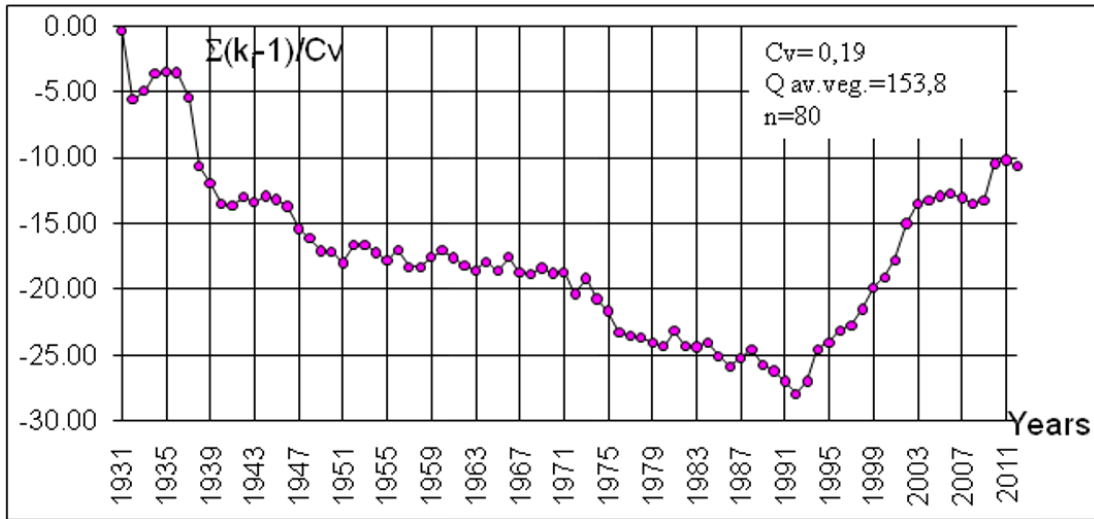


Figure 2.3.2.3. Differential integral curve of water flow, the Naryn River - Naryn town (1931-2012)

Let's consider the structure of flow in the vegetation period and the way the share of months of vegetation flow (HPNN data) was changed since 1992. The upper course of the Naryn River belongs to upland rivers with snow-glacial feeding and with maximum high water in July. The river hydrograph is multimodal, the first peak of high water originates from seasonal snow melting (April-June), the following from melting of glaciers and upland snows (July-September). In percentage ratio, the water content of the Naryn river (HPNN) in the vegetation period (high water) is distributed in the following way: 26% of runoff fall within July, 23% in June and August, 13 and 10% in May and September respectively, and only 5% in April.

Figure 2.3.2.4, based on the HPNN data, shows a permanent decrease of share of glacial feeding months in comparison to months with seasonal snow feeding. Thus, starting from 1992 the share of flow in July in total flow during the vegetation period fell down almost about 10% (**Figure 2.3.2.5**).

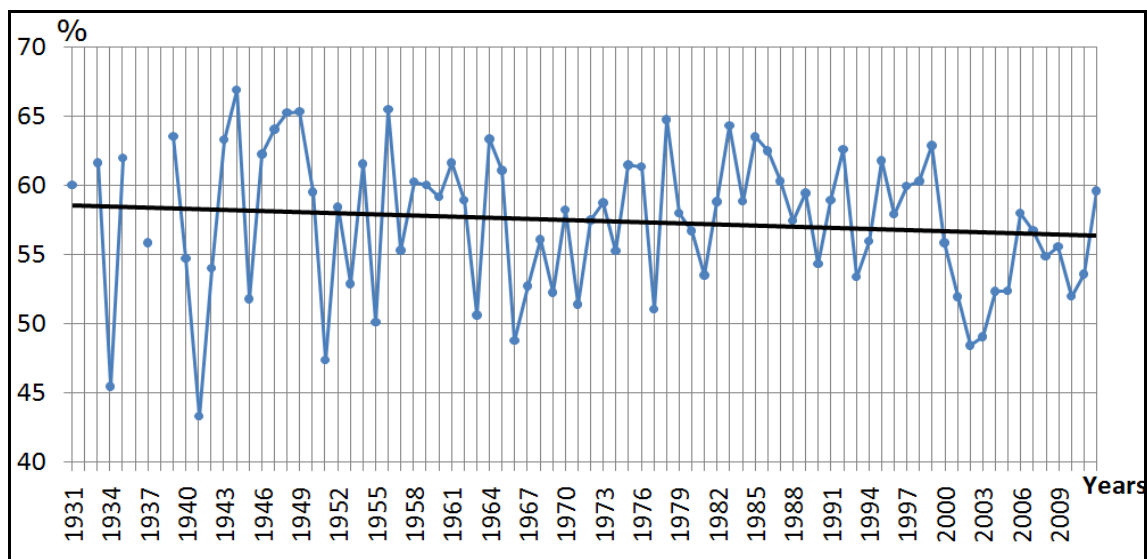


Figure 2.3.2.4. Ratio of months of glacial feeding (July-September) to months of seasonal snow feeding (April-June)

Since in July the river feeding is provided by both melting of seasonal snow and glaciers, this phenomenon may be linked to current glacier degradation and recession of neve line in the upstream of the Naryn River (see Kuzmichenok V.A. and Dikih A.N. [1.2]). Participation of glaciers in river feeding is observed later in August where share of flow didn't change in September as well although it increases slightly (about 1%). Share of flow of months with seasonal snow feeding increases from April to June. With such tendency, maximum high water will gradually move to earlier periods – from July to May-June.

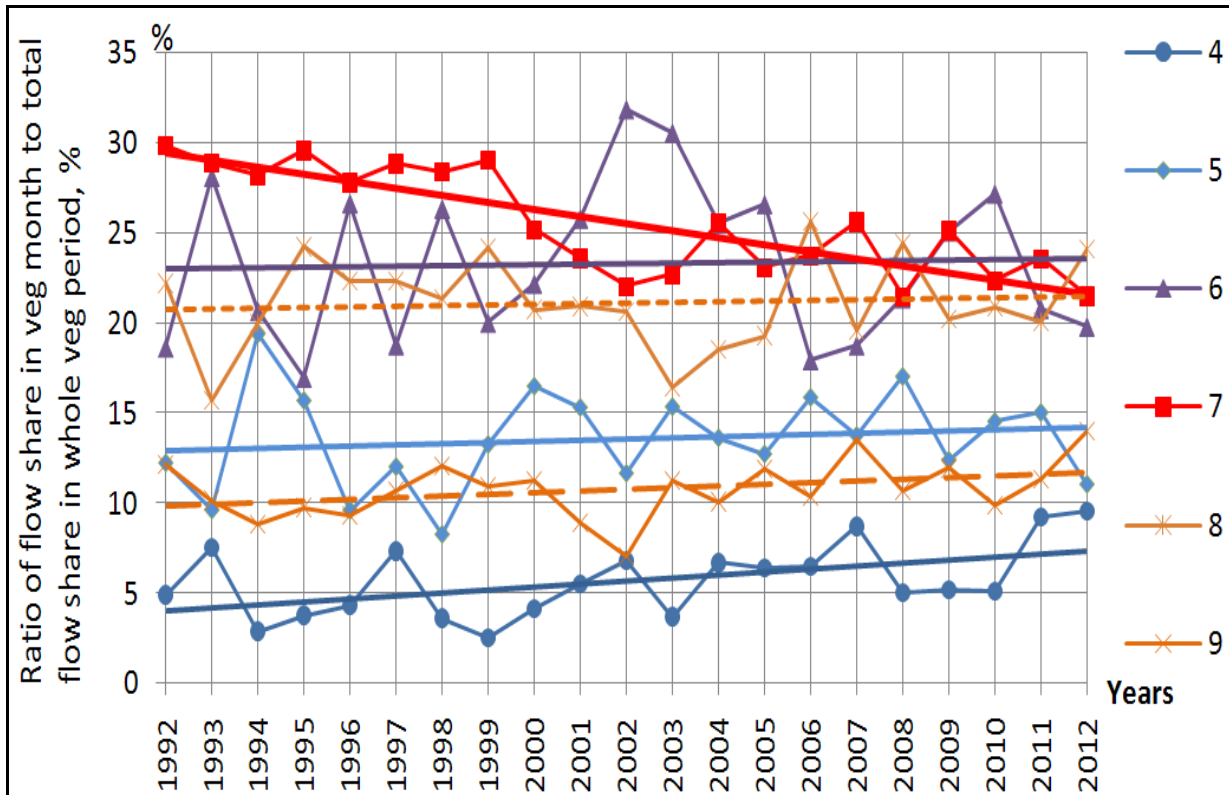


Figure 2.3.2.5. Change of flow proportion during vegetation months (%) to total flow during the vegetation period. Numbers: 4,5,6,7, 8 are months under the order.

Let's consider the climatic factors influencing the flow in the upper course of Naryn River in the vegetation period.

Figure 2.3.2.5 shows high water years when accumulation of seasonal snow was 120-150% of average long-term indicators. From 1998 to 2012 the precipitation in the upper course of the Naryn River significantly increased from October to March, according to data from the Tien Shan meteorological station – by 40 mm, the Naryn meteorological station – by 30 mm. This contradicts the view point of Dikih A.N. (1999) who addressed the tendency to a decrease of flow in the upper course of Naryn River due to precipitation reduction during the cold period from 1930 to 1998.

The biggest influence comes from seasonal accumulation of snow during the cold period (October-April) (**Figure 2.3.2.6**) which has a tendency to increase (**Figure 2.3.2.7**).

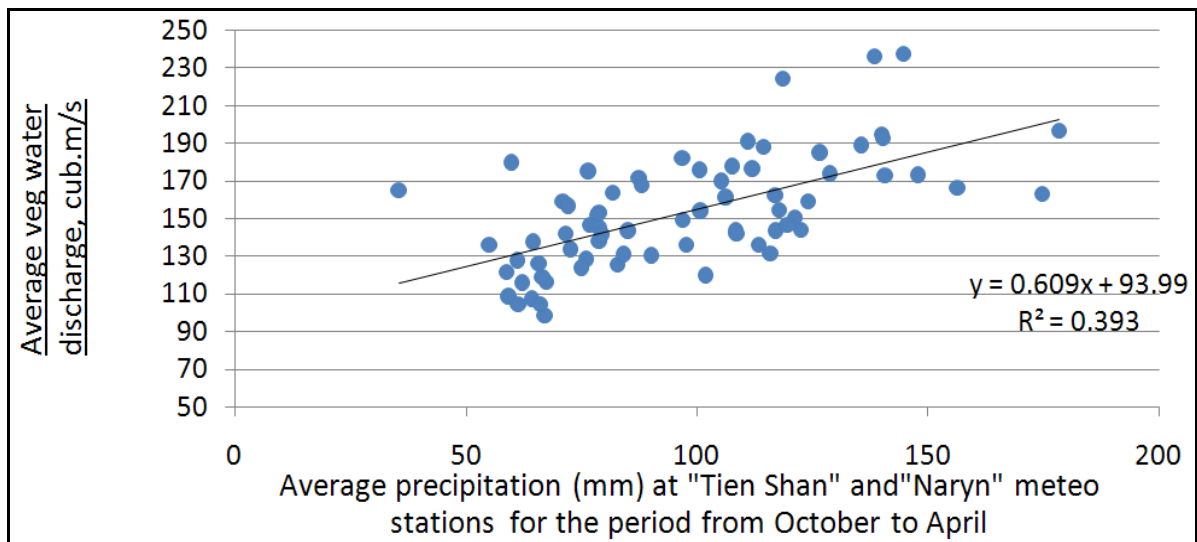


Figure 2.3.2.6. Dependence of average vegetation flows at the Naryn River – Naryn town points on average precipitation at the Tien Shan and the Naryn meteorological stations

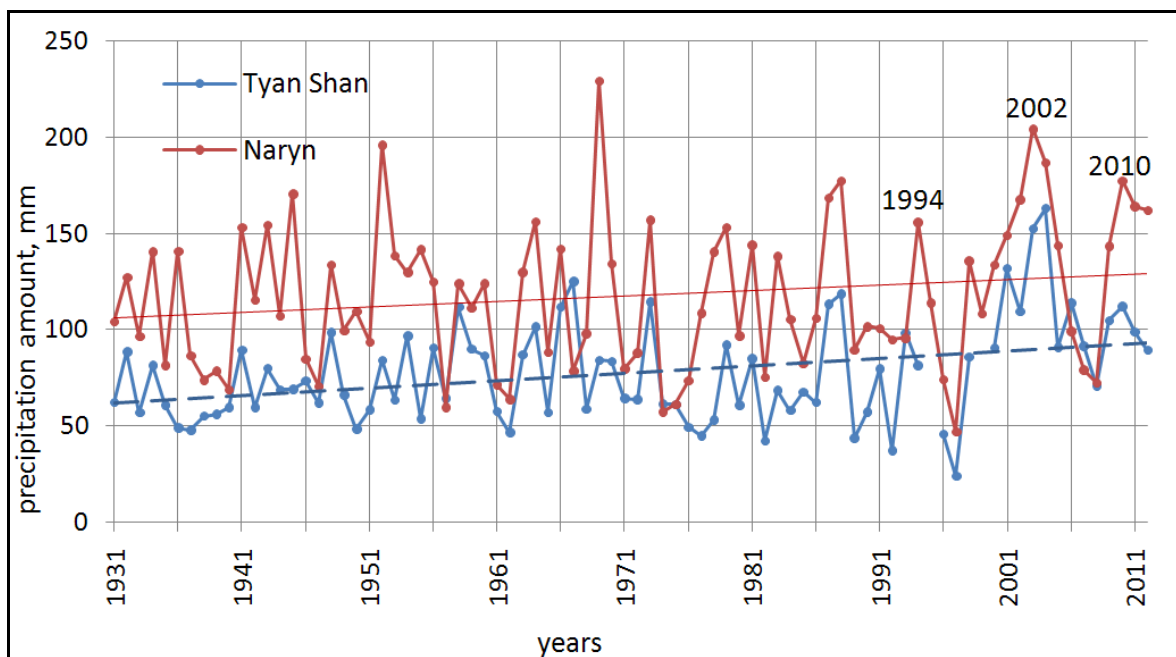


Figure 2.3.2.7. Change of precipitation (mm) within the period from October to April as measured by the “Tien Shan” and the “Naryn” meteorological stations

The river runoff during the vegetation period is influenced by melting of snow and glaciers in the catchment area which depends on:

- Sum of accumulated positive air temperatures (sum of active temperatures - an indicator of the amount of heat and is expressed as the sum of daily mean temperature of air or soil that exceeds a certain threshold of 0 degree. It is calculated as the sum of average daily temperatures for the days when the temperature exceeds the set threshold. The average daily temperature is calculated as the arithmetic mean of the thermometer) influencing the intensity of snow and glacier melting in the mountains (**Figure 2.3.2.8**);
- Duration of warm period – number of days with positive air temperature;

CHAPTER 2. CLIMATE AND WATER RESOURCES

- Date of transition of positive average daily temperatures though 0°C, their reading was made from January 1 if at least three days with positive air temperature were available.

Calculation of these parameters presents a difficult task for a highland zone as during the warm period regular decrease of average daily temperature is observed down to – 3-5 °C, but this is necessary because they influence the flow in the upper course of the Naryn River (HPNN) in the vegetation period.

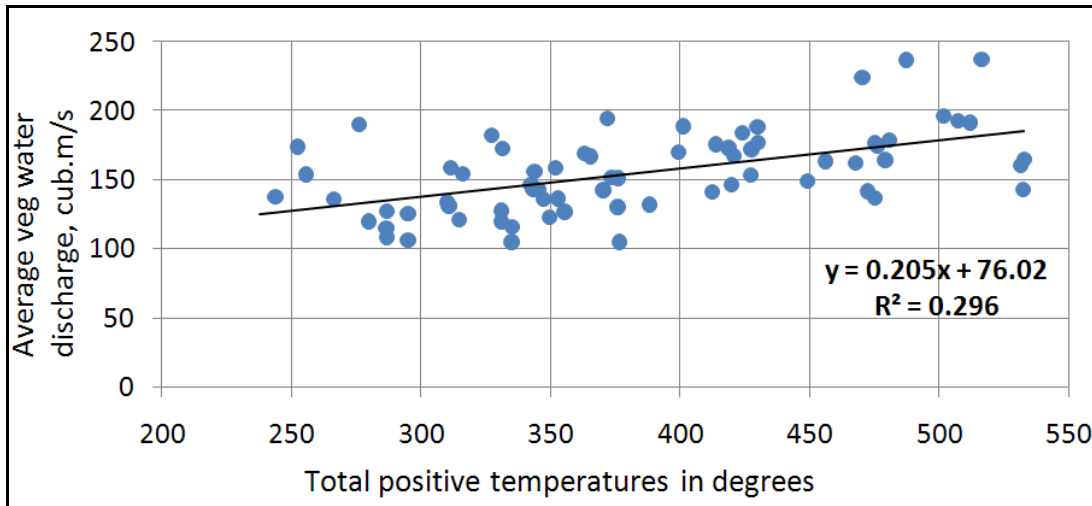


Figure 2.3.2.8. Dependence of average vegetation water discharge (HPNN) on total positive temperatures (the Tien Shan meteorological station)

Analysis of trends of data from the Tien Shan and the Naryn meteorological stations showed changes of climatic features in the upper course of Naryn River in the last 20-40 years.

The amount of positive air temperatures increased within the last twenty years in the upland zone and within the last forty years in the downstream of the catchment. Thus, according to the Tien Shan and the Naryn meteorological stations average total positive temperatures increased from 349 to 482°C and from 2531 to 2867°C, respectively (Figure 2.3.2.9).

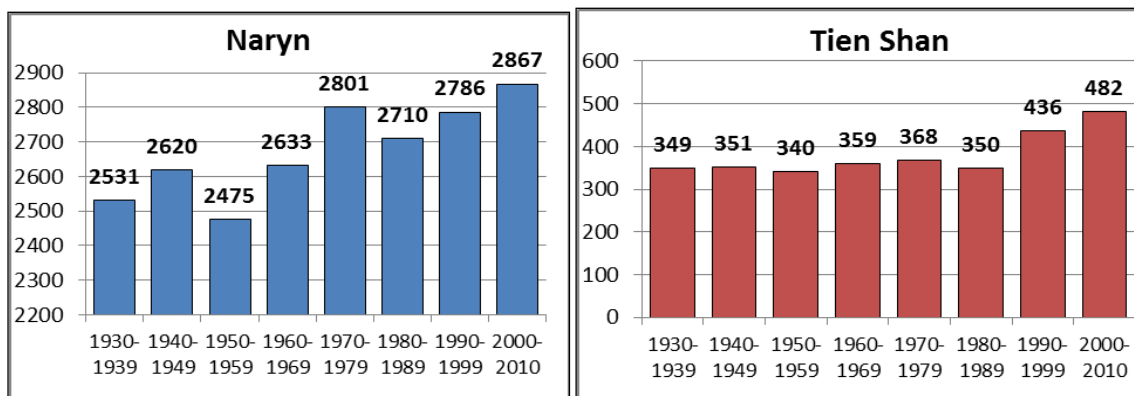


Figure 2.3.2.9. Average 10-year total positive temperatures at the Naryn and the Tien Shan stations

CHAPTER 2. CLIMATE AND WATER RESOURCES

Similarly to the total, the number of days with positive temperatures also increased in the upland zone within the last 20 year from 109 to 122 days, in the mid zone (catchment downstream) within the last 40 years from 220 to 236 days, respectively.

Analysis of trends of transition of average daily temperature via 0°C shows a gradual move to earlier periods, i.e. for the last 10-20 years at Tien Shan meteorological station from mid-May-June to April-May, at Naryn meteorological station from April-second half of March to the first half of March (**Figure 2.3.2.10**).

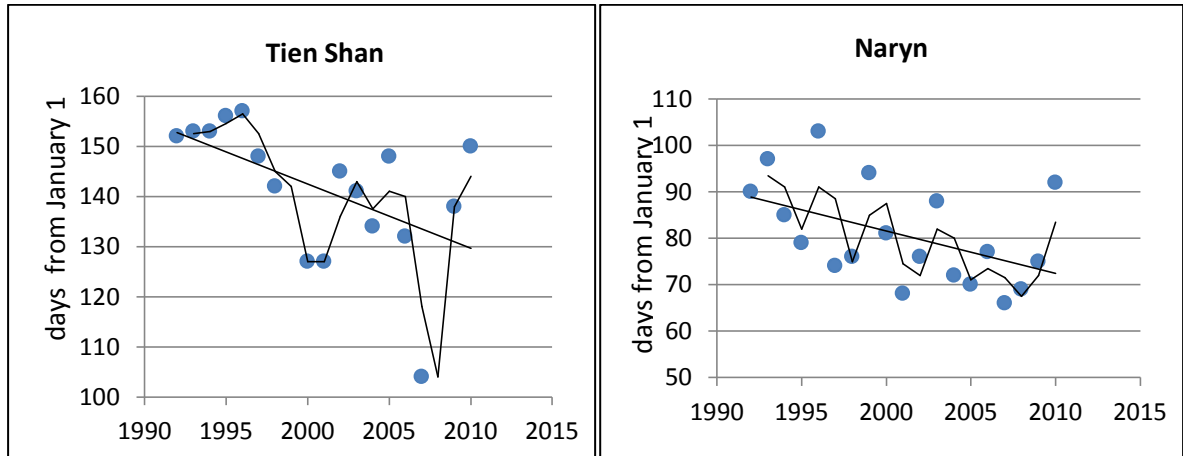


Figure 2.3.2.10. Dates of transition of positive temperatures via 0°C at “Tien Shan” and “Naryn” station for the last 20 years

During the study an analysis of the correlation of average vegetation water flows at HPNN and average monthly air temperature at the Naryn and the Tien Shan meteorological stations showed that the strongest correlation of the flow with air temperature is observed in summer period at Tien Shan meteorological station. This can be explained because the main flow in the upper course of the Naryn River during the vegetation period (72%) falls within summer months. Air temperature in summer months has a tendency to increase. From 1930 to 2012 air temperature in summer period increased by 1.2 °C (Figure 2.3.2.12) according to Tien Shan station data (**Figure 2.3.2.11**).

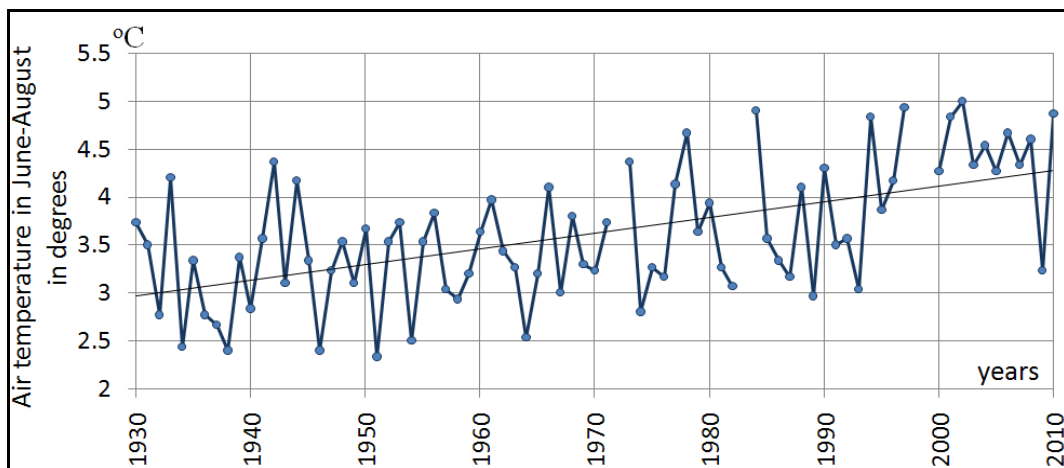


Figure 2.3.2.11. Change of average air temperature within June-August measured at the “Tien Shan” meteorological station

CHAPTER 2. CLIMATE AND WATER RESOURCES

Besides summer temperatures (or amount of positive air temperatures) and precipitations for the cold period (October-March), the Naryn river flow formation during the vegetation period is influenced by the previous low water flow (Figure 2.3.2.13). By estimation, the average flow in the low water period from 1992 to 2012 was 37.6 m³/sec or 126 % as compared with indicators of 1931-1991 when it was 29.9 m³/sec.

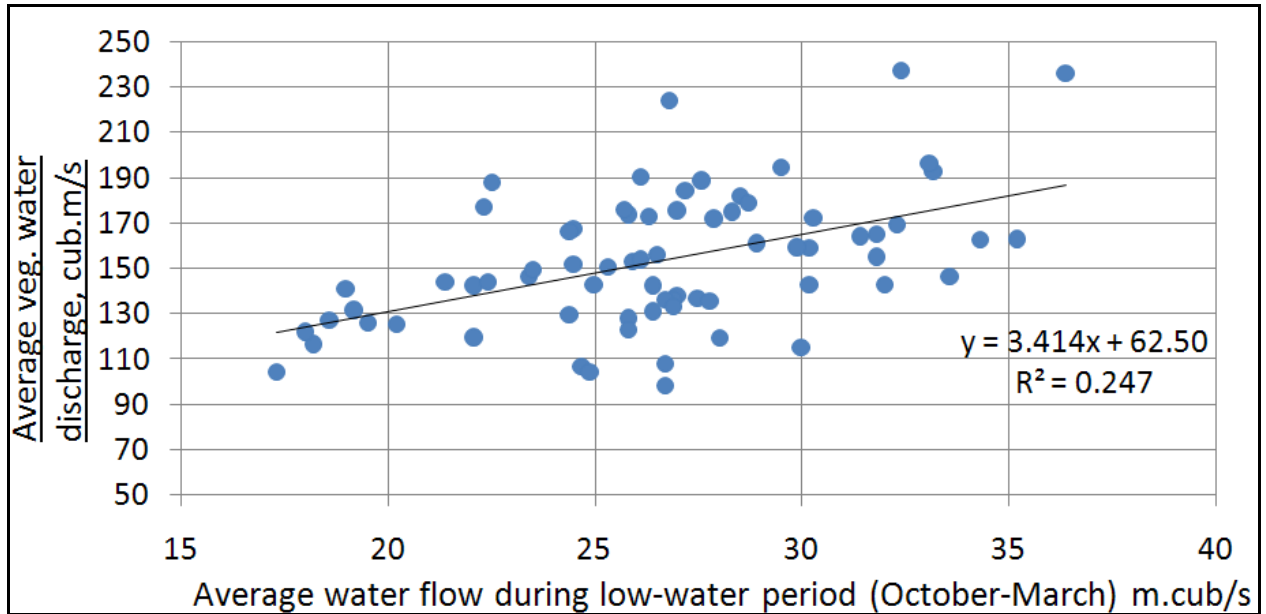


Figure 2.3.2.12. Dependence of average vegetation flows on average water flows during low water periods

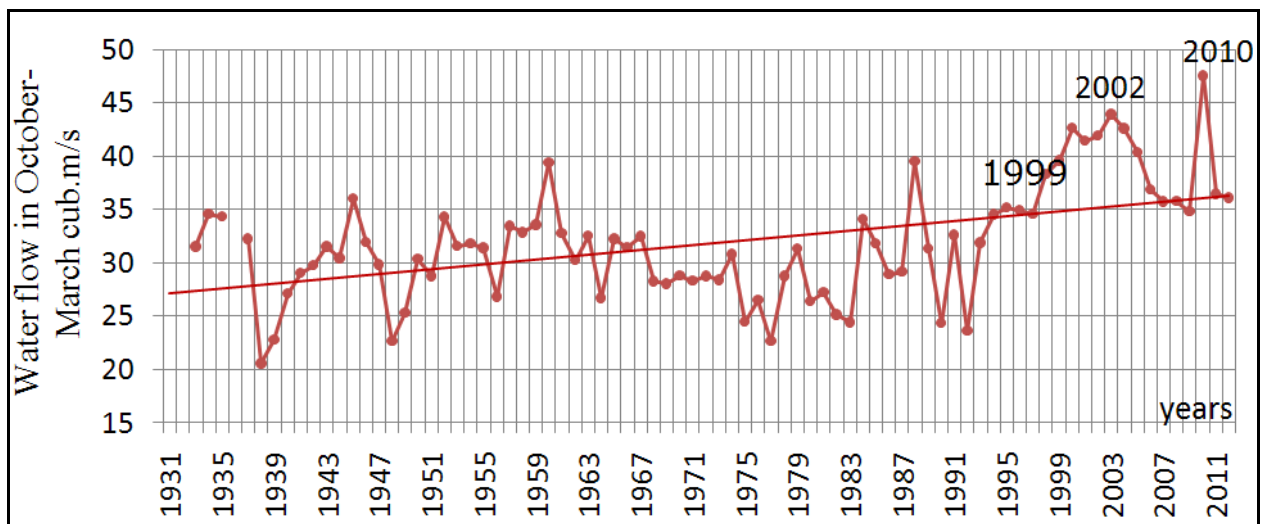


Figure 2.3.2.13. Change of water flow in the low water period, HPNN (m³/sec).

Summing up, we can point out at three factors (parameters) which impact the upstream of the Naryn River, HPNN (**Figure 2.3.2.14**):

- Precipitation amount for the previous cold period (October-March);
- Air temperature for summer period or amount of positive air temperatures;

– Previous low water period.

All three parameters have a tendency to increase since 1992 to date due to which the increase of Naryn River upstream is observed during this period.

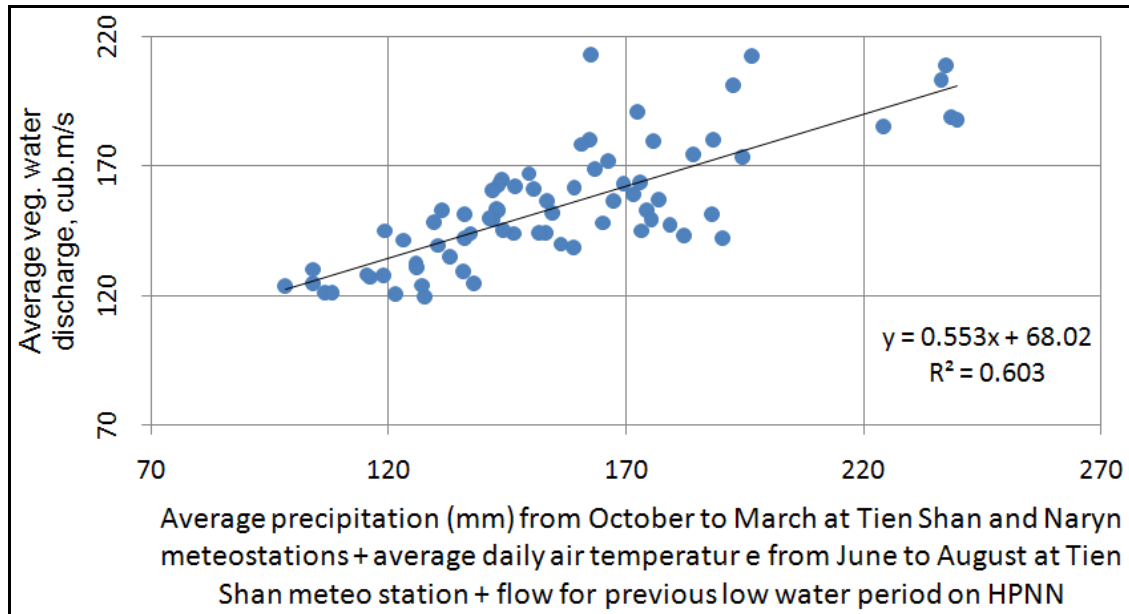


Figure 2.3.2.14. Dependence of average vegetation water discharge (HPNN) on average precipitation from October to March at Tien Shan and Naryn meteorological stations plus average air temperature within June-August measured at Tien Shan meteorological station + water flow in October-March HPNN

Thus, starting from 1992, the hydrological post Naryn River-Naryn town (HPNN) measures an increase of the flow of the upstream of Naryn River. The average vegetation flow for the period from 1992 to 2012 was 177 m³/sec or 122% as compared with the period from 1931 to 1991 when it was 145m³/sec.

Having glacial and snow feeding (with maximum high water in July-August [4]), the share of water flow of July, which is a month of glacial feeding, fell down almost at 10% from 1992 to 2012. As long as the share of seasonal snow feeding months (April-June) grows, the peak of high water will gradually move to May-June.

Starting from 1992, decrease of flow share in July is linked with glacier degradation and recession of the neve line.

Total precipitation plays the most significant role in flow generation in the cold period (October-March) when seasonal snow reserves are generated, increasing by 40mm (at Tien Shan station) and by 30mm (at Naryn station) from 1992 to 2012.

The total positive air temperature influencing the intensity of snow melting increased within the observation period by 349 to 482°C (Tien Shan station) and by 2531 to 2869°C (Naryn station).

The number of days with positive air temperature also increased within the observation period from 109 to 122 days (Tien Shan station) and from 220 to 236 days (Naryn station).

CHAPTER 2. CLIMATE AND WATER RESOURCES

Dates of transition of positive air temperatures via 0°C moved in the last 10-15 years to earlier periods: at Tien Shan station – from mid-May-June to April-May; at Naryn station from Second half of March - April to first half of March.

The strongest correlation of air temperature and flow HPNN was obtained in summer period at Tien Shan meteorological station, which also measured an increase of mean-temperature by 1.2°C in the long-term period of observations.

Indicated changes of main climatic parameters led to an increase of flow in the upper course of Naryn River within the vegetation period from 1992 to 2012.

Water discharges in the low water period (October-March) increased following the flow in the vegetation period. From 1992 to 2012 they amounted to 37.6 m³/sec or 126% compared with indicators of 1931-1991 (29.9 m³/sec).

Reference:

1. Dikih A.N. Glacial flow for Naryn river and scenario of its possible change in climate warming//Kyrgyz NAS. Problems of geology and geography in Kyrgyzstan. – Bishkek, Ilim, 1999. – p.74-79
2. Kuzmichenok V.A. Glaciation and flow in the Naryn river Basin. Inventory, temporal changes, forecast.// Study of formation factors and assessment of impact by reservoirs of the Lower Naryn cascades of hydropower stations on quality of water resources in the Naryn river basin using isotope methods. HAS. Part 1. – Bishkek, 2010. – pp. 19-39.
3. Mamatkanov D.M., Bajanova L.V., Romanovskiy V.V. Water resources of Kyrgyzstan at the modern stage// Kyrgyz NAS. Institute of water problems and hydropower. – Bishkek, Ilim, 2006. – p.266
4. Resources of surface water in the USSR. V.14. Edition 1. Basin of the Syrdarya river/Edited by Il'in I.A. – Leningrad: Gidrometeoizdat, 1969. – p.439
5. Schulz V.L. Mid Asia rivers. – Leningrad.: Gidrometeoizdat, 1965. – p.680
6. Chebotarev A.I. Glossary of Hydrology – Leningrad: Gidrometeoizdat, 1964 - pp. 182-183.

2.3.3. Change of annual flow of the Issyk-Kul basin in the long-term period.

The aim of this research is to study the change of annual river flow for 80 year-period of observations and to determine possible cycles and periods of change. The study of change in hydrological features of Issyk-Kul river basin was carried out at 23 water courses with natural flow for the observation period from 1930 to 2011 according to data from the hydrological post network of Kyrgyzhydromet (Kyrgyz Hydro- and Meteorological Service). Hydrological posts are located at the elevation of 1700 to 2100 m a.s.l. at the outlet of mountain gorges above intake facilities (channels etc.).

Peculiarities of the orographic structure of the Issyk-Kul Hollow determine the nature of the precipitation distribution on its territory. Passing the Chui Valley, humid western and north-western air masses lose a large portion of moisture, therefore, the western part of Issyk-Kul Lake has semi-desert and dry climate. Rivers have a low average annual flow

from 1 to 3 m³/sec. On the eastern coast of Issyk-Kul Lake is much more precipitation than on the western coast. Imbibition of air currents occurs over the warm non-freezing lake. Rivers of the north-eastern slope of Terskey Ala-Too range have the highest average annual values of flow – from 4 to 8 m³/sec.

According to the classification made by Schulz V.L., most of studied rivers have glacial-snow feeding except for the Djyrgalan River in Sovetskoe village, the Tyup River in the Sary Tologoi village and the Oi-Tal River in Oi-Tal village which have snow-glacial feeding [1.2].

With the purpose to identify the period of annual flow change and to study hydrological cycles, a correlation matrix and difference integral curves [3] of Issyk-Kul basin rivers were built. By dependence tightness – value of pair correlation (Rij) and nature of flow change it is possible to define three main river groups:

Group 1 (Figure 2.3.3.1):

The Chon Kyzyl Suu River – forest cordon; the Ak Suu River – Teplokluchenka village, the Djuukuu River – Djuukuchak river outlet, the Chon Djargylchak River – timber yard village; the Ton river – Tuura Suu village; the Chon Koi-Suu river – Sary Oy village; the Cholpon-Ata river – Cholpon Ata farm, the Ak Suu River – Semenovka village, the Ak-Sai River – Koek-Sai village, the Jety-Oguz River – timber yard village; the Barscoon River – outlet of Sasyl River; the Oi-Tal River – Oi-Tal village.

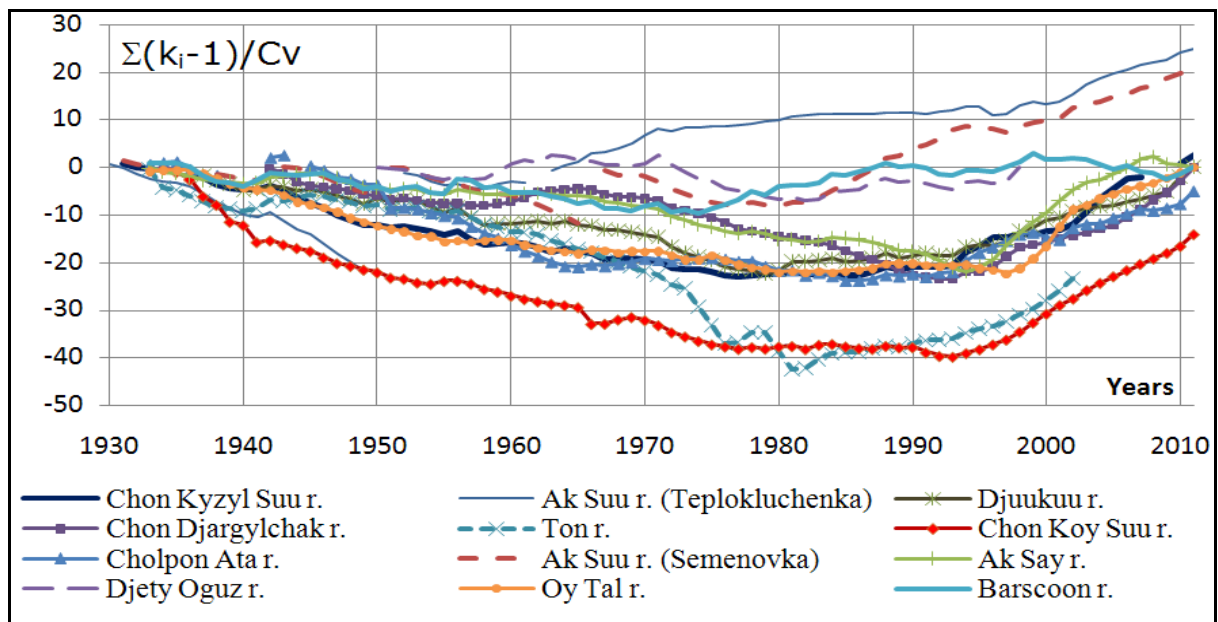


Figure 2.3.3.1. Differential-integral curves of average annual flow for rivers of Group 1

Despite of the different geographical location of catchments of these rivers, they have coefficients of pair correlation 0.57-0.72 that indicates the synchronism of fluctuations and similar hydrological cycles. This group is characterized with tendency to flow increase. On the most of river it is registered since 1990, on other rivers like Ton, Djety-Oguz, Djukuu and Ak-Suu (Semenovka village) it started earlier since 1980. on the Baskoon river – since 1970. Average annual runoffs of these rivers for the period from

1992 to 2011 increased significantly and were 107-171% of the values for the period from 1930 to 1991 (Figure 2.3.3.2). Within these periods just the flow of the Barskoon River didn't change, but it was included in the first group due to sustainable increase of flow and tightness of pair coefficients of correlations.

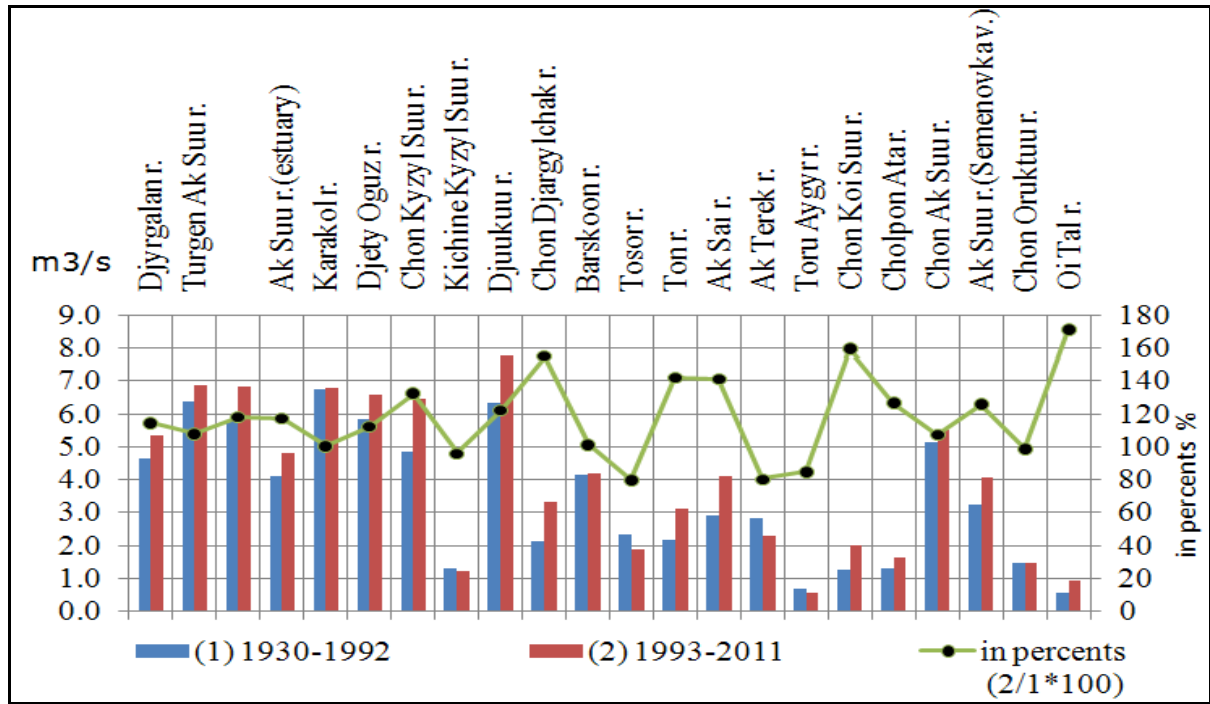


Figure 2.3.3.2. Average annual water flows and percentage ratio of flow for the periods of 1992-2011 and 1930-1991

Group 2 (Figure 2.3.3.3):

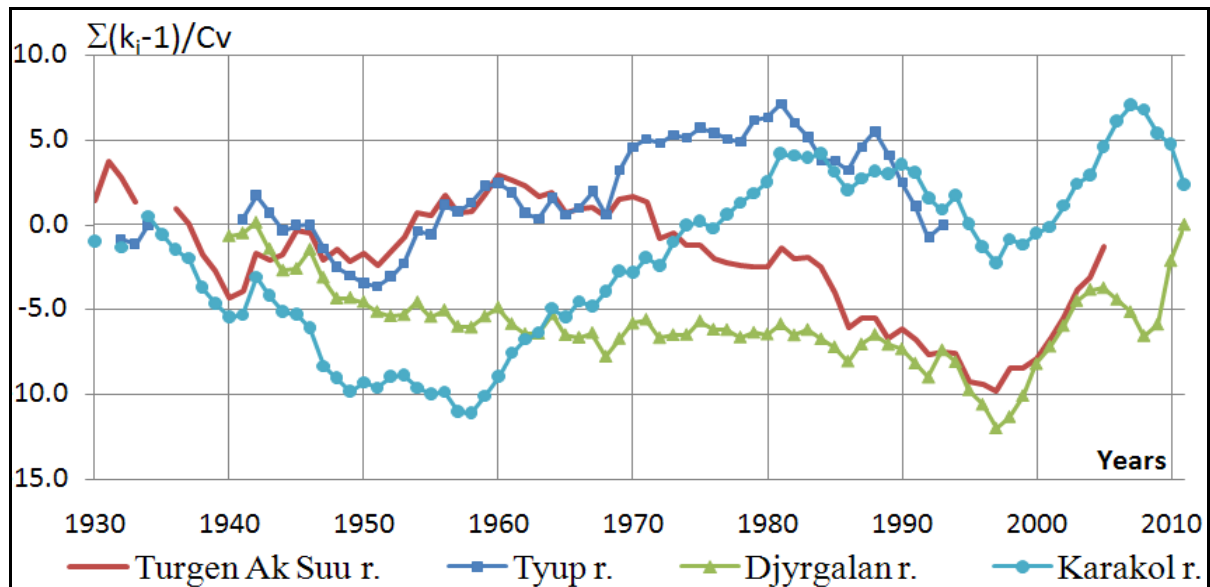


Figure 2.3.3.3. Difference-integral curves of average annual flow for rivers of Group 2

This group includes rivers of the eastern coast of Issyk-Kul lake with humid climate having mainly snow-glacial feeding: the Djyrgalan river – Sovetskoe village, the Tyup River – Sary-Tologoi village; and glacial-snow feeding – the Turgen Ak-Suu river –

timber yard village, the Karakol River – outlet of the Kashka-Suu River, and having pair coefficients of correlations 0.59-0.77. River flow for the periods from 1992 to 2011 and from 1930 to 1991 they have been increased slightly by 1-14% (**Figure 2.3.3.2**).

Group 3 (Figure 2.3.3.4):

Rivers of the southern slope of the Terskey Ala-Too with dry climate are: the Kichine Kyzyl-Suu River – Pokrovka village, the Tuura-Suu River – Ulahol village, the Ak-Terek River – Kyzyl-Tuu village, the Tamga River – Tamga village, the Tosor River – outlet of the Kodol River, the Chon Ak-Suu River – Grigoryevka village. They have pair coefficients – 0.56 – 0.62. On the rivers of this group, decrease of water level up to 20% is observed since 2000 (**Figure 2.3.3.2**).

There are also: the Toru-Aigyr River – outlet of the Kyzyl-Bulak River and the Chon Oryuk-Tuu – horse farm, which have rather low coefficients of pair correlation with the Issyk-Kul basin’s rivers.

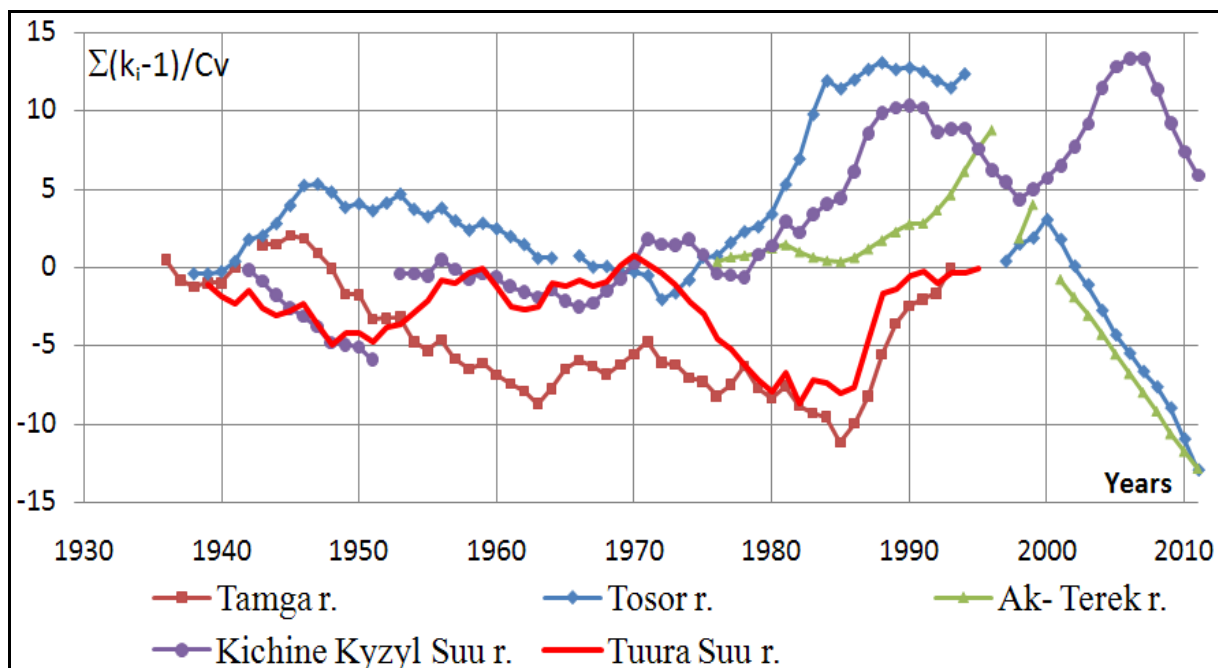


Figure 2.3.3.4. Difference integral curves of average annual flow for rivers of Group 3

In such a way, with the purpose to identify the period of annual flow change and to study hydrological cycles of Issyk-Kul Basin rivers, a correlation matrix and difference integral curves were built. By dependence tightness – value of pair correlation (R_{ij}) and nature of flow change it is possible to define three main river groups:

Group 1 includes such rivers as Chon Kyzyl-Suu, Ak-Suu, Djuukuu, Chon- Djargylchak, Ton, Chon Koi-Suu, Cholpon-Ata, Ak-Suu, Ak-Sai, Jety-Oguz, Barskoon, Oi-Tal. Their flows had a tendency to increase since 1990. On the Ton, Jety-Oguz, Djuukuu Rivers and Ak-Suu (Semenovka village) – since 1980, on the Barskoon River – since 1970. Average annual runoffs on these rivers for the period from 1992 to 2011 increased much and were 107-171% of the values for the period from 1930 to 1991.

CHAPTER 2. CLIMATE AND WATER RESOURCES

Group 2 includes rivers of the eastern coast of the Issyk-Kul Lake with humid climate having mainly snow-glacial feeding: Djyrgalan River, Tyup River; and glacial-snow feeding – Turgen Ak-Suu River and Karakol River. Rivers flow for the periods from 1992 to 2011 and from 1930 to 1991 increased slightly by 1-14%.

Group 3 embraces rivers of the southern slope of the Terskey Ala-Too with dry climate: Kichine Kyzyl-Suu, Tuura-Suu, Ak-Terek, Tamga, Tosor, and Chon Ak-Suu. On the rivers of this group, decrease of water level up to 20% is observed.

Reference:

1. Resources of surface waters in the USSR. V.14. Edition 2. Basin of Syr-Daria river.// Ed. by Bolshakova M.N. – Leningrad.: Gidrometeoizdat, 1973.- p.439.
2. Schulz V.L. Rivers of Mid Asia. - Leningrad.: Gidrometeoizdat, 1965. - p.680.
3. Chebotarev A.I. Hydrological Glossary – Leningrad: Gidrometeoizdat, 1964 - pp. 182-183.

2.3.4. Study of erosion processes and transportation of sediments in the pool of the Toktogul reservoir

Due to global climate change, the change of the surface flow in the Central Asian region becomes more important, as it is related to issues of high-quality water supply and land deterioration as a result of erosion.

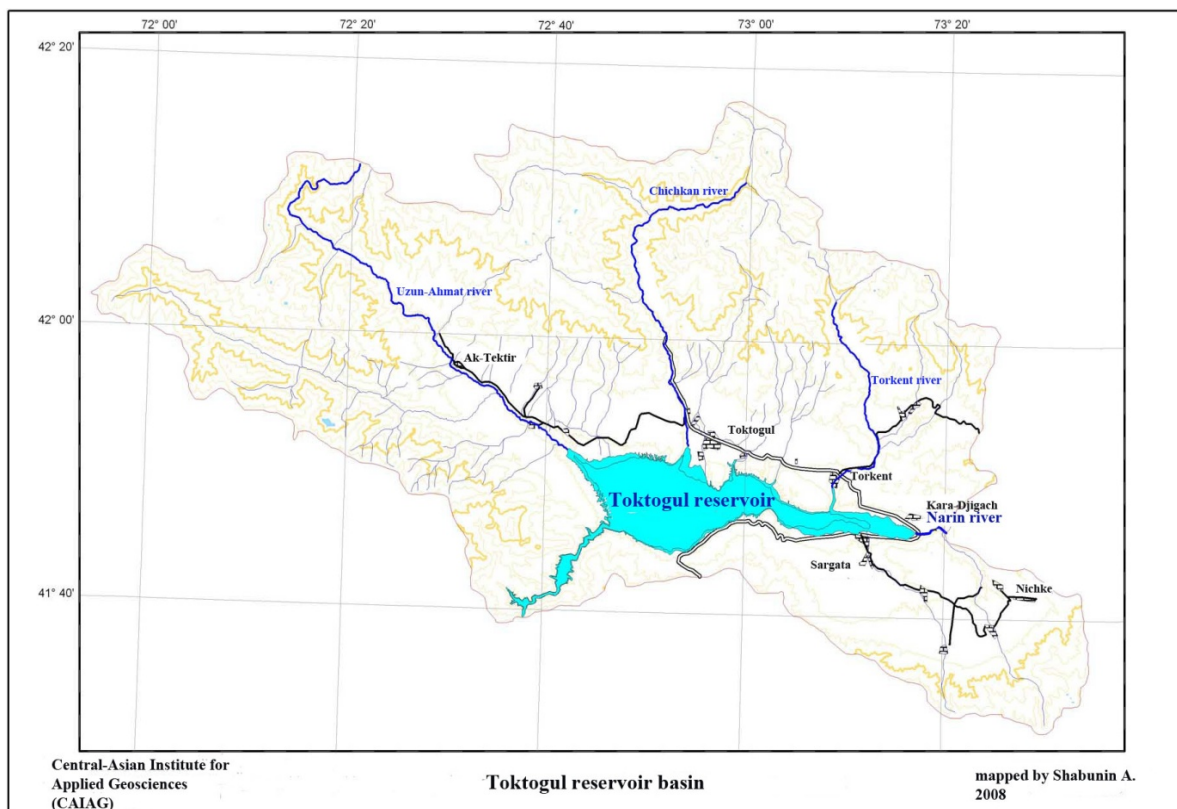


Figure 2.3.4.1. Individual hydrological basin of the Toktogul reservoir

The Toktogul reservoir is located in the vast Ketmen-Tube Hollow bordering the Talas and Suusamyр Ridges in the north, the Moldo-Too Ridge in the south and south-east, spurs of the Fergana range in the north-west, the Atoinok Ridge in the south-west, on the territory of the Toktogul district of the Osh Region, Kyrgyzstan.

Reservoir filling was started in July 1974.

Figure 2.3.4.1 shows a map of the individual hydrological basin of the Toktogul reservoir which was built using topographic maps of scale 1:100 000 and the Digital Elevation Model.

Relation of climatic parameters and surface flow

Assessment of climatic and hydrological conditions of the Naryn river basin was made using data from 16 meteorological stations and 20 hydrological posts which belong to the State Agency of Hydrometeorology under the Ministry of Emergency Situations. A map of their locations is shown in Figure 2.3.4.2.

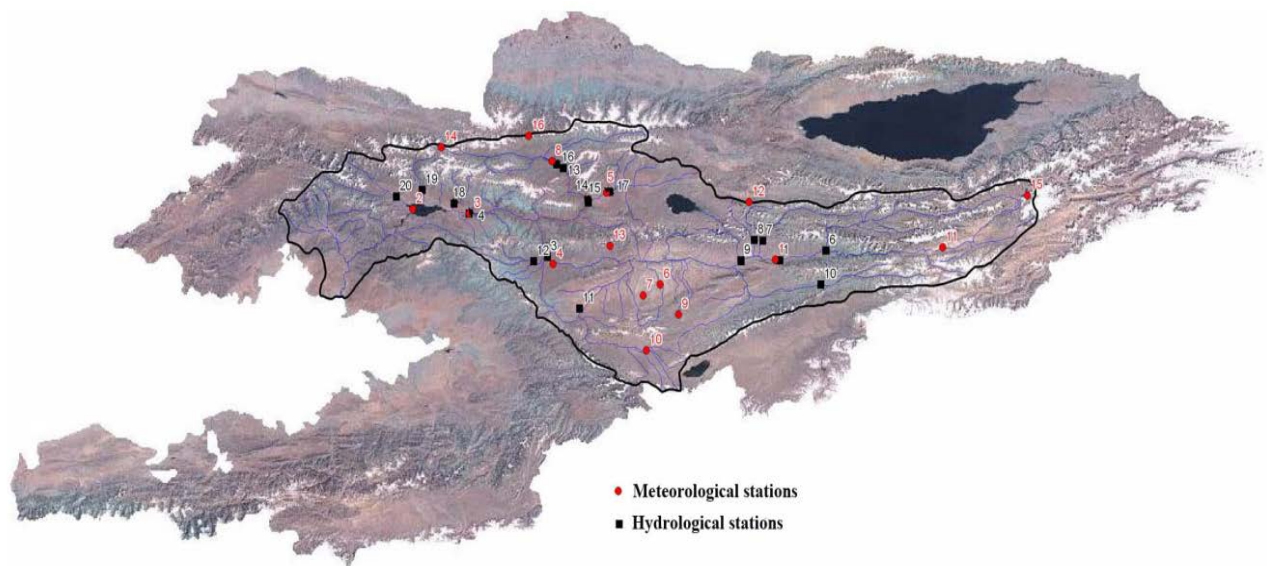


Figure 2.3.4.2. Map of locations of the meteorological stations and the hydrological posts in the Naryn River basin

Good linkage of coefficients of temperature value correlation was obtained during analysis of short series of observations to Naryn reference station. An increase of the average annual air temperature at the Naryn meteorological station was pointed out (**Figure 2.3.4.3**). A theory proposed an anthropogenic impact on air temperature change at the Naryn meteorological station in the period from 1954 to 1980.

It was shown that the most expressed trends of annual temperatures are related to short ranges of increases and decreases, considering the long-range trends make it obvious that they lie at nearly 0°C.

CHAPTER 2. CLIMATE AND WATER RESOURCES

In contrast to air temperature, the coefficients of correlation for pairs of reference and reducible stations of atmospheric precipitations varied in relatively wide ranges. This means that the main volumes of precipitations depend rather more on local conditions than on air temperature distribution. Such conditions may include terrain relief, physical and chemical properties of lower atmosphere, etc.

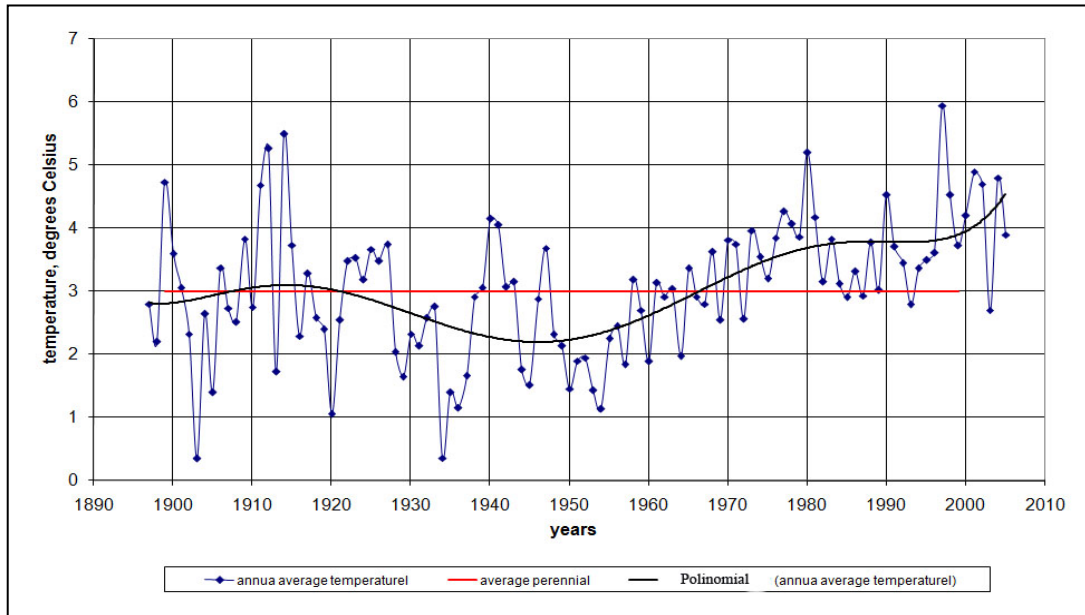


Figure 2.3.4.3. Trend of the average annual air temperature at the Naryn meteorological station

Most of the precipitation in the Naryn River basin is falling in the northern part on southern slopes of Talas range (633.799 mm), and on southern slopes of Moldo-Too Range (549 mm). In general, the Naryn river basin is known for small amount of precipitations – about 300 mm. The lowest amount is observed at the Taragai station (Karakol) located in a narrow gorge between the Djetim-Bel and the Naryn-Too Ranges where the average annual precipitation is 193 mm (**Figure 2.3.4.4**). Percentage distribution of precipitations by months is similar for all stations; however, maximum and minimum precipitations are slightly different for some groups of stations.

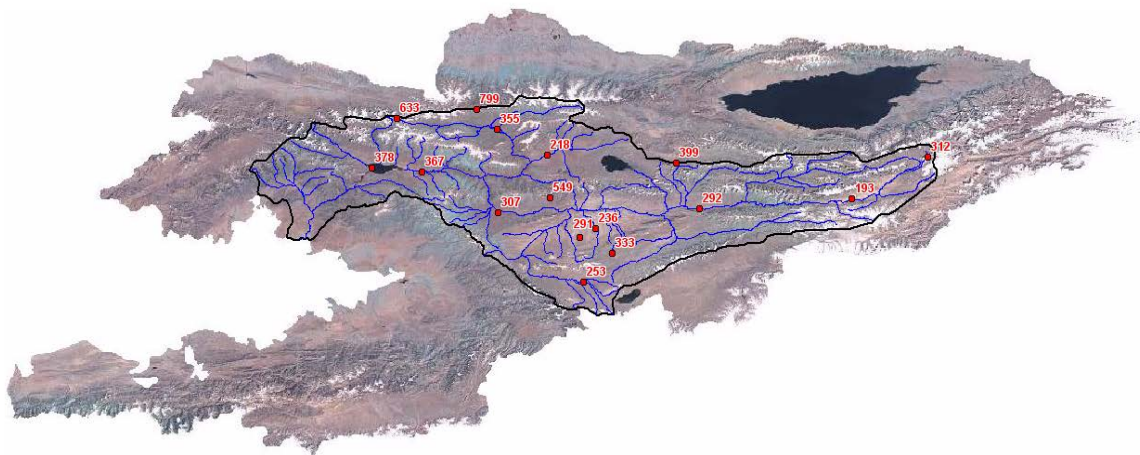


Figure 2.3.4.4. Average annual precipitation it the Naryn River basin during the observation period

CHAPTER 2. CLIMATE AND WATER RESOURCES

The study of the surface flow showed that on the way from Naryn river head to its mouth the peak of high water moves to earlier period thanks to inflows. If it falls on mid-July near Naryn town, it appears near Uchterek village end of June (Figure 2.3.4.5).

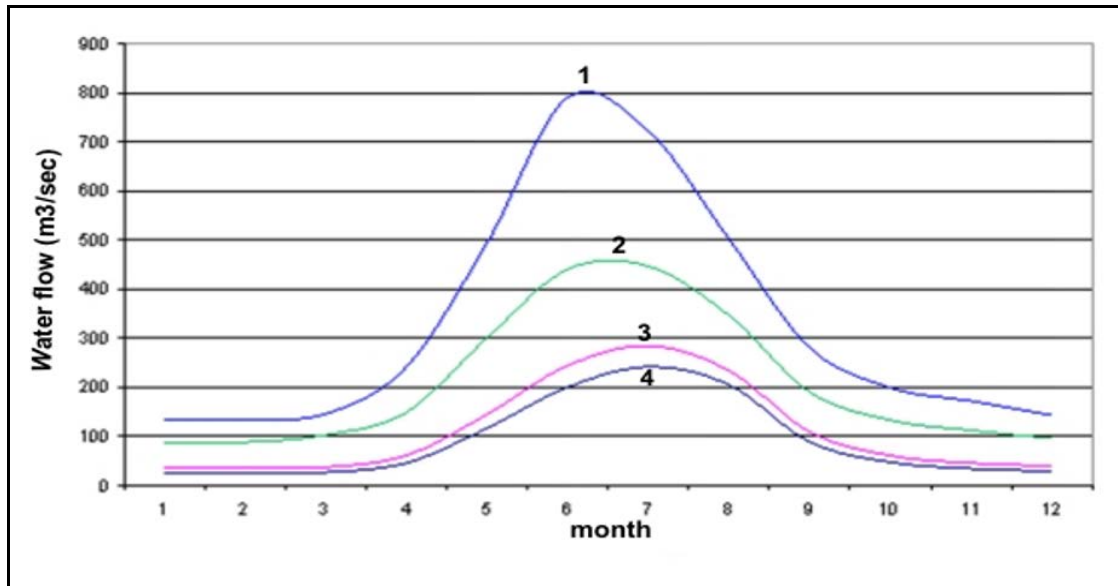


Figure 2.3.4.5. Average monthly hydrograph of the Naryn River's flow during the observation period. Hydroposts: 1-Uchterek, 2- estuary r. Kekirim, 3- estuary r. Kekdjerty, 4- Naryn

It was shown that the air temperature for the whole basin increases nearly at 0.01°C per year. Just for the eastern part of the Naryn Basin this increase is less obvious and is mentioned just in the one thousandth part.

Linear trends of precipitations give no uniform picture over the basin. They show precipitation decrease and increase at some stations. Besides, it might be noted that precipitation trends are not linked with the altitude of meteorological station, increase and decrease of annual precipitations are observed at all altitudes.

In the whole length of the Naryn River, from junction of the Big and the Little Naryn Rivers until the Naryn river inflow to the Toktogul reservoir, the water runoff trend is positive and increases from river head to its mouth. The same pattern is seen for the Kekemeran River. For the Big and the Little Naryn rivers, as for most of other inflows, the water runoff trend is negative. Positive trends are observed, besides for Naryn and Kekemeran rivers, only with the Ala-Buka and the Uzunahmat Rivers.

Geological and hydrological conditions

An assessment of transportation and distribution of suspended sediments in the Toktogul reservoir basin can't be made without the analysis of geological and hydrological conditions of the basin. For making the analysis, a digital geological map of the Toktogul basin (**Figure 2.3.4.6**) was built using geological maps of scale 1:200 000.

The study area is located on the junction of three principal structural-facial zones of Tien Shan: the Northern, the Chatkal-Naryn and the Southern.

CHAPTER 2. CLIMATE AND WATER RESOURCES

The Ketmen-Tube hollow is an utmost western link in the following southern chain of hollows in Mid-Tien Shan. It has west-north-western spread and is confined to the important structural line of Tien Shan (the Nikolaev line) to which the Fergana boundary fault adjoins from south-east.

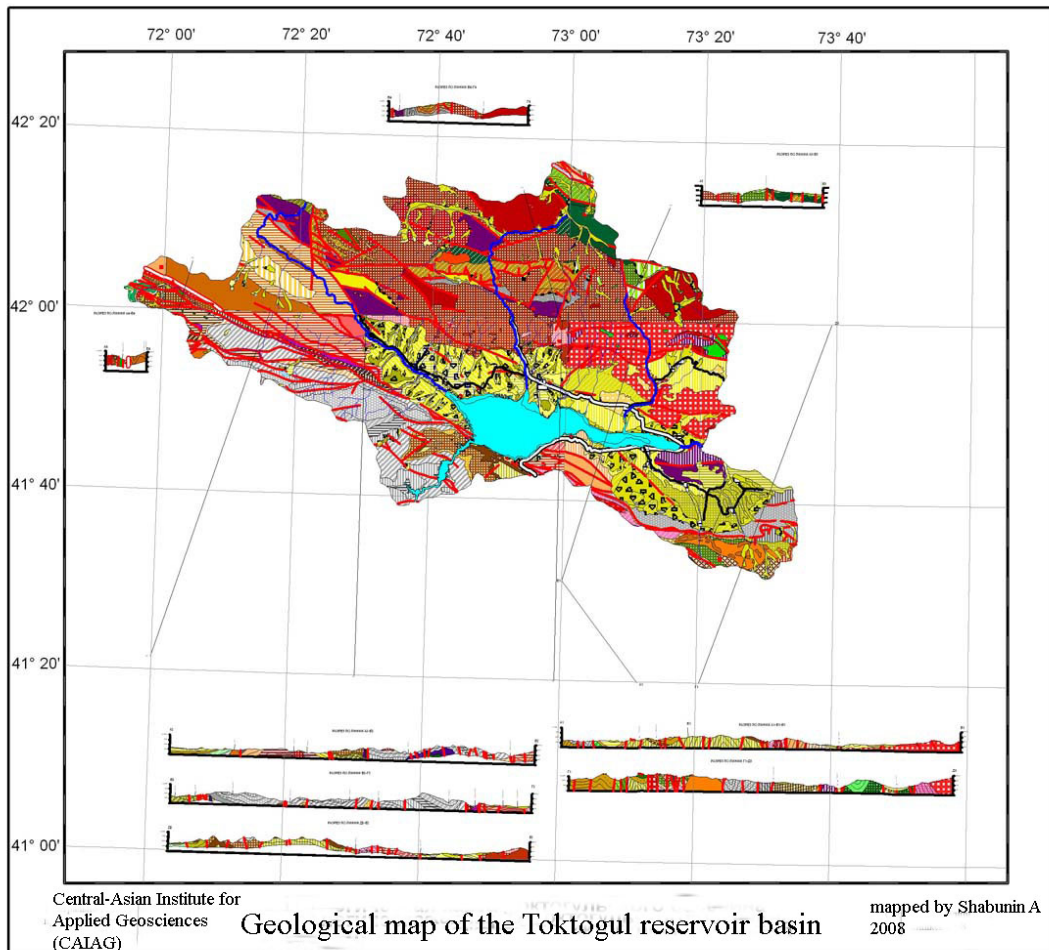


Figure 2.3.4.6. Geological map of the Toktogul reservoir basin

Ongoing tectonic movements in the study area lead to a dislocation of later Pleistocene and even Holocene terraces. In particular, Krestnikov V.N. (1960) draws a transverse Chychkan zone of disturbance which in generation is the most sagging part of the hollow in the downstream of Chychkan River.

Hydrological conditions of the Ketmen-Tube hollow are rather complex which are defined by non-uniformity of conditions for distribution, formation, filtration and discharge of ground waters.

Assessment of water sheet erosion

Assessment was made with regard to the change of areas of erosion which were formed in the Toktogul basin during the time of operation of the reservoir. This work was carried out by comparing satellite images for the time of reservoir construction and for the present time. Territorial complexes with a different degree of soil erosion can be traced and differentiated by the satellite images. However, for primary identification

CHAPTER 2. CLIMATE AND WATER RESOURCES

of soil type prone to any erosion, it is necessary to use factual materials on zoning of the area by erosion characteristics.

Assessment of the water sheet erosion can be made properly using the results of satellite image interpretation. The accuracy of such assessments mainly depends on resolution and quality of images as well as on the scale taken as a basis of the map.

Processes and phenomena related to linear erosion are not identified on Landsat images. They can only be with large zooming and, consequently, with large errors. Consequently, the interpretation of images with high resolution is required.

Major changes of horizontal erosion complexes took place in the riparian zones of the Toktogul reservoir. This is due to the filling of the reservoir and, therefore, increase of its area (from 92.41 km² in 1975 to 230.20 km² in 2001) resulting in flooding of adjacent territories and drastic reduction of their area (reduction of the area prone to water sheet erosion on irrigated lands for medium washed soil from 166.20 km² to 92.41 km² within the study period).

In other places within the Toktogul reservoir these changes are not significant which is mainly connected with the firmness of the soil cover in upland zones.

The outcome of the implemented activities was a digital map of soil erosion in the Toktogul basin for 2001 (**Figure 2.3.4.7**) which reflects the distribution of land prone to different types of water sheet erosion. For more detailed analysis of some places of the basin and types of erosion processes it is necessary to have a detailed basis and satellite images of high resolution.

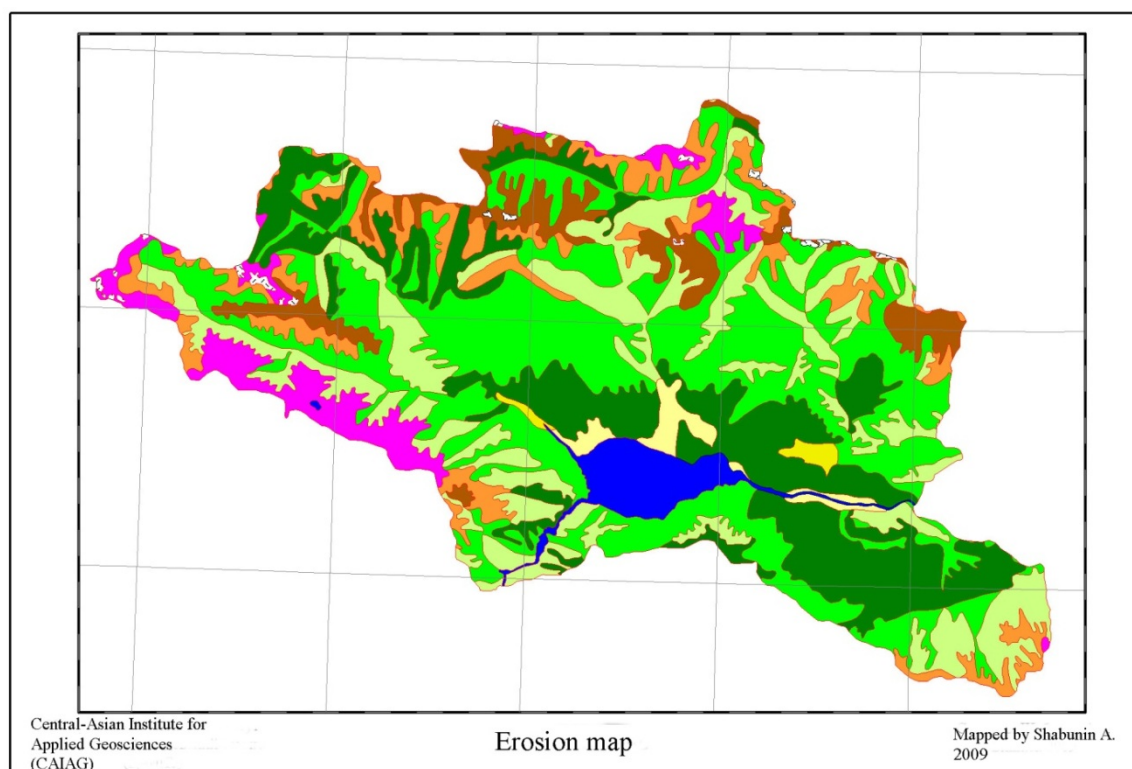


Figure 2.3.4.7. Digital map of soil erosion in the Toktogul Basin for 2001

Relation between water flow rate and suspended sediments in the Naryn River

Over 85% of water inflow to the Toktogul reservoir is provided by the Naryn River. Approximately the same percentage of solid flow is supplied by the Naryn River to the Toktogul reservoir. The importance to study this subject is that sediments settling in the reservoir reduce its net capacity and can largely change the river bed evolution in the estuarine part of the river flowing to the reservoir.

Relations of sediment flow with average monthly water flow for the same period were analyzed. For this purpose, pair coefficients of correlation were estimated between liquid and solid flows for each month within the 25-year period. The highest values of coefficients of correlation between liquid and solid flow are observed during 5 months (May-September). Precisely in these months, Naryn River is deepest and transports a major part of sediments. Estimations showed that in average during the 26-year summer period 70% of liquid flow and 80% of solid flow go through the Uch-Terek post during May-September.

Linear dependences of average annual values of sediment flow and average annual water flow values during the study period (**Figure 2.3.4.8**) were estimated as well as dependences of study values during May-September and October-April.

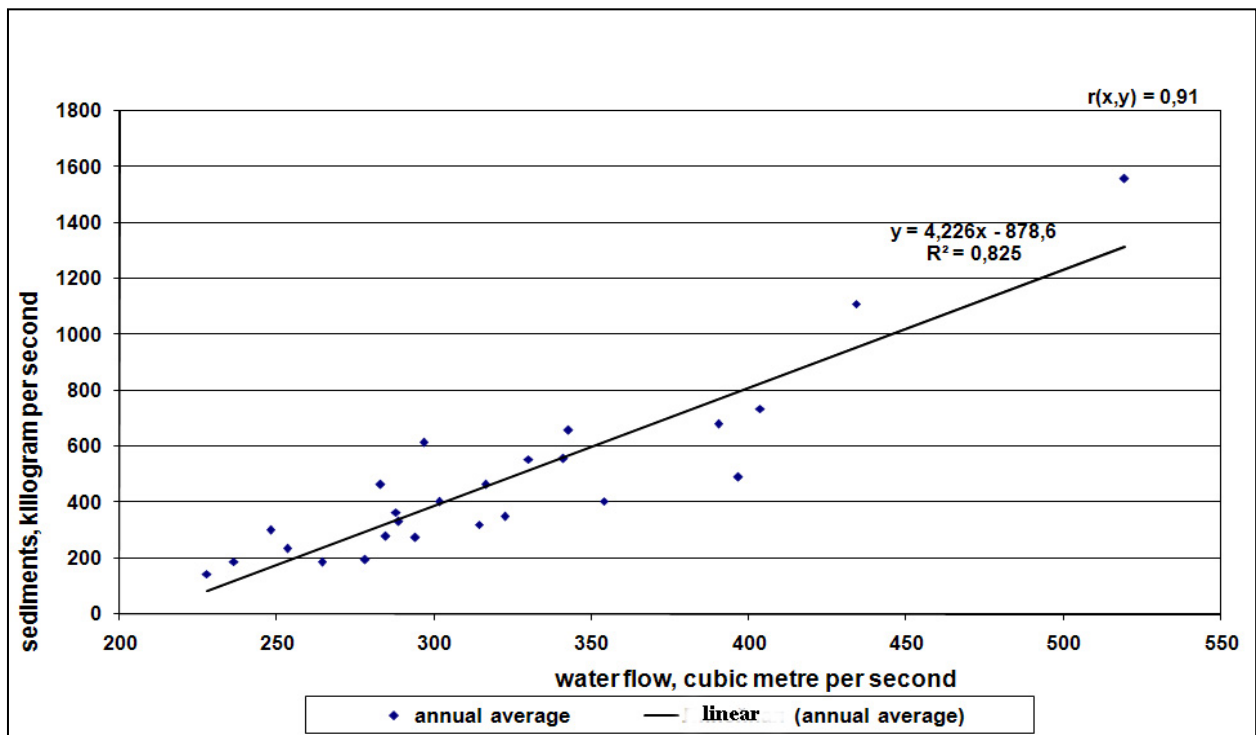


Figure 2.3.4.8. Dependence of sediment flows on water flow at Uch-Terek post (average annual values)

The average annual water flow at the Uch-Terek post (or volume of annual discharge) mainly determines the sediment (discharge) flow. Coefficient of correlation between these values is 0.91. Average liquid and solid discharges during 5 months (May-September) also have relation with coefficient of correlation equivalent to 0.91. and for

the remaining 7 months relation between these values is much worse (correlation coefficient is only equal to 0.56).

Estimation of siltation of the Toktogul reservoir during its operation period (1974-2099)

One of the main factors in estimating the dynamics of water reserves and regime of reservoirs' operation is the change of their area due to siltation, reformation of banks and soil subsidence in the reservoir floor.

This work aimed to assess the total content of sediments and their distribution throughout the reservoir water space. The method of bathymetric survey and the determination of altitudes in a dried part were selected for estimating volumes of siltation of the Toktogul reservoir. This method, as compared to other methods of reservoir siltation estimation, is the most accurate in estimating actual volumes of solid matter in the reservoir bowl.

Topographic maps of 1:25000 scale (survey of 60s, before reservoir construction) were used and a number of field studies were implemented to determine altitudes. These studies were carried out jointly with the Institute of Water Problems and Hydropower of the National Academy of Science and participants of the Project KR1430.

As a result of the field studies, 4 sets of data were obtained: point-by-point GPS measurements using Topcon GB-1000 in the dried part of the reservoir, bank measurements of the depth in selected places using echo sounding device Hummingbird PiranhaMAX 240, profiles on drained area using the "Leica" tachometer, and continuation of these profiles on the water space of the reservoir obtained with the use of echolocation system Ceeducer.

Based on the results digital contour maps before reservoir construction and for the present time were constructed (**Figure 2.3.4.9**).

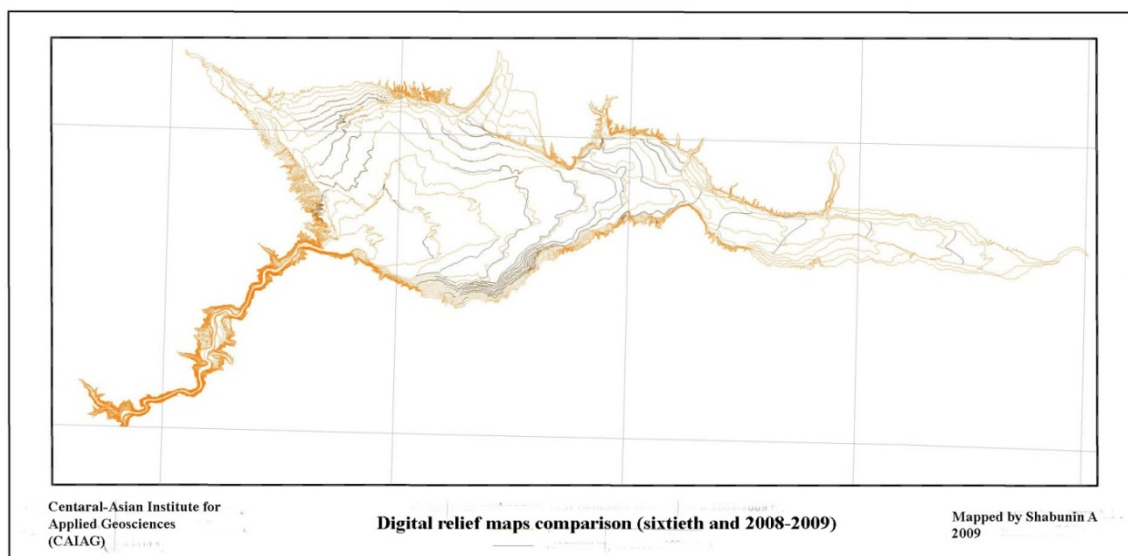


Figure 2.3.4.9. Comparison of digital contour maps of 60s and 2008-2009 (isobaths were made in 10 m)

CHAPTER 2. CLIMATE AND WATER RESOURCES

Estimations were made towards Toktogul reservoir siltation during its operation period. The siltation volume amounts to 0.52 bln m³. The distribution of sediments in the reservoir water space can be traced with the alignment of terrain layers on a 3D model (Figure 2.3.4.10). Theoretical assessment of sediment volumes showed a value (0.50 bln m³) close to the obtained one through direct measurements (0.52 bln m³).

Reservoir siltation occurs in the altitude interval of 900 – 770 m a.s.l. (in the Baltic height system). Above 900 m there are no changes of the terrain that is connected with reservoir filling. Below 770 m the change of the terrain was not determined because the terrain at these heights is presented by the canyon leading to the reservoir dam where measurements were not made due to bad visibility for satellite devices, refraction of reflections during echo ranging and small share of water volume in comparison with the main bowl of the reservoir.

In the altitude interval of 780-800 m there is a negative balance of sedimentation (0.24 bln m³) which is, in our opinion, linked with washing out of bed soil at these depths during reservoir filling.

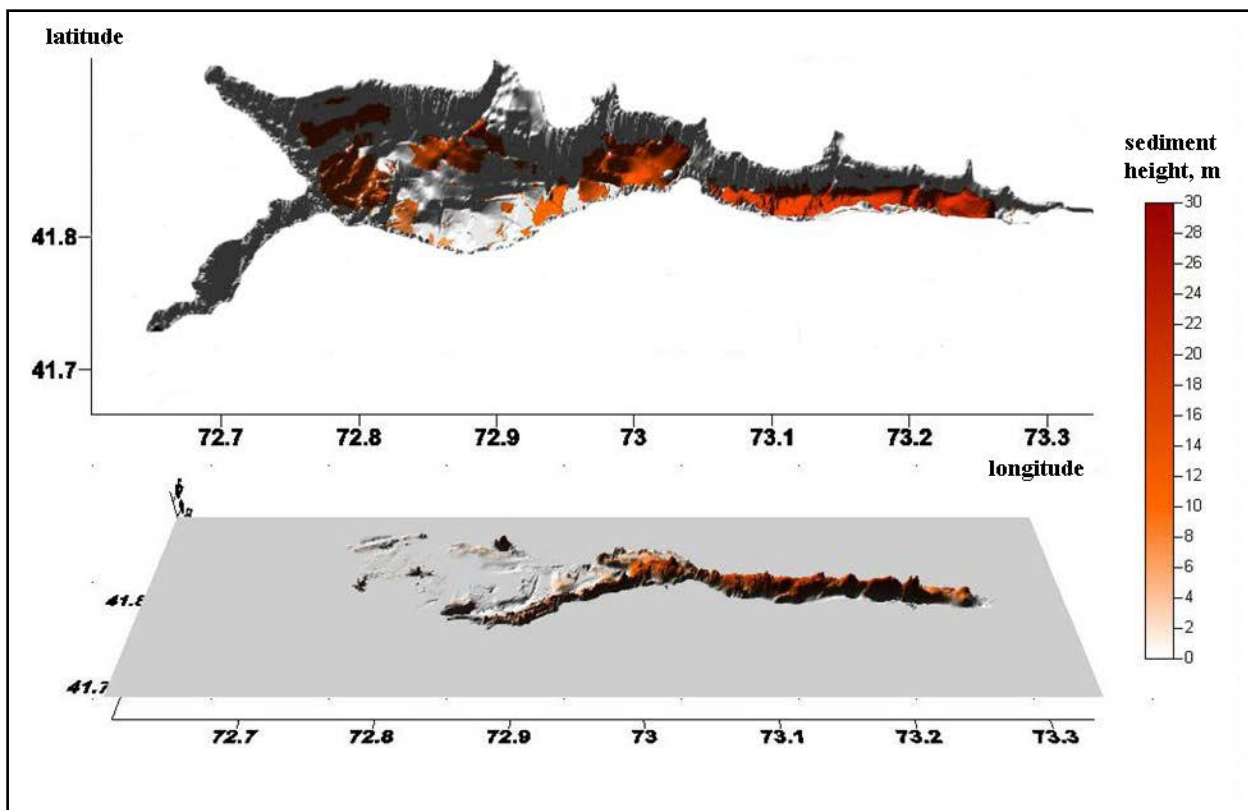


Figure 2.3.4.10. Distribution of sediments in the water space of the reservoir

The dead storage level (DSL) of the Toktogul reservoir is at a point of 837 m. To assess the distribution of volumes, we took the height of 840 m as a dead storage level. The assessment showed that 0.38 bln m³ of sediments suspended in the zone of the active storage capacity (2.3% of the total live capacity), and 0.14 bln m³ in the zone of dead storage capacity (2.2%).

CHAPTER 2. CLIMATE AND WATER RESOURCES

As a result of estimations by the topographic maps of 1960s, a value of the total storage capacity of 20.0 bln m³ at level of 900 m was estimated. However, according to Reference data this value is 19.5 bln m³. The reason of this discrepancy requires a thorough analysis together with other parties concerned.

Good linkage of coefficients of temperature value correlation was obtained during analysis of short series of observations to Naryn reference station.

A hypothesis was proposed an anthropogenic impact to meteorological station air temperature change at the Naryn meteorological station within the period from 1954 to 1980.

It was shown that the most obvious trends of month temperatures are related to short ranges of ups and downs, considering trends for long ranges shows that they are near 0°C.

An increase of the average annual air temperature at the Naryn meteorological station at 0.01°C was pointed out. Just in the eastern part of the Naryn basin this increase is less obvious and is noted

An area capacity curve of sediments of the Toktogul reservoir was built, and also bathygraphical and Burmester curves were worked out taking into account accumulated sedimentary material in the reservoir's bowl.

Calculations were made to derive the total values of the area, volume and average depth of the Toktogul reservoir for different heights of the water level taking into account accumulated sedimentary material. The volume of siltation was equal to 0.52 bln m³.

An area capacity curve of sediments of the Toktogul reservoir was built, and also bathygraphical and Burmester curves were worked out taking into account accumulated sedimentary material in the reservoir's bowl.

Calculations were made to derive the total values of the area, volume and average depth of the Toktogul reservoir for different heights of the water level taking into account accumulated sedimentary material.

Reference:

1. <http://www.cawa-project.net/>
2. V.D. Bykov, A.V. Vasilyev. Hydrometry. – L.: Hydrometry, 1977. – p.448.
3. Gzovsky M.V., Krestnikov V.N., Nersesov I.L., Reissner G.I. New principles of seismic zonation by an example of central part of Tien Shan // IAS USSR. Ser. Geophys. 1960. No.2. p. 77-94. No.3. pp. 353-370.
4. Resources of surface water of the USSR. Issue 1. Issue 1. Syrdarya River basin/ Ed. By I.A. Ilyin. – L.: Hydrometizdat, 1969. – p. 440.

2.3.5. Monitoring and assessment of mountain outburst lakes in the northern slope of the Terskey Ala-Too and the Kyrgyz Ridge.

Analysis of satellite data showed a significant reduction of the glaciers from 1971 to 2007 in the foothills of the Tien Shan, where the major cities are located. Most of the glacial lakes in the region began to emerge in 1980 when glaciers started to get reduced. In the mountains of Central Asia floods which were caused by the overflow of glacial lakes (GLOF) in 2002, 2008 and 2012 resulted in the death of people, serious damage to infrastructure and crops. These floods (GLOF) were not as destructive as in the Himalayas. However, with the development of glacial lakes flooding increasingly pose a threat to local communities.

Below there are results of the study of glacial lakes of the northern slope of the Terskey Ala-Too and the Kyrgyz Ridge performed in 2008-2012.

Outburst lakes on the northern slope of the Terskey Ala-Too.

Now on the northern slope of Terskey Ala-Too there are about seventy upland glacial lakes, of which thirteen are considered as potentially outburst lakes (**Figure 2.3.5.1**). If we consider the outburst glacial lakes of the northern slope of Terskey Ala-Too by separate administrative districts, they are measured at different number, size and scope. In the Ton district are twenty six alpine lakes in the upper basins of the Ton, Tosor, Tuura-Suu, Jer-Ai, Ak-Terek, and Ak-Sai Rivers; six of them are potential outburst lakes. In the Jety-Oguz region there are about forty alpine lakes, four of them are potentially outburst ones. The lakes are concentrated mainly in the upper reaches of the Barskoon, Jety-Oguz, Yrdyk, Kichi and Chon-Kyzyl-Suu Rivers. [1]

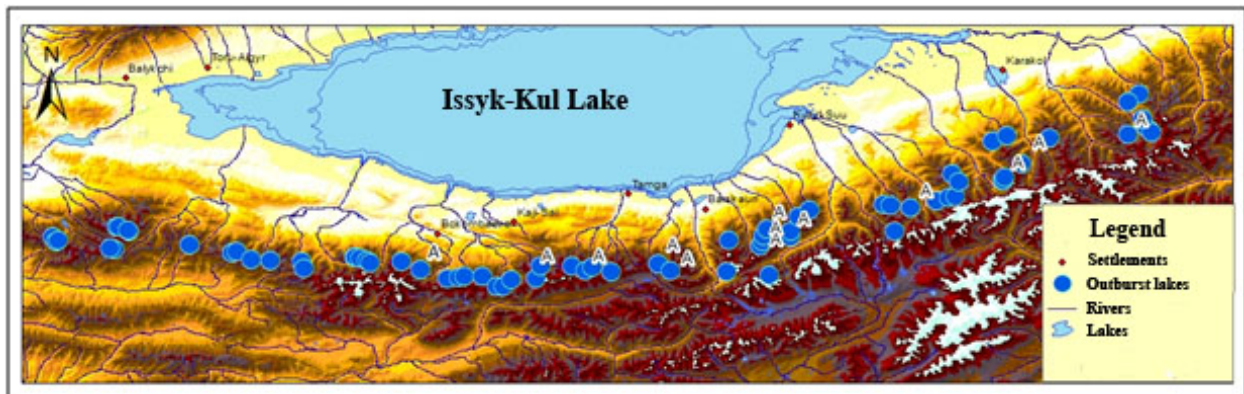


Figure 2.3.5.1. Location of outburst lakes in the northern slope of the Terskey Ala-Too

On the northern slope of the Terskey Ala-Too, a glacial mudflow formation area is located in the territories occupied by modern glaciation and moraines. The relief is characterized by rocky ridges of mountains, cirques, kars. The lower boundary is at the altitude of 3-3.5 thousand meters. In this area are favorable conditions for the formation of large amounts of snow and glacier melt waters. In this region, the glaciers' reduction in size was about 8% for the period of 1971-2002 and lakes' outbursts have been recorded since 1970.

CHAPTER 2. CLIMATE AND WATER RESOURCES

Field studies of several floods in the region during 2006-2009 showed that in mountainous areas stone-and-mud flows are the most powerful and destructive. For example, in the Ton Valley during the outbreak of englacial contents of the Anga-Sai glacier in 1980 on a substrate of gravitational deposits a large stone-and-mud flow of high density appeared, but it did not cause any casualties. It is known that the Angie Sai glacial lake outburst formed mudslides in 1974, 1975 and 1980. Also, in 1985 there was a flood due to the breakout of Suuk Tor Lake. The area flooded by mudflow due to Angie Sai glacial lake outburst, which occurred from June 25 to July 14, 1980, was mapped using satellite imagery Corona KH-4 (23.09.1971) and Hexagon KH-9 (07.09.1980).

In the study area, during 1999-2008 small mudflows during breakout of six glacial lakes No. 2, 16, 17, 24, 31, and 33 occurred. Volume increase $> 0.001 \text{ km}^2/\text{year}$ within 1999-2008 was typical for these lakes. The largest increase (0.0053 km^2 per year) was observed for East Zyndan Lake.

After intensive rainfalls on 24.07.2008, a breakthrough occurred in Zyndan Lake. This lake was formed during the two and a half months after snowmelt in May 2008. As a result of the breakthrough in the Zyndan river valley, a powerful mudflow emerged with the flow of $60\text{-}70 \text{ m}^3/\text{sec}$. The mudflow went along the Ton River and caused great destruction and human losses. Three people died and an enormous damage was observed, including destroyed bridges, roads, two houses and crops.

Ground-based observations and remote sensing methods were applied for the study of the lake. To estimate the changes in the lake's area, GPS (the instrument LeicaTCR 407) and bathymetric surveys were conducted. Shapes of the coastline were determined by the GPS receiver and RTK-GPS900 base (**Figure 2.3.5.2**).

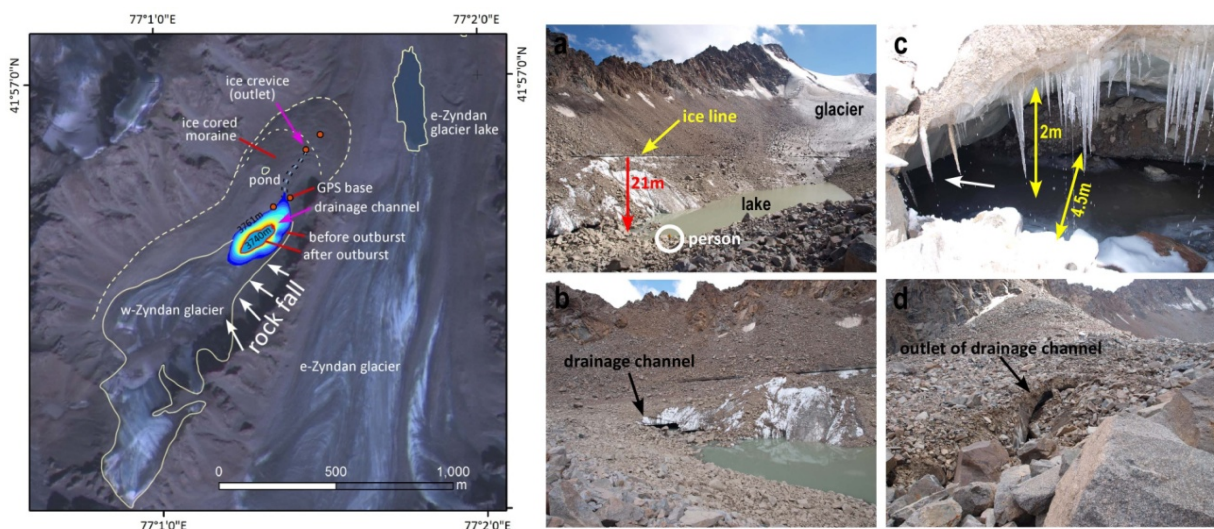


Figure 2.3.5.2. Change of the shoreline of western Zyndan Lake before and after the outbreak (July 24, 2008). Figures a, b, c, d show the previous water level in the lake and the size of moraine-glacial tunnel

To monitor changes in the water volumes of Western Zyndan Lake, a digital model of the study area was produced using GPS data (2008), based on the topographic maps of

scale 1:50 000 (1973), and SRTM3 DEM data (2000). The length and area of the flooded zone were surveyed using GPS and satellite data “ALOS/AVNIR-2” on August 4. 2008.

As a result of GPS and bathymetric survey in 2009, the following morphometric characteristics were defined: the lake lies at an altitude of 3759 m above sea level, the lake area before the outburst was 0.0422 km², after it 0.0083 km², the volume of water before outburst was 459.000 m³. The water flow during the outburst reached 86 m³/sec, the maximum depth 25 m [3].

Outburst lakes on the northern slope of the Kyrgyz Ridge.

Aerial and satellite imagery from different years and glacier topographic survey data delivered the information about glacier degradation at present time on the northern slope of the Kyrgyz Range. In case of a further retreat of glaciers, one can expect the emergence of numerous high-altitude lakes.

In the study of high-altitude lakes methods of remote sensing (RS) and GIS were used. Data of the Agency for Meteorology of the Kyrgyz Republic were used for analyzing climate change and water resources in the area. For area mapping, a digital elevation model (DEM) with a resolution of 30 meters was applied which was built according to the ASTER DEM radiometer. Polygon data on the lakes were recorded in the GIS with additional information about the location, area, height and attributive data. Using satellite images of ALOS PRISM/AVNIR-2 from 2006 to 2010, Landsat 7 ETM from 1999 to 2002 and LANDSAT 8 enabled to identify 194 mountain lakes, out of which 178 lakes are small lakes

Kol-Tor Lake lies in the middle of the Kol-Tor River valley – the right tributary of Kegety. Comparison of the bathymetric survey results in 2011 with the results of the surveys carried out by Shnitnikova [4] since 1971 showed an increase in size and volume of the lake. The depth of the lake gradually increases from the mouth of the feeding river to its natural dam. The greatest depth, measured on June 19. 1971. reached 8.4 m. It is indicated that from 1971 to 2011 lake level went up by 6.1 m. Currently the volume of the lake is 218.052 m³, the maximum depth is 14.6 m (**Figure 2.3.5.3**). Lake surface runoff occurs naturally in well-established channels.

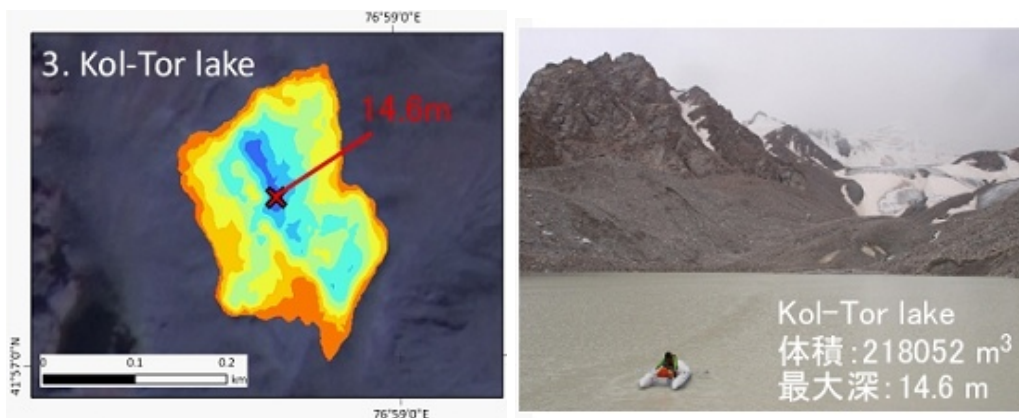


Figure 2.3.5.3. Bathymetric scheme of Kol-Tor Lake as of July 2011

CHAPTER 2. CLIMATE AND WATER RESOURCES

Now on the northern slope of the Kyrgyz Ridge there are about 6 outburst glacial lakes which are potentially dangerous for the community.

Most of the Kyrgyz Ridge lakes are located in the altitude range between 3100 and 3800 m. On the curve of the vertical distribution of lake location two peaks are seen – at altitudes of 3200-3300 and 3500-3800 m (**Figure 2.3.5.3**).

At noon on July 31, 2012, at the Adygene Gorge located 40 km from Bishkek, the outburst of alpine Tez-Tor Lake had occurred.

Tez-Tor Lake (42°32'23" N, 74°25'27"E) is located on the northern slope of the Kyrgyz Ridge, in the basin of the Ala-Archa River, in the headwaters of one of the tributaries of the Adygene River. Near the Tez-Tor glacier, above the moraine- complex, periglacial lakes No. 1 and No. 2 are located which are together called Tez-Tor Lake. The lake was formed originally as a relic above the moraine of down stage (moraine hill), and was much smaller than it is now. Later occurred a rock fall from the left side of the valley in the area of the moraine. Having closed up over the moraine, rocks created a solid dam with the width of about 10-13 m on the top and the height of about 2-4 m. Originally, a fairly shallow pot hole significantly increased in volume and got filled with water resulting in the appearance of a small lake. In the course of time, a moraine-glacial channel was formed in its underground part.

Highness of the lakes of Kyrgyz Ridge Ala-Too

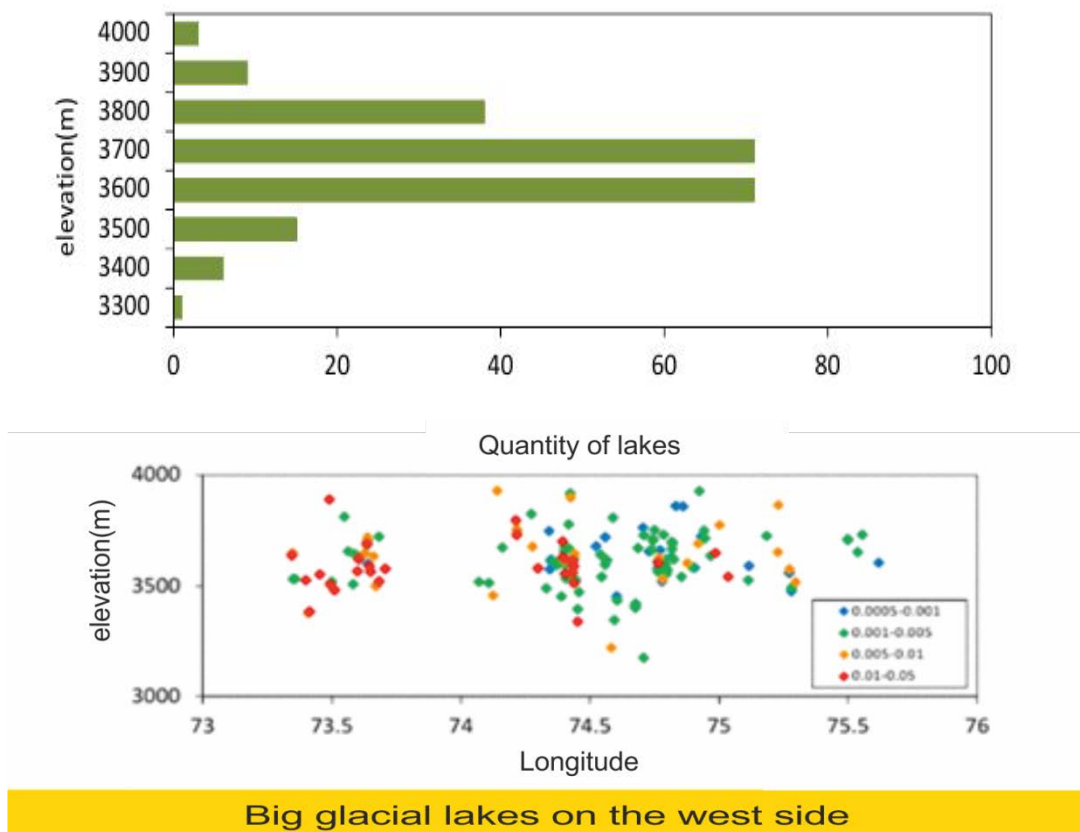


Figure 2.3.5.4. Number of lake, location by altitudes on the northern slope of the Kyrgyz Ridge

CHAPTER 2. CLIMATE AND WATER RESOURCES

At the end of July 2012 the water level in the lake was close to critical; the air temperatures in July 2012 exceeded the average monthly temperatures. According to some sources, the water level rose due to melting of glaciers. According to the Ministry of Emergency Situations water began to spill over the dam in Tez-Tor Lake at 9:30 a.m. At about 3:00 p.m. the water volume overflowed the dam was 7.8 m³/sec and destroyed the slopes of narrow valleys and was accompanied by proluvial-diluvial sediments and deposits.

The former line of the lake level was digitized manually in the ArcGIS 9.3 program (**Figure 2.3.5.5**). Periglacial Tez-Tor Lake contacts with the glacier on its southern shore. The moraine loam coastline which is washed out above the mountain-moraine rocks shows the maximum level of the lake before the outburst. The final moraine is 3-5 m higher than the water level of the lake, and a thickness of stagnant ice is under the moraine. The thickness of ice collapsed during high temperature and the moraines which were backed up on the ice were set free. In the meantime the lake was released. [2]

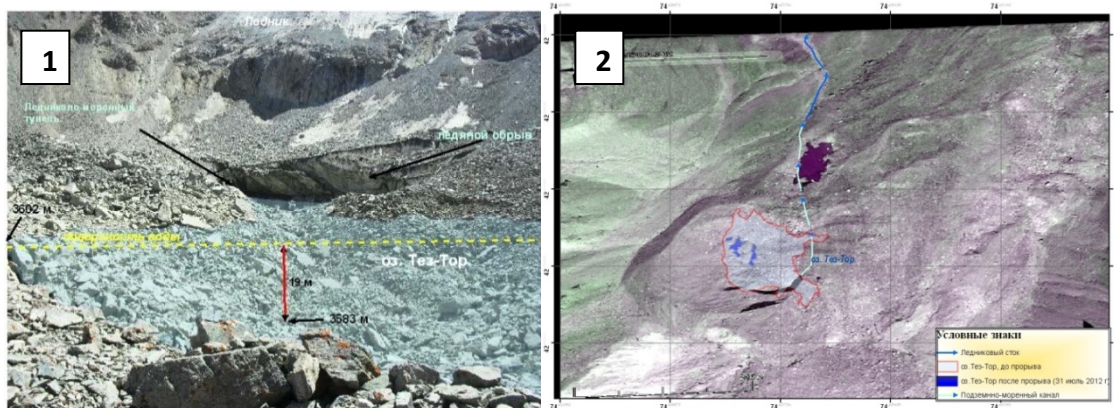


Figure 2.3.5.5. Tez-Tor Lake after outburst on July 31, 2012. The figure shows: the previous water level in the tunnel (1), change of the shoreline of Tez-Tor Lake (2)

Field calculations have shown that the discharge of the Adygene River in the mouth of the Ala-Archa River at 12:00 was 23 m³/sec, and at 14:00 it reached 27 m³/sec. Maximum flow rate was 150-200 m³/s.

Presently, a recreational complex with different types of ecological and adventure tourism and ski industry are actively developing in the Ala-Archa Gorge. In this regard, assessment of the outburst risk and state of lakes in Ala-Archa River basin, on the basis of geo-information modeling, will help to prevent possible adverse natural phenomena.

As a result of studies of glacial lakes of the northern slope of the Terskey Ala-Too and the Kyrgyz Ridge, several hundred glacial lakes were identified; the dynamics, levels, amounts of water were estimated; and areas flooded due to glacial lake outbursts were studied.

The main direction of future research can be a comprehensive analysis and modeling of complex multifactorial dependencies in the system "lake sediments - outburst risk - assessment of the risk mechanism."

Reference

1. Karamoldoev J., Daiyrov M., 2012. Assessment of modern state and natural precondition of Tez-Tor Lake outburst (the Ala-Archa river basin). International Conference on Eurasian Mountain's Cryosphere. Almaty, Kazakhstan. 30-31.
2. Narama C., Duishonakunov M., Kaab A., Daiyrov M. A, and Abdrakhmatov K. A. The 24 July 2008 outburst flood at the western Zyndan glacier lake and recent regional changes in glacier lakes of the Terskey Ala-Too Ridge, Tien Shan, Kyrgyzstan // Nat. Hazards Earth Syst. Sci., 10. 647–659. 2010.
3. Erokhin S.A. Engineering-geological study of dams of upland mudflow lakes on the territory of the Talas, Naryn, Chui and Issyk-Kul Regions of the Kyrgyz Republic. Report of the engineering geological crew of the Kyrgyz complex hydrogeological expedition 2000-2008. State Geology Agency. – Bishkek, 2008. – pp. 174-192.
4. Shnitnikov A.V. Climatology, hydrology and geophysics of the Inner Tien Shan Lakes (natural development tendency). L.: "Nauka", 1981. p. 244

2.3.6. Groundwater studies

Groundwater represents a significant part of the water resources in Kyrgyzstan. The groundwater volume, concentrated mainly in intermountain depressions in the Quaternary aquifer system is estimated to be around 650 km³, and the renewable groundwater flow rate to be 11 km³/year [2]. Groundwater has a great practical importance, since the water supply of Bishkek city is largely provided by groundwater.

In May 2012 we have started the monitoring of groundwater levels of the Ala-Archa deposits located within the city of Bishkek and its vicinities to study the variations of groundwater level and resources of the Quaternary aquifer system in the territory of the Chui depression of Kyrgyzstan. The monitoring instrument is the "OTT_ecoLog_500" [1], which was provided to CAIAG by "OTT Hydromet" (Kempton, Germany) for the purpose of scientific research. The sensor was installed in the borehole No. 1301-4. of the network of observation wells that belongs to the Kyrgyz integrated hydro-geological expedition of the Agency for Geology and Mineral Resources of the Kyrgyz Republic.

The borehole is located on the western edge of Bishkek (42°52'1.06"N 74°28'50.31"E, absolute elevation is 739 m). The location is shown in **Figure 2.3.6.1** and following the link:

<http://maps.google.com/maps/ms?ie=UTF&msa=0&msid=203965682782791499971.0004b53779c0491758c3a>.



Figure 2.3.6.1. Network of location of observation wells in the Chui Valley (red rectangle shows the position of the well 1301-4).

The well has a depth of 75 m and was drilled during the process of a detailed exploration of fresh groundwater in the producing Ala-Archa ground water deposits. The well taps the underground water reservoir that has age of Q II-III, and presented as an interstratification of pebbles, sand and gravel. The monitoring of groundwater levels has been conducted since 1986.

Now the sensor is located in the well 1301-4 at a depth of 19.5 m, 8-12 m below the groundwater level. Temperature and depth level measurements for 2012 and 2013 were conducted every 10 minutes and transferred by the cellular GSM network to the server of CAIAG. Since May 24, 2013, the measurement period is one hour. To get this information and to view a graph of changes in groundwater levels, please follow the link: (<http://gdbweb.caiag.kg/WATER/index.php>).

During the observation period from May 4, 2012 to May 4, 2013, the data on groundwater level and temperature changes were obtained. The water temperature at a depth of 19.5 m is constant during the annual measurement period, and equals to 12.6 - 12.7°C. A view of groundwater level fluctuations for a certain period is shown in **Figure 2.3.6.2**. The sharp level decrease of 1.2 m on April 4, 2013, at 17:40 was caused by a sudden sensor pressure rise. Therefore it was necessary to identify the distance of sensor displacement using the water level rates, to correct the position of the sensor. Besides, attention is drawn by irregular frequency and amplitude of level fluctuations starting from the third decade of November 2012 to mid-January 2013. They, apparently, are associated with low temperatures of -20°C, affecting the operation of the sensor, likely the capillary channel equalizing the pressure in the sensor.

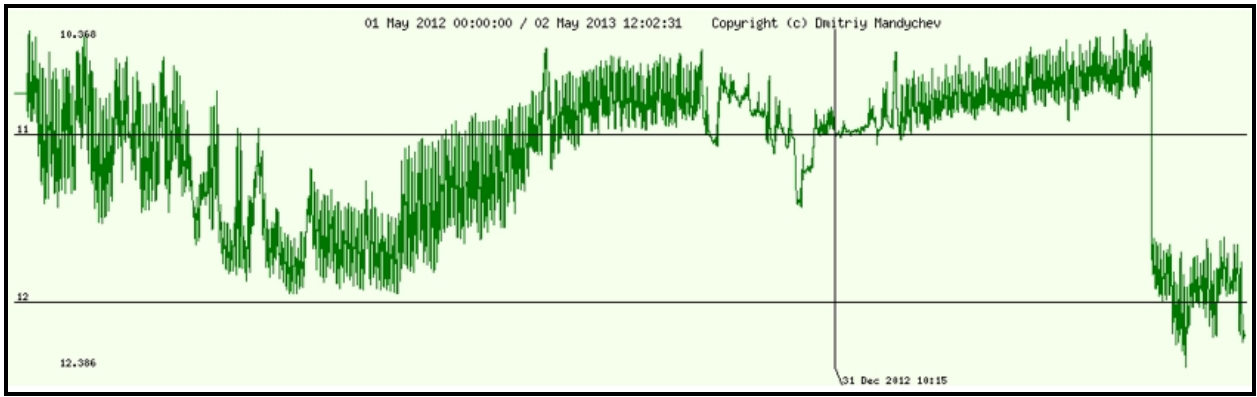


Figure 2.3.6.2. Fluctuations of groundwater levels. The large jump of a level - technical reason, is corrected by a raising upwards.

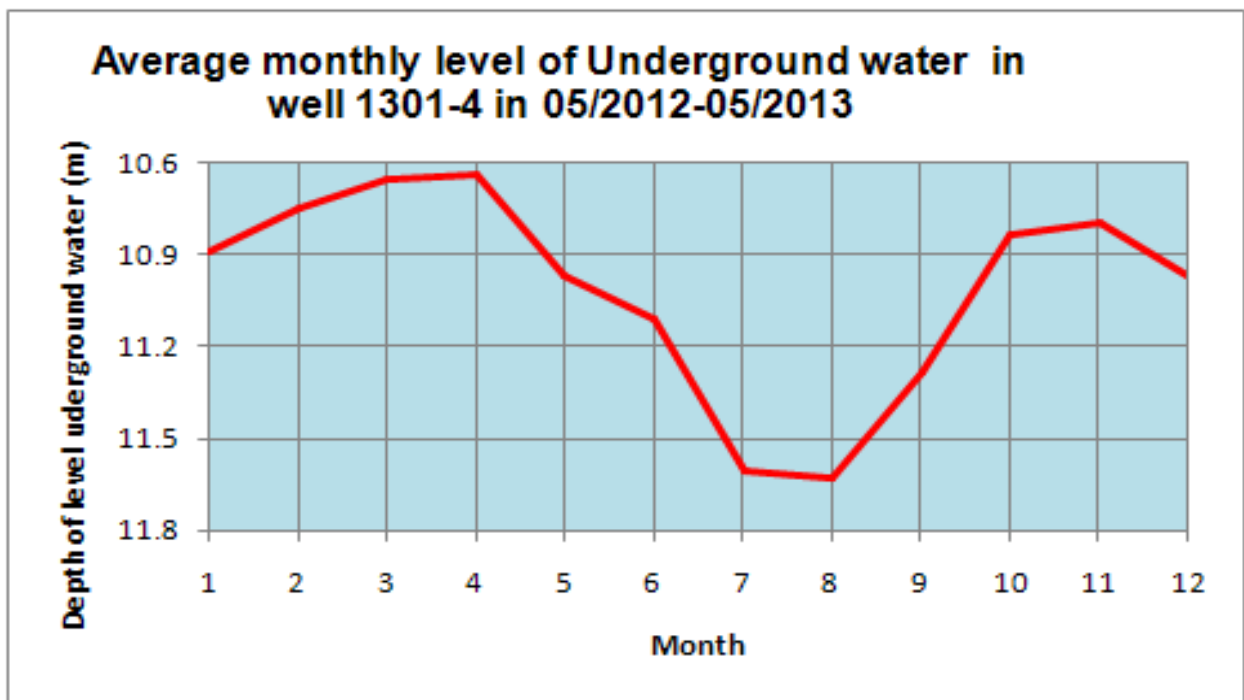


Figure 2.3.6.3. Water level fluctuations in the well 1301-4

As seen in **Figure 2.3.6.3**, long periods of fluctuations of the water level with amplitude of up to 1 meter, are observed in the seasonal section with a minimum value in July - August. In this period the depth level in the well is 11.63 m. The maximum level with a depth of approximately 10.64 m is observed in March-April. These seasonal fluctuations are due to the change of groundwater intake, and are similar to the fluctuations observed in other wells of the Chu basin.

Short periods of fluctuations in the well 1301-4 are associated with tide motions of the Earth's crust and depend on the position of the Moon and the Sun relative to the Earth. The tidal fluctuations occur daily as two peak and low groundwater levels, as shown in **Figure 2.3.6.3**. It should be noted that low levels match with high tides in the Earth's crust, while the peak levels match with low tides in the Earth's crust. [3].

The period between two daily low levels is about 12 hours, what corresponds to half a lunar day (12 hours 25 minutes). The time period between two peak levels is about 6 hours. As a rule, the first minimal level has larger amplitude than the second one, which corresponds to the second smaller tidal wave.

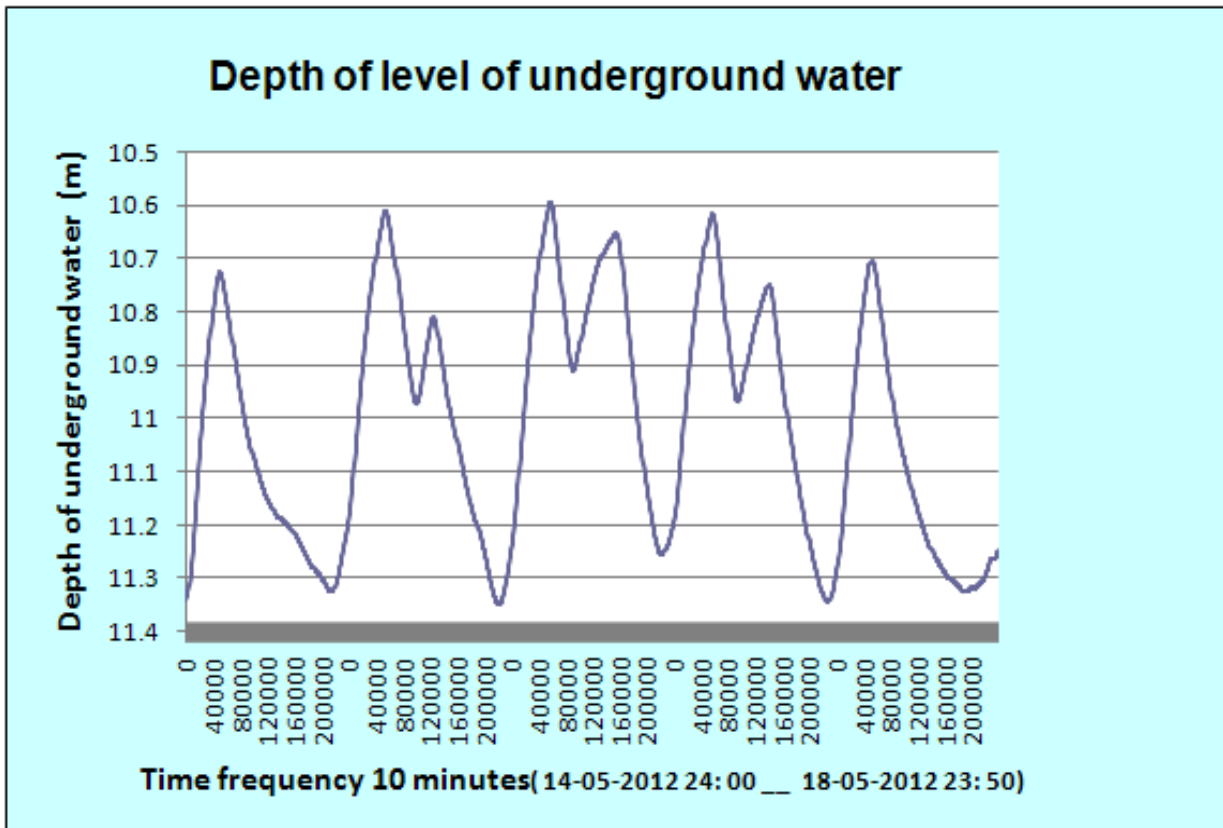


Figure 2.3.6.4. Depth of groundwater levels

In general case, the maximum amplitude is about 0.75 m, while the minimum is about 0.3-0.4 m. There are level fluctuations observed which have one maximum and minimum level within 24 hours, or have low-grade second maximum and minimum levels.

The longer periods of fluctuations shown in **Figure 2.3.6.5** have duration of 14-15 days and correspond to the half of sidereal lunar month with duration of 29.52 days. The maximum and minimum levels of these fluctuations correspond to the highest syzygies and lowest quadrature tides, which depend on the moon and the sun position. The groundwater level fluctuation amplitude is about 0.4 m. These fluctuations were most clearly observed in May-June 2012. Furthermore, their character was not expressed clearly.

Data of ground water level observations in the well 1301-4 allowed the identification of the characteristics of fluctuations in groundwater level caused by Earth tides within in the Chu basin. Besides, it allowed specifying the nature of seasonal changes in the year 2012-2013, which is similar to the previous years, as well as specifying the relative stability of the static groundwater level in the Quaternary aquifer in the Chui basin,

which is particularly used for drinking water supply for Bishkek city. The experience of the application of an automatic sensor for ground water level monitoring, and transmission of information using cellular connection to the Internet is important for the future design of an automatic groundwater observation network. The failures of sensor operation observed in the course of investigation observation in winter time are of importance, in order to improve the observation system.

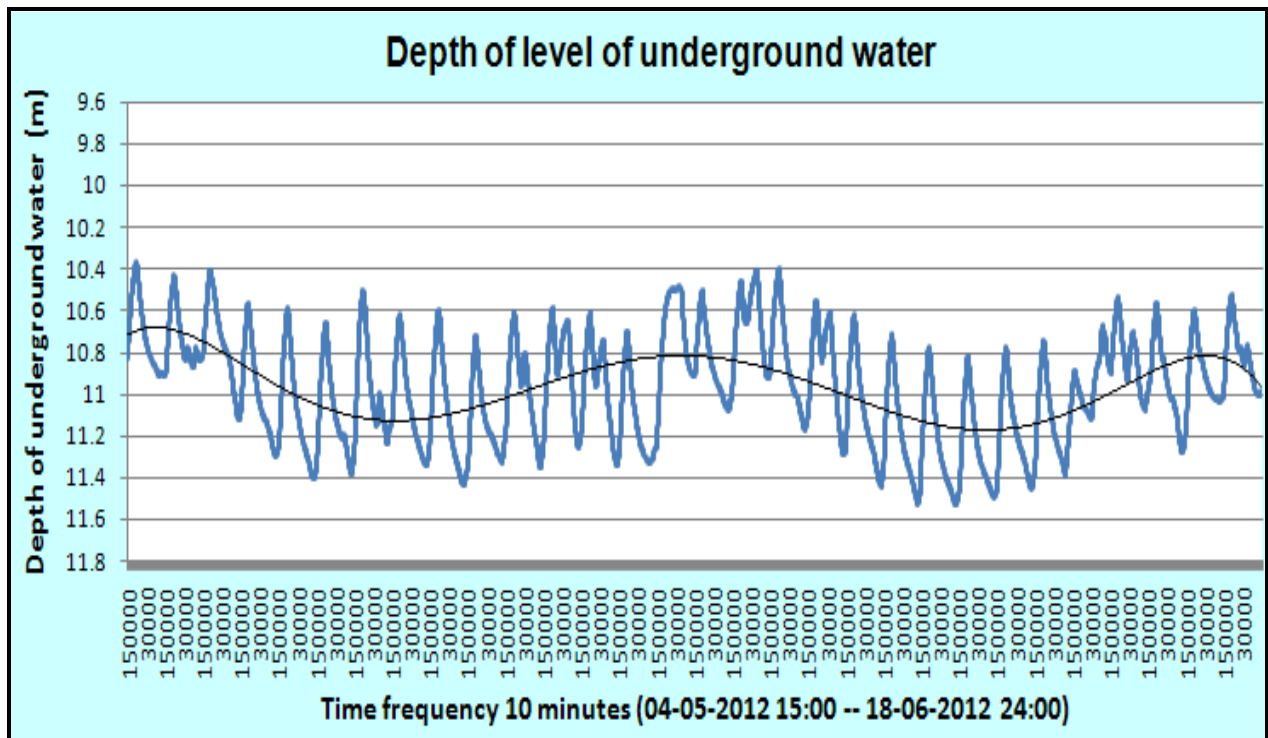


Figure 2.3.6.5. Depth of groundwater levels

Reference

1. http://www.hydrolab.com/web/ott_hach.nsf/id/pa_ott-orpheus-mini.html
2. Lange O.K. Groundwater of the USSR, part 1-2. M., 1959-1963.
3. Melchior P. Earth tides. - M: Mir, 1968. – p. 482.

2.3.7. Analysis of “Landsat 8” satellite imagery with respect to mapping of aquatic and terrestrial objects of Issyk-Kul Lake basin

The Landsat Program is the most long-term program to obtain satellite images of the Earth. The first satellite under this program was launched in 1972; to date, the last one Landsat 8 – on February 11, 2013. Landsat 8 acquires images in the visible range of light, in the short infrared and long infrared, with a resolution of 15 m, 30 m and 100 meters (panchromatic channel, multispectral channel and LWIR, respectively) [1].

CHAPTER 2. CLIMATE AND WATER RESOURCES

Interpretation of aquatic and terrestrial objects was made in the coastal and mountainous area in the Issyk-Kul Lake basin. As objects to be mapped in the coastal zone were selected: Issyk-Kul Lake, flooded areas and built-up areas (sites of mass developments). In the alpine zone objects of interpretation were alpine lakes and glaciers.

The main basic data during this work were the satellite images of Earth remote sensing (RS) – Landsat 8 (USGS site - <https://earthexplorer.usgs.gov/>), as well as a digital elevation model with a resolution of 30 meters built according to data of the ASTER radiometer located on the transnational research satellite TERRA (site of the National Aerospace Agency U.S., NASA – <http://earthdata.nasa.gov/>).

Methodology

For interpretation, the original Landsat 8 images were transformed into the GeoTIF format images of RGB compositions with different combinations of channels. To identify ground objects a combination of 432 “natural colors” was applied that uses the channels of the visible range, therefore the land surface objects look as they are perceived by the human eye. For aquatic objects a combination of 564 was used which includes short, middle infrared channels and red visible channel allowing to clearly distinguish the boundary between water and land and to highlight hidden details barely visible when using only the visible range channels. Further, the resolution of the obtained images was enlarged by using the 8th panchromatic channel. These changes were made in the software package ENVI 4.6.1. Mapping and calculation of morphometric characteristics of objects were made in the GIS MapInfo Professional 7.8.

It should be noted that the mapping was carried out in the original projection of satellite images UTM – Mercator (WGS 84). At the same time, to minimize errors associated with the conversion of basic material from one projection to another, binding of topographic maps was not made with a coordinate grid in the original projection, as it is accepted in the standard procedure for binding in GIS, but by co-registration of the material with Landsat satellite images in the projection UTM.

The first object for mapping, in order to estimate the area of Issyk-Kul Lake, became its coastline. The lake area is a very important parameter for assessing the evaporation from the water area, heat reserves, change of the coastal territory and as a result the impact of the lake on climate and environmental conditions in the basin [6].

As the following research objects, flooded areas along the shoreline of Issyk-Kul Lake were selected. These water bodies are the result of backwater of groundwater and are the consequence of raising Issyk-Kul Lake level at the present time [7] (**Figure 2.3.7.1**).

The following mapping objects were built-up areas: human settlements and holiday resorts. Freestanding buildings and groups of buildings were not used, but large-scale housings which quite accurately can be identified on Landsat satellite images.

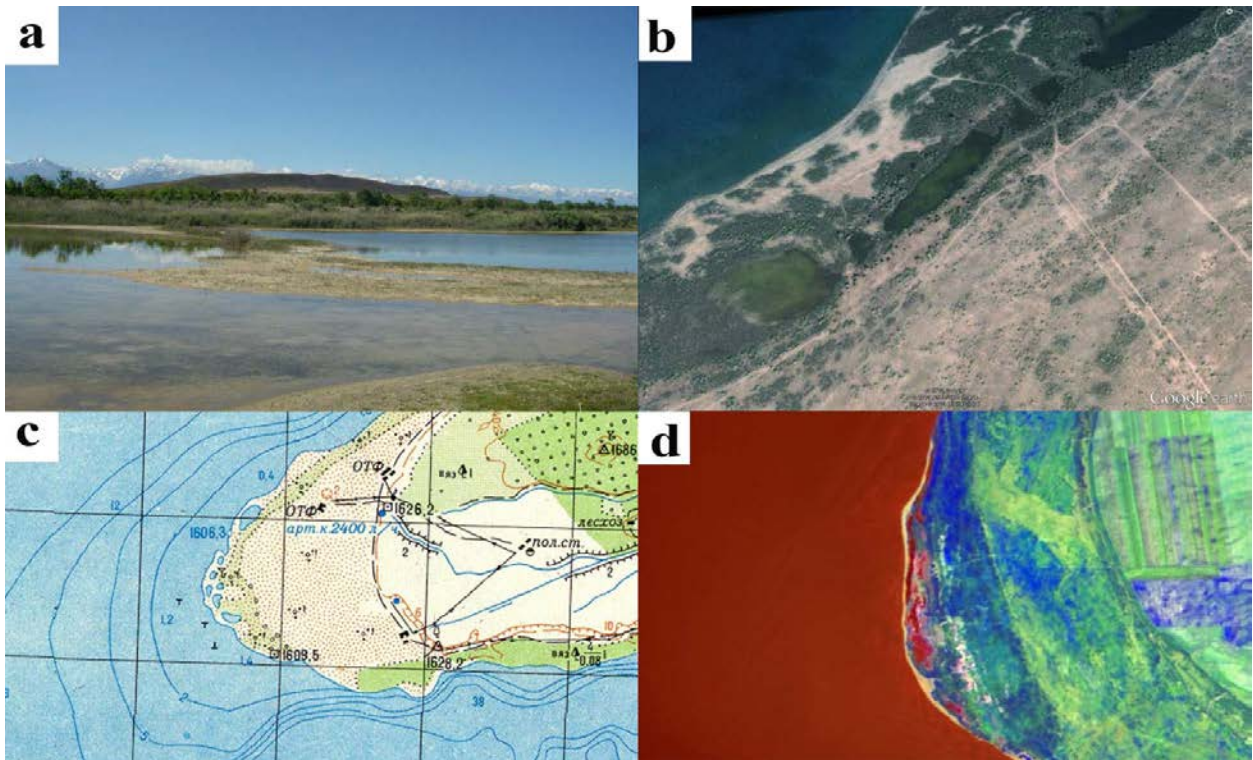


Figure 2.3.7.1. Flooded areas along the shoreline of Issyk-Kul Lake:

a – picture from Internet; *b* - Google Earth image; *c* – topographic map; *d* – “Landsat 8” picture.

In the high part of the Issyk-Kul Lake basin, a first interpretation of alpine lakes on the slopes and Kungei and Terskey Ala-Too was produced. In connection with the global warming and the retreat of glaciers, development of such lakes occurs throughout the country and, in many cases, outbursts of such lakes often can lead to catastrophic consequences. Efforts to monitor the dynamics of alpine lakes in the Kyrgyz Republic are taken by the engineering-geological crew of the Kyrgyz complex hydrogeological expedition. Conducting this type of work with field methods and helicopter flights certainly requires huge human and financial resources, but it is clearly necessary to prevent disasters. The remote sensing methods can be widely used for the preparation of such work and for regular monitoring of the situation in this area. Determination of the location of high mountain lakes as well as the development of a database of characteristics of these lakes were performed using lists and catalogues of the Ministry of Emergency Situations. [5]

As a result of mapping the shoreline of Issyk-Kul Lake, the following morphometric characteristics of the lake were obtained: the water area of the lake - 6206 km² and the coastline length of 673.2 km on the sphere. In the paper by VA Kuzmichenok [4], the author estimates the area of the lake basin as of mid-1968 to 6249.4 km² taking the height of the water level of 1607.6 m a.s.l. He also states that in case of the fall of the lake level by one meter (at water level of 1606.6 m a.s.l.) its water area will be equal to 6203.14 km². Given that on July 30, 2013, the water level was 1606.9 m a.s.l. and the area was 6206 km² one can conclude that mapping of the shoreline of Issyk-Kul Lake using Landsat 8 satellite images is acceptable for purposes of monitoring of morphometric parameters of the lake as its water area and coastline length.

CHAPTER 2. CLIMATE AND WATER RESOURCES

The main part of flooded areas is located along the eastern shoreline of the Issyk-Kul lake, less frequently such areas are found along the western and northern parts, while along the southern shoreline of the lake such territories are practically absent which is obviously related to the large slopes seen here. Mapping of such areas using Landsat imagery showed that in 2013 the number of such objects was 192. and their area was 2.87 km², while on the maps of 1986. these open water bodies were found only near the Pokrovka village (13 objects) with a total area of 0.17 km². Despite the various sources of information used for the analysis, it is obvious that the number and the flooded area increase with the rise of the water level of Issyk-Kul Lake, and it can have a negative impact on the territory adjacent to the lake (destruction of sandy beaches, coastal vegetation degradation, flooding of residential and commercial facilities etc.). Landsat images are suitable for monitoring of such areas and can be used to assess the extent and location of flooding.

Comparison of the decrypted satellite images of built-up areas with similar areas on maps of the 70s, scale 1:100.000 showed the following results. Massive development of the territory is observed around the perimeter of Issyk-Kul Lake, the largest number of such developments since the 70s of the last century to the present occurred on the northern shore of the lake in the central part (near Cholpon-Ata town).

Table 2.3.7.1 Change of sizes of built-up areas since the 1970-s and up to date in some settlements of the Issyk-Kul Lake basin

Settlements	Built-up areas in the 1970s	Built-up areas in August 2013
Karakol town	18.70 km ²	21.38 km ²
Balykchy town	13.26 km ²	17.64 km ²
Barskoon village	3.02 km ²	4.54 km ²
Darhan village	2.67 km ²	4.54 km ²
Bosteri village	2.03 km ²	3.33 km ²
Cholpon-Ata town	1.77 km ²	4.70 km ²
Korumdu village	1.09 km ²	1.58 km ²
Ichkesu village	0.77 km ²	1.29 km ²
Sary-Kamysh village	0.40 km ²	1.29 km ²

Table 2.3.7.2 Permanent population in the Issyk-Kul Oblast as per population census data from the National Statistics Committee of the Kyrgyz Republic

	1959	1970	1979	1989	1999	2013
Population	233 729	314 386	350 634	403 917	413 149	453 384

Table **2.3.7.1** shows the largest increases of built-up areas by settlements.

Due to the increasing population of the Issyk-Kul region (**Table 2.3.7.2**), the increase in built-up areas, the increase in the number of private holiday resorts and vacation houses, hence, the increase of anthropogenic load on the ecology of the lake and surrounding area, it is necessary to monitor on a regular basis these areas. Here satellite images give the best overview of the current distribution of land.

According to the results of alpine lakes mapping in the Issyk-Kul Lake basin, a digital lake map was produced with the database which includes information from the catalogues of the Ministry of Emergency Situations, as well as information obtained during mapping of these objects.

In the mountainous part of the Issyk-Kul Lake basin 472 lakes were counted according to the Landsat 8 satellite imagery for 2013 while 165 lakes were mentioned according to the catalogue of the Ministry of Emergency Situations for 2012. Such a large difference is due to the emergence of new lakes and to the fact that the Ministry of Emergency Situations catalogue included outburst lakes. In this work we mapped all alpine lakes identified on satellite imagery.

According to the results of alpine lake mapping and their verification by other satellite imagery, we conclude that the determination of their locations can be made with sufficient accuracy, but for practical use to assess their type, to determine the exact area and to monitor their development, satellite images of higher resolution than Landsat are required.

Identification of aquatic and terrestrial objects in the coastal and upland zone of Issyk-Kul Lake basin on the Landsat 8 satellite images showed fairly good results and can be used for large-scale studies also in other regions.

Clarification of morphometric characteristics of the Issyk-Kul Lake and determination of flooded areas along the perimeter of the lake, present a scientific interest for the purposes of assessment of its water balance, climate change in the basin, as well as the environmental situation in the region.

The data on increase of built-up areas since 1970-s and up to date in some settlements in the Issyk-Kul Lake basin are also of great interest for research in the field of socio-economic, migration and environmental issues.

Development of catalogues and geo-databases related to alpine lakes and glaciers in the Issyk-Kul Lake Basin undoubtedly has both theoretical and practical aspects.

The next step in this direction could be a more detailed study of the presented objects using different satellite and ground information and also dissemination of research data to other regions.

Reference

1. <http://landsat.gsfc.nasa.gov/>
2. Randolph Glacier Inventory: A Dataset of Global Glacier Outlines, Version: 2.0. 11 June 2012. // GLIMS Technical Report, 2012. -32 p.
3. USSR glacier catalogue, volume 14. edition 2.part 5. Leningrad: Gidrometeoizdat, 1976. – p.92
4. Kuzmichenok V.A. “Estimation of some detailed morphometric characteristics of Issyk-Kul Lake” // Study of hydrodynamics of Issyk-Kul Lake using isotope techniques, Part 1. Bishkek: Ilim, 2005. pp. 64-80.
5. Monitoring, forecasting of hazardous processes and phenomena in the Kyrgyz Republic (Ed. 8th rev. and ext.), Bishkek: Ministry of Emergency Situations, 2011.
6. Shabunin A.G. Hydrodynamic processes of Issyk-Kul Lake and their role in creating the environmental situation in its basin. // PhD Dissertation, Bishkek, 2006. – p. 106.
7. Shabunin G.D., Shabunin A.G. Climate change in Issyk-Kul and possible future changes in the water level. // Proceedings of NIGMI, 2010, edition 12 (257), pp. 117-127.

2.4. Study of the Makmal gold mine impact on environment

The European Commission’s EO-MINERS project was aimed at integrating new and existing earth observation tools to improve best practice in mining activities and to reduce the mining related environmental and societal footprint by:

- introducing innovative remote sensing tools to the mining industry;
- providing accuracy and quality measures for remote sensing products;
- demonstrating the application of earth observation in different case studies;
- fostering the dialogue between mining industry and environmental organizations based on EO-derived information;
- generalizing the obtained results to be used in operational mining applications in the future.

The main objective of this project was to develop EO tools for monitoring and observing environmental and societal impacts of mineral resources exploration and exploitation.

The project is primarily focused on the improvement of specialized software in selected demonstration areas around the world. New approaches were applied in processing of different data sets through various integration cycles. Certain algorithms for data integration and data processing have been tested and / or developed at this stage, given the conditions of the test site and the various thematic requirements were made available by mining companies and geological surveys.

A number of GIS thematic maps produced as a result of these activities were used to make the footprint and risk analysis. For example, risk assessment map of potential dam failure (**Figure 2.4.1**).

Three test sites were selected to achieve the objectives of the project:

CHAPTER 2. CLIMATE AND WATER RESOURCES

- In Europe, in densely populated areas: Sokolov lignite-brown coal pit located in the Czech Republic;
- Difficult-exploited areas in South Africa: Witbank black coal deposits, Province of Mpumalanga, South Africa;
- In Kyrgyzstan: Makmal gold mine, “Kyrgyzaltyn” JSC.

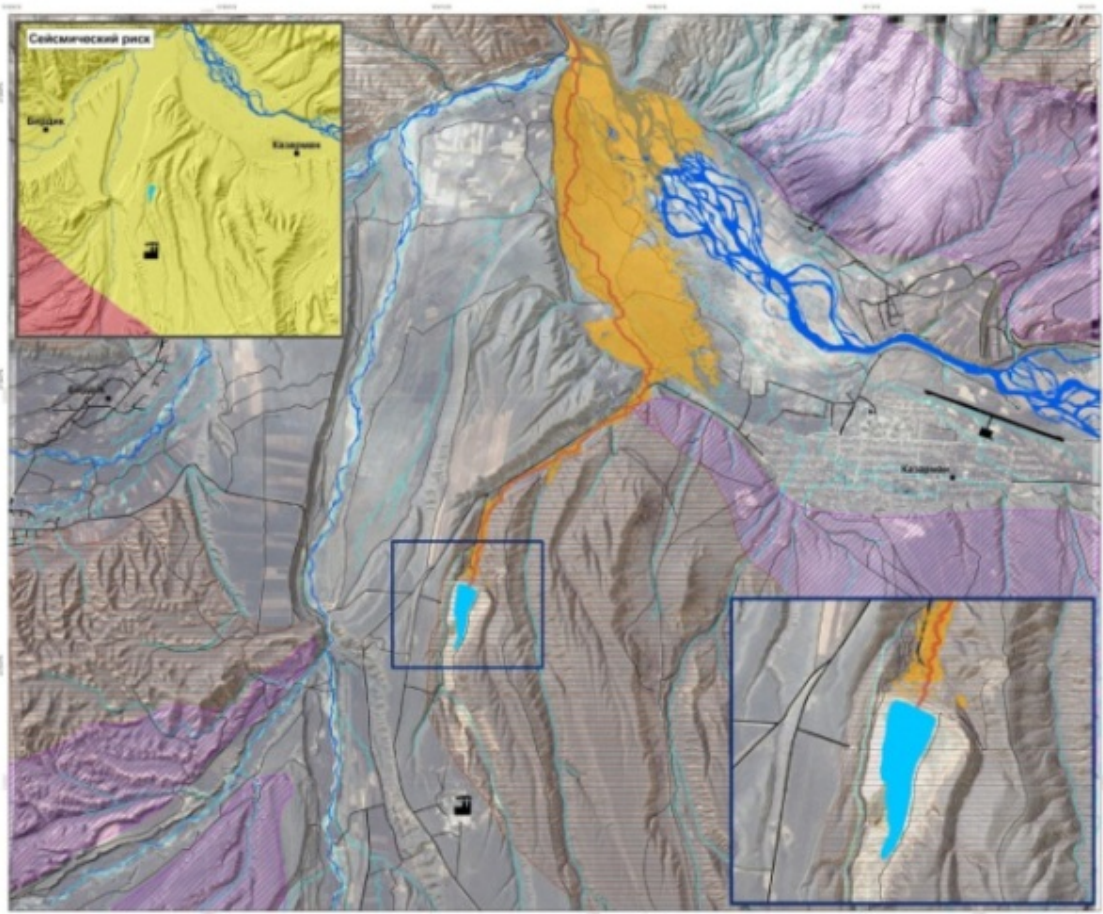


Figure 2.4.1. Risk assessment of potential dam failure

These three sites enabled to address the following issues with a particular focus on reducing the environmental footprint of mining industry, from survey work to full recovery. The work packages of the project paid particular attention to field works to obtain reliable information about the test site locations.

Object of the study. The object of the study in Kyrgyzstan is the impact of Makmal gold mine on the geo-ecological conditions of the environment and water resources. The gold extraction process is based on heap leaching using toxic materials (sodium cyanide) and subsequent stockpiling of refined products at the tailing pond.

Importance of the study. Kyrgyzstan is one of the leading mining countries of Central Asia. It keeps one of the first places in the world for gold production. Now the mining industry in our country is one of the most important sectors of economic development.

CHAPTER 2. CLIMATE AND WATER RESOURCES

Exploitation of mineral resources is associated with anthropogenic impacts on the environment. Mainly, it relates to the industrial regions with large reserves of mineral resources and therefore with a high concentration of mining production. In this case, it is the Toguz-Toro district in the Jalal-Abad Region.



Figure 2.4.2. Field works

Starting from the 1950s, mining and mineral processing in the country steadily increased, and at the same time we observe an increase of the rate and scale of landscape degradation, pollution and other negative impacts of mining. This fact proves the relevance of geo-ecological assessment and development of an effective monitoring system, using modern GIS technology in order to reduce the effects of mining on the environment and most important the impact of mines on trans-boundary water resources.

To obtain reliable data we have integrated field methods (**Figure 2.4.2**), chemical laboratory analysis of samples and GIS methods of data interpretation (**Figure 2.4.3**) demonstrating a map of cyanide dissemination in soil by results of chemical analysis with the use of GIS methods. CAIAG specialists worked closely together with their foreign counterparts in all fields of investigation.

The aim of the research work at the Makmal gold mine's tailing pond was to develop methods and tools that help to facilitate and improve the interaction between the mining industry and society using methods and tools based on Earth Observation (EO).

These methods allow to objectively assessing the potential environmental and socio-economic consequences for the life of a mining site, from exploration to final closure. The obtained products (results) will help to make the decision making process more transparent. They will secure transparency between the mining industry, regulatory bodies and other stakeholders such as local communities and non-government organizations (NGOs). It is important to note that the results and the provision of comprehensive geo information (i.e. interactive maps) increase the abilities of the public

CHAPTER 2. CLIMATE AND WATER RESOURCES

in their discussions with stakeholders who have different skills and different levels of basic knowledge. All this has been achieved through the integration of different data sets in separate EO products under the joint international project on Earth Observation to assess the environmental and social impacts from the extractive industries (EO-Miners).

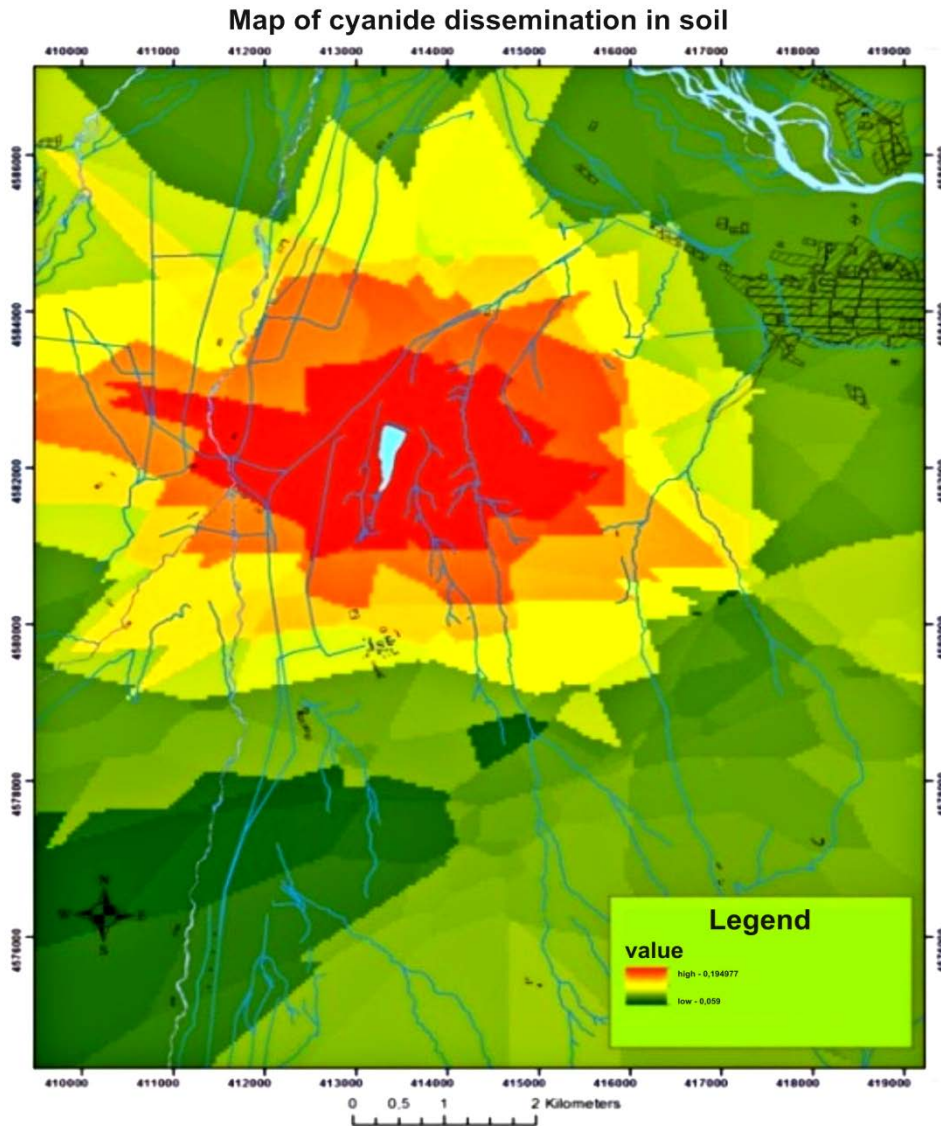


Figure 2.4.3. GIS-interpretation methods

The objectives of the work were also to use GIS tools to help to identify the scale of mining related impact on the environment and society. This, in turn, helped to reduce and improve the public perception of mining projects and related activities. To achieve this goal it was necessary to ensure objectivity and accuracy of the collected material. To meet these criteria, the data were collected using remote sensing techniques and were integrated with information collected in the field. It should be noted that in the framework of the EO-MINERS project the scientific data have been collected and presented only in the area around the Makmal processing plant near the Kazarman village and around the tailings dam. Thus, all the presented EO products reflect the situation around the area of one specific gold ore processing plant (gold extracting plant).

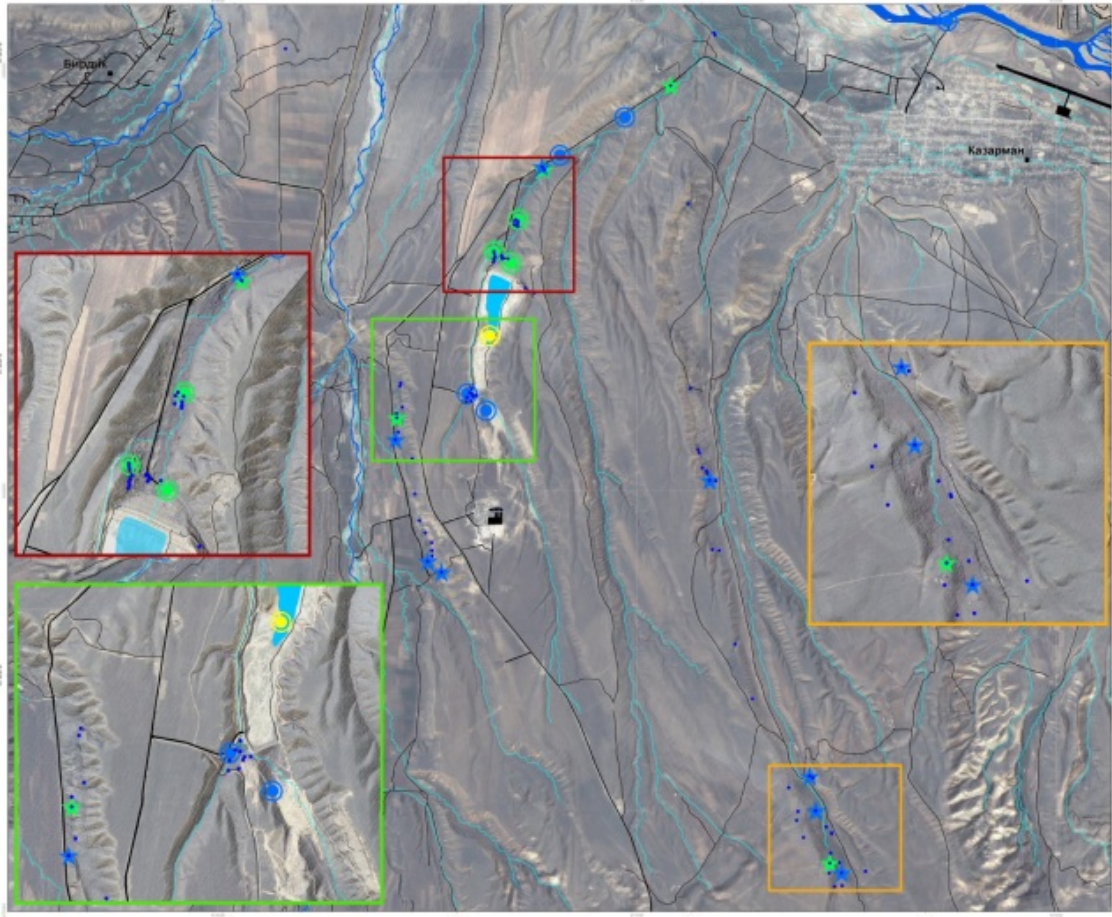


Figure 2.4.4. Places where soil and water samples were taken

As a result of the studies we have accomplished the following:

- geo-ecological assessment of mining impact using GIS technologies;
- environmental assessment of the mine's activities;
- virtually, there is no relation between local community morbidity and mine's activities;
- based on the geo-ecological assessment of the impact by the mining industry we determined the level of anthropogenic pressure on the different areas Toguz- Toro district and could show that the activity of Makmal mine didn't pose a serious threat to the health of the population (**Figure 2.4.4**) shows the points where soil and water samples were taken.

The practical significance of the work is that the developed specialized GIS-maps and the software allow to quickly assess the anthropogenic impact and to conduct a comprehensive monitoring. This makes the concept a powerful tool for decision-making and for the development of regional environment protection activities. Monitoring tools and specialized software will be transferred to Kyrgyzaltyn JSC and Makmal gold mine for future monitoring of the environment and water bodies in the local area.

The main results are:

CHAPTER 2. CLIMATE AND WATER RESOURCES

On the basis of analysis of soil, mineral and water resources, air quality, the activities of enterprises, an optimized set of factors and indicators was identified that characterize the state of ecological and geological systems.

The results of the study of mining activities and their impact revealed that:

- no negative environmental impact is made by the Makmal mine;
- a correlation between morbidity and gold mining activities in this district was statistically not proved;

The structure of a database of the environmental geographic information system was developed.

A system of GIS technology-based tools for integrated monitoring of human impact for effective environmental management of the Makmal gold mine was developed.

CHAPTER 3. NATURAL PROCESSES MONITORING AND GEOINFORMATION SYSTEMS

For the 10 years of its establishment CAIAG actively developed modern monitoring networks for geoenvironmental changes in the territory of Kyrgyzstan and transboundary areas of Central Asian countries.

Monitoring networks are interdisciplinary and include seismic, meteorological, hydrological, geodetic observations. Many observation stations are installed in areas where previously instrumental investigations were not conducted.

3.1. Monitoring Systems

The Central Asian region is known for its continental climate, high-mountain terrain, numerous rivers and low-water deserts. High tectonic activity results in devastating earthquakes with catastrophic aftermath. Integral to the region are landslides, avalanches, mudslides, floods and droughts. As a result, people suffer and infrastructure deteriorates. Therefore, creating a monitoring system to track natural hazards in quasi-real time is vital for the countries in the region. This work aims to build a geomonitoring and information system intended to collect, process and receive various types of information about the environment required to research the natural processes and disasters as well as opportunities to forecast them.

A schematic concept of the monitoring system is shown in Figure 3.1.1.

The system consists of:

1. Network of permanent multiparameter stations with a set of instruments (GNSS, seismic, hydrological, meteorological) and communications devices.
2. Information system to manage the monitoring stations and to collect the data.

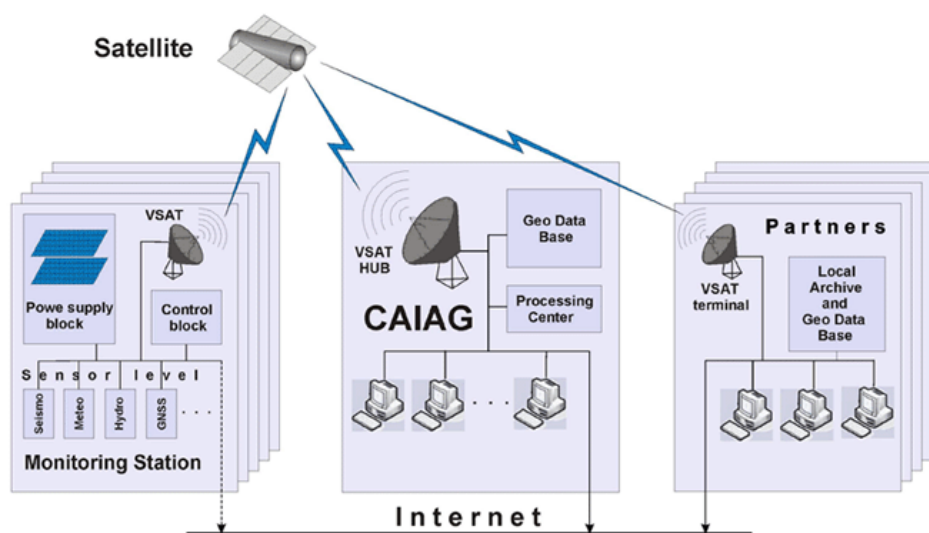


Figure 3.1.1. Schematic concept of the monitoring system.

CHAPTER 3. NATURAL PROCESSES MONITORING AND GEOINFORMATION SYSTEMS

The monitoring system receives data from observation stations via satellite or cellular networks, or via Internet in real time or quasi-real time, performs prompt analysis of the information received, identifies developing emergencies, enters data into a geodatabase in accordance with a predetermined hierarchy of data classes.

All monitoring stations are constructed based on similar schemes.

A typical monitoring station consists of basic subsystems – power, communication, station management – and includes a set of various sensors depending on the station's intended use. The power system is made of solar panels and includes batteries and a solar panel management block.

The composition of the communication system may vary depending on the station's location. In remote mountainous conditions, where communication with the outside is difficult, satellite communication channels - VSAT (Very Small Aperture Terminal) systems with 1.8 m antennas – are installed. The practice proves that such systems operate in a stable manner in all weather conditions. In areas where cellular communication is available, GSM modems are used to transmit data. Stations located in large cities are usually directly connected to Internet.

The station management system is based on an industrial computer assembled on the basis of the PC-104 board. The system's functions include controlling and managing individual parts of the station including temporal shutting-down to save energy, collecting sensors' data and transmitting them to the collection center.

Stations may include seismometers, GNSS receivers, and various meteorological and hydrological sensors. Their combination changes depending on the objectives set.

The system of station management and data collection includes communication channels and a collection and management center. Two options for data collection are possible: active and passive. In the case of the active option, stations independently transmit data to the collection center as the data emerges, and in the case of the passive option – special programs in the collection center send inquiries to stations one after another and collect new information.

3.1.1. Monitoring network

The first CAIAG monitoring stations were set up in 2008. Since then, the network has been continuously developed. The stations are located in the territory of Kyrgyzstan, Tajikistan and Uzbekistan.

The current state as of June 2014 is presented in Table 3.1.1. and in Figure 3.1.2.

CHAPTER 3. NATURAL PROCESSES MONITORING AND GEOINFORMATION SYSTEMS

Table 3.1.1. List of monitoring stations of CAIAG

№	Item	Year of setup	Parameters measured	Project	Location
1	Abramov Glacier (ABRA)	2011	Meteorological, GNSS	CAWa	Kyrgyzstan
2	Alay (ALAI, ALA1, ALA2, ALA3)	2013	GNSS	CAIAG +GFZ	Kyrgyzstan
3	Ayvaj (AYVA)	2012	Meteorological, GNSS	CAWa	Tajikistan
4	Aksay (ASAI)	2009	Meteorological, GNSS, Seismic	GCO	Kyrgyzstan
5	Arslanbob (ARSL)	2009	GNSS	RDP CAIAG	Kyrgyzstan
6	Bishkek (BIK0)	2006	GNSS	CAIAG +GFZ	Kyrgyzstan
7	Dupuli (DUPU)	2012	Meteorological, GNSS	CAWa	Tajikistan
8	Golubin Glacier (GOLU)	2013	Meteorological, GNSS	CAWa	Kyrgyzstan
9	Kara-Batkak (KRBK)	2008	GNSS	RDP CAIAG	Kyrgyzstan
10	Kerege-Tash (KRGT)	2008	GNSS	RDP CAIAG	Kyrgyzstan
11	Kokomeran (KEKI)	2010	Meteorological, GNSS	CAWa	Kyrgyzstan
12	Maydanak (MADK)	2012	Meteorological, GNSS	CAWa	Uzbekistan
13	Mertzbacher (MRZ1, MRZ2, ICED)	2009	Meteorological, GNSS, GNSS, Seismic	GCO	Kyrgyzstan
14	Sufi-Korgon (SUFI)		Meteorological, Seismic	CAREM ON	Kyrgyzstan
15	Taragay (TARA)	2008	GNSS, Seismic	CAWa	Kyrgyzstan
16	Tash-Komur (TKUM)	2009	GNSS	RDP CAIAG	Kyrgyzstan
17	Maidantal (MTAL)	2014	Meteorological, Hydrological, GNSS	CAWa	Uzbekistan

CHAPTER 3. NATURAL PROCESSES MONITORING AND GEOINFORMATION SYSTEMS

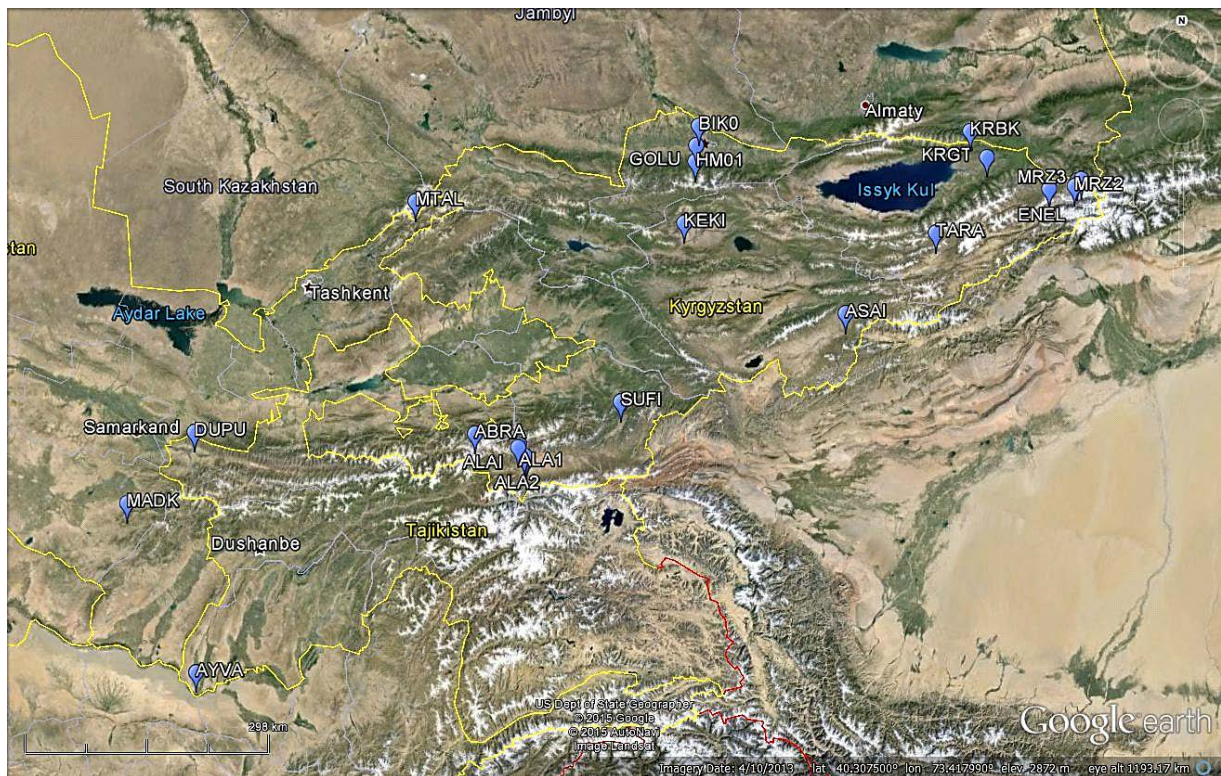


Figure 3.1.2. Location of the monitoring network stations in Central Asia

3.1.2. Seismic monitoring

The seismic monitoring network consists of own CAIAG stations and stations of other seismological networks.

Three CAIAG stations were set up in 2008-2009. These include Taragay (TARG), Aksay (ASAI) and Mertzbacher-1 (MRZ1) equipped with broadband STS-2 seismometers and Earth Data PS6-SC digitizers. Data is archived in miniseed format on a PC-104 computer that uses SeisComP v. 2.1 software to collect seismological data in a quasi-real time mode. After collection, data is transmitted via VSAT satellite antenna to the CAIAG server. In order to tie up precise time all stations use Trimble GPS antennas.

As part of the CASCADE Project (Central Asia Cross-Border Natural Disaster Prevention) the GeoForschungsZentrum (GFZ), Potsdam, Germany set up several seismic stations in 2009. One station – Sufikurgan (SUFI) – was handed over to CAIAG.

The SUFI seismic station is equipped with a Guralp broadband CMG-3ESP seismometer, CMG-5T accelerometer and CMG-DM24S6 digitizer. Data is stored in a CMG-EAM datalogger and is transmitted via VSAT to the CAIAG server. Scream software is used to collect data.

The CAIAG data collection and processing center uses the SeisComP3 server software. Data arrives at the seismic data collection server where it is automatically processed and also exchanged with other institutes and international data-centers. From the server

CHAPTER 3. NATURAL PROCESSES MONITORING AND GEOINFORMATION SYSTEMS

data is transmitted to 2 work stations: 1) in order to reflect seismic information and, simultaneously, 2) for manual processing.

SeisComP3 is a software package to collect, store and share seismological data in quasi-real time via Internet. The SeisComP3 software package ensures the following functions: collecting and storing data, quality control, data registration, data sharing in real-time mode, control of the network status, automatic processing in real time with a possibility to manual interaction, acoustic and visual event alarm, archiving wave forms, distributing wave form data, automatic identification of events and their locations, identification of events and their location on an interactive basis, archiving event parameters, ensuring free access to relevant information about stations, wave forms and latest earthquakes (Figure 3.1.3.).

SeisComP3 automatically calculates the following magnitudes: ML, MJ, mb, mB, Mw(mB), Mwp, Mw(Mwp). In order to notify users about earthquakes, Seiscomp3 utilizes “a system of prompt notification” for immediate mailing of notifications. The primary goal is to provide stakeholder organizations, scientists and the public with prompt and reliable information.

In 2011, CAIAG was admitted as a member of FDSN (The International Federation of Digital Seismograph Networks). Membership in this organization enables to exchange seismological data within this network free of charge. As a result, CAIAG receives data from more than 30 seismic stations of the FDSN network in real-time for earthquake processing.



Figure 3.1.3. Example of a message (notification) on a seismic event by SeisComP-3.

The system uses SEISAN software for manual processing of seismological data that was recommended on seismology courses run by GFZ as part of the IASPEI training program. The SEISAN seismic analysis system consists of a full set of software and a

172

CHAPTER 3. NATURAL PROCESSES MONITORING AND GEOINFORMATION SYSTEMS

simple database for the analysis of earthquake records, both analogue or digital. SEISAN allows entering phase parameters; localize events; edit the event parameters received; identify spectral characteristics, earthquake moment and azimuth of arrivals for 3-component stations; receive graphic representation of epicenters. The entire set of programs of the system is connected to the general database. The program allows searching for events in the database based on various criteria for selection of events, enables to work with subsets of events without extracting from the database. In order to expand capabilities of SEISAN, the system was augmented with a series of research software programs such as Q code, synthetic modeling, as well as a full system of seismic hazard identification (Havskov and Ottemoller, 1999).

According to processing results primarily two catalogs are prepared. The first one on the basis of the SeisComP system. An operator analyzed the catalog of automatic solutions and, in cases of major scattering of source data, performed a manual picking of phases. For the second catalog, an operator reviewed the continuous flow of wave forms and, in case of the identification earthquakes not located by SeisComP, cut out such records and processed them with SEISAN. This catalog included weak events whose amplitudes were lower than the threshold values for the automatic location. Data from the two catalogs was combined into one.

3.1.3. Hydrometeorological monitoring

Hydrometeorological monitoring is conducted by automatic stations. The system of collecting and primary processing of meteorological and hydrological information at certain time intervals to collect information on satellite links and presents it in a convenient form. Monitoring system in quasi-real time controls the parameters as air temperature and humidity, atmospheric pressure, wind speed and direction, level of rain precipitation, soil temperature and moisture, solar radiation, etc.

The majority of stations – Baytik (HM01), Golubin Glacier (GOLU), Taragay (TARA), Enilchek (ENEL), Aksay (ASAI), Kokomeren (KEKI), Abramov Glacier (ABRA), Dupuli (DUPU), Ayvaj (AYVA), Maydanak (MADK), Maidantal (MTAL) – are equipped with ROMPS meteorological stations (Remotely Operated Multi-Parameter Stations) (GFZ, Department 1.2) [T. Schöne, 2013] and set up as part of the CAWa and GCO-CA projects.

The stations are managed by a station computer on the basis of the PC-104 board. In addition the stations have a power management system. Data collection is done by a Campbell Scientific CR1000 datalogger. Two satellite communication systems are used: a primary (main) VSAT to transmit data to the collection center and a secondary (auxiliary) Iridium for station management in case of emergencies. Power supply for the devices is normally arranged via six 125 W solar panels and 6 batteries 240 Ah each.

Sensors include:

CHAPTER 3. NATURAL PROCESSES MONITORING AND GEOINFORMATION SYSTEMS

- atmospheric pressure sensor (Barometric Pressure Transducer, model 278, Setra, USA),
- air temperature and relative humidity sensor (Temperature & Relative Humidity Probe HMP45, Vaisala, Finland),
- solar radiation sensor (Net Radiometer NR01, Hukseflux, Netherlands),
- precipitation gauge (Tipping Bucket Rain Gauge 52203, RM Young, USA),
- wind speed and direction gauge (Wind Monitor 05103, RM Young, USA) installed on a 10-meter mast,
- soil temperature sensors (Soil Temperature Sensor 107, Campbell Scientific, UK),
- soil moisture sensors (Soil Water Content Reflectometer CS616, Campbell Scientific, UK),
- GNSS receiver (Topcon GB-1000 or Septentrio NV AsteRx2e) whose antenna is normally mounted on a metal tube.

Some stations support devices to measure the snow pack (Snow Pack Analyzing System - SPA, Sommer, Austria).

If there is a river with a bridge near a station, a water level and flow speed sensor are installed on the bridge (Discharge System RQ-24, Sommer, Austria) and connected to the primary station via a radio modem channel (Figure 3.1.4.).

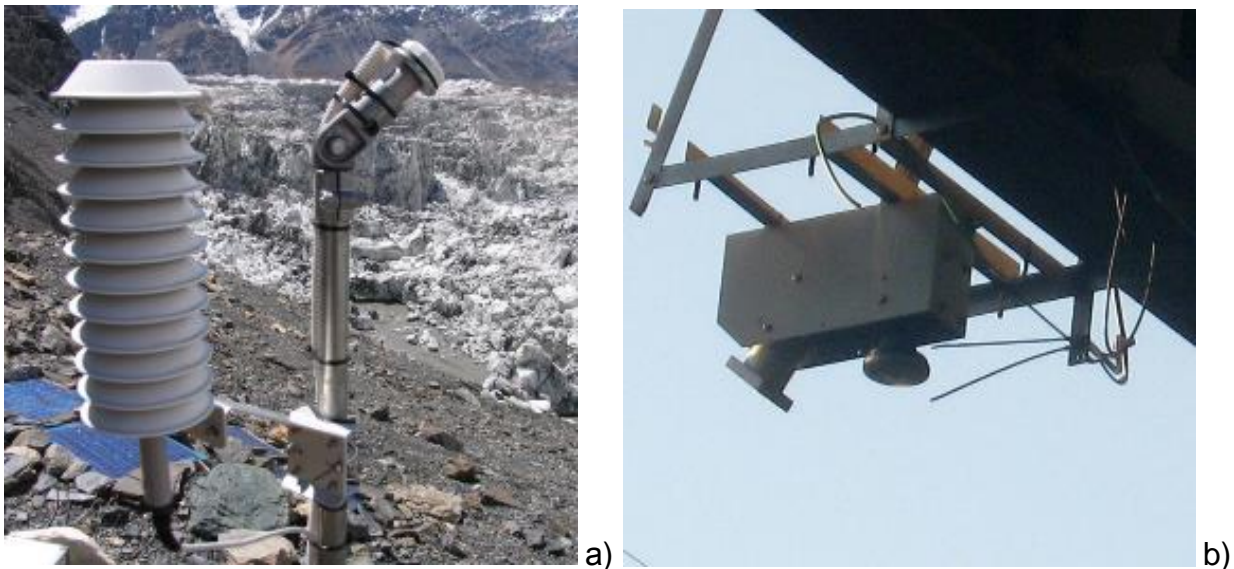


Figure 3.1.4. Meteorological sensors on the Enilchek glacier (a) and Doppler water flow meter in Dupuli (b).

The hydrometeorological monitoring network covers the territories of Tajikistan (DUPU and AYVA), Uzbekistan (MADK) and Kyrgyzstan (the other stations). Bishkek Station (BIK0) utilizes a Vaisala meteorological station.

Values from the database for any measured parameter and any station can be plotted (Figure 3.1.5.) using the SDS (see below).

CHAPTER 3. NATURAL PROCESSES MONITORING AND GEOINFORMATION SYSTEMS

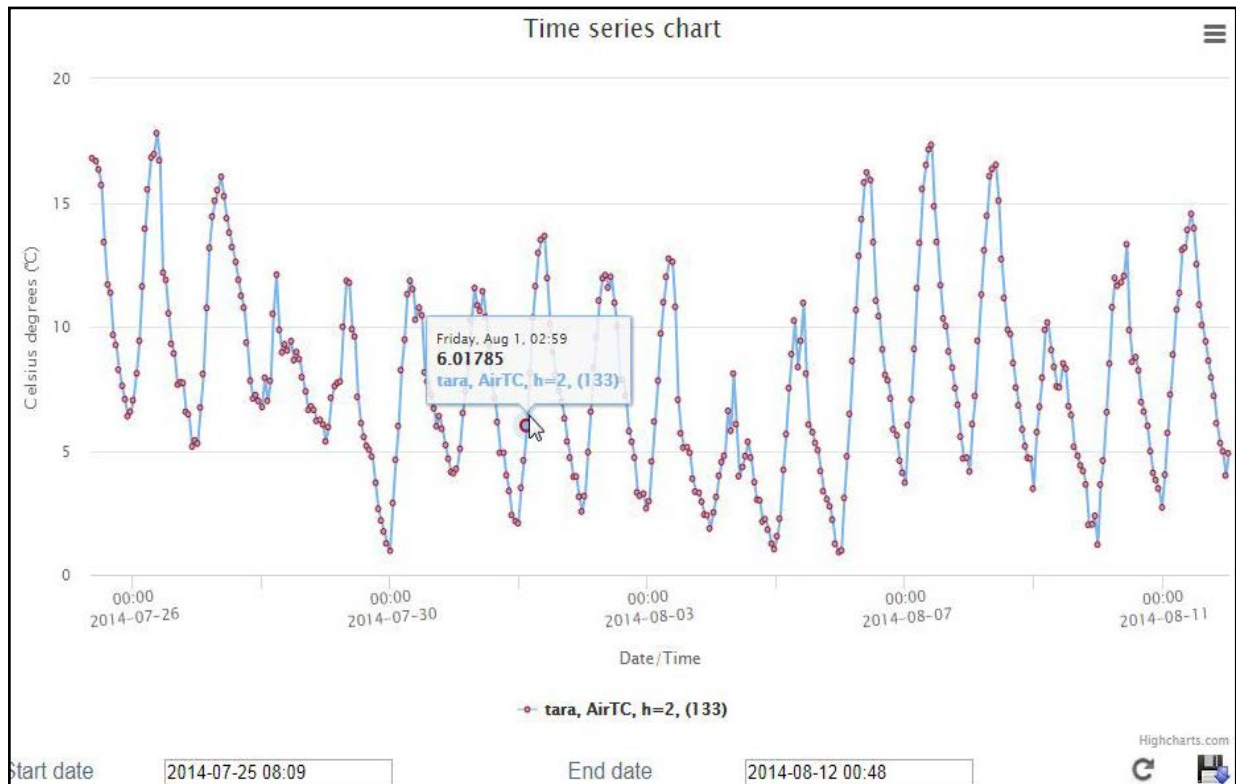


Figure 3.1.5. Example of a plot of the air temperature for the Ayvaj Station

3.1.4. GNSS monitoring

Earlier GNSS-based observations in the territory of Kyrgyzstan, Kazakhstan and Tajikistan identified significant regional non-homogeneities of velocity fields and deformation fields (Figure 3.1.6.) [A.V. Zubovich, 2013].

Their correspondance with geological structures (correspondence of areas of high deformations to fault zones, correspondence of primary parameters of deformation fields based on GNSS data to parameters of seismo-tectonic deformations) allows to conclude that the spatial distribution of deformations of the Earth crust has been consistent and stable over a long period of time.

The continuation of measuring campains in the territory of Central Asia to determine velocity or deformation fields is unlikely to yield new information compared to what is already available. Therefore, CAIAG's main efforts with respect to GNSS monitoring aimed to develop a network of permanent stations that, in addition to the already available static distribution of deformation fields in terms of area, can provide more detailed information in terms of dynamics.

GNSS monitoring is performed by all network stations (except for the Sufikurgan Station) as shown in Figure 3.1.2. and Table 3.1.1. All stations use dual-band and dual-mode GNSS receivers; information is automatically transmitted via communication lines (Internet, satellite, radio modem and GSM communication) to the CAIAG data collection

CHAPTER 3. NATURAL PROCESSES MONITORING AND GEOINFORMATION SYSTEMS

center and recorded on the file server. Meta-information is stored in a database. Information about the delivery of GNSS data is given on the CAIAG web server.

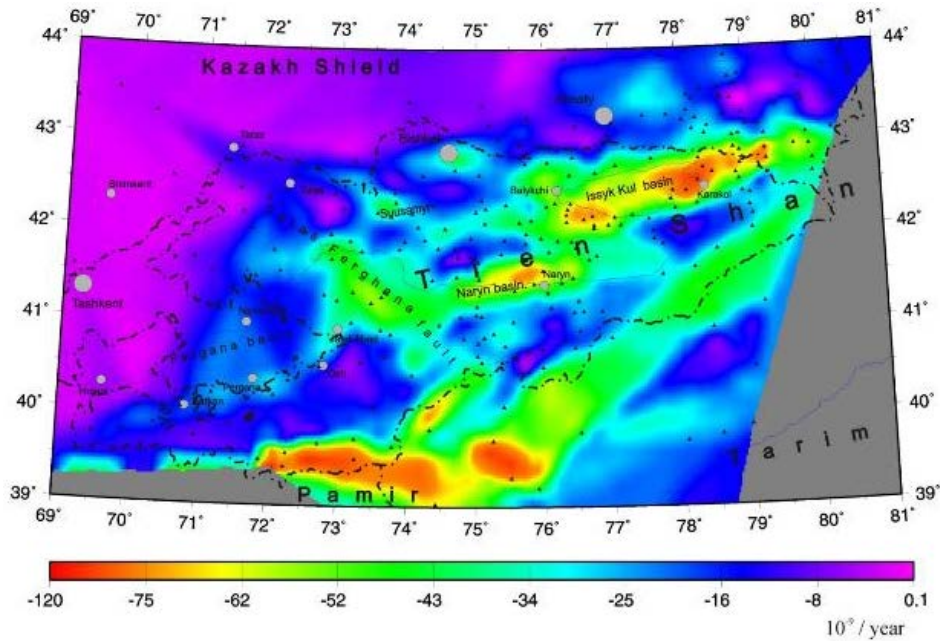


Figure 3.1.6. Field of deformation velocity (maximum shortening) of Tien-Shan

Processing of GNSS data is performed by the GAMIT/GLOBK software package developed by the Massachusetts Institute of Technology, USA [Herring, 2004; King and Bock, 2004].

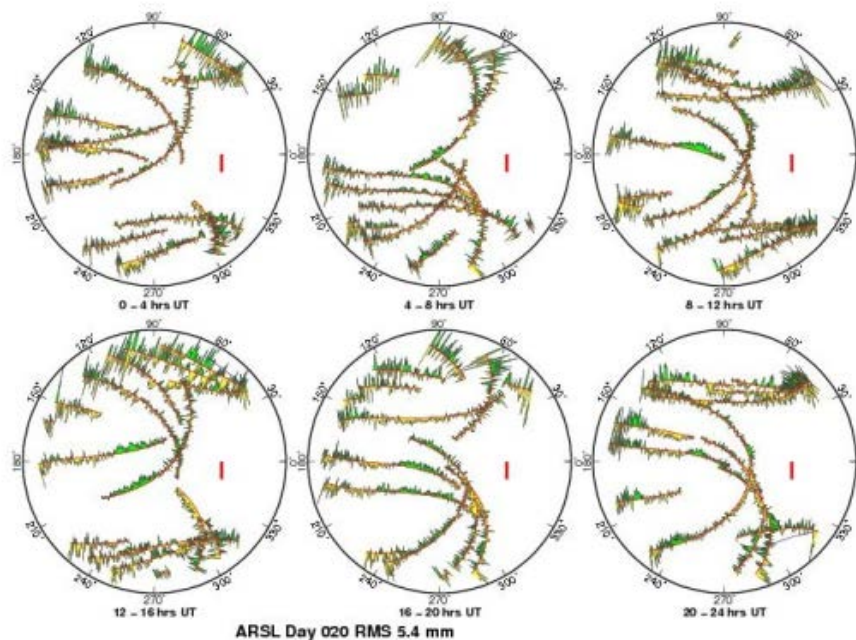


Figure 3.1.7. Sky map for Arslanbob station showing measurement error for each satellite observed along the trajectory of their movement

For all GNSS stations the quality of measured data was analyzed based on “sky maps” (Figure 3.1.7.) representing the measurement error along the trajectories of satellites for

CHAPTER 3. NATURAL PROCESSES MONITORING AND GEOINFORMATION SYSTEMS

every 4 hours. For all stations the mean-square deviations are within the allowable ranges. This means that the stations have insignificant noise background, receivers and antennas function properly, and re-reflection of the signal from surrounding objects is not observed or is insignificant.

3.2. Information Systems and Geodatabase

In CAIAG conducted a number of projects for various organizations and agencies, solving the tasks on providing the spatial and non-spatial data, geoprocessing, digital mapping, and use them for effective planning and management of enterprises, forecast and assessment of natural disasters risks.

Implementation of the projects was carried out with use of geoinformation systems technology, databases, web mapping and applied programming. In selecting software components, preference was given to OpenSource software products as for financial reasons, and on the fact that they are free from corporate liabilities and more committed to observance of international standards on data formats and data exchange protocols. So, used in all the projects below the web mapping technology, Open Geospatial Consortium (OGC) standards based, provides services to enable the exchange of data between OGC-servers and jointly use them to create a common mapping projects available throughout the Internet community.

Geodatabase based on PostgreSQL and PostGIS, are also OpenSource products and as good as commercial products as Imformix, MS SQL Server or ArcGIS Server in productivity and functionality, and the area of their use is expanding all the time.

Using the single bundle of geodatabase on PostgreSQL/PostGIS and web mapping services based on OGC standards allowed to obtain construction providing effectiveness, efficiency, functionality of systems of storage, distribution and exchange of spatial data at the lowest cost.

3.2.1. Sensor Data Storage System

Sensor Data Storage System (SDSS) was developed for the CAIAG monitoring data received via Internet or satellite or other radio communication channels. The system is based on PostgreSQL.

SDSS prototype system is SOS (sensory observations service - <http://www.opengeospatial.org/standards/sos>), which is designed for a wide range of applications and can be used to store almost any sensor data. But like any tool of too general application, it does not take into account the specifics of individual data. Therefore, the system for sensor data storing was developed. The advantage of SOS, which has passed to SDSS is strict structure of the database (fixed number of tables),

CHAPTER 3. NATURAL PROCESSES MONITORING AND GEOINFORMATION SYSTEMS

that does not change with the addition of new sensors, stations, measurement parameters.

The central element of SDSS is the Measurement Block. A Measurement Block is a timeseries of one "Property" (e.g., temperature or wind speed) measured by a Sensor Device with a preset serial number at one Station in indicated Units of Measure. If conditions of measurement change (a sensor is replaced or its location changes), a measurement block is considered finished and a new one is started. Quite frequently, one measurement device identified by its serial number can contain several sensors thus measuring several parameters simultaneously (for instance, air temperature and relative humidity).

SDSS management is performed by a special software accessible via a web interface and consisting of 4 module pages. The main page contains a welcome message and brief instructions on how to use the system. The Equipment page hosts all tools needed to work with instrumentation.

A major role in for this application plays a sensor model that represents a certain type of a measurement device. The sensor model has technical specifications such as range of working temperatures, precision of sensor, etc. Models of sensors are combined into groups. The Measurements page is intended to work with blocks of measurements (Figure 3.2.1.).

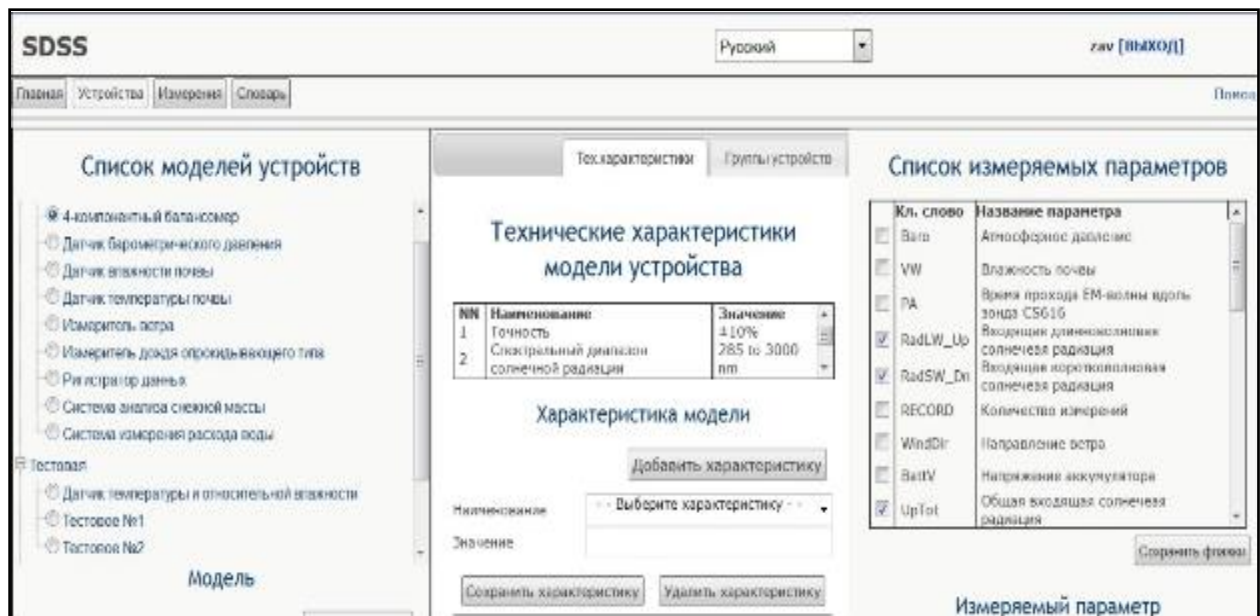


Figure 3.2.1. View of a page for handling measurement instrumentation

The page "Measurement" is designed to work with blocks of measurements (Figure 3.2.2.), the filter criterias are specified in the left pane of the page. The right panel is used for displaying and editing blocks and their parameters.

The SDSS has visualization facility of sensor data as graphs, allowing you to obtain a visual imagination about characteristics and features of changes in blocks of measurement (Figure 3.2.3.).

CHAPTER 3. NATURAL PROCESSES MONITORING AND GEOINFORMATION SYSTEMS

SDSS Система Управления Сенсорными Данными

Имя параметра: все | Очистить

Станция: все | Очистить

Модель устройства: все | Сервом. | все | Очистить

Единица измерения: все | Очистить

Список измеренных параметров

№	Кл. слово	Название свойства
1		
2		
3	Ваво	Атмосферное давление
4	VW	Влажность почвы
5	PA	Время приема СВ-волны единь блока CS616
6	RadW_Up	Входящая длинноволновая солнечная радиация
7	RadSW_Dn	Входящая коротковолновая солнечная радиация
8	NEC08D	Количество измерений
9	Rad_M_Sc	Отраженная длинноволновая солнечная радиация
10	WindDir	Направление ветра
11	BatV	Напряжение аккумулятора
12	UpTot	Общая мощность солнечной радиации
13	NetTot	Общая остывающая солнечная радиация
14	DeTot	Общая отражающая солнечная радиация
15	Rain_Tot	Общая количество осадков за время отчета
16	RQ_0	Объем воды в реке
17	NetB	Остывающая длинноволновая солнечная радиация
18	NetBo	Остывающая коротковолновая солнечная радиация
19	HN	Относительная влажность
20	Albedo	Отражательная способность
21	RadW_Dn	Отраженная длинноволновая солнечная радиация
22	Rad_M_Sc	Отраженная коротковолновая солнечная радиация
23	RadSW_Dn	Скорость ветра
24	WindSp	Скорость течения поперек реки
25	RQ_1	температура
26	DirTC	Температура воздуха
27	DirTC	Температура почвы
28	HR03T	Температура у дна реки
29	HR03T	Уровень воды в реке
30	RQ_WL	

Список блоков измерений

№	ID	Имя	Сущность	Высота	Нач. время	Кон. время
1	85	dirTC	kali	2	2007-03-31 00:00:00	2009-12-31 00:00:00
2	220	dirTC	tara	2	2008-01-31 22:30:00	2009-12-31 23:59:59
3	133	dirTC	tara	2	2008-01-31 22:30:00	2009-12-31 23:59:59
4	203	dirTC	madk	2	2008-01-31 22:30:00	2009-12-31 23:59:59
5	592	dirTC	nrz1	2	2011-08-03 10:14:00	2009-12-31 23:59:59
6	43	dirTC	abra	2	2011-08-28 08:00:00	2009-12-31 00:00:00
7	358	dirTC	ayva	2	2012-06-02 00:00:00	2009-12-31 23:59:59
8	1	dirTC	asa1	2	2012-07-04 00:00:00	2009-12-31 00:00:00
9	177	dirTC	goku	2	2013-09-26 00:00:00	2009-12-31 23:59:59
10	305	dirTC	bfo	2	2014-04-05 06:45:00	2009-12-31 23:59:59
11	672	dirTC	ntal	2	2014-09-29 08:07:00	2009-12-31 23:59:59
12	102	dirTC	kali	2	2007-03-31 00:00:00	2009-12-31 00:00:00
13	221	dirTC	hny1	2	2008-01-31 22:30:00	2009-12-31 23:59:59
14	204	dirTC	madk	2	2008-01-31 22:30:00	2009-12-31 23:59:59
15	134	dirTC	tara	2	2008-01-31 22:30:00	2009-12-31 23:59:59
16	593	dirTC	nrz1	2	2011-08-03 10:14:00	2009-12-31 23:59:59
17	44	dirTC	abra	2	2011-08-28 08:00:00	2009-12-31 00:00:00
18	359	dirTC	ayva	2	2012-06-02 00:00:00	2009-12-31 23:59:59
19	2	dirTC	ntal	2	2012-07-04 00:00:00	2009-12-31 23:59:59
20	170	dirTC	goku	2	2013-09-26 00:00:00	2009-12-31 23:59:59
21	673	dirTC	ntal	2	2014-09-29 08:07:00	2009-12-31 23:59:59
22	716	dirTC	kali	1.5	2007-03-31 00:00:00	2009-12-31 00:00:00
23	222	dirTC	hny1	1.5	2008-01-31 22:30:00	2009-12-31 23:59:59
24	205	dirTC	madk	2	2008-01-31 22:30:00	2009-12-31 23:59:59
25	135	dirTC	tara	2	2008-01-31 22:30:00	2009-12-31 23:59:59
26	594	dirTC	nrz1	2	2011-08-03 10:14:00	2009-12-31 23:59:59
27	45	dirTC	abra	2	2011-08-28 08:00:00	2009-12-31 00:00:00
28	360	dirTC	ayva	1.5	2012-06-02 00:00:00	2009-12-31 23:59:59
29	3	dirTC	asa1	1.5	2012-07-04 00:00:00	2009-12-31 00:00:00
30	179	dirTC	goku	2	2013-09-26 00:00:00	2009-12-31 23:59:59
31	306	dirTC	ayva	1.5	2014-09-29 08:07:00	2009-12-31 23:59:59
32	674	dirTC	ntal	2	2014-09-29 08:07:00	2009-12-31 23:59:59
33	856	BatV_Avg	hny1	2	2008-03-12 06:06:00	2008-12-31 23:59:59
34	88	BatV_Min	kali	1.5	2007-03-31 00:00:01	2009-12-31 00:00:00
35	223	BatV_Min	hny1	1.5	2008-01-31 22:30:00	2009-12-31 23:59:59
36	206	BatV_Min	madk	1	2008-01-31 22:30:00	2009-12-31 23:59:59
37	136	BatV_Min	tara	1.5	2008-01-31 22:30:00	2009-12-31 23:59:59
38	46	BatV_Min	abra	1.5	2011-08-28 08:00:00	2009-12-31 00:00:00
39	361	BatV_Min	ayva	1.5	2012-06-02 00:00:00	2009-12-31 23:59:59
40	4	BatV_Min	asa1	1.5	2012-07-04 00:00:00	2009-12-31 00:00:00
41	595	BatV_Min	nrz1	1.5	2011-08-03 10:14:00	2009-12-31 23:59:59
42	180	BatV_Min	goku	1.5	2013-09-26 00:00:00	2009-12-31 23:59:59
43	675	BatV_Min	ntal	1.5	2014-09-29 08:07:00	2009-12-31 23:59:59
44	596	DeTot_Avg	nrz1	2	2011-08-03 10:14:00	2009-12-31 23:59:59
45	89	DeTot_Avg	kali	2	2007-03-31 00:00:00	2009-12-31 00:00:00
46	267	DeTot_Avg	madk	2	2008-01-31 22:30:00	2009-12-31 23:59:59
47	224	DeTot_Avg	hny1	2	2008-01-31 22:30:00	2009-12-31 23:59:59
48	137	DeTot_Avg	tara	2	2008-01-31 22:30:00	2009-12-31 23:59:59
49	598	DeTot_Avg	nrz1	2	2011-08-03 10:14:00	2009-12-31 23:59:59
50	87	DeTot_Avg	abra	2	2011-08-28 08:00:00	2009-12-31 00:00:00

a)

SDSS Система Управления Сенсорными Данными

Имя параметра: все | Очистить

Станция: все | Очистить

Модель устройства: HNP45C | Сервом. | все | Очистить

Единица измерения: все | Очистить

Список моделей устройств

№	Модель	Название
1	HR01	4-компонентный датчик скорости
2	278	Датчик барометрического давления
3	CS616	Датчик влажности почвы
4	HNP45C	Датчик температуры и относительной влажности
5	107	Датчик температуры почвы
6	05103	Измеритель ветра
7	52203	Измеритель дожде
8	CR1000	Регистратор данных
9	SFA	Система анализа опенкой насы
10	RQ-24	Система измерения расхода воды

Список блоков измерений

№	ID	Имя	Сущность	Высота	Нач. время	Кон. время
1	85	dirTC	kali	2	2007-03-31 00:00:00	2009-12-31 00:00:00
2	133	dirTC	tara	2	2008-01-31 22:30:00	2009-12-31 23:59:59
3	203	dirTC	madk	2	2008-01-31 22:30:00	2009-12-31 23:59:59
4	220	dirTC	hny1	2	2008-01-31 22:30:00	2009-12-31 23:59:59
5	592	dirTC	nrz1	2	2011-08-03 10:14:00	2009-12-31 23:59:59
6	43	dirTC	abra	2	2011-08-28 08:00:00	2009-12-31 00:00:00
7	358	dirTC	ayva	2	2012-06-02 00:00:00	2009-12-31 23:59:59
8	1	dirTC	asa1	2	2012-07-04 00:00:00	2009-12-31 00:00:00
9	177	dirTC	goku	2	2013-09-26 00:00:00	2009-12-31 23:59:59
10	305	dirTC	bfo	2	2014-04-05 06:45:00	2009-12-31 23:59:59
11	672	dirTC	ntal	2	2014-09-29 08:07:00	2009-12-31 23:59:59
12	102	dirTC	kali	2	2007-03-31 00:00:00	2009-12-31 00:00:00
13	238	dirTC	hny1	2	2008-01-31 22:30:00	2009-12-31 23:59:59
14	130	dirTC	tara	2	2008-01-31 22:30:00	2009-12-31 23:59:59
15	280	dirTC	madk	2	2008-01-31 22:30:00	2009-12-31 23:59:59
16	614	dirTC	nrz1	2	2011-08-03 10:14:00	2009-12-31 23:59:59
17	60	dirTC	abra	2	2011-08-28 08:00:00	2009-12-31 00:00:00
18	375	dirTC	ayva	2	2012-06-02 00:00:00	2009-12-31 23:59:59
19	18	dirTC	asa1	2	2012-07-04 00:00:00	2009-12-31 00:00:00

Выбор устройства

F2650065, F294005, atal32R, atal3H, F0150011, F2940004, F2940038, G4610027 2011, HNP 45 AC, F0150012 3333

b)

Figure 3.2.2. View the page to work with blocks of measurement (a) and with viewing of location(b).

CHAPTER 3. NATURAL PROCESSES MONITORING AND GEOINFORMATION SYSTEMS

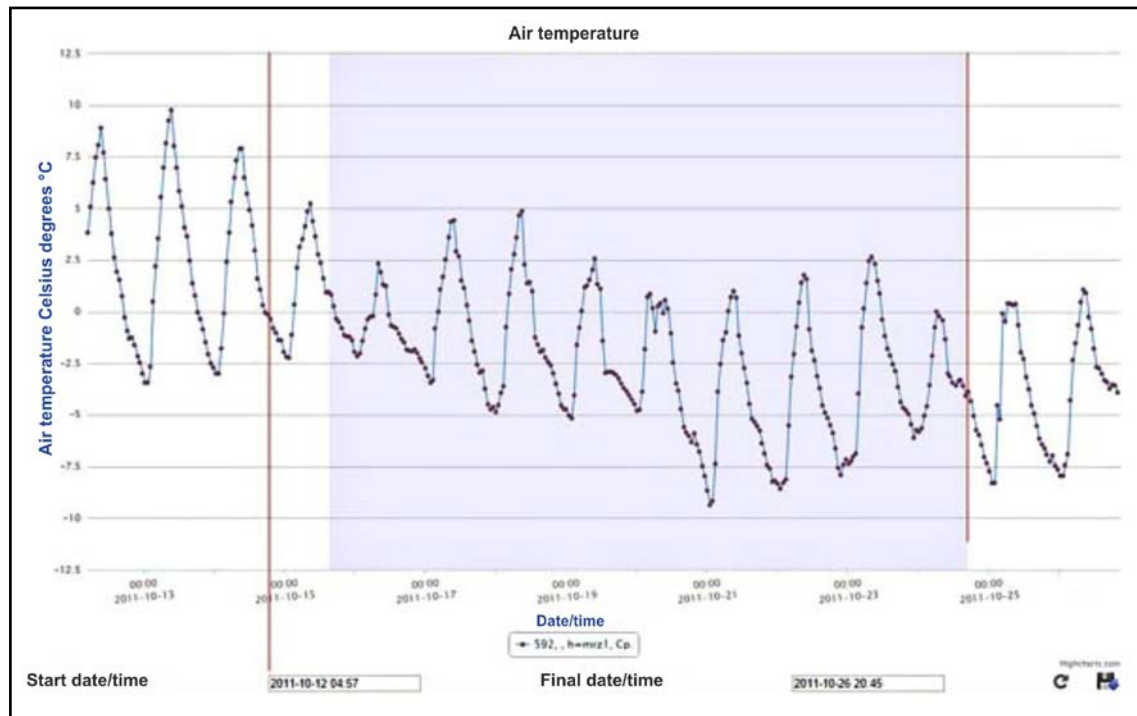


Figure 3.2.3. The graphic visualization of measurement blocks.

Currently available version of SDSS v. 1.1 (<http://192.168.20.52/sdss>).

3.2.2. Geodatabase

Information about the subject of research is a key to any scientific research. In the case of geosciences, this includes information about processes taking place on the Earth and within it. Such information is of spatiotemporal nature and can be provided in the form of topographic and thematic maps, satellite and aerial imagery, radar data, various geophysical and geodetic data (topographic, gravimetric, electromagnetic, seismological, meteorological and many others) in the form of binary records or tables. For an effective use of this geodata, an information system is implemented that is based on a Geodatabase (GDB).

The GDB must include regional and individual data accumulated from various sources. The topographic basis of the database is determined for various spatial levels, which enables to enter data of varying spatial sources. In addition to the spatial data, the GDB contains geophysical and geodetic data of observations of various stages of processing, received from monitoring stations or external sources like global datacenters. The Central Asian GDB serves as a starting point for the integration of data from ground stations, external archives, manufacturers or partners of CAIAG. On the other hand, the GDB serves as an interface for the access to information by the scientific community.

The goal was to draft and create a regional geodatabase (GDB) accessible by a wide circle of specialists from Central Asia and other regions. The intended use of the GDB was storing various types of data, ensuring a quick search and sampling of information

CHAPTER 3. NATURAL PROCESSES MONITORING AND GEOINFORMATION SYSTEMS

by both local and remote users. Access to the database should use state-of-the-art web technologies. In addition to the attributive information, GDB must also contain metadata that describes this information. Overall, the geodatabase was supposed to become a basis for the analysis and interpretation of information about endogenous and exogenous processes occurring in the Earth system with a focus on natural calamities and early warning in Central Asia.

The schematic concept is shown in Figure 3.2.4. Its main principle is: exclusivity of data and multiplicity of applications. This means that the same data must not be duplicated but many applications can exist that use the same data.

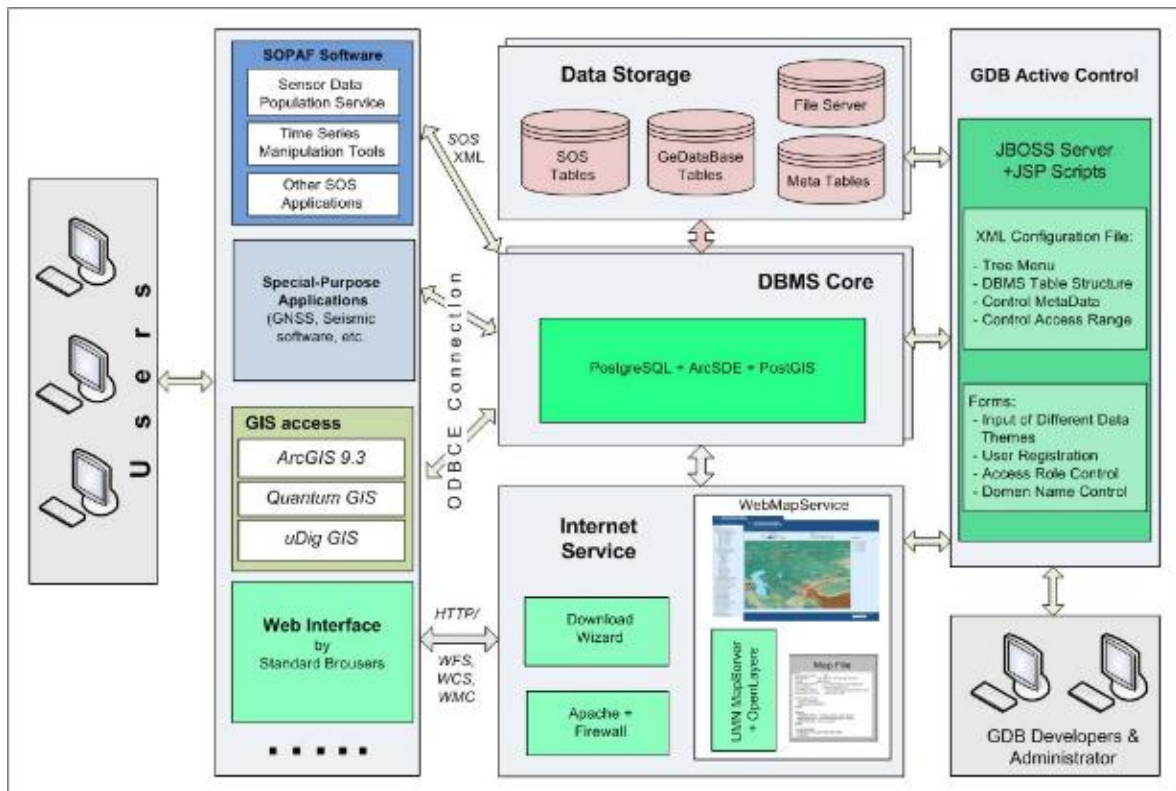


Figure 3.2.4. Schematic concept of GDB

GDB interface simple and intuitively understandable. It provides tools and methods for defining the thematic, spatial and temporal queries to find the required data, spatial navigation and basic information on the project by click (Figure 3.2.5.).

Currently, a new version of GDB is being developed, which supports the formation, editing and distribution of interactive web maps in OGC standards and based on the concept of geo-data platform (working title - JointMap). Working with the geodatabase, experience with projects from 3 sources, as well as global trends in the development and use of databases have highlighted a number of requirements, which were not provided earlier in Geodatabase, but that should be followed during its development. Some of them are mentioned below:

- ✓ The data should be managed by those who are associated with their creation and modification

CHAPTER 3. NATURAL PROCESSES MONITORING AND GEOINFORMATION SYSTEMS

- ✓ The data should be available in formats of recognized standards
- ✓ It must be possible combination of data from various sources in the air
- ✓ The system of restrictions and permissions of access rights to the data should be simple, reliable, flexible, and visual
- ✓ Language system with its vocabularies should be simple, intuitive and flexible
- ✓ There should be a maximum decentralization of information system

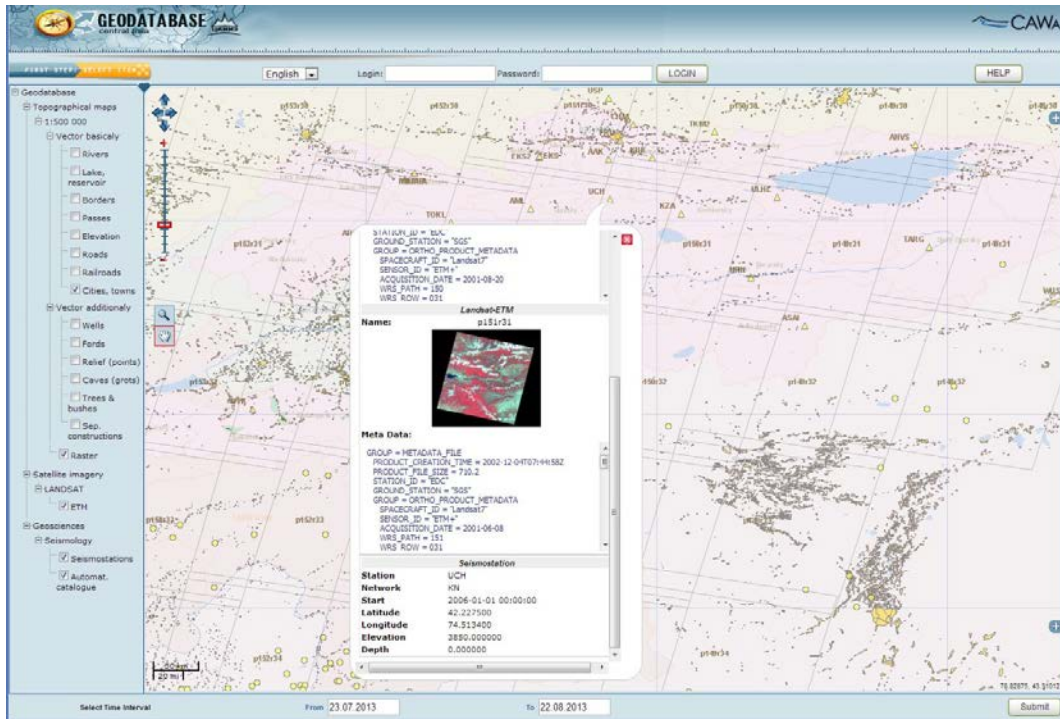
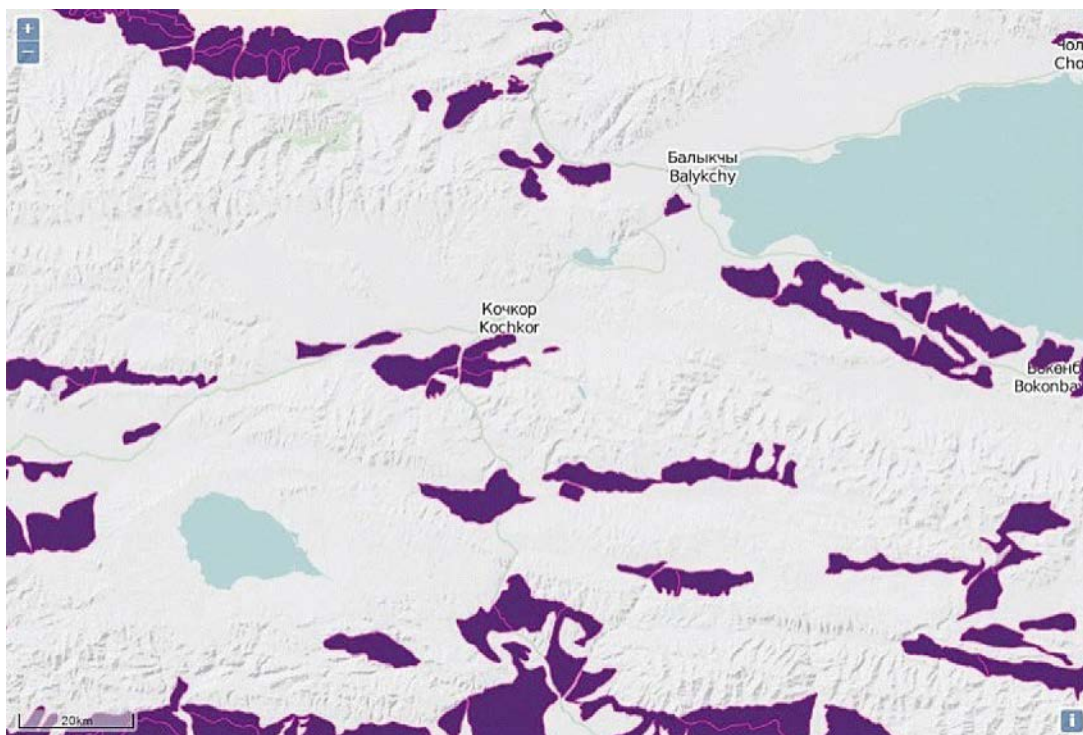


Figure 3.2.5. GDB user interface



CHAPTER 3. NATURAL PROCESSES MONITORING AND GEOINFORMATION SYSTEMS

Figure 3.2.6. GDB user interface- JointMap

Such requirements are met by program-information systems under the name Data Platform. As distinct from Geodatabase they have user-friendly interface, less centralization and more openness. Any registered user can enter data into the Platform and to determine the level of access to their data for others (Figure 3.2.6.). He can independently in interactive mode build their own maps from own layers or layers to which he has access. JointMap internal structure consists from a set of interrelated management tables. In accordance with the management structure the management system is created and designed in the form of web-applications and consists of the following modules: Layer, Map, User, Group, schedule (from SDSS), Dictionary.

3.2.3. Geoinformation Systems in engineer communications services

Geoinformation systems are important tools for an effective planning and management of urban infrastructure. This project creates digital maps of three Issyk-Kul towns and a database of their water and sanitation systems. Lake Issyk-Kul is one of the largest Alpine lakes in the world. A surprising clarity and cleanness of the Issyk-Kul water makes this lake a popular rest and recuperation destination not only for people of Kyrgyzstan but also for foreign tourists.

The GIS developed in the framework of ADB project on Issyk-Kul sustainable development helps effectively to manage water and sanitation services (WSS) of Balykchi, Cholpon-Ata and Karakol while reducing the adverse impact of urban development on the environment of the Issyk-Kul Biosphere Reservation.

For the implementation of the project were used: software ArcGIS and ENVI - to create GIS project and satellite image processing, geodatabase on the database PostgreSQL / PostGIS, a specially designed program based on QuantumGIS library - client of geodatabase, web server UMN MapServer for organization of the web-cartography services and set of equipment for high-precision geodesic surveying TPS GB-1000 and Leica TC802.

In Balykchy, Cholpon-Ata and Karakol towns were conducted inventory of assets and updating of WSS services system, geodesic surveying of WSS objects, vectorization of cadastral and topographic maps and input of semantic information, and based on them developed geographic information system which allows:

- Display, store, edit and print objects of WSS system, cadastral and topographic maps, zoning and land use maps, urban areas satellite images stored in geodatabase servers of each city.
- Provide access to GIS project from client applications with the right of editing or just viewing with web-cartographic services of geodatabase using existing communication networks.

CHAPTER 3. NATURAL PROCESSES MONITORING AND GEOINFORMATION SYSTEMS

- Provide input of new facilities and networks, edit existing objects of WSS system, to conduct quick search, create different queries and reports, generate various forms of paper work with including fragments of maps and semantic data about objects and networks.

At the stage of inventory of assets were composed communication networks schemes, updated the semantic data, conducted high-precision geodesic survey of locations of all WSS objects on 4694 points (Balykchy - 1153, Cholpon-Ata – 872, Karakol - 2669) with an accuracy of about a centimeter.

To prepare the vector layers of digital maps used 290 raster cadastral and topographic maps with scale 1: 2000 (Balykchy - 138, Cholpon-Ata - 54, Karakol - 99).

Topographic maps were 30-40 years old and failed to reflect the current state of landscape and urban plans. Therefore, in order to actualize digital maps as a basis for geodetic coupling of raster maps, we used actual satellite images WorldView-01/02 and QuickBird-2 with high spatial resolution of 0.5 - 0.6 meters and most relevant time for survey.

Following a geodetic survey the adjustment of georeference of the satellite images and orthorectification was performed using results of GPS survey. The necessity of orthorectification was triggered by significant geometric distortions in the satellite pictures caused by and the roughness of the terrain. The most important element in the orthorectification procedure is the digital model of the location synthesized using results of a GPS survey, elevation points on topographic maps and data of radiolocation surveys – SRTM. As a result of the adjustment of satellite imagery, the initial georeference error of 10-15 meters was reduced to one meter.

The geodesic coupling of cadastral and topographic maps was finally conducted on the basis of the adjusted satellite imagery.

Vectorization was performed based on geodetically coupled maps; however, in case of discrepancies between the map images and satellite imagery, the vectorization was based on a satellite image. Overall, 31 cartographic layers were vectorized and prepared: Topography – 10 layers, cadastral – 4 layers, land tenure – 1 layer and WSS facilities – 16 layers for each town (Figure 3.2.7.).

The delivered system for the management of assets of municipal water and sanitation services built on a client-server scheme including a server containing a PostgreSQL geodatabase and support of a web cartographic service and several client nodes in different locations – Vodokanal (Water Supply Company), Glavarhitektura (Chief Architecture Agency) and Meriya (Mayor Office).

Access to the geodatabase is provided in two ways: via a web access by an Internet viewer or via a specialized WSS-GIS application.

Web-GIS access to the geodatabase is intended to be used in a read-only mode. Information is displayed on a screen using standard web browsers (Figure 3.2.8.a.).

CHAPTER 3. NATURAL PROCESSES MONITORING AND GEOINFORMATION SYSTEMS



Figure 3.2.7. Fragment of Balykchy town (a) with WSS objects and GIS, Cholpon-Ata town (b).

CHAPTER 3. NATURAL PROCESSES MONITORING AND GEOINFORMATION SYSTEMS

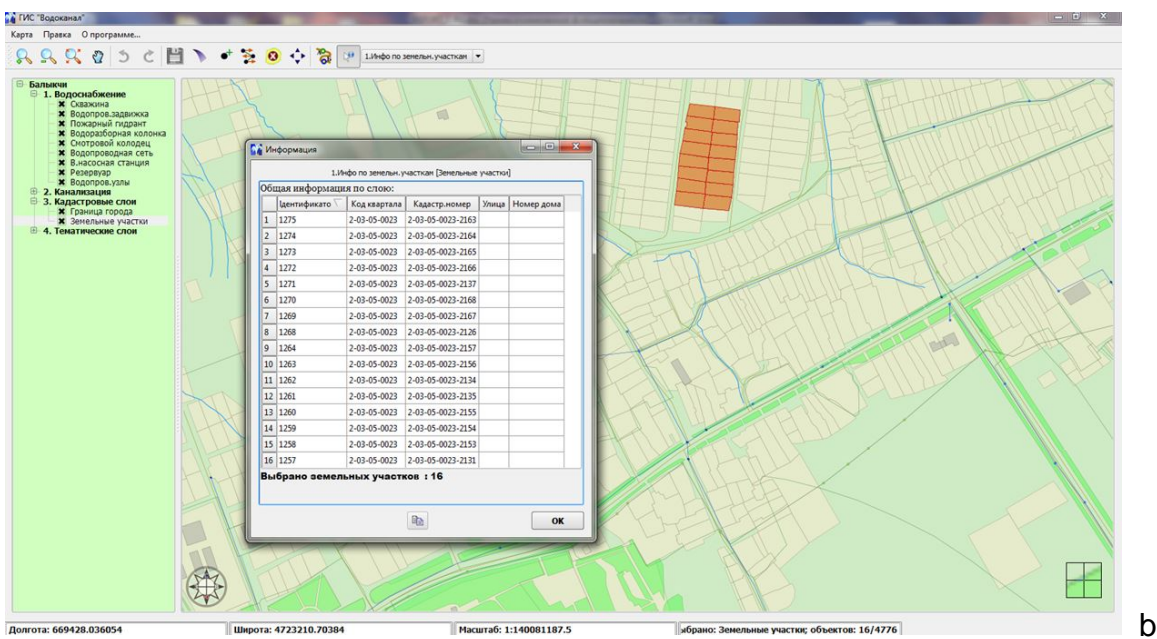
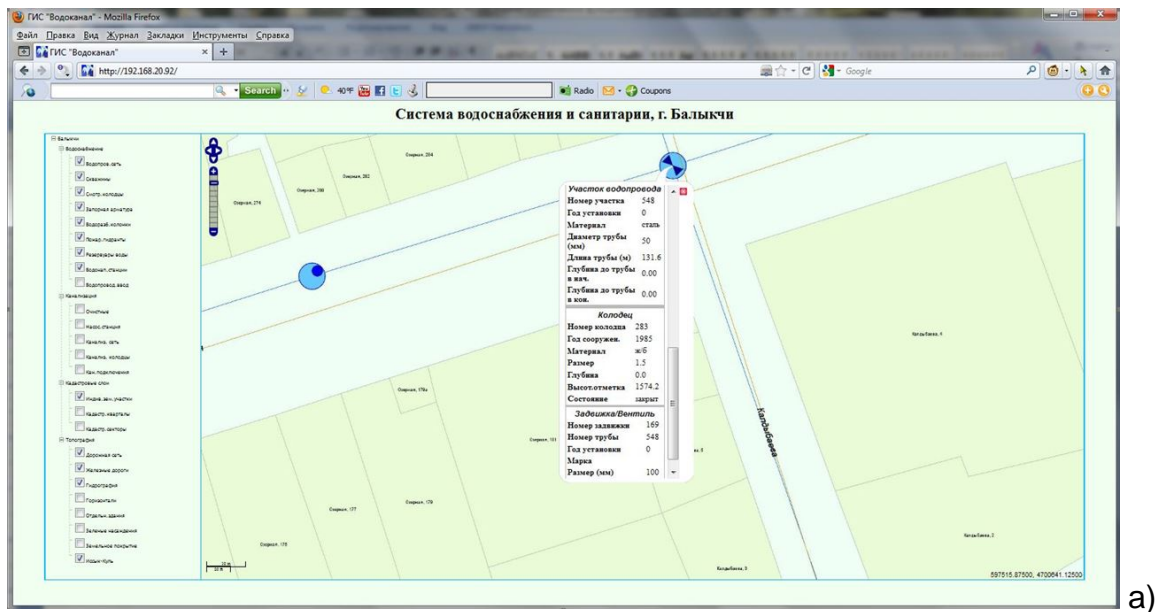


Figure 3.2.8. Access to WSS geodatabase via Internet viewer (a) and client application WSS-GIS (b).

The displayed layers are split into 4 thematic groups: Water, Sanitation, Cadaster Layers and Topography. When working with the map, one can activate the following functions:

Turn on/off any layer from the menu list to display them on the map.

Change the map scale and navigation.

Display signs for individual layers when scaling up.

Receive information about individual facilities.

CHAPTER 3. NATURAL PROCESSES MONITORING AND GEOINFORMATION SYSTEMS

To manage the geodatabase and editing objects and WSS schemes was developed WSS-GIS software which uses libraries of QuantumGIS (Figure 3.2.8.b.).

In every town in the Vodokanal offices (Water Supply Company) installed the servers of geodatabase, additional equipment (scanners, printers), established Internet domains to host geodatabase and made the connection to Internet. Additionally installed computers in offices of Glavarhitektura (Chief Architecture Agency) and Meriya (Mayor Office) that are connected to the WSS geodatabase.

3.2.4. School and Preschool Safety Information System

To assess the schools and preschools in terms of security and vulnerability to natural disasters was conducted large-scale work to collect data on structural and functional safety of buildings carried out by Kyrgyz Scientific Research and Design Institute for Seismic Resistant Construction and database that provides quick access to the data using a web-cartographic technology created in CAIAG.

The basis for development of information system was a document entitled “Methodology and Toolkit for Assessment of Schools and Preschools of Kyrgyzstan” drafted by UNICEF and adapted by Kyrgyz specialists on seismic construction and disaster risk mitigation. Database and web-server were installed on separate server (<http://schooldb.caiag.kg/index.php>).

During development of Information System were used following OpenSource softwares:

- Apache – to organize the website,
- UMN Map-Server – to display Web-GIS maps,
- PostgreSQL – to manage the database,
- PostGIS – to store geographic coordinates in the database,
- QuantumGIS – to enter and edit graphic data in the database (optional).

The database structure contains 16 tables, among them 5 - are administrative formations: country, provinces, districts, rural districts and settlements (residential points), each of them have a geometry column. The other 7 tables contain data on schools and preschools. Only one table of those contains coordinates. All the rest contain information on the 4 forms of safety, background on schools and preschools and photos. Another table contains a map of seismic zoning. The three remaining tables are service types and are required for the functionality of the information system.

Views are more complex. The database has 74 of them. Views are virtual tables that are generated from source tables or other views only when accessed. Views allow applying various filters to the source tables, for instance, to separate schools from preschools, combine several tables into one, calculate final information, for instance, the number of schools or students by district, province, etc.

CHAPTER 3. NATURAL PROCESSES MONITORING AND GEOINFORMATION SYSTEMS

The School and Preschool Safety Information System is organized as a WEB-GIS website containing 12 pages (Figure 3.2.9.).

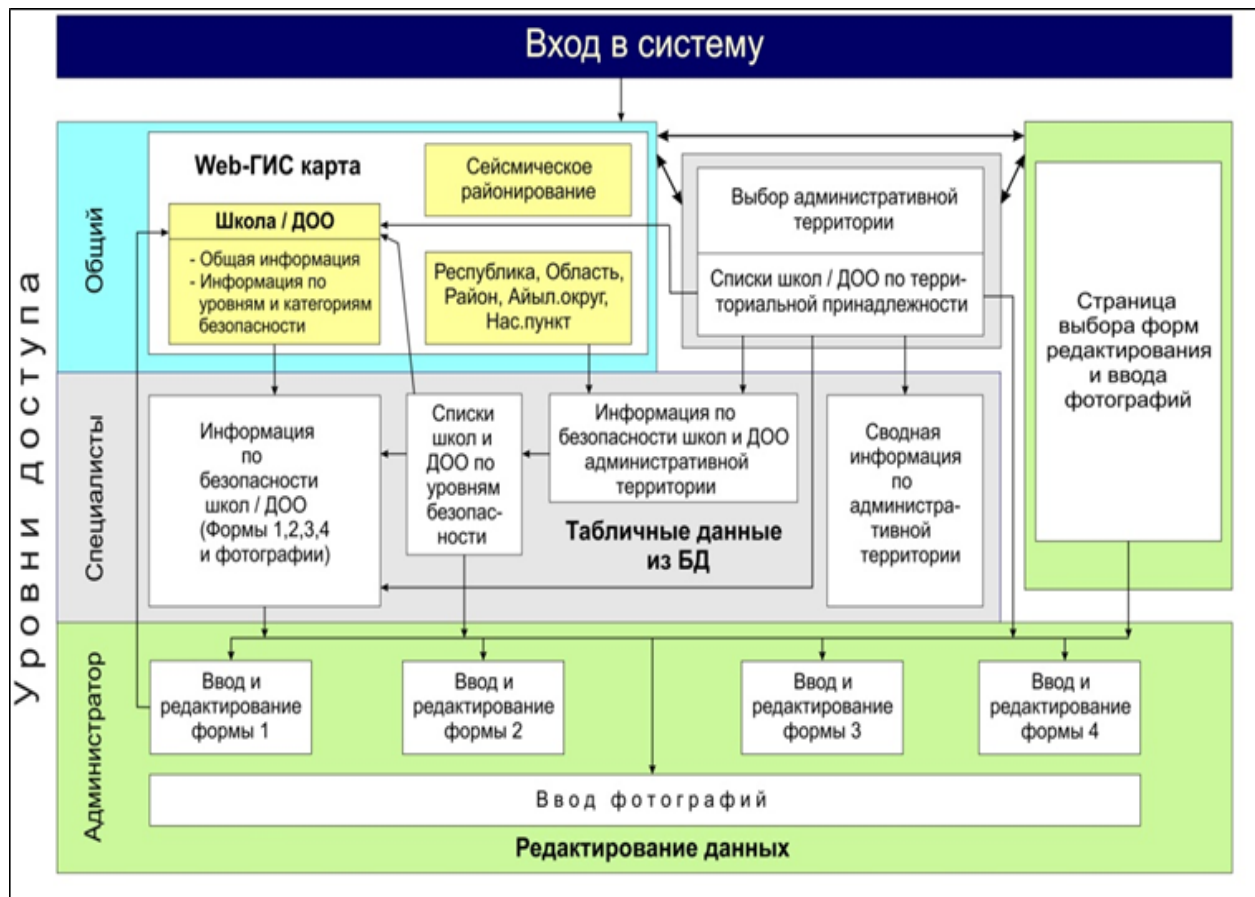


Figure 3.2.9. Web-GIS site organization scheme

To access Web-GIS site and database the next access levels were set up: general (default) –used to only view GIS maps and background information on schools and preschools, specialist – full set of functions to view, administrator – ability to enter and edit data and photos, super administrator – access right to Information System to registered users. The Levels 2 and 3 is available only after special registration of user account.

HTML was used to create the webpages. Coding for the server part was based on PHP, while the client part was coded in JavaScript.

As a result, information on more than 3 thousand schools and preschools of Kyrgyzstan was entered into the database under 4 parameters of safety: structural safety, disaster risk safety, safety of services and infrastructure, functional safety (Figure 3.2.10.).

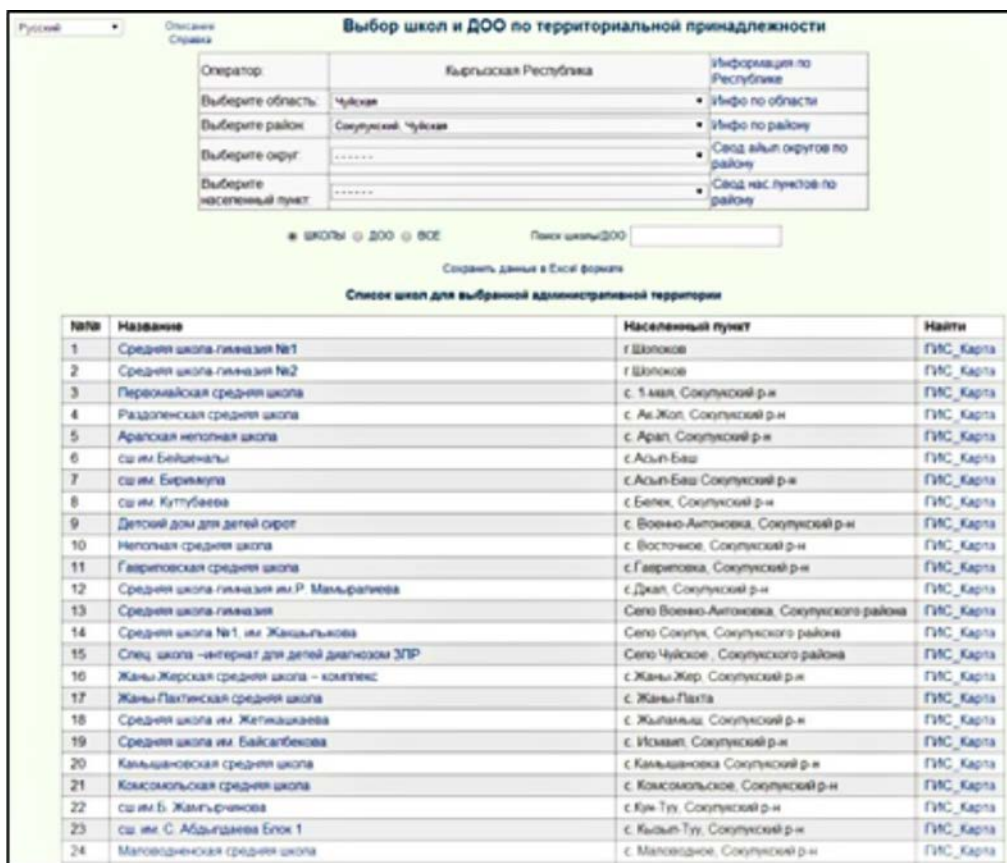
The Reduction of Children Vulnerability to Disasters in Kyrgyzstan was implemented in collaboration with Ministry of Education and Science of Kyrgyz Republic, Ministry of Emergencies of Kyrgyz Republic, supported by UNICEF and funded by the U.S. Federal

CHAPTER 3. NATURAL PROCESSES MONITORING AND GEOINFORMATION SYSTEMS

Emergency Management Agency (FEMA) and United States Agency for International Development (USAID).



a)



b)

Figure 3.2.10. View of web-page WEB-GIS with map (a) and table (b)

3.2.5. Platform of data on risks of natural disasters in Kyrgyzstan

The Kyrgyz Republic Disaster Risk Data Platform supports effective and efficient decisions on disaster risk management in Kyrgyzstan and is used for Capacity Building purposes. The platform is the primary place to store, search, disseminate, display, enter and analyze data aimed at reducing the risk and mitigating the aftermath of disasters, while providing various sectors of the public sector, private sector and the public with more complete information and tools for decision making.

The Disaster Risk Data Platform (DP) is designed to provide specialists in disaster monitoring and forecast and specialists in disaster prevention and management with relevant and factual information in form of cartographic layers, aerial and satellite imagery, textual and tabular data and maps.

Spatial and non-spatial data is stored on servers and accessible from any computer via Internet using a standard Internet browser. The data is compatible to international standards as necessary for GIS data exchange and use. Users working in the area of disaster risk are able to locate the necessary data, view and download them onto their computers. DP has tools to create maps based on available cartographic layers, print and publish them on the Internet in the form of interactive web maps.

To build the Data Platform was selected the GeoNode software system. The Data management tools embedded into GeoNode allow creating layers, maps, documents and metadata and visualize them. Each dataset in the system can be used either public or by restricted users. Such social functions as user profiles and comments and ranking systems allow developing communities around each platform to make it easier for users to use, manage and control the quality of data.

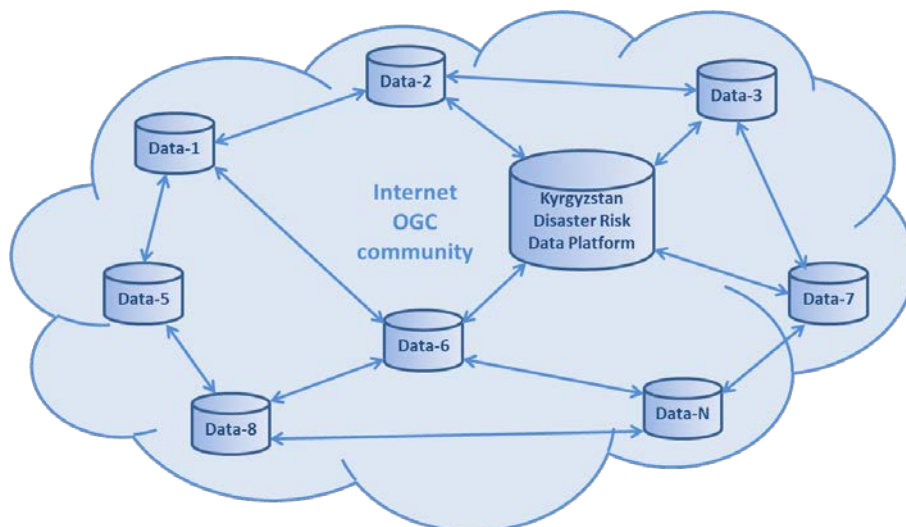


Figure 3.2.11. Data exchange between OGC-servers

Another important advantage of GeoNode is its ability to exchange spatial data with other nodes supporting OGC standards (Open Geospatial Consortium).

CHAPTER 3. NATURAL PROCESSES MONITORING AND GEOINFORMATION SYSTEMS

The data contained in the DP can be made available to users of other OGC-servers (Figure 3.2.11.), as well as the contents of other OGC-servers can be used by users of DP, taking into account the access restrictions set on the data.

The Data Platform is an Internet geo-website (<http://geonode.mes.kg/>) (Figure 3.2.12.) on which users save their spatial and non-spatial data, provide access to them for other users, create maps and publish them, share data with other communities of OGC server networks, discuss the content and comment it.

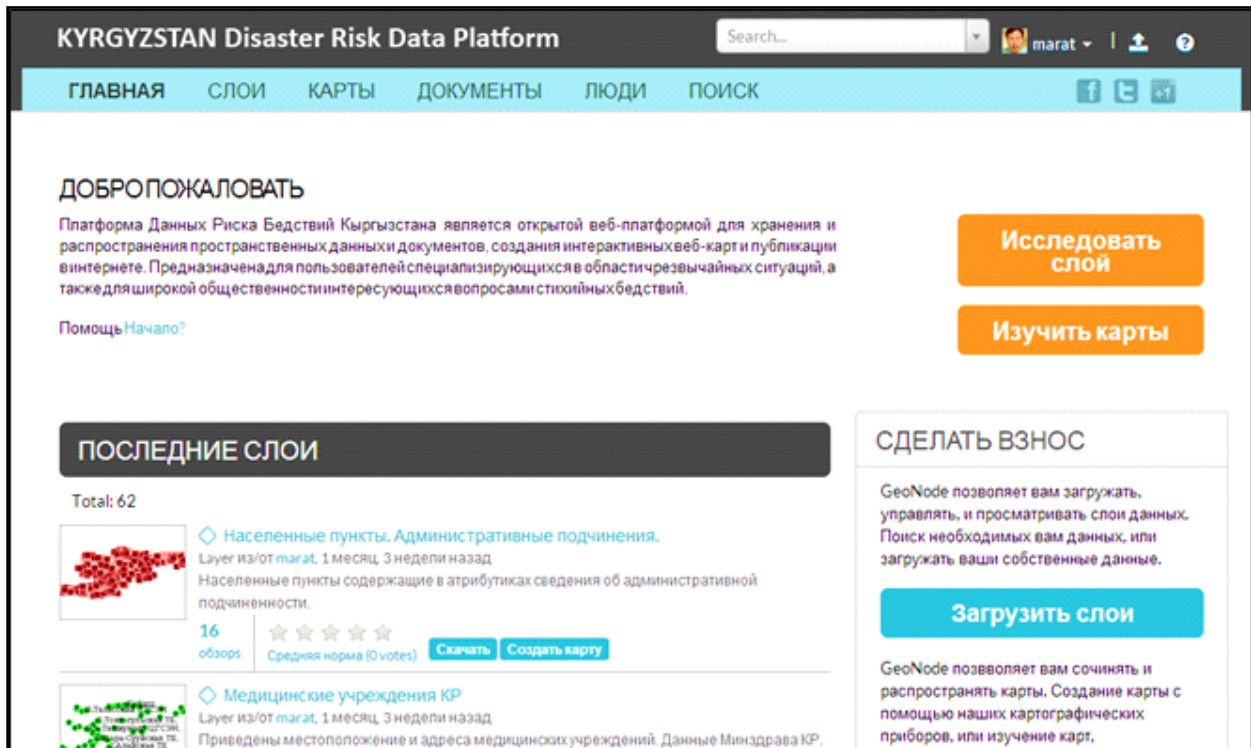


Figure 3.2.12. Main page of Data Platform geo-website

The user interface is generally rather simple and intuitive even for inexperienced users. Only map creation and setup of styles to display layers and signs may trigger some degree of difficulty.

Spatial data is shared between the Data Platform and other OGC-compatible nodes via the protocols WMS, WFS, WCS and others that allow transmitting and receiving spatial data in the form of images, vectors, covers, etc.

Figure 3.2.13. shows the integration of WMS-layers provided by Information System on the safety of schools and pre-schools, into Data Platform for disaster risk mitigation.

Thus, one can create maps by using not only Data Platform-based layers but also layers from other OGC-compatible nodes.

CHAPTER 3. NATURAL PROCESSES MONITORING AND GEOINFORMATION SYSTEMS

The created maps can be easily published on Internet pages in the form of interactive maps that can be moved, sized up and down, and clicked on to receive attribute information about the facilities shown, etc.

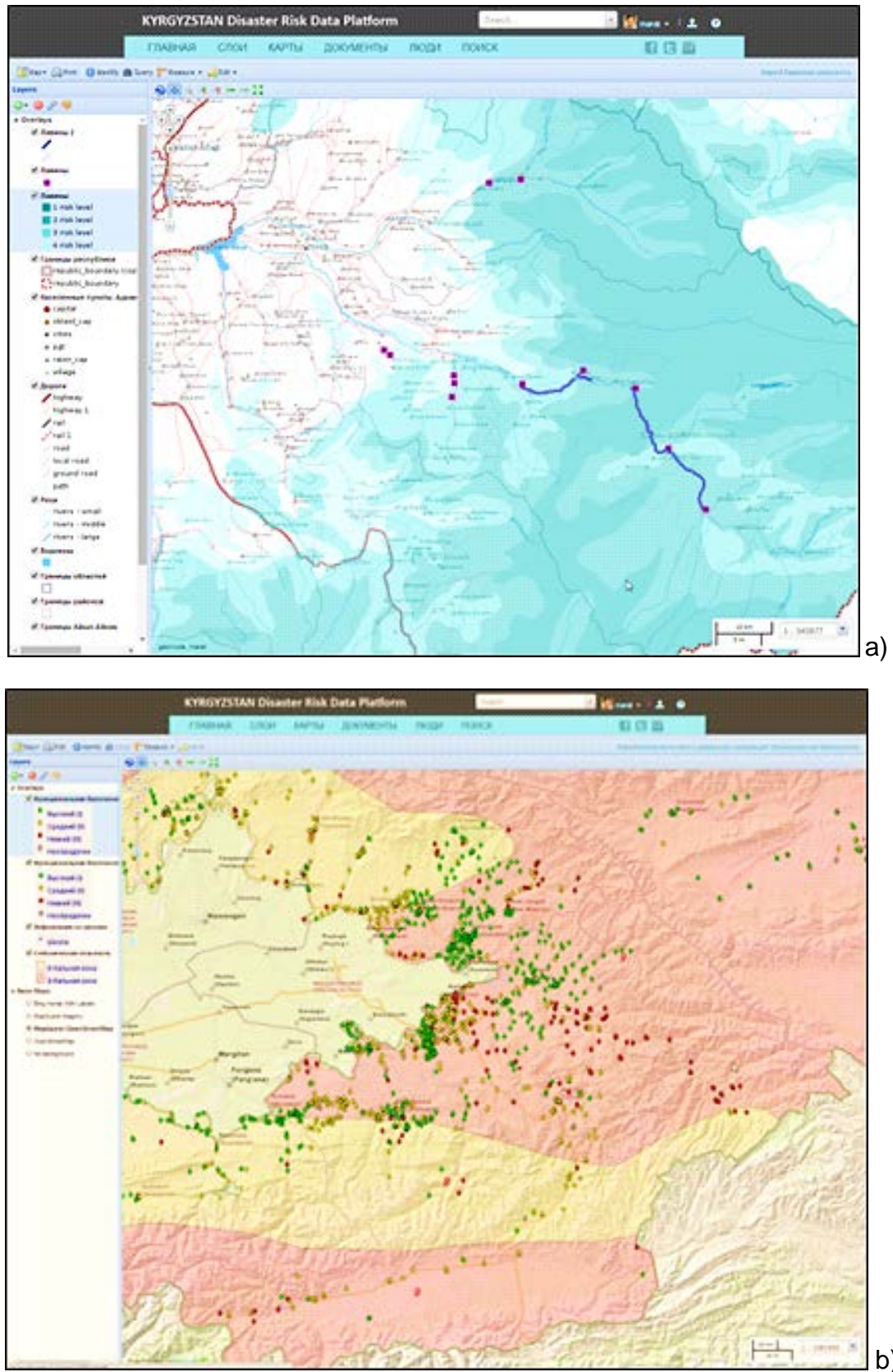


Figure 3.2.13. Map of landslides risks (a) and school safety (b) in Data Platform

References

1. A.B. Bakirov (edit.) *Zemnaya kora i verkhnyaya mantiya Tyan-Shanya v zvyazi s geodinamikoi i seismichnostyu* (Earth Crust and Upper Mantle of Tien-Shan due to Geodynamic and Seismicity). Bishkek: Ilim. 2006. p. 116.
2. Grin T.P. *Skorostniye razrezy seismoaktivnogo sloya i glubiny ochagov zemletryaseniy na osnove detalnogo volnovogo polya* (Velocity Profile of a Seismic Layer and Depth of Earthquake Focuses Based on a Detailed Wave Field). A Ph.D. in Physics and Mathematics dissertation, Moscow: IFZ, 1987. p. 149.
3. Zubovich A. V., Mukhamediyev Sh. A. *Metod nalozhennykh triangulyatsiy dlya vychisleniya gradiyenta skorosti gorizontalnykh dvizheniy: prilozheniye k tsentralno-aziatskoi gps-seti* (Method for Superimposed Triangulations to Calculate Gradient of Velocity of Lateral Movements: Annex to the Central Asian GPS Network // Geodynamic and Tectonic Physics. 2010. Vol. 1. # 2. p. 169-185
4. Kalmetyeva Z.A., Mikolaychuk A.V., Moldobekov B.D., Meleshko A.V., Jantayev M.M., Zubovich A.V. (2009) *Atlas zemletryaseniy Kyrgyzstana* (Atlas of Earthquakes of Kyrgyzstan). Bishkek: CAIAG, p. 213. ISBN 978-9967-25-829-7. www.caiag.kg
5. Abdybachaev U.A., Bragin V.D., Haberland Ch., Jusupova K., Kalmetyeva Z.A., Matiks A.I., Mechie J., Meleshko A.V., Moldobekov B.D., Orunbaev S.J., Schurr B. and Usupaev Sh.E. Active Seismic Investigation of December 22, 2009 Detonation at Kambarata (Kyrgyzstan) Site for a Dam Fill Construction. Geophysical Research Abstracts Vol. 13, EGU 2011-140-2, 2011 EGU General Assembly 2011, 3-8 April 2011 in Vienna, Austria.
6. Havskov J. and Ottemoller L. SeisAn Earthquake analysis software, *Seis. Res. Lett.*, 70, 1999.
7. T. Schöne, C. Zech, K. Unger-Shayesteh, V. Rudenko, H. Thoss, H.-U. Wetzels, A. Gafurov, J. Illigner, and A. Zubovich. A new permanent multi-parameter monitoring network in Central Asian high mountains – from measurements to data bases. *Geoscientific Instrumentation, Methods and Data Systems*, 2, 97–111, 2013, www.geosci-instrum-method-data-syst.net/2/97/2013/
8. Herring T.A.(2004), *GLOBK: Global Kalman Filter VLBI and GPS Analysis Program Version 4.1*, Mass. Inst. of Technol., Cambridge.
9. King, R.W. and Y. Bock (2004), *Documentation of the MIT GPS Analysis Software: GAMIT*, Mass, Inst. of Technol., Cambridge.

CHAPTER 4. CAPACITY BUILDING AND SCIENTIFIC COOPERATION

4.1. Scientific cooperation

In the post-Soviet period the state of academic structures in Kyrgyzstan has been deteriorated significantly: despite the high scientific capacity, the development of science was poorly supported by the government. Therefore, cooperation between CAIAG and Kyrgyz scientific and research organizations is of great interest: capacity building, targeted use of resources, information sharing, training of young scientists etc. The Institute continues to deepen its cooperation with national partners transitioning to level of practical implementation of plans.

The Ministry of Emergency Situations of the Kyrgyz Republic remains the main partner interested in obtaining scientific results from the Institute. CAIAG researchers provide the Ministry with data from seismic stations and assess consequences of disasters on site. Annually, CAIAG researchers work out and present forecasting materials on expected most common natural hazards in the territory of the Kyrgyz Republic for their further publication in the Ministry's annual report "Book of Forecasts of Emergency Situations."

CAIAG is a member of the National Disaster Platform under the Ministry of Emergencies and renders consulting support to decisions made by the Platform Secretariat. The Institute participates in periodic meetings of the Platform and preparation of the Disaster risk Reduction Action Plan that provides for the creation of a regional early warning system, improvement of specialist training, awareness-raising in local communities and cooperation among regional platforms.

As a member of the Scientific and Technical Council under the Interdepartmental Commission for Civil Protection of the Kyrgyz Republic, CAIAG participates in discussion of issues and results of operations of state authorities, international organizations and NGOs in the sphere of disaster risk management in Kyrgyzstan.

Participating in several engineering seismology projects, CAIAG continues to make contributions to improvement of institutional frameworks for seismic-resistant construction and risk assessment in settlements. Such academic institutions as the Institute of Seismology and Institute of Geology under the National Academy of Sciences of the Kyrgyz Republic and relevant organizations such as the Kyrgyz Science and Research Institute for Designing and Seismic-Resistant Construction, the State Agency for Architecture, and municipal authorities are engaged in this process now. CAIAG holds periodic meetings with representatives of these organizations at which its officials present results of their scientific-applied projects.

CAIAG liaises with educational institutions of Kyrgyzstan. In addition, CAIAG officers are part-time instructors in universities engaging undergraduate, graduate and post-graduate students of such universities in the Institute's activities and offering field trips

CHAPTER 4. CAPACITY BUILDING AND SCIENTIFIC COOPERATION

and internships as well as consultations of specialists. The educational partners involved include:

- Kyrgyz State University of Construction, Transportation and Architecture;
- Kyrgyz-Russian Slavic University;
- Kyrgyz State University named after J. Balasagyn (Faculty of Geography);
- Bishkek Humanities University (Faculty of Ecology);
- Institute of Mining and Mining Technologies under the Kyrgyz Technical University named after I. Razzakov.

In addition, CAIAG offers opportunities to conduct international internship for foreign students who are engaged in CAIAG daily work.

The development of international cooperation and its form are considered one of the preconditions for the Institute's prospects. CAIAG has defined such important directions as: conduction of scientific research in cooperation with foreign scientific centres, science information exchange, conduction of international scientific conferences, publication of scientific articles with foreign partners, usage of various forms of international cooperation for improving qualification of CAIAG researchers, specialist exchange, joint usage of equipment, organizing and hosting of conferences, editorial projects, cooperation with scientific communities, implementation of third-source projects, and managing scholarships.

CAIAG and international academic scientific centres express their mutual interest in cooperation to implement science projects in the Central Asian region. Within implementation of the joint scientific and research projects, over 10 years CAIAG signed more than 70 Cooperation Agreements with various national and international organizations. In future, this cooperation will only be solidified. Interest in CAIAG operations on part of international scientific centres and organizations is growing as evidenced by an increasing flow of offers of running joint activities.

4.1. Capacity building

CAIAG gained its first experience in implementation of educational activities after organization of the international training course "Seismology and Seismic Hazard Assessment" which was held from August 20 to September 23, 2006. Prominent scientists from Kyrgyzstan, Russia, USA and Europe made presentations and held practice sessions on state-of-art methodologies in seismology and visited historical earthquake sites in Issyk-Kul, Suusamyr, Chon-Kurchak, and Ala-Archa in which concrete examples were used to show signs of ancient and contemporary seismic dislocations and seismic catastrophes. As a result of this training, CAIAG partnered with GFZ-Potsdam and the Institute of Seismology of the National Academy of Science of the Kyrgyz Republic to publish a manual on field trips. At that time applications for the training course were received from 60 candidates from various countries, among which

CHAPTER 4. CAPACITY BUILDING AND SCIENTIFIC COOPERATION

26 specialists from Kyrgyzstan, Kazakhstan, Russia, Uzbekistan, Tajikistan, China, Mongolia, Afghanistan, and Iran were selected. The 5-week course was funded by GFZ-Potsdam, the German Ministry of Foreign Affairs, InWEnt-Berlin, CTBTO-Vienna, UNESCO-Paris, and CAIAG. This training course is arranged annually by GFZ-Potsdam as part of UNESCO's educational and training program in the sphere of geosciences and disaster mitigation.



Figure 4.2.1. Training Resource Group

During December 3-7, 2007, CAIAG held the international training program “Community-Based Disaster Risk Management based on the Hyogo Framework for Action.” The training was organised by the initiative of the Global Platform for Disaster Risk Reduction, ISDR/UN and co-funded by the Swiss Agency for Development and Cooperation (SDC) in Tajikistan. The organizational and technical support of the training was provided by CAIAG. The purpose of the training was to promote the Hyogo Framework for Action for 2005-2015: Building the resilience of nations and communities to disasters. The training was attended by representatives of ministries of emergency situations, Red Cross and Red Crescent societies, NGOs, UNDP national offices, UNICEF disasters components from Kazakhstan, Kyrgyzstan, Tajikistan, Turkmenistan, Uzbekistan and Serbia. Falak Nawaz, the Manager of Training Resource Group of the Asian Disaster Preparedness Center (Thailand) (Figure 4.2.1.) was the chief speaker. Also there were presentations run by ISDR/UN, the Swiss Agency for Development and Cooperation, CAIAG, FOCUS, DRR, and experience shared by UNDP Resident Office in Kyrgyzstan, the Ministry of Emergency Situations, the National Red Crescent Society of Kyrgyzstan. Research fellows of CAIAG's Department of Climate, Water and Geoecology made presentations.



Figure 4.2.2. Experts in outburst-prone lakes

On May 20-21, 2008, CAIAG arranged the international workshop “Glacial Outburst-Prone Lakes in Central Asia” funded by the Swiss Agency for Development and Cooperation (SDC, Switzerland). The purpose of the workshop was discussion of issues of outburst-susceptible glacial lakes in the Central Asian region, identification of existing and necessary scientific, technical and logistical means and tools, and recognition of primary trends, deficits and resources needed to resolve this problem in Central Asia. The workshop was attended by more than 40 experts in outburst-prone lakes and representatives of stakeholder organizations from Kyrgyzstan, Uzbekistan, Tajikistan, Kazakhstan, Russia, Germany, Austria, Czech Republic, Canada, and Nepal. The workshop resulted in recommendations to underlie better cooperation in outburst-prone lake mitigation and data and information monitoring, processing and management.

In 2008, the German Ministry of Foreign Affairs approved funding of a regional project “Cross-Border Disaster Prevention in Central Asia” implemented by the international capacity building company InWEnt (Germany), in cooperation with GFZ and CAIAG. The project was divided into two important components: a scientific one, in the framework of which the regional CAREMON network was created under scientific and technical supervision of GFZ; and an educational one, aimed at capacity building of representatives of authorities responsible for planning, seismic-resistant construction and emergency risk management, and instructors of relevant higher education institutions. This component was coordinated by CAIAG. The regional meeting in Bishkek held on April 6-8, 2009 was attended by national partners for discussion of the plan of activities. From April to September 2009, within the project CAIAG ran the following activities:

A regional training “Seismic-Resistant Construction” was held on May 27-29 in Almaty, Kazakhstan. The training was dedicated to such topics as design of buildings and

CHAPTER 4. CAPACITY BUILDING AND SCIENTIFIC COOPERATION

facilities in seismic areas, contemporary software products to measure and survey buildings and facilities in seismic areas, designing high-rise buildings, controlling quality of construction and installation works. CAIAG also invited Central Asian specialists from seismic-resistant construction institutes and architecture and construction organizations. National technical trainings “GIS for Emergency Situation Management.” CAIAG ran three-day practice sessions on applying GIS tools to assess vulnerability in 4 countries (Kazakhstan, Kyrgyzstan, Uzbekistan, and Tajikistan) for specialists of the ministries of emergency situations, institutes of seismology and aseismic construction and instructors of higher education institutions.

Regional training “Infrastructural Aspects of Preparation for Earthquakes,” August 11-13, Tashkent, Uzbekistan. Topics of three-day trainings included seismic hazards and risks in Central Asia, arrangement of seismic protection, non-structural safety at industrial sites, public buildings and residential houses, monitoring of the seismic situation in the territory of Central Asian countries, planning and optimum placement of infrastructure of large cities of Central Asia for sustainable development amidst high seismicity.

Regional workshop “Risk Assessment and Analysis,” September 28-29, Dushanbe, Tajikistan. Workshop goal: to discuss needs of national counterparts in local trainings in seismic risk assessment for representatives of architecture and urban planning organizations and Ministries of Emergency Situations.

Within the project, trainings for more than 100 participants from Central Asia were held. Training materials and licensed GIS software provided by ESRI, via Z_GIS Centre of the University of Salzburg were distributed among the participants. Successful participants were awarded certificates of attendance. Many participants wished more training sessions like those were held as they facilitated the improvement of qualification of young specialists as well as experience and knowledge sharing.

Within the project “Awareness Raising in Local Comprehensive Disaster Risk Management implemented” implemented by CAMP Ala-Too, CAIAG ran a risk assessment in a pilot territory of River Zerger Watershed in South Kyrgyzstan. In addition, six CAIAG officers attended the training in CAMP Ala-Too in holding trainings with local communities on disaster awareness-raising as part of that project. Following the TOT, the project conducted 16 field seminars in the territory of River Zerger Watershed and 11 field seminars in pilot rural aimaks (rural districts) funded by the UNDP Disaster Risk Management Project. Disaster risk awareness-raising is a priority objective for CAIAG and is mentioned as the main activity in the CAIAG Charter.

Therefore, specialists engaged in trainings with the public facilitate the meeting of CAIAG obligations and help improve the Institute’s stature and reputation in the country. Participation of CAIAG in an international symposium “Awareness-Raising in ICT Application in Disaster Risk Management” organized by the Ministry of Emergencies of the Kyrgyz Republic and the Japanese Aerospace Exploration Agency (JAXA) and the

CHAPTER 4. CAPACITY BUILDING AND SCIENTIFIC COOPERATION

United Nations Economic and Social Commission for Asia and the Pacific (ESCAP) held on 25-27 February 2009 in Bishkek opened up opportunities for the integration into the Pacific scientific and technical community. CAIAG joined the Sentinel Asia project coordinated by JAXA having gained official membership in the project and the right to receive free-of-charge satellite imagery from ALOS, IRS, KARI and THEOS upon request in case of disasters in the region.

On October 13-14, 2008, CAIAG held a project workshop “Water of Central Asia.” The workshop was attended by representatives of hydrometeorological services of Kyrgyzstan, Kazakhstan, Tajikistan, and Germany. The meeting discussed the current state of a network of hydrometeorological stations and hydrological posts and needs for the network expansion and instrumentation, procedures for handover, processing, and storage of data and gaining access to it, procedures for sharing parameters of CA, needs for creating a data bank for hydrometeorological parameters to develop a hydrological climate model for Central Asia.

On December 2-5, 2008, CAIAG and GFZ held the training in Bishkek “Seismic Microzonation.” The training was attended by seismology scientists of Central Asia: Tajikistan, Kazakhstan, Turkmenistan, Uzbekistan, and Kyrgyzstan. The project goal was to contribute to seismic risk mitigation in Central Asia.

On June 8-16, 2009, CAIAG, the Institute of Geology under the National Academy of Science of the Kyrgyz Republic, in collaboration with the ILP Project Topo-Central Asia and ERAS (Earth Accretion System), arranged an international geological travel route along the Kyrgyz side of the Tien-Shan, with a follow-up 2-day workshop in Bishkek. The activity goal was to compare geological structures and formation of the Tien-Shan in the Kyrgyz and Chinese territories, present and discuss unpublished data, and negotiate prospects of international cooperation on geological and geophysical research in the Central Asian orogenic belt including the seismogeological profile from North China to Siberia. During the 8-day long field trip, participants looked at sections of the Northern, Medial and Southern Tien-Shan to compare properties of formations as well as structural and metamorphic restructurings in the adjacent territories of Kyrgyzstan and China and discuss evolution of the Tien-Shan as part of the overall Central Asian geology. The follow-up workshop offered opportunities to present new findings and discuss prospects of joint research. The workshop also resulted in the publication of a guide and a collection of articles by workshop participants.

In 2009, CAIAG together with the Northern Eurasia Earth Sciences Partner Initiative (NEESPI), GFZ, University of Idaho, Institute of Geography of the Russian Academy of Sciences (IG RAS) and the Chief Geophysical Observatory RosGidromet held a series of educational activities:

- September 8-13 – a six-day scientific and educational seminar on mountainous ecosystems of Northern Eurasia and a regional seminar of the NEESPI scientific group (high-mountain regions).

CHAPTER 4. CAPACITY BUILDING AND SCIENTIFIC COOPERATION

- September 8-9 – a young scientists school “Environmental Studies in High Mountains” during which instructors from USA, Russia, Germany, Uzbekistan and Kyrgyzstan, including CAIAG, made presentations on the state of environment in high mountains and contemporary methods of studies;
- September 10-13 – an international workshop on current and planned NEESPI projects. The workshop resulted in recommendations on the improvement of research of high-mountain regions of Northern Eurasia. The workshop was attended by 50 participants from various countries.

The EMCA Project (Earthquake Model of Central Asia) was created as part of the GEM Program (Global Earthquake Model) and coordinated by GFZ, in collaboration with CAIAG. The project goal was to assess trans-border seismic hazards and risks in Central Asia. This scientific project was implemented in cooperation with science counterparts from Kyrgyzstan, Kazakhstan, Tajikistan, Uzbekistan and Turkmenistan working on seismic hazards, micro-zoning, vulnerability and risks. The EMCA Program enabled the parties to the project participate in various workshops and trainings. The participants received access to state-of-the-art software developed to assess seismic hazards and risks and analyse data of satellite sensing. The EMCA Project held the following workshops:

A kick-off workshop under the EMCA Project held in CAIAG in June 2011 attended by lead specialists of relevant research institutes as well as representatives of Ministries of Emergencies of Kazakhstan and Kyrgyzstan who today are the project beneficiaries. The workshop discussed all issues associated with the implementation of this project.



Figure 4.2.3. A) Starting seminar in June 2011; B) seminar of seismic construction in March 2011; C) seminar on harmonization of a single model of seismic zoning

In March 2012, within the EMCA Project there was a seminar for specialists in seismic construction dedicated to seismic vulnerability of large cities and settlements of Kyrgyzstan. This seminar discussed issues of seismic vulnerability of cities and settlements and the creation of a database of classifications of vulnerability of buildings based on GEM standards which are a part of actions to reduce seismic risks.

CHAPTER 4. CAPACITY BUILDING AND SCIENTIFIC COOPERATION

A workshop in June 2012 which completed, together with all partner countries, the harmonization of the unified model of seismic zoning for Central Asian countries which represents one of the main deliverables of the EMCA Project.

A workshop on using GIS-systems for vulnerability data processing and management was held in September 2012 for specialists of the Institute of Innovative Technologies in Bishkek to assess seismic vulnerability of buildings in Kyrgyzstan.



Figure 4.2.4. Seminar of the use of GIS systems for processing and managing data vulnerabilities

An EMCA-GEM workshop on assessment of seismic vulnerability of buildings was conducted on December 14-19, 2013, and was arranged by GFZ in collaboration with CAIAG. The workshop summarized all activities in assessing seismic vulnerability of buildings for Central Asian countries by project counterparts in compliance with the TAXONOMY vulnerability model. During the workshop, international lead specialists from GEM made presentations on the use of this model and contemporary methods and technologies in vulnerability assessment. For five days, international experts from GEM and partner experts from Central Asia worked to agree the unified harmonized system of classification of vulnerability of buildings using the data secured over the 2 years of the project and following relevant international standards.

Within the European Union project “Climate Change Impact on Glaciers and Mitigation Strategies in European Alps, Swedish Lapland and Tien-Shan Mountains,” in collaboration with the University of Vienna (the leading organization), Central Agency for Meteorology and Geodynamics (Vienna, Austria), Blekinge Institute of Technology (Sweden), CAIAG and GFZ, on August 13-17, 2012, held a workshop “Assessment and Mitigation of Climate Change Triggered by Geological Hazards based on the Example of Suburbs of Bishkek.” The workshop was attended by researchers from European and Kyrgyz universities, graduate students and representatives of state authorities. The

CHAPTER 4. CAPACITY BUILDING AND SCIENTIFIC COOPERATION

workshop presented results of a research group which prove the climate change over the past decade, glacial retreat, increase in geological hazards of glaciation, and looked at a particular example of an outburst of a glacial lake near Bishkek that occurred in June 2012. The workshop participants were offered a two-day field trip and experiences in geological hazard assessment in the Ala-Archa Gorge. Workshop materials and hydrometeorological, satellite and GIS data, as well as manuals and references were also presented in the form of a virtual training platform installed in CAIAG for the first time. Later, this platform was used for dissemination of project results and exchange of knowledge.

Within the international scientific and practice conference “Mountains and Climate,” dedicated to the 10th Anniversary of the International Day of Mountains, on 10 December 2012, CAIAG held a round table “Water Resources and Natural Hazards in Mountainous Regions Caused by Climate Change,” supported by the CAWa project. The meeting was attended by representatives of hydrometeorological services of Central Asia, CAWa project partners, science institutes and universities, and representatives of international organizations. The conference also saw interim reports of the CAWa project delivered by participants from GFZ, DLR, CAIAG and hydrometeorological services of Central Asia.

As part of collaboration with the Kazakhstan National Centre for Aerospace Studies and Technologies, CAIAG held 2 technical trainings for officers of that centre on the processing of GNSS and InSAR data. The training program was prepared and delivered by specialists of CAIAG Department 3.

On August 5-9, 2013, CAIAG, within the CAWa project, conducted a training course “Remote Sensing for Hydrological Monitoring” designed at the Department of Remote Sensing of the University of Wurzburg, Germany. The course was aimed to use opportunities of remote sensing in water resource management and use of the ArcGIS 10 software. The course participants processed individual projects related to their professional activities. The training course was attended by 26 participants representing all 5 Central Asian countries.

On December 9-13, 2013, CAIAG hosted another training course of the CAWa project “Statistical Analysis in Hydrology: Introduction to R Programming Language.” This free-access program was aimed to explain how to use the R language for statistical analysis purposes (<http://www.r-project.org/>). This open access program allows analysing, processing and rendering of graphic pictures of time rows, data and remote sensing and climate models. R is a powerful and easy-to-learn programming language which is used for scientific purposes to process information. The training course was attended by 24 participants from universities and scientific institutions of 5 countries including Afghanistan.

In order to further disseminate results of the SENSUM Project, on January 28-29, 2014, being supported by UNDP, CAIAG and GFZ held a symposium on earthquake and

CHAPTER 4. CAPACITY BUILDING AND SCIENTIFIC COOPERATION

mudslide risk in Central Asia and Caucasus: use of remote sensing and management of geospatial information. The symposium was attended by researchers from Germany, Norway, Great Britain, Italy, Japan, Turkey, Tajikistan, and Kyrgyzstan. Report topics included research and mitigation of natural catastrophes using contemporary technologies. Conference reports were presented in the form of presentations and posters. One of the symposium's main objectives was to bring together efforts of scientific researchers and representatives of local authorities and the Ministry of Emergencies in effective emergency management. The symposium also saw attendance by representatives of various organizations such as WB, GIZ, UNDP and ICCO COOPERATION that too implement joint projects in Kyrgyzstan aimed at disaster risk reduction.



Figure 4.2.5. Remote Sensing for Hydrological Monitoring training course participants



A

B

Figure 4.2.6. Statistical Analysis in Hydrology: A) Introduction to R Programming Language; B) learning of rendering the information.

CHAPTER 4. CAPACITY BUILDING AND SCIENTIFIC COOPERATION



Figure 4.2.7. General photo of the participants of the symposium SENSUM Project

As part of cooperation between CAIAG and the University of Wurzburg, from April 25 to May 8, 2014, CAIAG ran a training course “GIS and Remote Sensing Data Processing Methods. The training program was prepared and delivered by Prof. Christopher Conrad and graduate student Alexandra Breiter of the University of Wurzburg. The training was attended by CAIAG officers, instructors of the University of Central Asia (Mountain Societies Research Institute) and the Kyrgyz Technical University.

On September 9, 2014, CAIAG will host an international conference “Remote- and Ground-Based Earth Observations in Central Asia” dedicated to the 10-year anniversary of the Institute. The goals include: discuss the most important results of remote and ground-based Earth observations in Central Asia received over the past years, identify high-priority scientific directions in this research, share experience in both information research and processing, storage and management. The conference expects to see about 110 presentations by prominent scientists from Central Asia and Europe, Russia and USA distributed between 4 thematic sections:

- Geohazards and georisks
- Climate, water and nature management
- Geoinformational technologies and monitoring systems

Conference materials will be published in the Conference Proceedings Manual.

GRATITUDE

CAIAG expresses its deep gratitude for contribution to development of the Institute to scientists and representatives of State Bodies. With their assistance and tireless support the Institute development were created and implemented for 10 years.

To all of them we express sincere gratitude: Prof. Rajgber H., Prof. Ehtler G., Prof. Emmermann R., Dr. Raiser B., Prof. Gize E., Prof. Khuttl R.Yu., Dr. Mikhailev VN., Wetzell H.-U., Resner Z., P. Offermann, Prof. Chow J., Prof. Holzle., Dr. Schone T., Unger-Shaste K., Parolay S. from the German side. Dr. Dzhumagulov AD (Ambassador of the Kyrgyz Republic in Germany), ex-ministers of the Ministry of Emergency Situations of the Kyrgyz Republic: Urmanaeva S.I., Eshmanbetova R.B., Chyrmashev S.C., Rustembekov Zh.S., Dzhunushaliev T.Sh., Borbiev BB., Minister Boronov K.A. Academicians of the National Academy of Sciences of the Kyrgyz Republic: Bakirov A.B., Mamatkanov D.M., Kutanov A.S., Prof. Khristoforov A.V. (Russia), Saidova M.S. (Tajikistan), Mikhailova N.N. (Kazakhstan), Torkoyev I. To employees of the Department of monitoring and forecasting of MES KR: Sarnoyev A., Aitaliev A., Azhybaev T.A., Ibatulina H.V., Mokrousov V.V.

**CENTRAL ASIAN INSTITUTE FOR APPLIED GEOSCIENCES
(CAIAG)**

**REMOTE AND GROUND BASED EARTH EXPLORATIONS
IN CENTRAL ASIA**

Printed:
LLC “City Print”
Angarskii street 13, Bishkek
+996 (312) 88-21-10
+996 (312) 88-23-80
e-mail: cityprintkg@mail.ru

2016